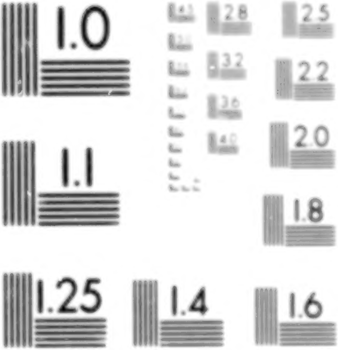
1.0
2.8
2.5
3.2
2.2
3.6
4.0
2.0
1.1
1.8
1.25
1.4
1.6

MICROCOPY RESOLUTION TEST CHART
NATIONAL BUREAU OF STANDARDS
STANDARD REFERENCE MATERIAL 1010a
(ANSI and ISO TEST CHART No. 2)

NASA Conference Publication 3072

Earth Sciences Requirements for the Information Sciences Experiment System

(NASA-CP-3072) EARTH SCIENCES REQUIREMENTS FOR THE INFORMATION SCIENCES EXPERIMENT SYSTEM (NASA) 220 p CSCL 05B
N90-27140
--THRU--
N90-27161
Unclas
H1/43 0287622

Proceedings of a workshop held in
Williamsburg, Virginia
May 1-4, 1989

NASA

NASA Conference Publication 3072

Earth Sciences Requirements for the Information Sciences Experiment System

Edited by
D. E. Bowker
S. J. Katzberg
and R. G. Wilson
Langley Research Center
Hampton, Virginia

Proceedings of a workshop sponsored by
the National Aeronautics and Space
Administration and held in
Williamsburg, Virginia
May 1-4, 1989

NASA
National Aeronautics and
Space Administration
Office of Management
Scientific and Technical
Information Division
1990

PREFACE

This report contains the papers presented at a workshop sponsored by the NASA Langley Research Center and held in Williamsburg, Virginia, May 1-4, 1989. The purpose of the workshop was to further explore and define the Earth sciences requirements for the Information Sciences Experiment System (ISES), a proposed onboard data processor with real-time communications capability intended to support the Earth Observing System (Eos). A review of representative Eos instrument types is given, and a preliminary set of real-time data needs has been established. An executive summary is included.

PRECEDING PAGE BLANK NOT FILMED

CONTENTS

PREFACE iii

ATTENDEES vii

EXECUTIVE SUMMARY 1

INTRODUCTION 5
David E. Bowker

SPACE STATION ATTACHED PAYLOADS 7
Lenwood G. Clark

INFORMATION SCIENCES EXPERIMENT SYSTEM 21
Stephen J. Katzberg, Nicholas D. Murray, Harry F. Benz,
David E. Bowker, and Herbert D. Hendricks

BASIC DATA REQUIREMENTS FOR MICROWAVE RADIOMETER SYSTEMS 33
R. W. Lawrence

RADARS IN SPACE 45
Victor E. Delnore

LIDAR INSTRUMENTS PROPOSED FOR Eos 61
William B. Grant and Edward V. Browell

Eos VISIBLE IMAGERS 69
W. L. Barnes

SAGE III: A VISIBLE WAVELENGTH LIMB SOUNDER 83
W. P. Chu, M. P. McCormick, J. Zawodny,
and L. R. McMaster

DESCRIPTION OF SAFIRE FOR ISES 89
Jae H. Park

ERBE AND CERES BROADBAND SCANNING RADIOMETERS 91
William L. Weaver and John E. Cooper

TROPOSPHERIC SOUNDERS 105
H. A. Wallio

DATA ANALYSIS TECHNIQUES 115
Steve Park

ONBOARD PROCESSOR TECHNOLOGY REVIEW 123
Harry F. Benz

PRECEDING PAGE BLANK NOT FILMED

BRIEF STATE-OF-THE-ART REVIEW ON OPTICAL COMMUNICATIONS FOR THE NASA ISES WORKSHOP 131
Herbert D. Hendricks

APPLICATIONS OF ISES FOR GEOLOGY 139
David E. Bowker

APPLICATIONS OF ISES FOR THE ATMOSPHERIC SCIENCES 145
James M. Hoell, Jr.

APPLICATIONS OF ISES FOR THE OCEANS 159
W. E. Esaias

APPLICATIONS OF ISES FOR COASTAL ZONE STUDIES 165
D. S. Bartlett

APPLICATIONS OF ISES FOR VEGETATION AND LAND USE 169
R. Gale Wilson

APPLICATIONS OF ISES FOR SNOW, ICE, AND SEA STATE 189
Alfred T. C. Chang and Victor E. Delnore

APPLICATIONS OF ISES FOR METEOROLOGY 197
Paul D. Try

APPLICATIONS OF ISES FOR INSTRUMENT SCIENCE 213
William B. Grant

APPENDIX A. Eos INSTRUMENTS 217

APPENDIX B. Eos BASELINE PLANNING SCENARIO 221

APPENDIX C. Eos INSTRUMENT ACRONYMS 225

ATTENDEES

Name	Organization	Phone
Marc Allen	CTA, Inc.	873-2020
Bill Barnes	NASA Goddard, Code 625.0	88-888-8117
Dave Bartlett	NASA Langley, ASD-ASB	864-5850
Harry Benz	NASA Langley, ISD-IPTB	864-1493
David Bowker	NASA Langley, ISD-IPTB	864-1528
Al Chang	NASA Goddard, Code 624.0	88-888-8997
Bill Chu	NASA Langley, ASD-ARB	864-2675
Lenwood Clark	NASA Langley, SSO-Tech off.	864-6023
Vic Delnore	NASA Langley, PRC	864-1812
Wayne Esaias	NASA Goddard, Code 671.0	88-888-5465
Ed Foudriat	ODU	683-4255
Bill Grant	NASA Langley, ASD-CDB	864-5846
Paul Hayes	NASA Langley, ISD-IPTB	864-1491
Herb Hendricks	NASA Langley, ISD-IPTB	864-1536
Jim Hoell	NASA Langley, ASB-ASD	864-5826
Milt Holt	NASA Langley, ISD	864-1596
Syed Ismail	STX	864-2719
Steve Katzberg	NASA Langley, ISD-IPTB	864-1531
James Koziana	Space Tec Ventures, Inc.	865-0900
Wes Lawrence	NASA Langley, GCD-AMRB	864-1821
Karen Looney	NASA Langley, ISD-IPTB	864-1492
Nick Murray	NASA Langley, ISD-SAB	864-1712
Mike Neely	CTA, Inc.	873-2020
Charlie Nichols	NASA Langley, ISD-IPTB	864-1490
Jae Park	NASA Langley, ASD-CDB	864-5811
Steve Park	William and Mary	253-4545
Steve Ruggles	NASA Langley, ISD-IPTB	864-1514
Mark Shipham	NASA Langley, ASD-DMO	864-5618
Sonya Smith	CTA, Inc.	873-2020
Paul Try	STC	863-0012
Bill Weaver	NASA Langley, ASD-DMO	864-5606
Drew Wallio	NASA Langley, ASD-CDB	864-5366
Bobby Wills	NASA Langley, ISD-SAB	864-1710

ATTENDEES

Name	Organization	Phone
Gale Wilson	NASA Langley, ISD-IPTB	864-1530
Steve Young	NASA Langley, ISD-SAB	864-1709

EXECUTIVE SUMMARY

A Langley-sponsored workshop was held at the Holiday Inn, Williamsburg, VA, May 1-4, 1989, to develop a list of potential real-time Earth Observing System (Eos) experiments and pertinent algorithms essential for the design of the proposed Information Sciences Experiment System (ISES) onboard computational facility and to bring Eos sensor specialists together for a discussion of potential multiple sensor output products. The 35 invited attendees were limited to the Langley Research Center, Goddard Space Flight Center, and local contractor personnel. Results of the meeting are summarized below.

SOME GENERAL OBSERVATIONS TAKEN FROM MEETING

1) Remote-sensing operations using field sampling teams can generally benefit from real-time satellite data, including quick-look data for determination of satisfactory program support.

2) High-resolution channels (such as the 250-m channels on the Moderate Resolution Imaging Spectrometer (MODIS)) are very important for real-time operations, but do not need to be transmitted routinely.

3) During support for field experiments, the onboard computations may be intensive, but only need to be done over a restricted set of data and area.

4) ISES can provide benefits from direct access to the instrument outputs and not just the Local Area Network (LAN).

5) Individual scientist's experiences and interests have limited the real-time data needs various panels have established. This suggests that additional panel efforts will yield even more provocative real-time data needs.

STATE-OF-THE-ART (SOA) INFORMATION ANALYSIS

Virtually all techniques have been developed for and implemented on large mainframe-type computers. Therefore, the associated software (typically in FORTRAN) may not move easily into the ISES environment. That doesn't mean ISES can't perform SOA information extraction. With some clever algorithm development and the use of associated good programming techniques, ISES can support a significant amount of real- or near-real-time scientific computing.

SOA PROCESSING TECHNOLOGY

Two processor technologies (80C86 and 1802) are available with radiation-hardening and single-event-upset (SEU) tolerance. The near-term projection is for a ×10 increase in capability, e.g., using the Generic VHSIC Spaceborne Computer (GVSC). Memory technology, with a 1 × 4096 bit chip, is currently available, with a projection to a 1 × 256,000 bit chip. Auxiliary mass storage mag tapes (10^8 bits) are currently available with optical disks available soon with 10^{12} bits. Near-term processor specs are 40 kG, 300 W, and 25 Million Instructions Per Second (MIPS).

SOA LASER COMMUNICATIONS (Com)

Low Earth Orbit (LEO) to ground optical com with 100 Mbits has not yet flown but is well within the SOA, particularly with known ground stations and available ephemeris. LEO to Geosynchronous Earth Orbit (GEO) com are fundamentally acquisition and tracking limited, not laser limited. GEO to ground Advanced Communications Technology Satellite (ACTS) is a (currently) developed concept weighing approx. 100 kg. LEO to ground will weigh less than 75 kg.

INSTRUMENTS

Most instruments have a low data rate but their processing may not be very low. Some facility instruments have a very high rate. Look-ahead (approx. 8 min) is definitely possible with some instruments, e.g., MODIS T, limb sounders and limb emission instruments, for intra-orbit applications. Inter-orbit look-ahead will be possible with MODIS T and N, and other instruments with latitude dependence. ISES can provide additional benefits from access to instrument outputs, not just the LAN. Targets of opportunity are a possible major use for onboard processing, but require instruments that are operating though not necessarily transmitting to ground. A major concern is the availability of instrument parameters of sufficient accuracy for onboard processing.

PANEL HIGHLIGHTS

GEOLOGY, VOLCANOLOGY, AND EARTHQUAKES

A real-time need exists for detecting volcanic events early by searching for warning signs such as gases, hot spots, and smoke plumes. With the exception of rain- or snow-induced slides and major wind storms, most of the major dynamic geologic events involve only damage and impact assessments. High-resolution visible imaging is the most desirable data source for this, aided by the all-weather capability of Synthetic Aperture Radar (SAR).

ATMOSPHERIC SCIENCES

This panel primarily addressed tropospheric science programs with in situ sampling; opportunities in the stratosphere, mesosphere, and ionosphere remain to be assessed. Support for field experiments through simple feature maps from TRACER/MOPITT, Laser Atmospheric Wind Sounder (LAWS), high-resolution imagery, and tropospheric instruments was evoked. A general observation for the atmospheric sciences was that triggering events, such as CO_2 outfluxes and stratospheric heating, can be used to alert ground crews to begin field operations. This area offers considerable opportunity and will be the subject of more development.

OCEANS

Real-time data are needed to support field experiment strategy and target chasing. Laser com and oceanography are compatible (if you can't see the ocean surface, there is no need to communicate). Chlorophyll and temperature maps, and sea state and sea/ice interface maps are extremely important for support of both science field experiments and industrial applications and should be registered over the user's area of interest. However, omni-directional broadcasts of quick-look, low-resolution data are needed on a regular basis.

COASTAL ZONE

Support for coastal zone field experiments would benefit in similar ways as oceans; e.g., chlorophyll, temperature, and turbidity maps in real-time will identify and locate features for scientific field parties. Operational uses may include early warning and tracking of toxic algal blooms ("red tides"), which is a current National Oceanic and Atmospheric Administration (NOAA-NesDIS) activity relying on the Advanced Very High Resolution Radiometer (AVHRR). Low spatial resolution of most Eos sensors limits some coastal zone applications. Large concentrations of population and dynamic environments suggest many potential applications to be determined (TBD) for sediment/pollution tracking, thermal effluents, estuarine circulation, etc. All weather and high-resolution data from SAR would be extremely useful for storm damage, erosion, and snow/ice applications in the coastal zone.

VEGETATION, FORESTRY, AND LAND USE

This domain requires support for field experiments and crop management operations in areas such as disease, senescence, and pollution events. However, high spectral and spatial resolution of the High Resolution Imaging Spectrometer (HIRIS) instrument is required for scientific investigations. Real-time quick-look data would be useful as a supplement to NOAA/Landsat data. Transient events may be the major payoff in this area, such as biomass burning, flood damage, and assessment of crop drying hours.

SNOW, ICE, AND SEA STATE

Passive microwave instruments with low resolution and low data rates have simple computational requirements. With SAR and scatterometer data (which are more computationally intensive) a wide range of parameters are available. A real-time need was established for such items as hurricane wind fields at sea, ice/water interface, ice/leads ratio for input to meteorology programs, snow/rain ratio in storms, and snow melting rates for input to hydrology programs.

METEOROLOGY

There is a real-time need for identifying and tracking large storms and hurricanes. Microwaves can determine the wind field pattern which is not always concentric with the eye of a hurricane. The Lightning Detector output may relate to the amount of rainfall during a storm, and cloud height (temp.) is related to the maximum storm center. Mapping noctilucent clouds, high cirrus clouds, and cirrus clouds in real time is important during such events as Space Shuttle reentry, which is sensitive to atmospheric density. Also, cloud inventory is a general parameter needed for meteorology, navigation, and several other scientific applications.

INSTRUMENT SCIENCE

Examples where instrument cooperation would improve both output and performance are given for four areas:

1) The decision to acquire data because of some important occurrence detected by Eos instruments: e.g., detection of an SO_2 or aerosol plume suggesting a volcanic eruption, or the use of lightning strikes to study the generation of NO and other trace gases.

2) The decision not to acquire data: e.g., not operating lasers when optically dense clouds obscure the ground, thus increasing life of the instrument.

3) The decision to acquire additional data to improve data quality: e.g., increase the transmitted power level when low signal-to-noise ratios are found, such as with lidar or active microwave instruments.

4) The process of combining data from several sources to enhance data quality: e.g., when using MODIS data to generate chlorophyll maps, use ozone data from the Total Ozone Mapping System (TOMS) to correct for attenuation in the Chappuis band. When generating data sets that rely on in situ data for calibration, such as sea surface temperature, relay in situ data to the Eos platform for inclusion in the algorithm.

CONCLUSIONS

A significant number of applications were identified that needed onboard processing and real-time data transmission. They spanned the time range from continuous output, such as ocean chlorophyll and temperature maps, to selected area output, such as sea/ice interface and support for local remote-sensing experiments, and finally to rapid response to emergency events, such as large storms and earthquakes. An additional need was established for continuous search of instrument data for warning signs, such as volcanic gases and surface thermal events. With regard to continuing efforts in support of ISES, several items were identified:

1) There should be a thorough analysis made of each potential instrument to better understand it's capabilities and how it can interact with and support other instruments.

2) An Earth Sciences Workshop should be convened with a more varied panel of scientists and users to drive out an even more convincing list of real-time applications.

3) More thought should be given to the direct connection of some instrument output channels to ISES, such as the two 250-m resolution channels on MODIS N or one of the volcanic gas channels on an atmospheric instrument, which may not be part of the main data stream, but can be interrogated by ISES on a random basis.

INTRODUCTION

David E. Bowker

The Earth Observing System (Eos) satellites, as well as Space Station Freedom, will produce a vast amount of data, and this data deluge could make the ground processing time required to uncover an anomalous event unreasonably long. To avoid delay and to assist the user who would like to have access to some form of instrument output in near real time, the Information Sciences Experiment System (ISES) has been proposed. ISES is an onboard computer that will process data, generate geophysical products, and then direct-broadcast the output to the user. It is by design not to interfere with the normal operation of the satellite; i.e., it will send quick-look, early-warning, and convenient data to users on a timely basis with their full knowledge that a more thoroughly processed data product will be available at a later time, if desired.

Before the onboard processor architecture can be established, a list of potential processing algorithms and data rates must be defined. The purpose of this workshop is to take a preliminary look at the Earth sciences requirements for ISES; a parallel effort may focus on information sciences requirements at a later date. The first part of this report discusses the generic instrument types that may be included on Space Station Freedom and Eos. Following that discussion is a state-of- the-art (SOA) review of required technology, and finally a discussion of the real-time data needs in each of the major Earth science areas.

One of the major findings of this workshop is that there is a large number of applications in which real-time data are desired, beyond what has traditionally been called quick-look data. Each of the fields of Earth science can benefit from direct broadcast, with some needs more pressing than others. An executive summary highlights the results of the meeting.

N90-27141

SPACE STATION ATTACHED PAYLOADS

Lenwood G. Clark
NASA Langley Research Center
Hampton, Virginia

Before considering Space Station Freedom and its planned provisions for accommodating attached payloads, a brief discussion of the evolution of the space station is warranted.

The concept of the space station goes back at least to 1869 when Edward Everett Hale mentioned the "Brick Moon" in the Atlantic Monthly. As illustrated in Figure 1, Hale proposed a spherical space station made of bricks, 60 meters in diameter, that would have a crew of 37, and be located in a 6000-km orbit. The station was envisioned to serve as a navigation aid for ships: communications were to have been by Morse code, with signals created by the station's occupants jumping up and down on the station's exterior surface.

Although there were many other early concepts, serious thinking about actually building a space station began in the late 1940's and into the 1950's with many groups focusing on the practical uses of such a facility. With the 1960's devoted to the Apollo/Saturn program and the 1970's to developing a reusable space transportation system, the space station activity was relegated to the back burner.

When the first space shuttle flew in April 1981, once again the space station was considered the next logical step in manned space flight, and in 1984 the Reagan Administration committed the nation to the goal of developing a permanently manned space station. President Reagan also invited U.S. friends and allies to help with building the space station , thereby creating an international program involving the U.S. and some 15 other countries.

The space station configuration has evolved considering the various requirements of nearly 300 proposed payloads. Figure 2 illustrates the "ideal space station" with some of these user requirements superimposed on a space station configuration. Two things are evident from this figure, first some user requirements conflict with others, and secondly users generally want more than could be afforded. NASA has, however, used these user requirements to shape the space station into the current configuration which also reflects the impact of the Challenger accident as well as budget considerations.

The current space station configuration, shown in figure 3, represents the so-called revised baseline configuration. Eventually this configuration is supposed to grow into an enhanced version which is shown in figure 4. The evolution of the space station configuration will, however, greatly depend on the ultimate use envisioned for the station in the future.

PRECEDING PAGE BLANK NOT FILMED

The detailed design is under way with the U.S. and its international partners each working on their parts of the programs. Figure 5 shows the division of responsibilities between the various program participants. The U.S. part of the program has been divided into four work packages as follows:

WORK PACKAGE 1

The Marshall Space Flight Center (MSFC) and its contractor, Boeing Aerospace, will design and manufacture: the astronaut's living quarters - the Habitation Module; the U.S. Laboratory Module; the logistics elements; the resource node structures connecting the modules; the Environmental Control and Life Support System; and the Thermal Control and audio-video systems located within the pressurized modules. It also is responsible for the technical direction of the Work Package 2 contractor for the design and development of the engine elements of the propulsion system. In addition, MSFC is responsible for operations capability development associated with Freedom Station payload operations and planning.

WORK PACKAGE 2

The Johnson Space Center (JSC) and its prime contractor, McDonnell Douglas Astronautics Company, will manufacture: the integrated truss assembly; the propulsion assembly; the mobile transporter system; the outfitting of the resource node structures provided by Work Package 1; the Extravehicular Activity (EVA) system; the external Thermal Control system; the attachment systems for the Space Shuttle and experiments packages; the Guidance, Navigation and Control System; the Communications and Tracking System; the Data Management System; and the airlocks. It is also responsible for the technical direction of the Work Package 1 contractor for the design and development of all man systems. In addition, JSC is responsible for flight crews, crew training and crew emergency return definition, and for operation capability development associated with operations planning.

WORK PACKAGE 3

The Goddard Space Flight Center and its prime contractor, the Astro-Space Division of General Electric Company, will manufacture: the servicing facility, the flight telerobotic servicer, the accommodations for attached payloads, and the U.S. unmanned free-flyer platforms.

WORK PACKAGE 4

The Lewis Research Center and its prime contractor, the Rocketdyne Division of Rockwell International, will manufacture the electrical power systems.

The other countries involved in the space station program include Canada, Japan, and the 13 member countries of the European Space Agency. Canada plans to provide the Mobile Servicing Center which together with a U.S.-provided, rail-mounted, mobile transporter will play the main role in Space Station Freedom's assembly and maintenance, moving equipment and supplies around the station, releasing and capturing satellites, supporting EVA activities and servicing instruments and other payloads attached to the station. Japan plans to provide a multipurpose laboratory which consists of a pressurized module, an exposed facility for attached payloads, and an experiment logistics module. The European Space Agency plans to provide attached and free flying laboratories and an unmanned polar platform.

The program organization is shown in figure 6 and includes level I in NASA Headquarters being responsible for policy and overall program direction; level II, the Space Station Program Office in Reston, Virginia being responsible for program management and technical content; and level III, the various centers involved with the work packages. Included in level III is the Kennedy Space Center with responsibility for launch operations and the Langley Research Center with responsibility for the evolutionary definition of the space station.

The assembly sequence for the station is shown in figures 7 and 8. The assembly begins in 1995 and proceeds from manned-tended capability, to assembly complete capability in some 20 Space Transportation System (STS) flights over a 4-year period. This assembly sequence is continuously being revised as the configuration becomes more defined. There are 13 flights associated with the manned base, 2 outfitting flights, and 4 logistics flights. Congress has also included an extended duration orbiter flight to involve some early activity with attached payloads.

The station will provide a research laboratory in space with the ability to support all types of experiments as indicated in figure 9. The combination of pressurized laboratories, a structure for attached payloads, and unmanned platforms, together with the permanent presence of an interactive crew, will enhance a number of research disciplines. Each research discipline has unique requirements that are satisfied by the station. Life sciences, for example, involves activity inside the pressurized laboratories with continuous crew interaction. Materials processing also requires use of the pressurized laboratories together with high power and low gravity. Earth sciences research is more focused toward the attached payload activity with minimum contamination to instrument visibility. Potential Earth sciences research on the space station is summarized in figure 10 and includes research on geodynamics, land processes, oceanography, and atmospheric dynamics and radiation.

Potential attached payload locations on the space station structure are shown in figure 11 where the Earth-viewing direction is towards the bottom of the figure. There are a number of locations for attached payloads and depending on the class of payload, different payload accommodation requirements which must be provided by the station as shown in figure 12. Major attached payloads, for example, may require active thermal cooling and provisions for pointing by means of a station-provided payload pointing system. Attached payloads could even be as small as distributed sensors in non-standard locations with modest needs for power and data management.

For accommodating attached payloads the space station has attached payload accommodations equipment as shown in figures 13 and 14. This equipment is designed to support payloads that weigh up to 25,000 lbs and provides for power, data management, and active cooling. The multiple payload/deck carrier is designed to accommodate multiple payloads, major payloads, and payloads which require pointing capability. The payload pointing system planned for the station is shown in figure 15 and is designed for 3 axes pointing with provisions for power, active cooling, data management, and payload sensor input for pointing.

To completely cover the station's attached payload capability, additional reference should be made to the Japanese Experiment Module pictured in figure 16. This module has an exposed facility for accommodation of attached payloads. Some of the activity planned on the exposed facility, such as exchange of experimental equipment and construction of large structures in space will require frequent crew access. However, by using a local manipulator and an experiment airlock, both operated within the pressurized module, this access can partially be accomplished while minimizing extravehicular activity.

The station will also be designed to accommodate so-called small and rapid response payloads as indicated in figures 17 and 18. Small and rapid response payloads include trunnion/keel small payloads, genic small payloads and small payloads proposed to be located on the Japanese exposed facility. These types of attached payloads do not require the previously mentioned attached Payload Accommodations Equipment, but include provisions for power, thermal control, and data management.

An important concern for attached payloads is payload visibility. With large panels associated with the station's photovoltic power system and with radiators for heat rejection, etc., the visibility of attached payloads varies greatly depending on payload location. Figure 19 shows some of the viewing restrictions for both space-viewing and Earth-viewing payloads. For Earth-viewing payloads on the lower surface of the station structure the field-of-view varies from 55 to 75 degrees depending on payload location outboard or inboard of the radiator panels.

In summary, the Space Station Freedom is being designed and developed with user requirements being used to shape the configuration. Plans include accommodation provisions for a wide variety of attached payloads including the Earth sciences research activities which are the focus of this conference. The station program is even beginning some preliminary payload manifesting which involves planning for accommodation of payload during the station's assembly flights. Potential payload organizations should be aware of the station's plans for payload accommodations so as to guide their own payload activities for future space station use.

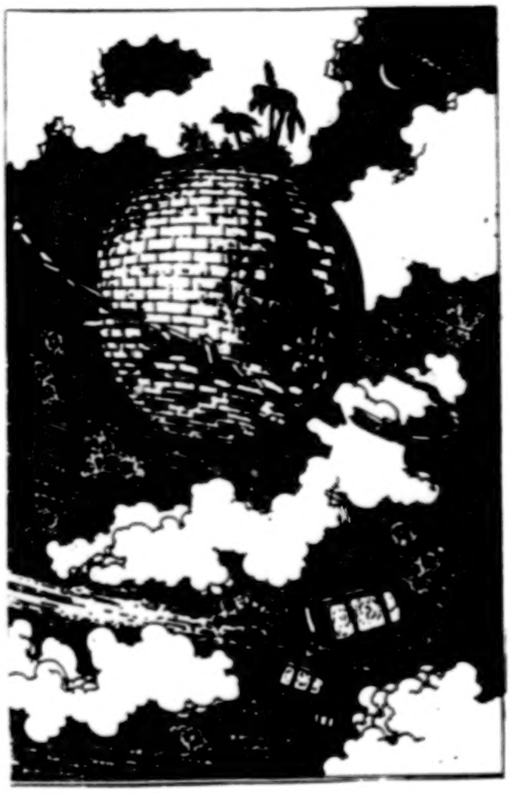

Figure 1: Space Station Concept From 1869 Atlantic Monthly

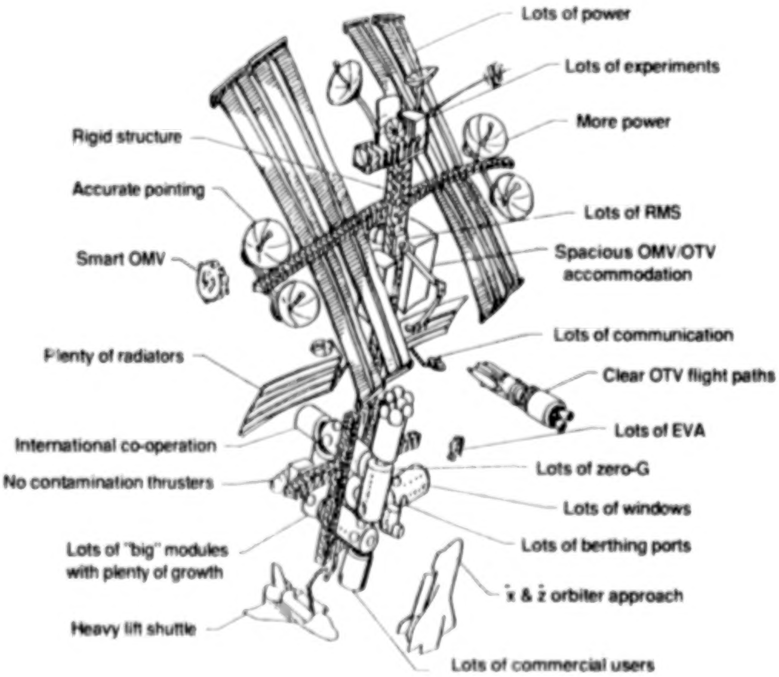
Lots of power
Lots of experiments
More power
Rigid structure
Accurate pointing
Lots of RMS
Spacious OMV/OTV accommodation
Smart OMV
Lots of communication
Plenty of radiators
Clear OTV flight paths
Lots of EVA
International co-operation
Lots of zero-G
No contamination thrusters
Lots of windows
Lots of berthing ports
Lots of "big" modules with plenty of growth
ẋ & ż orbiter approach
Heavy lift shuttle
Lots of commercial users

Figure 2: The Ideal Space Station

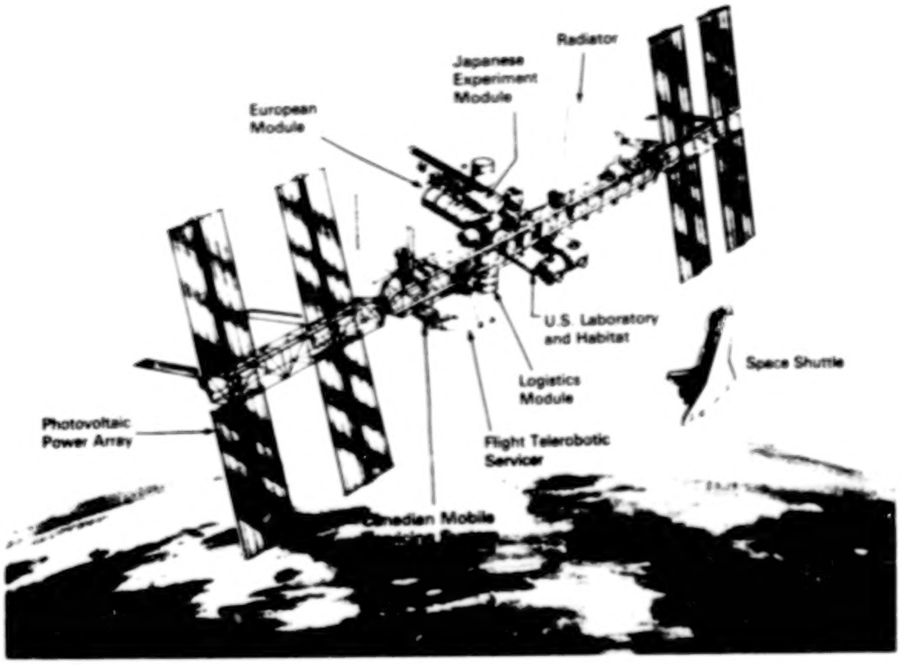
Radiator
Japanese Experiment Module
European Module
U.S. Laboratory and Habitat
Space Shuttle
Logistics Module
Photovoltaic Power Array
Flight Telerobotic Servicer
Canadian Mobile

Figure 3: Revised Baseline Configuration

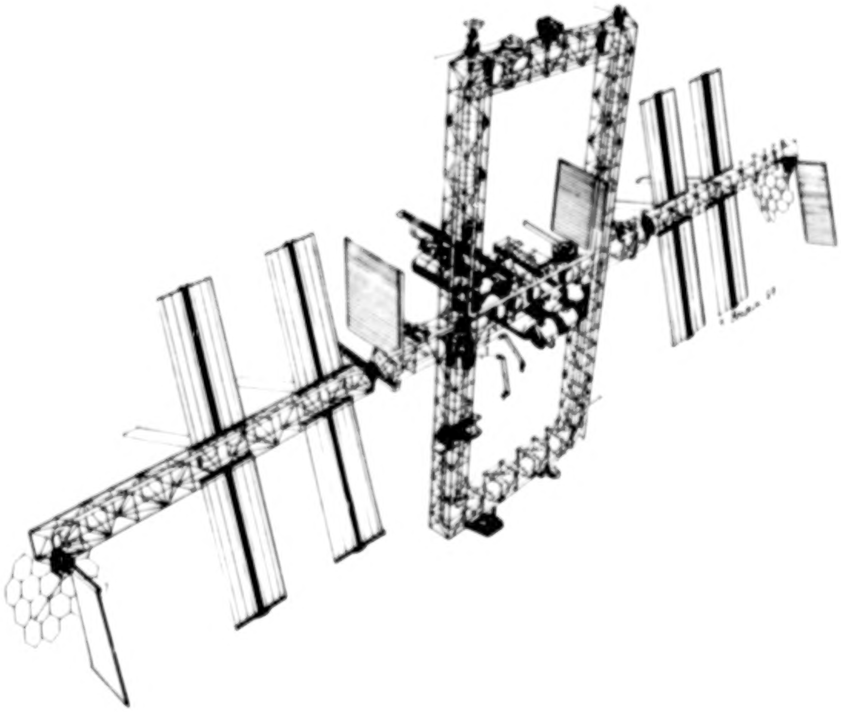

Figure 4: Evolutionary Growth Option

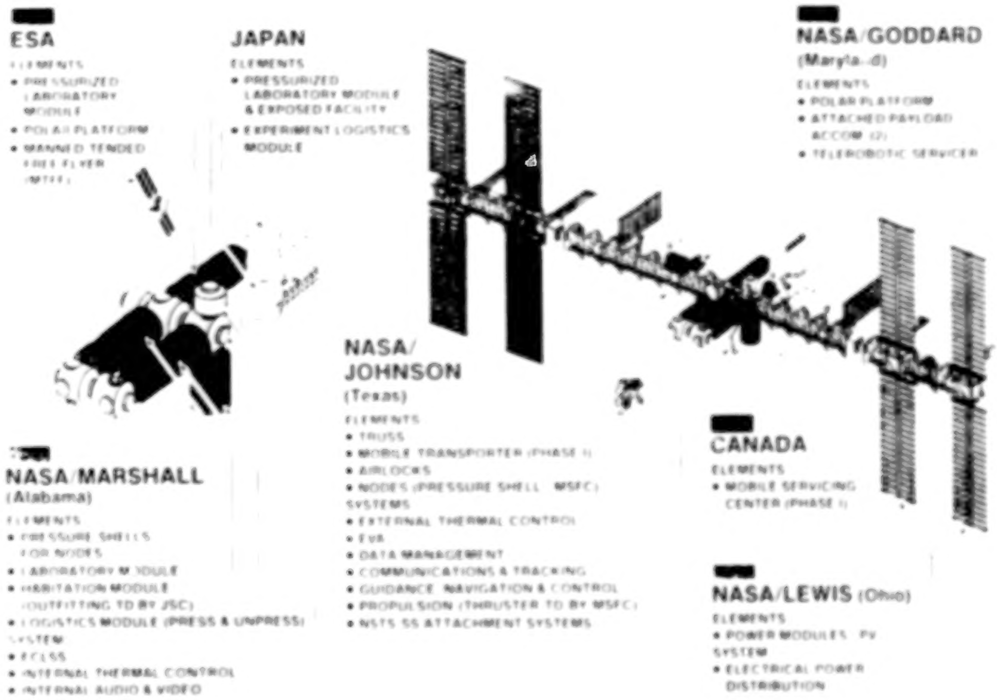
ESA
ELEMENTS
• PRESSURIZED LABORATORY MODULE
• POLAR PLATFORM
• MANNED TENDED FREE FLYER (MTFF)
JAPAN
ELEMENTS
• PRESSURIZED LABORATORY MODULE & EXPOSED FACILITY
• EXPERIMENT LOGISTICS MODULE
NASA/GODDARD
(Maryland)
ELEMENTS
• POLAR PLATFORM
• ATTACHED PAYLOAD ACCOM (2)
• TELEROBOTIC SERVICER
NASA/JOHNSON
(Texas)
ELEMENTS
• TRUSS
• MOBILE TRANSPORTER (PHASE I)
• AIRLOCKS
• NODES (PRESSURE SHELL - MSFC)
SYSTEMS
• EXTERNAL THERMAL CONTROL
• EVA
• DATA MANAGEMENT
• COMMUNICATIONS & TRACKING
• GUIDANCE, NAVIGATION & CONTROL
• PROPULSION (THRUSTER TD BY MSFC)
• NSTS SS ATTACHMENT SYSTEMS
CANADA
ELEMENTS
• MOBILE SERVICING CENTER (PHASE I)
NASA/MARSHALL
(Alabama)
ELEMENTS
• PRESSURE SHELLS FOR NODES
• LABORATORY MODULE
• HABITATION MODULE (OUTFITTING TD BY JSC)
• LOGISTICS MODULE (PRESS & UNPRESS)
SYSTEM
• ECLSS
• INTERNAL THERMAL CONTROL
• INTERNAL AUDIO & VIDEO
NASA/LEWIS (Ohio)
ELEMENTS
• POWER MODULES - PV
SYSTEM
• ELECTRICAL POWER DISTRIBUTION

Figure 5: Space Station Freedom Elements and Responsibilities

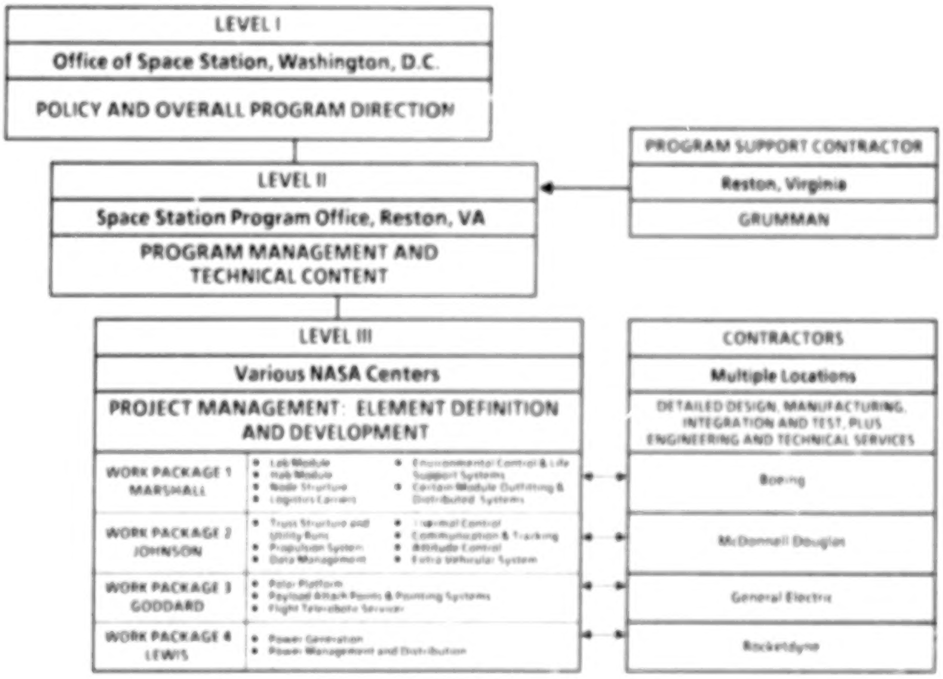
LEVEL I
Office of Space Station, Washington, D.C.
POLICY AND OVERALL PROGRAM DIRECTION
PROGRAM SUPPORT CONTRACTOR
Reston, Virginia
GRUMMAN
LEVEL II
Space Station Program Office, Reston, VA
PROGRAM MANAGEMENT AND TECHNICAL CONTENT
LEVEL III
Various NASA Centers
PROJECT MANAGEMENT: ELEMENT DEFINITION AND DEVELOPMENT
CONTRACTORS
Multiple Locations
DETAILED DESIGN, MANUFACTURING, INTEGRATION AND TEST, PLUS ENGINEERING AND TECHNICAL SERVICES
WORK PACKAGE 1 MARSHALL
• Lab Module
• Hab Module
• Node Structure
• Logistics Carriers
• Environmental Control & Life Support Systems
• Certain Module Outfitting & Distributed Systems
Boeing
WORK PACKAGE 2 JOHNSON
• Truss Structure and Utility Runs
• Propulsion System
• Data Management
• Thermal Control
• Communication & Tracking
• Attitude Control
• Extra Vehicular System
McDonnell Douglas
WORK PACKAGE 3 GODDARD
• Polar Platform
• Payload Attach Points & Pointing Systems
• Flight Telerobotic Servicer
General Electric
WORK PACKAGE 4 LEWIS
• Power Generation
• Power Management and Distribution
Rocketdyne

Figure 6: NASA Space Station Freedom Program Organization

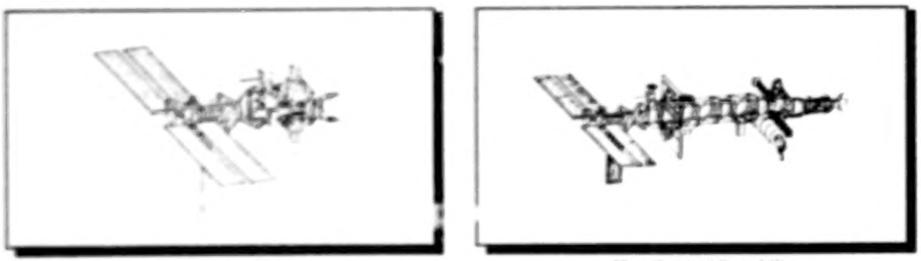

First Element Launch

Man-Tended Capability

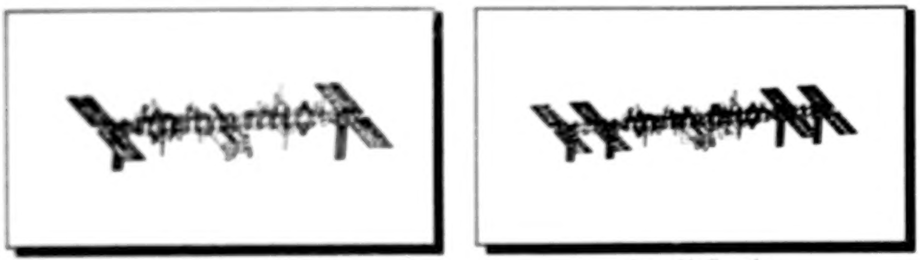

Permanently Manned Capability

Assembly Complete

Figure 7: Assembly Sequence Capability Build-Up

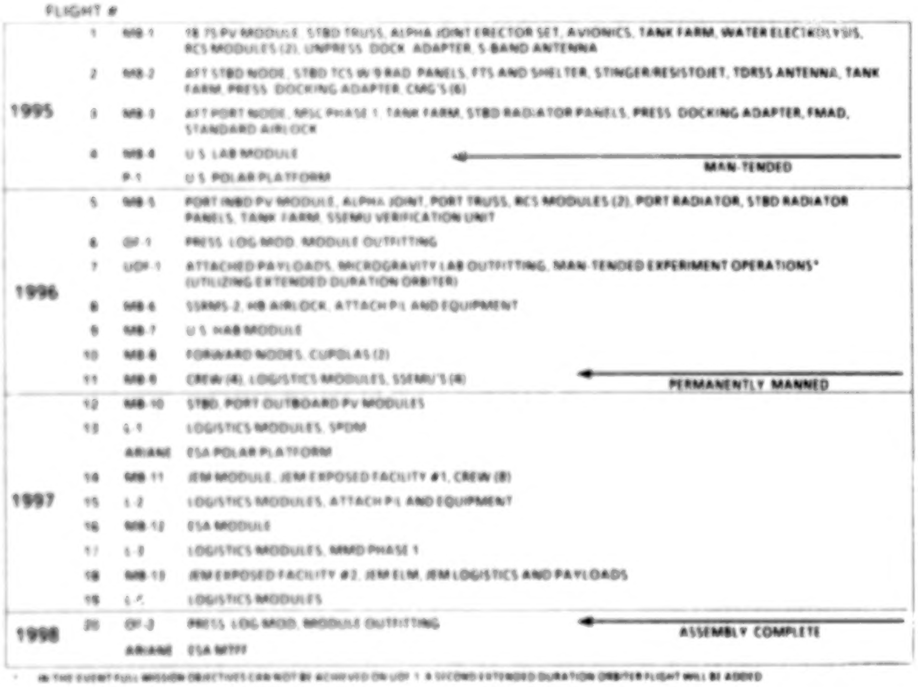

	FLIGHT #			
1995	1	MB-1	18.75 PV MODULE, STBD TRUSS, ALPHA JOINT ERECTOR SET, AVIONICS, TANK FARM, WATER ELECTROLYSIS, RCS MODULES (2), UNPRESS. DOCK. ADAPTER, S-BAND ANTENNA	
	2	MB-2	AFT STBD NODE, STBD TCS W/9 RAD. PANELS, FTS AND SHELTER, STINGER/RESISTOJET, TDRSS ANTENNA, TANK FARM, PRESS. DOCKING ADAPTER, CMG'S (6)	
	3	MB-3	AFT PORT NODE, MSC PHASE 1, TANK FARM, STBD RADIATOR PANELS, PRESS. DOCKING ADAPTER, FMAD, STANDARD AIRLOCK	
	4	MB-4	U.S. LAB MODULE	← MAN-TENDED
		P-1	U.S. POLAR PLATFORM	
1996	5	MB-5	PORT INBD PV MODULE, ALPHA JOINT, PORT TRUSS, RCS MODULES (2), PORT RADIATOR, STBD RADIATOR PANELS, TANK FARM, SSEMU VERIFICATION UNIT	
	6	OF-1	PRESS. LOG MOD. MODULE OUTFITTING	
	7	UDF-1	ATTACHED PAYLOADS, MICROGRAVITY LAB OUTFITTING, MAN-TENDED EXPERIMENT OPERATIONS* (UTILIZING EXTENDED DURATION ORBITER)	
	8	MB-6	SSRMS-2, HB AIRLOCK, ATTACH P/L AND EQUIPMENT	
	9	MB-7	U.S. HAB MODULE	
	10	MB-8	FORWARD NODES, CUPOLAS (2)	
	11	MB-9	CREW (4), LOGISTICS MODULES, SSEMU'S (4)	← PERMANENTLY MANNED
1997	12	MB-10	STBD, PORT OUTBOARD PV MODULES	
	13	L-1	LOGISTICS MODULES, SPDM	
		ARIANE	ESA POLAR PLATFORM	
	14	MB-11	JEM MODULE, JEM EXPOSED FACILITY #1, CREW (8)	
	15	L-2	LOGISTICS MODULES, ATTACH P/L AND EQUIPMENT	
	16	MB-12	ESA MODULE	
	17	L-3	LOGISTICS MODULES, MMD PHASE 1	
	18	MB-13	JEM EXPOSED FACILITY #2, JEM ELM, JEM LOGISTICS AND PAYLOADS	
	19	L-4	LOGISTICS MODULES	
1998	20	OF-2	PRESS. LOG MOD. MODULE OUTFITTING	← ASSEMBLY COMPLETE
		ARIANE	ESA MTFF	

* IN THE EVENT FULL MISSION OBJECTIVES CAN NOT BE ACHIEVED ON UDF-1 A SECOND EXTENDED DURATION ORBITER FLIGHT WILL BE ADDED

Figure 8: Assembly Sequence Flights

STATION ELEMENTS

- Pressurized laboratories
- Structures for attached payloads
- Unmanned platforms

STATION ATTRIBUTES

- Permanent presence
- Interactive crew
- Repetitive access
- High level of power
- Gravity force nearly zero

DISCIPLINES ENHANCED

- Life sciences
- Materials processing
- Astrophysics
- Earth sciences
- Technology

Figure 9: Space Station Capability as a Research Laboratory

GOAL: To investigate the Earth as a system, from its interior through the inner magnetospheric boundary.

- **GEODYNAMICS**
  - Crustal Dynamics
  - Gravitational and Magnetic Fields
- **LAND PROCESSES**
  - Terrestrial Ecosystems
  - Hydrology
  - Geology
  - Remote Sensing
- **OCEANOGRAPHY**
  - Ocean Topography
  - Ice Formations
- **ATMOSPHERIC DYNAMICS AND RADIATION**
  - Global Climate Studies
  - Meteorology
  - Aerology

Figure 10: Earth Sciences Research on Space Station

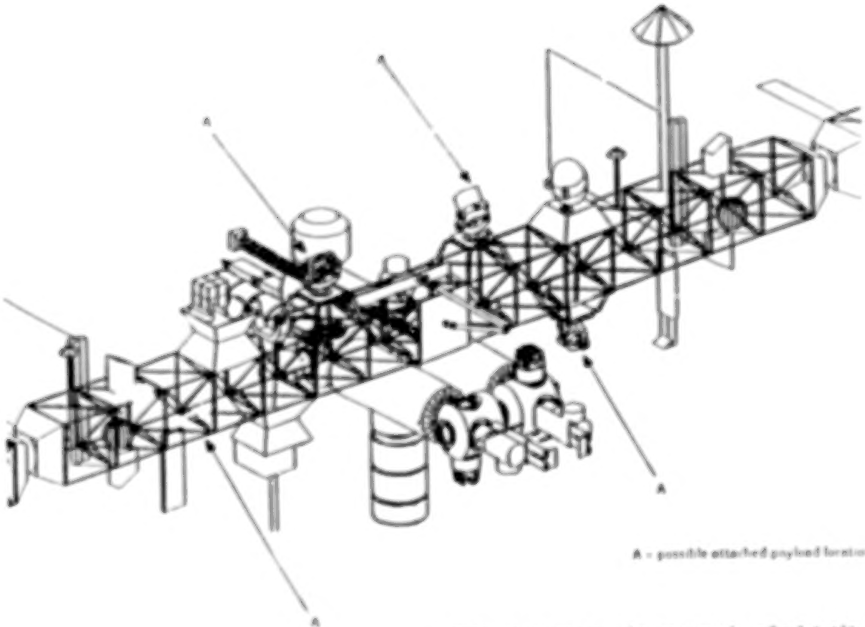

A = possible attached payload locations

NOTE Could utilize more than one truss cube surface but utility port provided resources would have to be shared

Figure 11: Potential Attached Payload Locations

PAYLOAD CLASSIFICATION

CLASS	PAYLOAD FEATURES
MAJOR	• LARGE • REQUIRES MAJOR APAE RESOURCES • ACTIVE THERMAL COOLING • SOME NEED PPS FOR POINTING • LONG STAY
SMALL AND/OR RAPID RESPONSE	• SMALL • NO ACTIVE THERMAL COOLING • MODEST POWER/DATA RESOURCES • VARIETY OF FIELDS OF VIEW • SET ASIDE RESOURCES
DISTRIBUTED SENSOR	• CAN BE VERY SMALL IN SIZE (LIKE ACCELEROMETER) • NON-STANDARD LOCATIONS • MODEST POWER/DATA RESOURCES • CAN BE ANALYTICALLY INTENSIVE • CAN HAVE UNIQUE PACKAGING

Figure 12: Manned Base Attached Payload Accommodations

MANNED BASE ATTACHED PAYLOAD ACCOMMODATIONS

APAE DESIGN CAPABILITY

DESIGNED FOR:

MULTIPLE PAYLOADS **MAJOR** **POINTING PAYLOADS**

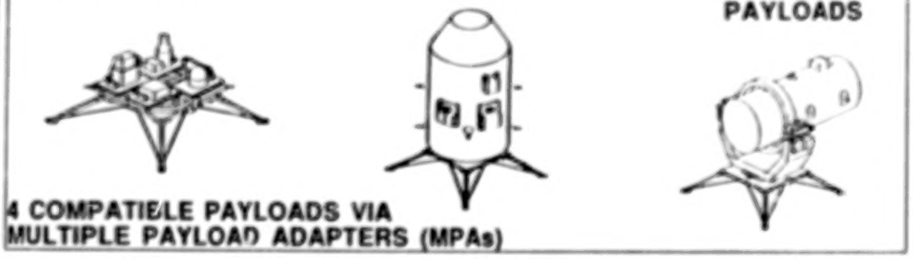

4 COMPATIBLE PAYLOADS VIA MULTIPLE PAYLOAD ADAPTERS (MPAs)

- **APAE DESIGNED TO SUPPORT UP TO 25,000 LB PAYLOAD**
- **PROVIDES: 10kW POWER**
  50 MBPS DATA RATE } **PAYLOAD(S)**
  10 kW ACTIVE COOLING
- **STRUCTURAL SUPPORT FOR POINTING CAPABILITY (60 ARC SEC ACCURACY) FOR 6000 kg PAYLOAD**

Figure 13: Attached Payload Accommodation Equipment (APAE) Design Capability

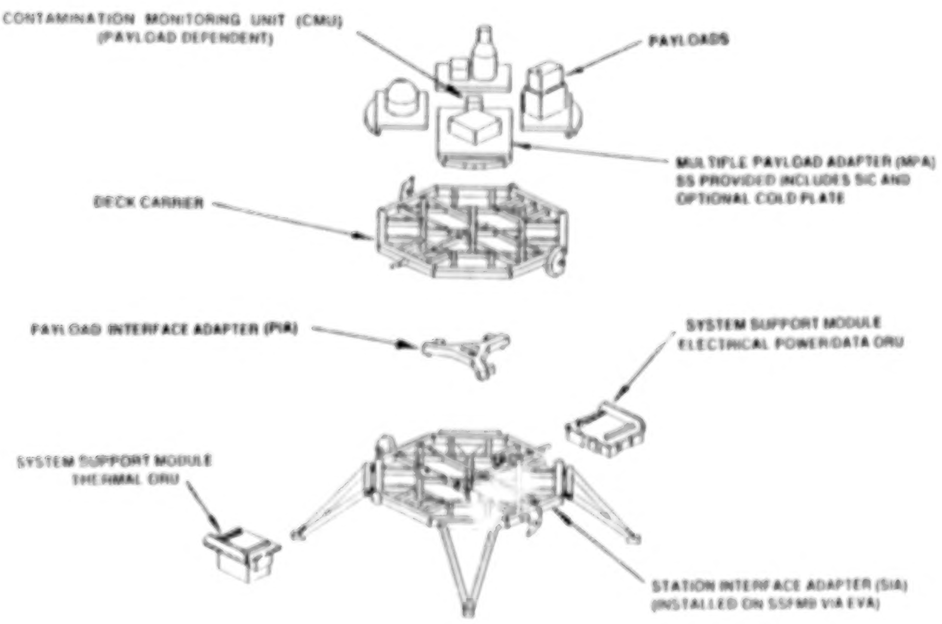
CONTAMINATION MONITORING UNIT (CMU)
(PAYLOAD DEPENDENT)
PAYLOADS
MULTIPLE PAYLOAD ADAPTER (MPA)
SS PROVIDED INCLUDES SIC AND
OPTIONAL COLD PLATE
DECK CARRIER
PAYLOAD INTERFACE ADAPTER (PIA)
SYSTEM SUPPORT MODULE
ELECTRICAL POWER/DATA ORU
SYSTEM SUPPORT MODULE
THERMAL ORU
STATION INTERFACE ADAPTER (SIA)
(INSTALLED ON SSFMB VIA EVA)

Figure 14: Multiple Payload/Deck Carrier Configuration

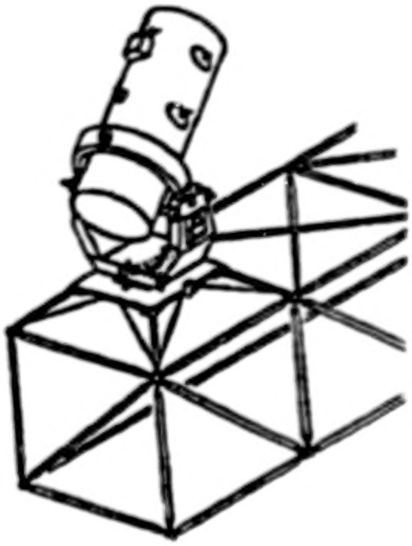

- 1 ARC MINUTE POINTING ACCURACY
- 30 ARC SECOND POINTING STABILITY (OVER 1800 SECS)
- 15 ARC SECOND/SECOND JITTER
- 3 AXES
- 5 kW OF POWER/ACTIVE COOLING
- 50 MEGABITS HIGH RATE DATA/IMAGERY
- 6000 kG PAYLOAD - 3 METERS WIDE, C.G. TO BASE 2.5 METERS
- ACCEPTS PAYLOAD SENSOR INPUT FOR POINTING

Figure 15: Payload Pointing System (PPS)

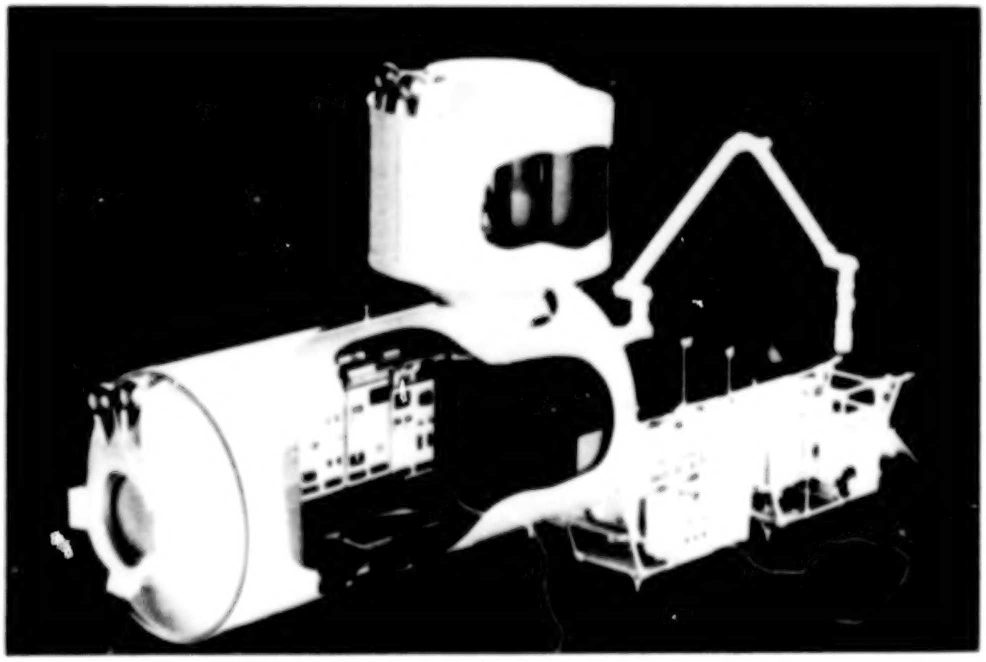

Figure 16: Japanese Experiment Module

ORIGINAL PAGE
BLACK AND WHITE PHOTOGRAPH

EXTERNAL SARR PAYLOAD ENVELOPE & PROPOSED CONSTRAINTS

TRUNNION/KEEL (T/K) SARR PAYLOAD:

FIT INTO 4M X 1.25M X 2M ENVELOPE (MAX VOL < 10 M3)

- ≤ 900 kG
- ≤ 900 WATTS
- ≤ 0.3 MBPS UPLINK/2.0 MBPS DOWNLINK
- ≤ 100 MB DATA STORAGE/ORBIT

CAN ACCOMMODATE MORE THAN ONE PAYLOAD

RMS GRAPPLE FIXTURE (ON T/K CARRIER)

GENERIC (GEN) SARR PAYLOAD:

FIT INTO 1.25 M X 1.25 M X 1.25 M ENVELOPE (MAX VOL ≤ 2 M3)

- ≤ 300 kG
- ≤ 300 WATTS
- ≤ 0.3 MBPS UPLINK/2.0 MBPS DOWNLINK
- ≤ 100 MB DATA STORAGE/ORBIT

ORU COMPATIBLE I/F (ORU TOOL)

Figure 17: Small and Rapid Response Payloads

INTERFACE COMPARISON CHART FOR RELATIVELY SMALL ATTACHED PAYLOADS* ON TRUSS AND JEM EF (PROPOSED)

Interface or Physical Constraint	PAYLOAD		
	SARR Trunnion Keel	SARR Generic	JEM Exposed Facility
Weight	≤ 1980 lbs ≤ 900 kg	≤ 660 lbs ≤ 300 kg	typically 1100 lbs or 500 KG
Volume Limitations Physical Dimensions	~ 10m3 1.25m x 2.0m x 4.0m	~ 2m3 1.25m x 1.25m x 1.25m	~ 2m3 0.8m x 1.0m x 1.85m (0.8m x 1.0m footprint)
Thermal Cooling	only passive	only passive	≤ 6kW active cooling
Power Constraint	≤1.5kW	≤0.3kW	≤6.0kW
Data Rates Downlink Uplink	 2.0 Mbps 0.3 Mbps	 1.4 Mbps 0.3 Mbps	 4 Mbps 4 Mbps
Access to Pressurized Module	None	None	Possible thru JEM Airlock
Pointing Capability Provided	None	None	None

* These do not require an APAE

Figure 18: Small and Rapid Response Payloads Interface Comparison

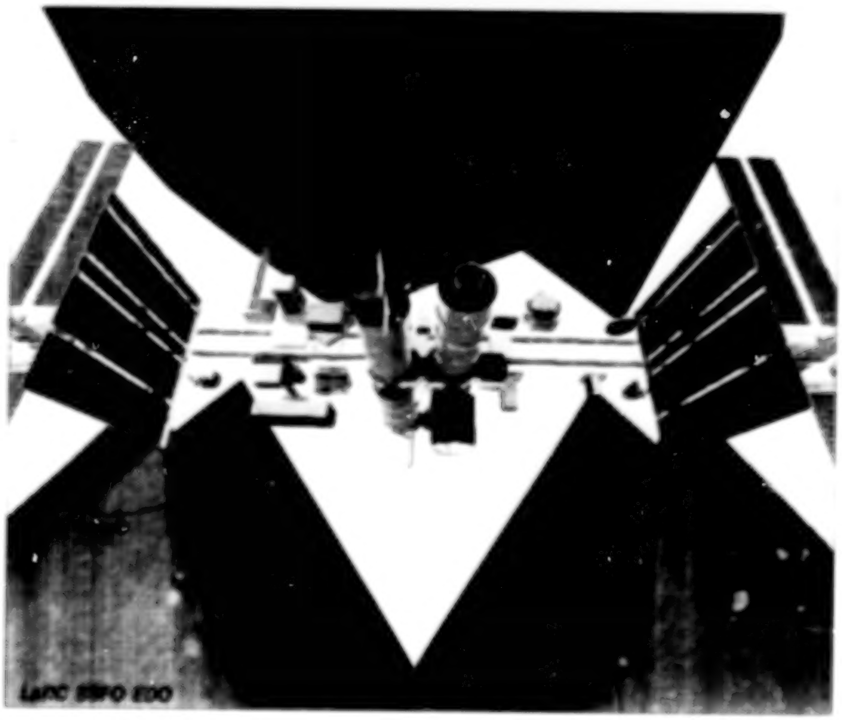
LaRC 89PO 800

Figure 19: Maximum Unobstructed Symmetric Fields of View

N90-27142

INFORMATION SCIENCES EXPERIMENT SYSTEM

Stephen J. Katzberg, Nicholas D. Murray, Harry F. Benz,
David E. Bowker, and Herbert D. Hendricks
NASA Langley Research Center
Hampton, Virginia

Abstract

The rapid expansion of remote sensing capability over the last two decades will take another major leap forward with the advent of the Earth Observing System (Eos). An approach is presented in this paper that will permit experiments and demonstrations in onboard information extraction. The approach is a non-intrusive, eavesdropping mode in which a small amount of spacecraft "real estate" is allocated to an onboard computation resource. This paper discusses how such an approach allows the evaluation of advanced technology in the space environment, advanced techniques in information extraction for both Earth science and information science studies, direct to user data products, and real-time response to events, all without affecting other onboard instrumentation.

Introduction

The United States Space Program is about to undertake its most ambitious effort yet in remote sensing of the Earth's environment. The centerpiece of this activity is the Earth Observing System (Eos) which is a joint endeavor of NASA's Space Station Program and NASA's Office of Space Science and Applications. As the Space Station "Freedom" is a major step forward for the United States in space infrastructure, the Eos will be a major step forward for the United States in environmental monitoring.

Since the Space Station Constellation (Core Station and Polar Platform) is planned to be of very long life and use, it is important to ensure that its capability has provision for growth. Capability growth can come from a variety of sources, not the least of which is the application of new technologies and techniques as time goes on. Unfortunately, space flight systems rarely have provision for excess capacity (data, weight, power, etc.) to permit accommodation of additional functions.

Without the opportunity to evaluate potential technologies and techniques in space, the necessary "confidence-building" to convince program managers and project engineers to use new technologies or techniques is lacking. A "Catch 22" ensues in which new approaches are proposed to be tried in the space environment, but are rejected for use because they don't have the requisite space flight experience. New technology is rarely used because it is not mature; and by the time it gets mature, it is no longer new. On the other hand, the need for more rapid application of new technologies is never more apparent than in the Eos. The Eos is in many respects the continuation of a long line of remote-sensing systems which have provided far more data than can sensibly be absorbed. The historical "data glut problem" is very much in evidence in the Eos. One instrument, called the High Resolution Imaging Spectrometer (HIRIS), has an anticipated internal data rate nearly twice the capacity of the data relay satellites sent to the ground.

This paper provides some background on the Eos and discusses the "data glut problem" particularly concerning Eos. A systems approach is presented, allied with Eos objectives, that addresses some important issues related to space remote-sensing systems capability. This system, called the Information Sciences Experiment System (ISES) has as its objective onboard information extraction for use either directly to the ground or on-board. This paper also shows how the Eos offers a unique opportunity to apply this new approach, and how the ISES can effectively address (1) the insertion and evaluation of new technology and techniques for space use without adversely impacting overall system performance, (2) the "data glut problem", (3) the increase of the onboard use of assets, (4) the use of real-time response to events, and (5) the provision of direct-to-user data products. Finally, some comments related to the applicability of the ISES approach to the Core Space Station are made.

The Earth Observing System (Eos)

The Eos is, in part, an outgrowth of early Space Station Program thinking, where both equatorial and polar orbiting spacecraft were contemplated to be derived from the same flight hardware. The polar orbit was important to supplement the near equatorial orbit of the manned space station supporting science applications. Only through high orbital inclination can complete global coverage be obtained from a low-Earth orbit. Independently, but contemporaneously, NASA's Office of Space Science and Applications had begun studies to determine what the next step should be in remote sensing of the environment. The result of these studies pointed to a need to look at the Earth from a unified perspective recognizing the interdependence of the processes shaping our environment.

The details of the scientific rationale for what first became "System Z" and then the Eos can be found in Reference 1, and will not be discussed here. The current state of the Eos concept is, in fact, one with a wide variety of remote sensors that look up, look down, back, and sideways, detecting radiation from very high energies to very long wavelength phenomena. Magnetometers are included as are electric field meters. Environmental targets include crops, water resources, atmospheric chemistry, ice, oceanic processes, lightning, air glow, and so on. Again, the interested reader is directed to Reference 1. What is of interest are the results of the Science and Mission Requirements Working Group (SM&RWG), which give the requirements that must be met to realize a practical system to enable a unified approach to Earth studies. Of the five recommendations, two specifically address the data and information aspects in an implementation strategy (Reference 1).

Within the current Eos concept is an extensive ground data network with considerable resources and capabilities to receive, preprocess, store, distribute, and exchange data sets. A schematic of this concept is illustrated in Figure 1 (and abstracted from Reference 2), which shows a very simplified ground and flight data system. When one looks for the equivalent access to data systems resources in the flight element, one is struck by its relative absence.

The lack of onboard computational capability is remarkable when it is realized that of the three types of experimenters participating in Eos, one is "Multidisciplinary Investigators." The Eos, proposed as enabling a unified approach to Earth studies, has no real provision for addressing that goal on the spaceflight vehicle itself. The reason for this situation lies in the dichotomy of the Eos and the spacecraft on which it flies. The Eos is a system of remote-sensing instruments and outlines an approach to Earth studies that is hosted on a spacecraft developed as part of the Space Station Program. Eos and the polar platform on which it flies are separate and distinct.

The Space Station Program as the host generally supplies certain basic services to its users and customers such as power, thermal rejection, spacecraft ephemeris, time code, communication, and other housekeeping information. Because of the extreme diversity of potential users, the complexity and attendant cost of providing general computational services was not deemed to be protected. If a user has a need for special services, it is that user's responsibility to provide those services and bear the cost.

On-Orbit Data Processing and Eos

NASA has been well aware of the problem posed by remote sensors, particularly high volume/high data rate systems. The earliest weather satellites and Earth resources satellites were already creating considerable archives of data in the late 1960's and early 1970's. A typical early example was the Multispectral Scanner (MSS) of the Landsat spacecraft, which was a four-band imager. The data rate for this instrument was 15 MBits/second. At that time, a typical 1,200-foot reel of 800 bpi magnetic tape held about 108 bits. Archiving data from the MSS would fill a reel of such tape every 7 seconds.

The situation just described has remained in an uneasy equilibrium in the ensuing years. New data processing and data storage technology have come on the scene, to be pressed even harder by new high volume, high data rate remote sensors. A somewhat arbitrary but still reasonably accurate illustration of the historical trends is shown in Figure 2. The growth in Data Processing Technology and Data Storage Technology is compared to demands from spaceborne remote sensors. It is arguable that even with the very impressive strides made in data systems technology, sensor systems continue to overwhelm the systems required to work with them.

Included in the figure is a point to represent the Eos. Most of the Eos data is generated from a handful of instruments such as HIRIS, Moderate Resolution Imaging Spectrometer (MODIS), and Synthetic Aperture Radar (SAR). It is also true that these are very powerful instruments with a phenomenal number of spectral channels or ground resolution. It is hard to imagine any further development on these sensor concepts. However, the upper limit is nowhere near reaching its fullest development.

A rough calculation of the ultimate data rate and data volume potential shows something of the top end. Assuming a Landsat or Eos orbital altitude of 800 km with a ground track speed of 6.5 km/second, and an imager with a 1-m diameter mirror operating at 1 micrometer wavelength, one can arrive at the possible data rate. For assurance of complete access to any point on the Earth, the field of coverage would be 1,700 km per orbit. A 1-m mirror at 1 micrometer has a diffraction limit at 800 km of about 1 m, assuming there are two-to-one overlapped ground sampling 2×10^{10} samples per second per spectral channel. For 10-bit encoding and for the 100 or so channels of an Eos MODIS instrument, a final figure of 2×10^{13} bps is produced.

It should also be noted that geostationary platforms would offer some improvement, but not much. Assume that the 1-micrometer resolution is held at the 40,000-km range of a geostationary platform, and assume that one complete scan every hour would still be close to 10^{11} bits/second. As mentioned earlier, NASA was and has been well aware of the developing "data glut problem" and has moved to address it. The result was the NASA End-to-End Data Management System (NEEDS) program which started in the mid 1970's. The NEEDS Program had as an objective of 1,000 to 1 improvement in the rate of conversion of data to information (Reference 3). The NEEDS Program had various elements, but was divided into a ground element and a flight element. It is fair to say that the objective of improving the information extraction rate by three orders of magnitude was not achieved, and that the greatest disappointment in the NEEDS was in the flight element. No hardware developed for the flight element has been included on a NASA spacecraft. The irony is that some rather capable hardware was developed for the flight element. Flight upgradable hardware was produced which was fast enough to do step-wise linear corrections to sensor nonlinearities, provide gain and offset correction, and do real-time cloud editing. Geometric resampling was also close to being realized at real-time rates.

The reason that the NEEDS flight hardware was never flown can be ascribed to a variety of reasons, but three are of interest here. First, the objectives of moving very simple processing functions to orbit were not really cost effective. Second, the hardware was demonstrated on the ground with no "confidence building" space flight experiment to demonstrate its power. Third, capabilities that the flight element demonstrated did address significant data system problems. However, scientists and other end users of the remote-sensing data were looking for diverse end products with ultimate accuracy generated by complex algorithms yet to be determined. With this set of difficulties, the flight element of the NEEDS Program foundered. Yet it is intuitive that there is much that can and should be done on orbit. Some of the fundamental obstacles to both flight and ground elements in the NEEDS Program were in fact our lack of understanding of the physical relationships between what can be sensed and what we are trying to derive. There was no algorithm engraved in stone, which when applied to multispectral sensor data, would tell us how much corn was being grown on a particular patch of soil in Kansas.

The Eos: An Opportunity Regained

In light of what has been discussed previously, the Eos concept now should be considered. The Eos is most radical in its departure from prior U.S. Earth observation spacecraft in that it has been, from its inception, aimed at broad spectrum scientific objectives and the interplay among them. The Eos recognizes that major Earth processes interact with one another. In fact even in the past, it was recognized that observations were contaminated, obscured, or significantly impacted by outside effects: crop signatures blurred and modified by atmospheric effects, Lidar measurements sensitive to water vapor aerosols, sediments affecting chlorophyll signatures, and so forth.

To make significant statements about major Earth processes, it may be much more beneficial to reasonably define the multi-input, multi-output process than to continue to develop and fly more and more complex sensor systems, when the problem is in the physical understanding and not the hardware. Thus, models including good if not perfect algorithms may be perfectly adequate for Eos objectives.

ISES: The Information Sciences Experiment System

A concept has been proposed called ISES, which can avoid many of the problems encountered in the NEEDS Program, and at the same time address some very major issues of onboard information extraction. The key to the ISES concept is the commitment by the flight project of some "real estate" on the spacecraft: power, weight, access to the data system, and a time slot in the communications stream.

Basically, what is proposed is a "black box" attached to the spacecraft data bus or LAN. To the spacecraft the "black box" appears to be just another remote sensor requiring power, heat rejection, interfaces, adding weight, and requiring time on the data management and communication system. In reality, the "black box" is a programmable computational resource which eavesdrops on the data network, taking data and producing selectable science information back on the data network. An added element to the ISES is a proposed laser communication experiment for direct-link-to-ground experiments. The incorporation of the ISES into the Eos flight is shown in figure 3, where it can be seen that the "black box" simply interfaces into the Eos platform data network, like other instruments and, like them, communicates to the ground through the two radio frequency (RF) links. (The two RF links are: the primary Telemetry Data Relay Satellite (TDRS) and, on a non-interference basis, a proposed NOAA/NASA, 100-MBit/second, direct-to-user RF link.)

A system can therefore be instituted characterized by, among others, the following six items:

(1) Conducting onboard information extraction experiments and demonstrations.
(2) Not modifying investigators' data.
(3) Avoiding "mission critical" constraints.
(4) Making real-time event response possible.
(5) Defining flight experience as "confidence building."
(6) Identifying desirable technology areas.

Item (1) is made possible by eavesdropping on instrument data as it either passes around a LAN or is placed on the data bus. With the ability of picking up data from a variety of instruments as they are being taken comes the possibility of executing information extraction experiments in the "black box." Since the "black box" is a computational resource, algorithms can be run (which according to Eos provisions must be freely shared) to extract whatever end product is desired. More particularly, data retrieval that requires inputs from other data sets ("sensor fusion") can be executed. High data rate or low data rate experiments can be run on selected subsets of data by "frame snatchers." Thus, significant experiments can be performed on a modest size computational resource with modest data storage capability. Once finished with the experiment, the results are then prepared for transmission and presented back to the Eos data system. It is anticipated that information extraction experiments will be run in both the areas of Earth resources and information sciences and that those experiments will be defined by a science team representing both groups.

Item (2) is important, since as has been discussed previously, one of the major concerns with onboard information extraction has been the principal investigator's objection to irreversible modification of data when the ultimate algorithms are as yet undiscovered. The ISES avoids this by running in parallel with the actual investigator's experiment by copying the data into its memory, and by not handling the data in any way. Consequently, this approach allows timely comparisons of investigator data with whatever quick-look data or other early processing that is planned.

Item (3) answers the question of adding advanced technology to flight systems which might be considered immature concerning reliability. Failure of some or all of ISES does not result in the failure of anything except experiments ISES hosts. Treating the computational resource as a payload relieves some of the reliability and quality assurance rigors, since payloads would not be considered "mission critical."

Item (4) refers to the possibility of responding to events that may be observable from Eos in real-time. Data from experiments observing weather phenomena, for example, could be monitored continuously for suspicious features by ISES, and if something is identified, a priority communication could be executed or high-resolution sensors commanded to examine the feature more closely.

Item (5) is reasonably self-evident. Nothing develops confidence in space flight hardware than actual demonstration and use in space. The more flight time the hardware logs, and the more routine use it gets, the more actual experimental data base is developed and the more comfortable mission managers become in supporting future applications.

Item (6) is a side benefit from trying technology that shows promise and points to areas that could benefit from further development. Special-purpose hardware and special functions being performed could yield results that are extremely useful, but far from being fully exploited.

Whereas the approach of flying the onboard processing system as a payload rather than part of the spacecraft support hardware obviates many objections, ISES is then left with justifying itself in its own arena. The most serious obstacle to ISES in a head-to-head competition with other potential payloads is the lack of a developed advocacy in the science community. Such a lack is something like the "chicken and egg" dilemma: Without prior access to onboard, real-time computational capability, there is no opportunity for experiments or participation. Without opportunity, advocacy community cannot be developed; without advocacy community, there can be no onboard computation. Since ISES has elected the payload approach, its justification must survive competition against the other potential payloads. Thus, one major element in defining ISES is the development of science and user requirements for peer review and program cost-benefit assessment.

A science team made up of two sub-groups, an Earth sciences team and an information sciences team, develops ISES requirements. Given the nature of Eos, the information sciences team must develop its experiments and demonstrations in and around those developed by the Earth sciences team.

At this point, it is worthwhile noting that the science teams must develop a set of requirements in the form of experiments and demonstrations. The ISES concept distinguishes among three classes of activities: (1) experiments, where there are competing concepts, algorithms, theories, etc.; (2) demonstrations, where a leading approach, algorithm, etc., has been identified, tested, and evaluated; and (3) operational systems, where the relevant demonstration has been done, effectiveness and utility proven. ISES has the objective of addressing elements (1) and (2).

A second major activity in the ISES approach is the definition and development of the physical ISES flight and ground system, including hardware and software, etc. The science requirements, converted to quantitative experiment scenarios, with algorithms, are mapped against potential hardware options. An optimization process must maximize the science return (with prioritized experiments) within the expected allocation of platform resources (power, weight, volume, heat rejection, etc.) Thus, the ISES concept [illegible] predicated on technology driven by science rather than technology for technology's sake.

Regarding other payloads that might include internal information extraction or data processing, ISES is neutral. Whatever other instruments do to their data, whatever information extraction the Principal Investigator and his Science Team will allow as "in-line" processing, simplifies the task for ISES, so long as there is available knowledge of final output. ISES operates in parallel with other instruments, and its structural relationship to internal instrument processing can be illustrated as shown in figure 4. ISES deals with instrument data as a constraint, but one which is a legitimate consequence of the ISES eavesdropping, non-intrusive, approach.

Direct-to-Users

An aspect of the ISES concept which has considerable potential for magnifying both the range of experiments and the extent of participation is direct-to-user information transmission. The baseline communication method for ISES is through the Eos space-to-ground link (the Telemetry Data Relay Satellite System (TDRSS)). After performing the information extraction experiment or demonstration, ISES typically would wait its turn and when appropriate, feed its information into the LAN, which in turn, would send the data to the platform data and communication package for transmission through TDRSS to the ground.

Two other paths to ground, including "in-the-field" users exist. First is what was originally proposed to be NOAA's direct broadcast communication link. The second path is part of the ISES concept and is a proposed laser communication demonstration.

The NOAA link, as originally proposed, was composed of four elements: A VHF or UHF data collection transponder, a VHF Automatic Picture Transmission (APT) subsystem, an S-Band High Resolution Picture Transmission (HRPT) subsystem, and a 100 Mbit/sec Landsat-like subsystem. Scattered throughout the world, there are about 800 APT-compatible stations, 76 HRPT-compatible stations, plus a few Landsat-compatible stations (Reference 4).

It is likely that NOAA instruments or communications packages will NOT be on the first Eos platform, and consequently, discussions have taken place for alternative suppliers of the direct-to-users link. One option is for ISES to support the formatting of data for the physical RF system, including the generation of substitutes for the original NOAA data and the ISES experiment results.

The HRPT stations are of considerable interest, since they represent digital data receiving capability. The HRPT format consists essentially of a 0.665-Mbit/sec data stream that is derived from the AVHRR joined to atmospheric sounder, limb scanner, and radiation monitor data. A digital data format similar to that in HRPT can be considered quantitative as opposed to the qualitative data from the analog APT system. With all the necessary RF receiving station hardware, antennas, preamplifiers, bit synchronizers, etc., already established and ready, using such ground stations offers many more potential experiments for ISES to perform, particularly regarding contemporaneous and location specific applications. It is possible to imagine universities, local governments, or perhaps, companies participating much more readily in the global environmental studies or applications, if their involvement is direct. The ISES concept offers a flexible approach to tailoring the powerful and broad capabilities of the sensing systems on Eos to the specific concerns under the spacecraft's flight path.

Basically, the HRPT output is just a digital data stream which happens to be formatted from line scan imagery data with atmospheric and radiation environment data appended in each data frame. The content in the frame in the Eos context could be anything that the experimenter wants, abstracted from any of the various sensor systems on Eos. Some simple adaptation of the current HRPT systems may be necessary to avoid interference with the NOAA TIROS satellite frequency at S-Band. Users may have to purchase new crystals, etc. and software would have to be modified. Nevertheless, the resulting systems would be an inexpensive way to receive data from the most powerful remote sensing system ever flown and to widen participation in a dramatic way.

An example of applying new technology to the space environment is the laser communication experiment in the ISES proposal. This experiment represents a demonstration of the ISES approach to evaluating new technology such as semiconductor diode lasers in a space-to-ground link. As currently envisioned, the laser communication experiment will be split into two major portions: the first portion is a moderate data rate, direct-to-earth science-field users objective in which the ability to establish enough bi-direction communication to fill an empty personal computer fixed disk in one pass of the polar platform is demonstrated. Since this represents about 15 minutes from horizon-to-horizon, a rate of about 10 bits/second is enough, which is a low rate. The second portion of the experiment will support information sciences with an objective of gigabit rate links near the poles. The very difficult job of acquisition and tracking is greatly ameliorated by the stated accuracies to be provided in the polar platform ephemeris. (The position is known to be better than plus or minus 10 m.)[*] The demonstration of bi-directional space-to-ground optical communication has many desirable features and stands as an already defined experiment in ISES (fig. 5).

Relation to the Core Space Station Freedom

At this point, it is worth commenting on the application of the ISES concept to the Core Space Station Freedom, that will be in a low-inclination orbit. The Eos will be in a high-inclination polar orbit, placed there by an expendable launch vehicle and it will be very likely that whatever hardware placed there will be capable of easy change out. The Eos ISES will rely very heavily on a fixed hardware environment and a versatile software environment to support simulations and emulations. The Core Space Station Freedom, on the other hand, represents the permanent manned presence. The Core Station is, by design, maintainable, evolvable, and repairable, lending itself to supporting an ISES concept with a far more flexible hardware environment. Thus, experiments and evaluations of novel hardware become a reality. Items such as optical processors, neural nets, and other hardware treated as coprocessors or firmware are possible. Moreover, the Core Space Station is itself the subject of study as a complex, somewhat flexible flying machine. The types of experiments that might be supported in an ISES environment become more generalized than just Earth sciences. Experiments in controls, structures, and artificial intelligence are possibilities as well as those related to Earth observations.

Conclusions

A concept called ISES has been proposed and discussed in this paper which makes use of a new opportunity, the Eos, to evaluate the role of onboard information extraction in space flight systems. Onboard information extraction is a possible part of the solution to the growing "data glut problem" associated with Earth-viewing remote sensors. The ISES concept offers additional opportunities in better use of onboard instrumentation, real-time response to events, and a way to evaluate new technology in space without jeopardizing mission safety. Finally, the applicability of the ISES concept to the core station was discussed, including important differences between a possible Eos version and core station version of the ISES concept.

---

[*] Part Three: Eos Science, Operations, and Data Management, Background Information Package (BIP) Announcement of Opportunity, No. OSSA-1-88, NASA, Goddard Space Flight Center.

References

1. Earth Observing System Working Group Report, Volume 1, NASA TM-86129, August 1984.
2. The Earth Observing System Data and Information System Report of the Eos Data Panel, Volume IIa, NASA TM-87777, June 1986.
3. Remote Sensing of Earth from Space: Role of "Smart Sensors" Progress in Astronautics and Aeronautics, Vol. 67, Roger A. Breckenridge, ed. 1979.
4. Yates, Harold W., Meteorological Satellites and Cooperative Programs, Advances in Space Research, Vol. 3, No. 7, pp.133-137, 1983.

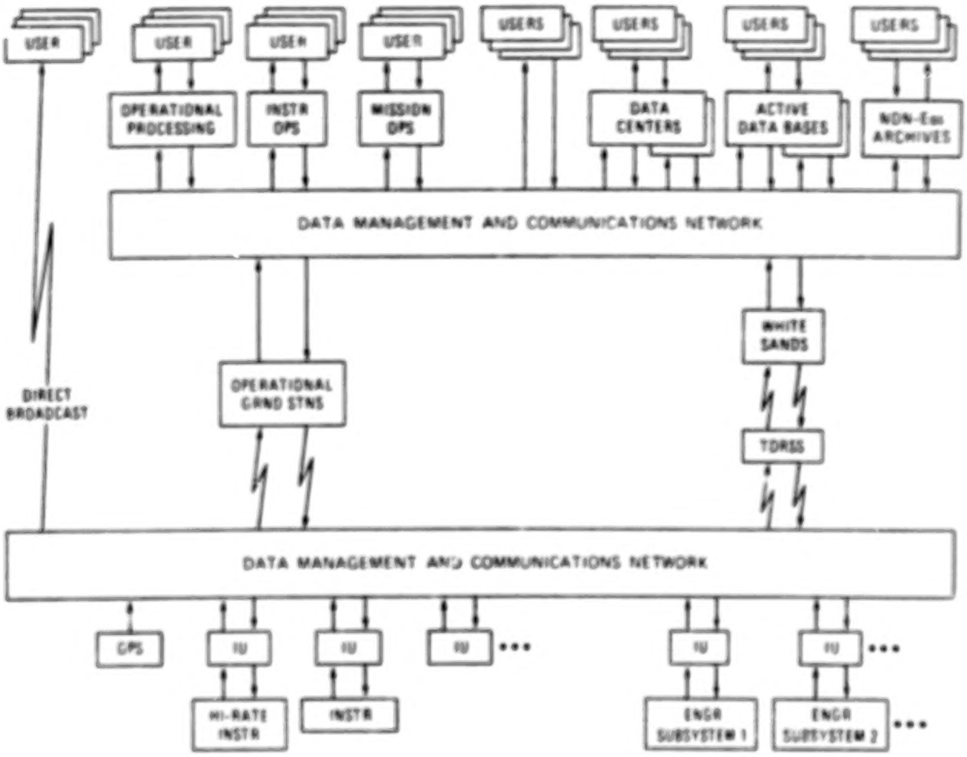
USER
USER
USER
USER
USERS
USERS
USERS
USERS
OPERATIONAL PROCESSING
INSTR OPS
MISSION OPS
DATA CENTERS
ACTIVE DATA BASES
NON-Eos ARCHIVES
DATA MANAGEMENT AND COMMUNICATIONS NETWORK
WHITE SANDS
DIRECT BROADCAST
OPERATIONAL GRND STNS
TDRSS
DATA MANAGEMENT AND COMMUNICATIONS NETWORK
GPS
IU
IU
IU
IU
IU
HI-RATE INSTR
INSTR
ENGR SUBSYSTEM 1
ENGR SUBSYSTEM 2

Figure 1. Current Eos data systems schematic showing ground element and flight element.

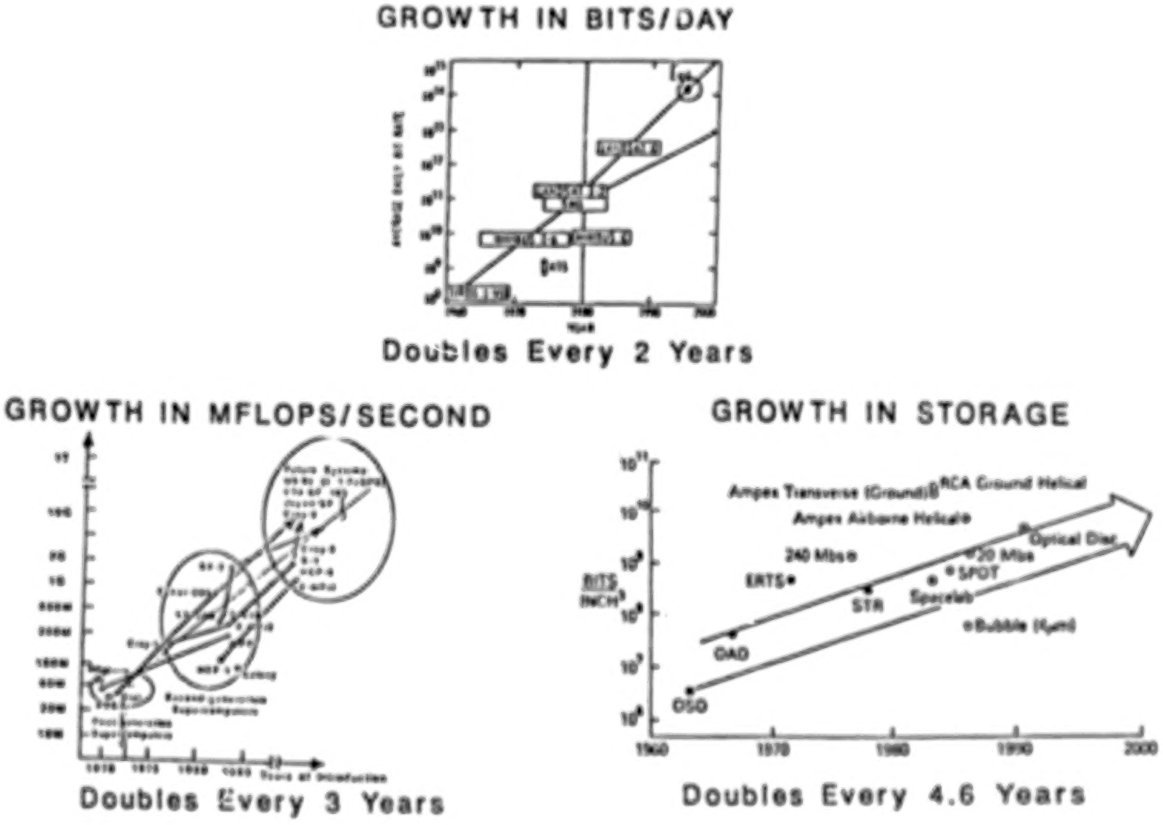

Figure 2. Illustration of historical trends in sensor data rates, compared with trends in data processing speed and data storage technology.

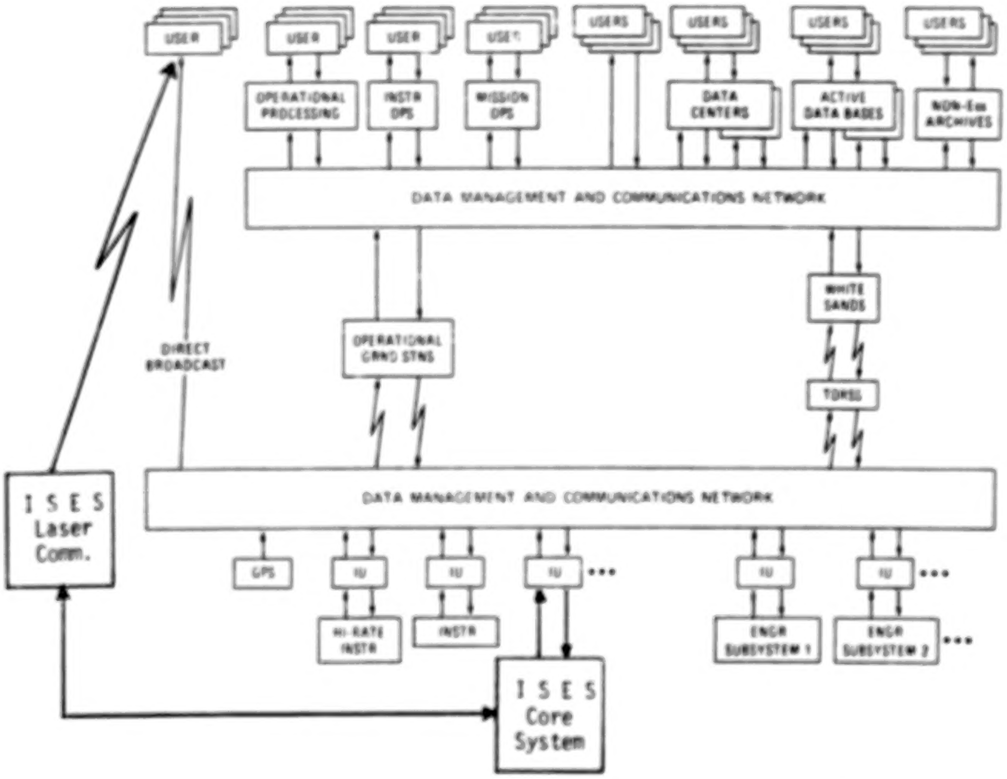
USER
USER
USER
USER
USERS
USERS
USERS
USERS
OPERATIONAL PROCESSING
INSTR OPS
MISSION OPS
DATA CENTERS
ACTIVE DATA BASES
NON-Eos ARCHIVES
DATA MANAGEMENT AND COMMUNICATIONS NETWORK
WHITE SANDS
OPERATIONAL GRND STNS
DIRECT BROADCAST
TDRSS
ISES Laser Comm.
DATA MANAGEMENT AND COMMUNICATIONS NETWORK
GPS
IU
IU
IU
IU
IU
HI-RATE INSTR
INSTR
ENGR SUBSYSTEM 1
ENGR SUBSYSTEM 2
ISES Core System

Figure 3. ISES concept integrated into Eos flight element showing eavesdropping access to real-time instrument data.

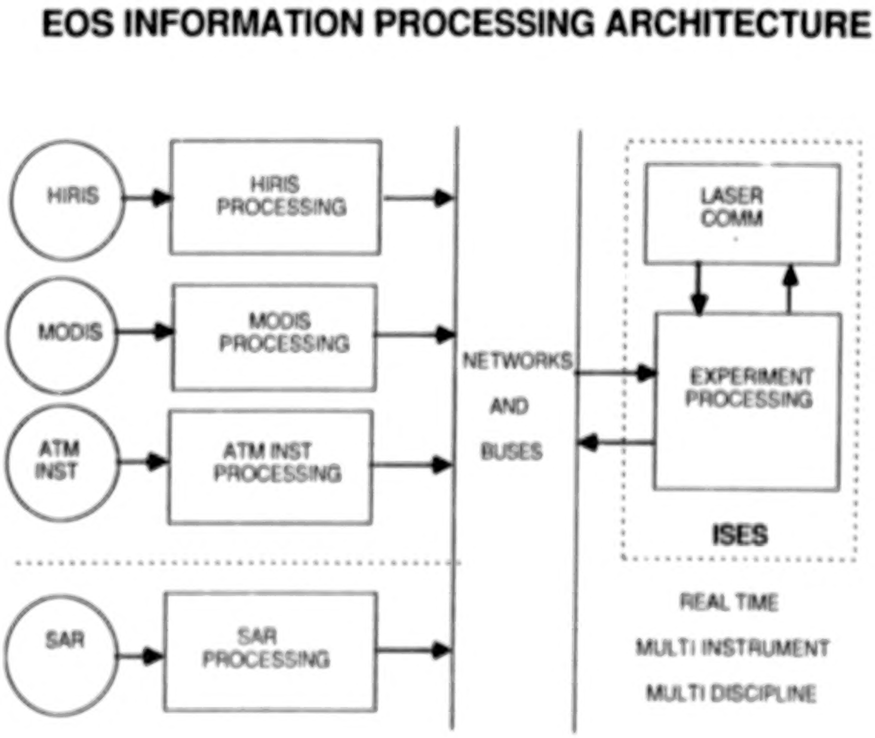
EOS INFORMATION PROCESSING ARCHITECTURE
HIRIS
HIRIS PROCESSING
MODIS
MODIS PROCESSING
ATM INST
ATM INST PROCESSING
SAR
SAR PROCESSING
NETWORKS AND BUSES
LASER COMM
EXPERIMENT PROCESSING
ISES
REAL TIME
MULTI INSTRUMENT
MULTI DISCIPLINE

Figure 4. Relation of ISES to other onboard sensor processing such as internal-to-the-instrument data processing.

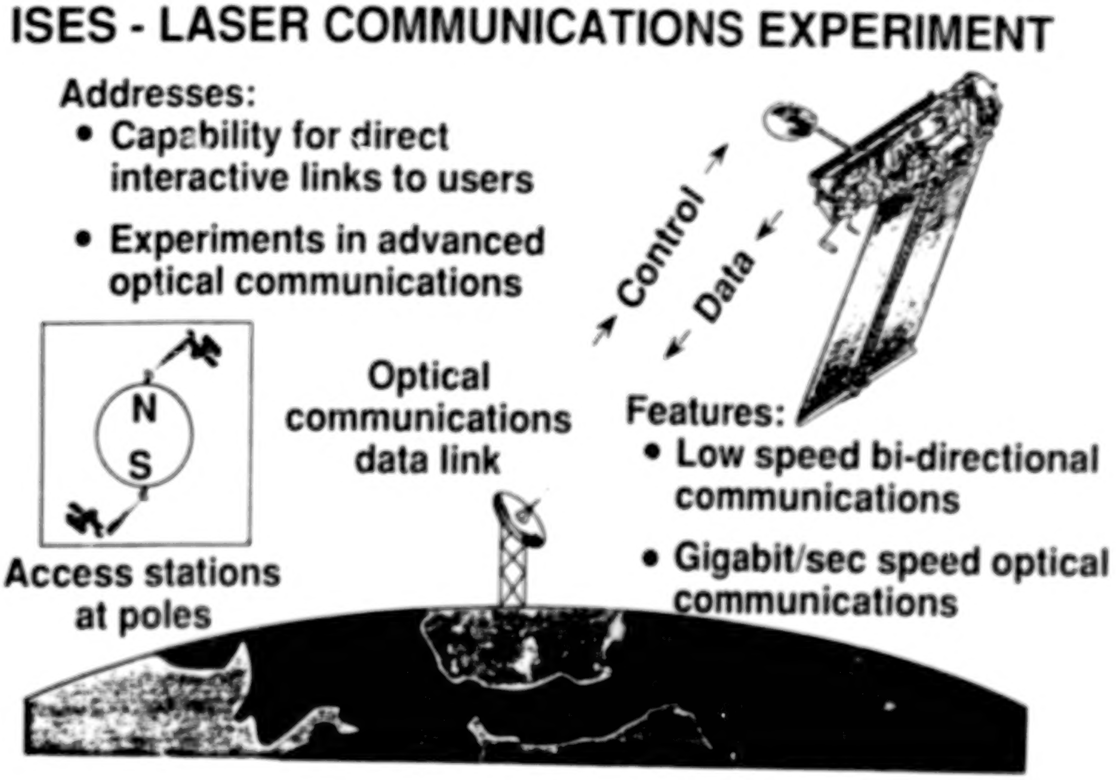

ISES - LASER COMMUNICATIONS EXPERIMENT

Addresses:

- Capability for direct interactive links to users
- Experiments in advanced optical communications

Features:

- Low speed bi-directional communications
- Gigabit/sec speed optical communications

Control
Data
N
S
Access stations at poles
Optical communications data link

Figure 5. Illustration of potential advanced technology demonstration on ISES: laser communication for direct-to-user experiments.

N90-27143

BASIC DATA REQUIREMENTS FOR MICROWAVE RADIOMETER SYSTEMS

R. W. Lawrence
NASA Langley Research Center
Hampton, Virginia

Microwave Radiometry has emerged over the last two decades to become an integral part of the field of environmental remote sensing. Numerous investigations have been conducted to evaluate the use of microwave radiometry for atmospheric, oceanographic, hydrological, and geological applications. Remote sensing of the earth using microwave radiometry began in 1968 by the Soviet satellite Cosmos 243, which included four microwave radiometers (Ulably, 1981). Since then, microwave radiometers have been included onboard many spacecraft, and have been used to infer many physical parameters.

The development of the required algorithm to determine these physical parameters from radiometric measurements is clearly an extremely broad area and is beyond the scope of this paper. Rather, in this paper, some of the basic concepts of radiometric emission and measurement will be discussed. Several radiometer systems will be presented and an overview of their operation will be discussed. From the above description of the radiometer operation the data stream required from the radiometer and the general type of algorithm required for the measurement will be discussed.

As noted above the radiometer has been shown to be useful in the measurement of many physical properties. This is accomplished by measuring the energy the object emits. All substances at a temperature above absolute zero radiate electromagnetic energy. Atomic gases radiate electromagnetic energy at discrete frequencies according to specific transition of an electron from one energy level to another. For liquids and solids, the increased particles interaction results in a continuous spectrum. A radiometer is simply a very sensitive receiver which can be used to accurately measure this radiated energy and thus infer physical properties.

The power P emitted by an object in thermal equilibrium is a function of its physical temperature T and in the microwave region P is directly proportional to T. The maximum power an object can emit for a given T is given by P_{bb}, the ideal black body radiation. If a microwave radiometer is completely surrounded by perfectly absorbing material, i.e. a black body, the power received by the antenna would be

$$P_{bb} = kTB \qquad (1)$$

where k is Boltzmann's constant and B is the noise bandwidth of the radiometer. The term *brightness* temperature T_b can be used to characterize the energy emitted by a material of constant physical temperature by the following equation

$$T_b = \frac{P}{k\ B} \qquad (2)$$

where P is the power emitted by the material over the bandwidth B. For materials that are not perfect absorbers (not black bodies) the power received will be less than the maximum P_{bb}, and the material is said to have an emissivity $e = T_b/T$. The radiometers measurement of T_b can then be used to determine the emissivity of an object which may be related to physical parameters.

The radiometer must estimate the power P radiated from an object. The power level of this received signal may be lower than the receiver noise level. Thus, a radiometer must make a very precise measurement of a very small signal. Clearly this requires the gain and receiver noise to be well known and very stable. Several radiometer systems have been developed to facilitate this measurement and will be discussed below.

The ***total-power radiometer*** is a straightforward configuration consisting of an antenna, amplifier stages, a detector, and a low-pass filter or integrator. An ideal system is shown in figure 1. Here the system is dependent on the receiver noise and gain to be stable between calibrations. The internal receiver noise is represented as an additive noise source and the front end amplifier stage is considered noise free. If the detector is assumed to be a square law device, then the voltage out of the detector will be proportional to the noise power at the input. That is,

$$V_{out}(t) = V_{dc} + V_{ac}(t) \qquad (3)$$

where

$$V_{dc} = G_s(T_A + T_{REC}) \qquad (4)$$

where G_s is the system gain. The dc portion is a measure of the power into the square law device, i.e. a measure of the input noise temperature. The ac portion represents the statistical uncertainty in the measurement. The low-pass filter (or integrator) will reduce this uncertainty. It can be shown [Ulably, 1981] that integrating a random process with a noise bandwidth B for a time τ will reduce the variance of the output process by $B\tau$. Therefore,

$$\frac{\{V_{ac}\}_{rms}}{V_{dc}} = \frac{1.}{\sqrt{B\tau}} \qquad (5)$$

If the term ΔT is defined as the standard deviation of the output in terms of the input antenna temperature measurement

$$\Delta T = \frac{\{V_{ac}\}_{rms}}{G_s} \qquad (6)$$

Then,

$$\Delta T = \frac{T_A + T_{REC}}{\sqrt{B\tau}} \qquad (7)$$

where ΔT can be considered as the minimum detectable change in the radiometric antenna temperature. In the above expression, ΔT is defined as the radiometric sensitivity of an ideal total power radiometer. Uncertainty in the measurement because of gain fluctuations can be written

$$\Delta T_G = \frac{\Delta G_s}{G_s} \qquad (8)$$

then the total uncertainty can be written

$$\Delta T = T_{sys}\left\{ \frac{1}{B\tau} + \left(\frac{\Delta G_s}{G_s}\right)^2 \right\} \qquad (9)$$

Equation 9 is the radiometric sensitivity of a total power Dicke radiometer including the effects of noise and gain fluctuations.

One method to reduce the effect of gain fluctuations was developed by Dicke in 1946 using a modulation technique to reduce these effects. Figure 2 shows a simplified block diagram of a *Dicke radiometer.* The system is essentially a total power radiometer with the addition of two switches (often called Dicke switches). This allows the input to the radiometer to be alternately switched from the antenna to a reference load of known noise temperature. The output for these two switch positions are subtracted before averaging. If the switches are operated at a rate in excess of the highest component of the spectrum of the gain fluctuation, then the effective system gain G_s can be considered constant for both switch positions. Since the gain is identical for each half cycle, the average voltage out of the square law detector can be written

$$\bar{V}_{d_{ant}} = G_s kB(T_A + T_{REC}) \quad \text{for } 0 \le t \le \tau_s/2 \qquad (10a)$$

$$\bar{V}_{d_{REF}} = G_s kB(T_{REF} + T_{REC}) \quad \text{for } \tau_E/2 \le t \le \tau_s \qquad (10b)$$

where T_{REF} is the known reference noise source and τ_s is the period of the switching cycle. The average output voltage, V_{out}, can be written

$$\bar{V}_{out} = \frac{1}{2} G_s (T_A - T_{REF}) \qquad (11)$$

The ΔT of the Dicke radiometer will be determined by first finding the ΔT for each half cycle. The noise uncertainty during the antenna portion

$$\Delta T_{ANT} = \frac{T_A + T_{REC}}{\sqrt{\frac{B\tau}{2}}} \qquad (12)$$

For the reference portion

$$\Delta T_{REF} = \frac{T_{REF} + T_{REC}}{\sqrt{\frac{B\tau}{2}}} \qquad (13)$$

The effect on gain fluctuations

$$\Delta T_G = (T_{REF} - T_A)(\Delta G_S / G_S) \tag{14}$$

Since these fluctuations are independent the total uncertainty or ΔT for the Dicke radiometer can be written

$$\Delta T = \left[\frac{2(T_A + T_{REC})^2 + 2(T_{REF} + T_{REC})^2}{B\tau} + \left(\frac{\Delta G_S}{G_S} \right)^2 (T_A - T_{REF})^2 \right]^{1/2} \tag{15}$$

If the antenna temperature, T_A, equals the reference temperature in equation 15 the effects of gain fluctuations are virtually eliminated. The ΔT for this *Balanced Dicke radiometer*, shown in figure 3, then becomes

$$\Delta T = \frac{2(T_{REF} + T_{REC})}{\sqrt{B\tau}} \tag{16}$$

or

$$\Delta T = 2\Delta T_{IDEAL}$$

There are several techniques which may be used to ensure the above condition is met and the radiometer is balanced. These techniques use a control loop such that the error signal adjusts the system gain during one half cycle, varies the reference temperature, or adds noise to the antenna port to balance the loop. These approaches have various advantages and disadvantages and the specific approach is not important to this discussion.

The sensitivity for the *Total Power, Dicke (unbalanced)*, and *Balanced Dicke* is shown in equations 9, 15, and 16 respectively. The sensitivity is important to the information scientist since the required precision or word length is dependent on the sensitivity of the radiometer. These expressions allow the information scientist to determine the likely digital word length requirements from either the science requirements or from a hardware description of the proposed radiometer system.

In the above discussion, the RF components in the radiometer front-end have been assumed to be perfectly impedance matched, that is, no reflections exits between components. In actuality, although these reflections can be minimized they can never be completely eliminated and, as will be shown, their effect on radiometer performance can be significant.

If the radiometer measurement is assumed to be linear over the range of interest, then the output of the radiometer (counts, volts, duty cycle, etc.) can be expressed as

$$N_{counts} = M\,T_A + b \tag{17}$$

For the ideal (perfectly impedance matched) case the intercept, b, can be calculated from system parameters for some radiometer configurations. The slope M can then be found by calibration. In practice, accurate characterization of the instrument including the effects of mismatch requires calibration at two reference temperatures. This allows the independent determination of M and b. To the extent that the reflection coefficients of the radiometer front end remain constant, their effect can, in principle, be accounted for by the calibration of the effects of the reflection coefficients.

The effect of impedance mismatch and loss in the radiometer front end can be understood by the analysis of the simplified front end network shown in figure 4. The effective noise temperature at the input to the receiver T_{IN} can be shown to be [Ulably, 1981], [Kerns, 1967]

$$T_{IN} = \alpha_m Y T_{ANT} + \alpha_m (1-Y) T_c + (1-\alpha_m) T_{REC} \qquad (18)$$

where

$$\alpha_m = \frac{(1-|R_{2S}|^2)(1-|R_R|^2)}{|1-R_R R_{2S}|^2}$$

$$Y = \frac{1}{L_S}\left\{\frac{(1-|R_G|^2)(1-|S_{11}|^2)}{|1-S_{11}R_G|^2(1-|R_{2S}|^2)}\right\}$$

and

$$R_{2S} = S_{22} + \frac{S_{21}S_{12}R_G}{1-S_{11}R_G}$$

$$L_S = \frac{Z_{02}}{Z_{01}} \frac{(1-|S_{11}|^2)}{|S_{21}|^2}$$

The first term in equation 18 is the net-delivered noise temperature from the antenna; the second term is the net-delivered noise temperature generated by the losses in the network; the third term is the net-delivered noise temperature emitted by the receiver itself. The purpose of the calibration, in addition to compensating for gain constants, etc. in the receiver, is to allow the extraction of T_{ANT} from the measurement of T_{IN}. Fortunately, the calibration can be performed, and an algorithm to convert from the indicator (counts) to engineering units (T_A) developed without knowledge of the specific relationship between the various reflection coefficients and the factors of equation 16. However, equation 16 indicates the dependence of the calibration constants on temperature. Clearly, the second term is directly a function of temperature and all the reflection coefficients could be temperature dependent.

For this reason, radiometric front ends are generally temperature stabilized, and the algorithm from counts to T_A will be temperature dependent. Although the method used to include this temperature dependence is hardware specific, a technique commonly used for thermally controlled systems is to perform calibrations at operating temperatures, and correct only for temperature dependence of significant losses as shown below.

$$T_{ANT} = \sum_{i} \alpha_{i} (T_{PHY_{i}} - T^{CAL}_{PHY_{i}}) + M\, N_{COUNTS} + b \qquad (19)$$

The information scientist wanting to provide estimates of T_A must extract from the data stream the measured T_{IN} for the available calibration sources or ground truths. From the "known" noise temperatures of the sources the coefficients M and b are then found for one set of physical temperatures within the front end. For small changes in physical temperatures and for time periods for which the radiometer system is stable T_A can be estimated from equation 17. The required precision of the operation of equation 17 would be similar to those found for N_{COUNT}. Required data rate and calibration intervals are again instrument/mission specific; however, some "typical" values are shown in table 1.

Thus far, the discussion has focused on transforming the radiometer output to antenna temperature T_A (noise temperature delivered by the antenna). Although not discussed here, for completeness it should be noted that a second transformation is generally required to convert the antenna temperature to the scene brightness temperature. This transformation is dependent on detailed antenna characteristics and the incidence dependence of the brightness temperature.

This transformation from T_A to T_B is closely related to the spatial resolution and antenna pattern of the radiometer. The spatial resolution of a microwave radiometer is often specified by its *instantaneous field of view* (IFOV). The IFOV is defined as the area on the ground contained by a specified portion of the antenna pattern (often the 3 dB contour). Of course the actual antenna temperature is a weighted average of the noise temperature received over the entire antenna pattern. In general, careful antenna design and definition of the IFOV will ensure that the transformation from T_A to T_B can be performed separately for each pixel or IFOV. However, if there is enough spatial sampling it may be possible to partially deconvolve the antenna pattern and brightness temperature to improve the trade off between spatial and temperature resolution. This could be of interest to onboard real-time users of radiometric data. In developing such an algorithm, the information scientist would require very specific information about the imaging aspects of the instrument. A possibly more trackable problem would be to develop a deconvolution algorithm that could correct the radiometric image for larger antenna side lobes. This may allow processing of nearest cells only.

In summary, although this paper is clearly not an in-depth study of possible applications of onboard processing in radiometry, it is hoped that it does provide the information scientist with an appreciation of the general data requirements for radiometric systems. An overview of general radiometer concepts has been presented with hopes that the information scientist can estimate the type of algorithms or processing which could be required in a generic sense for various applications.

REFERENCES

1. Ulably, S. T., Moore, R. K., and Fung, A. K.: Microwave Remote Sensing, Volume I, Addison Wesley Publishers, Reading, Massachusetts, 1981.

2. Kerns, D. M., and Beatty, R. W.: The Basic Theory of Waveguide Junctions and Introduction To Microwave Network Analysis, Volume III, Pergammon Press, New York, 1967.

Table 1. Data Rates and Calibration Intervals

DATA RATE

• T_A	> INTEGRATION TIME – 47 ms ESMR(NIMBUS 5) – 32 ms RADSCAT(SKYLAB) – 128 ms – 256 ms
• PHYSICAL TEMPERATURES	> THERMAL TIME CONSTANT
• CALIBRATION	> TOTAL POWER - SECONDS > DICKE - MINUTES > DICKE BALANCED - HOURS ⇒ DAYS

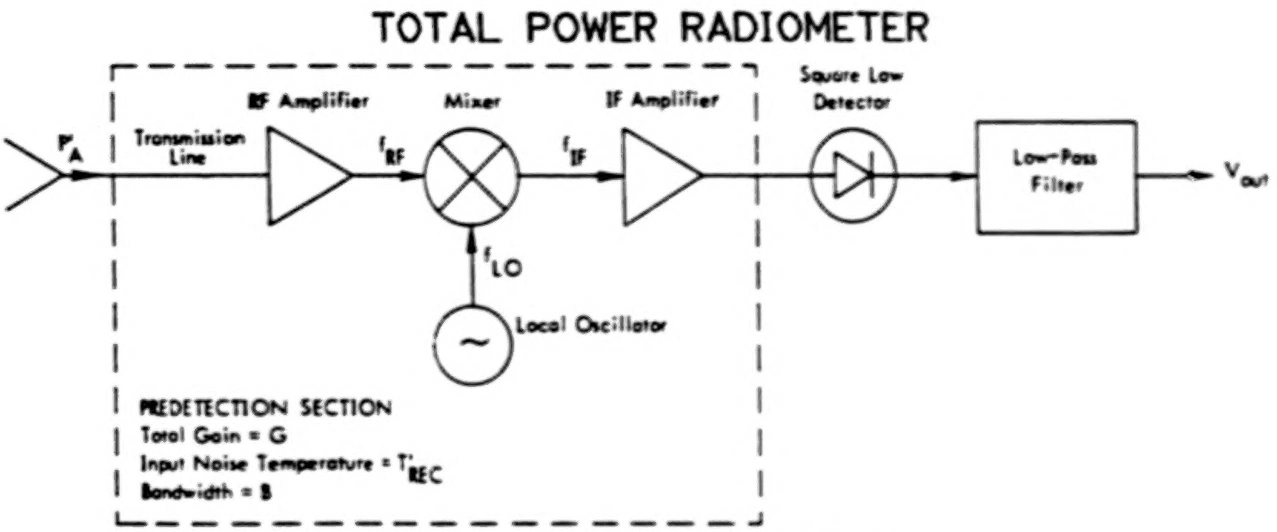
TOTAL POWER RADIOMETER
P'_A
Transmission Line
RF Amplifier
f_{RF}
Mixer
f_{IF}
IF Amplifier
Square Law Detector
Low-Pass Filter
V_{out}
f_{LO}
Local Oscillator
PREDETECTION SECTION
Total Gain = G
Input Noise Temperature = T'_{REC}
Bandwidth = B

(a) Block Diagram of Total-Power Radiometer

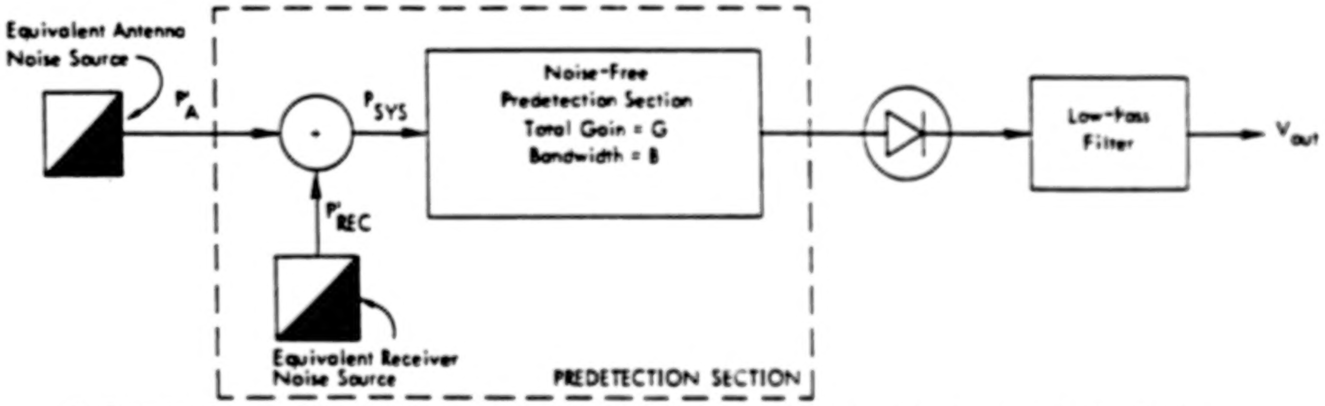
Equivalent Antenna Noise Source
P'_A
P_{SYS}
Noise-Free Predetection Section
Total Gain = G
Bandwidth = B
Low-Pass Filter
V_{out}
P'_{REC}
Equivalent Receiver Noise Source
PREDETECTION SECTION

(b) Equivalent Representation of (a) in Terms of a Noise-Free Receiver and Equivalent Noise Sources at the Receiver Input

Figure 1. Total power radiometer.

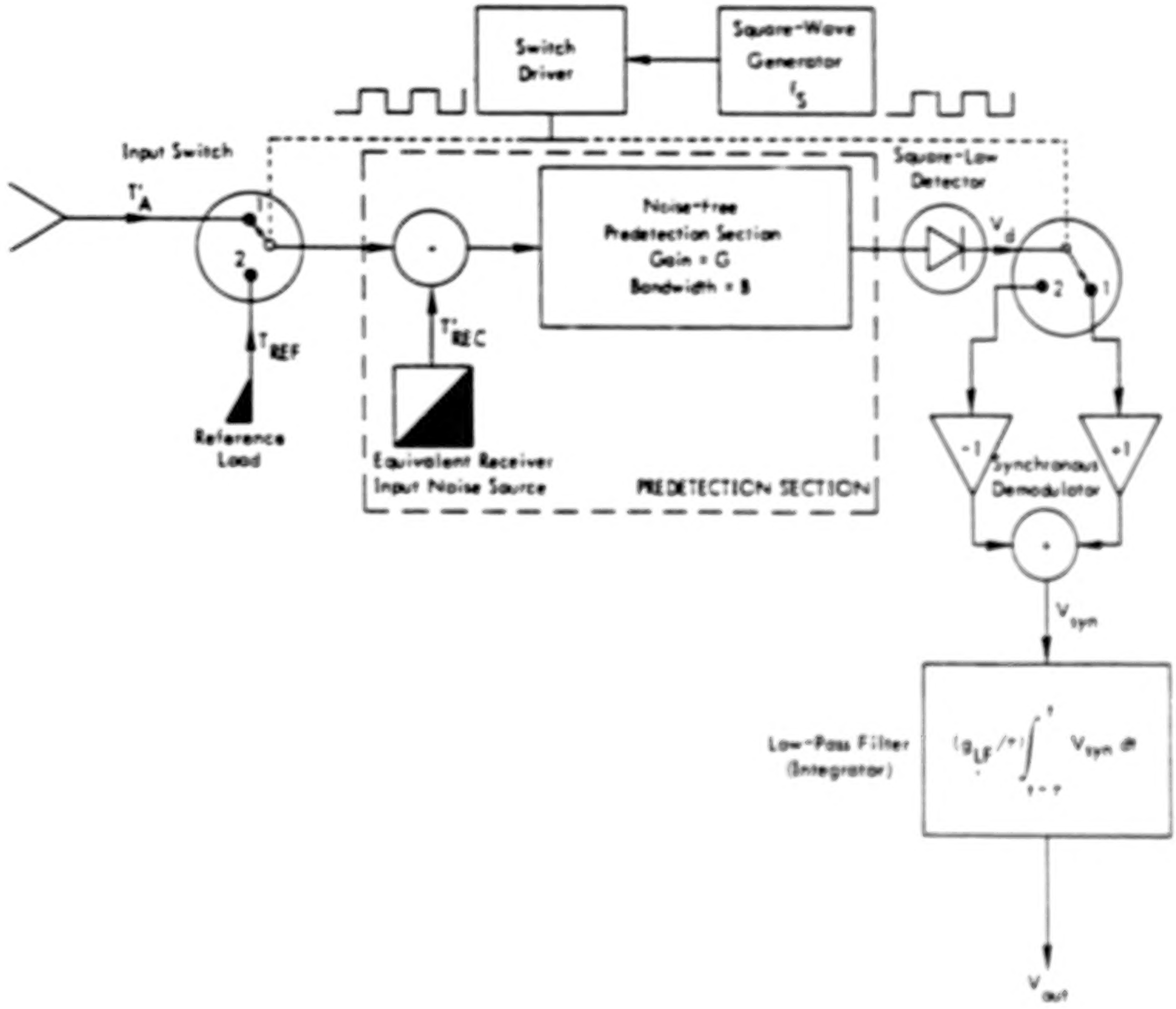
Switch Driver
Square-Wave Generator
f_S
Input Switch
T'_A
1
2
T_{REF}
Reference Load
T'_{REC}
Equivalent Receiver Input Noise Source
Noise-free Predetection Section
Gain = G
Bandwidth = B
PREDETECTION SECTION
Square-Law Detector
V_d
2
1
-1
+1
Synchronous Demodulator
V_{syn}
Low-Pass Filter (Integrator)
$(g_{LF}/\tau)\int_{t-\tau}^{t} V_{syn}\,dt$
V_{out}

Figure 2. Dicke radiometer.

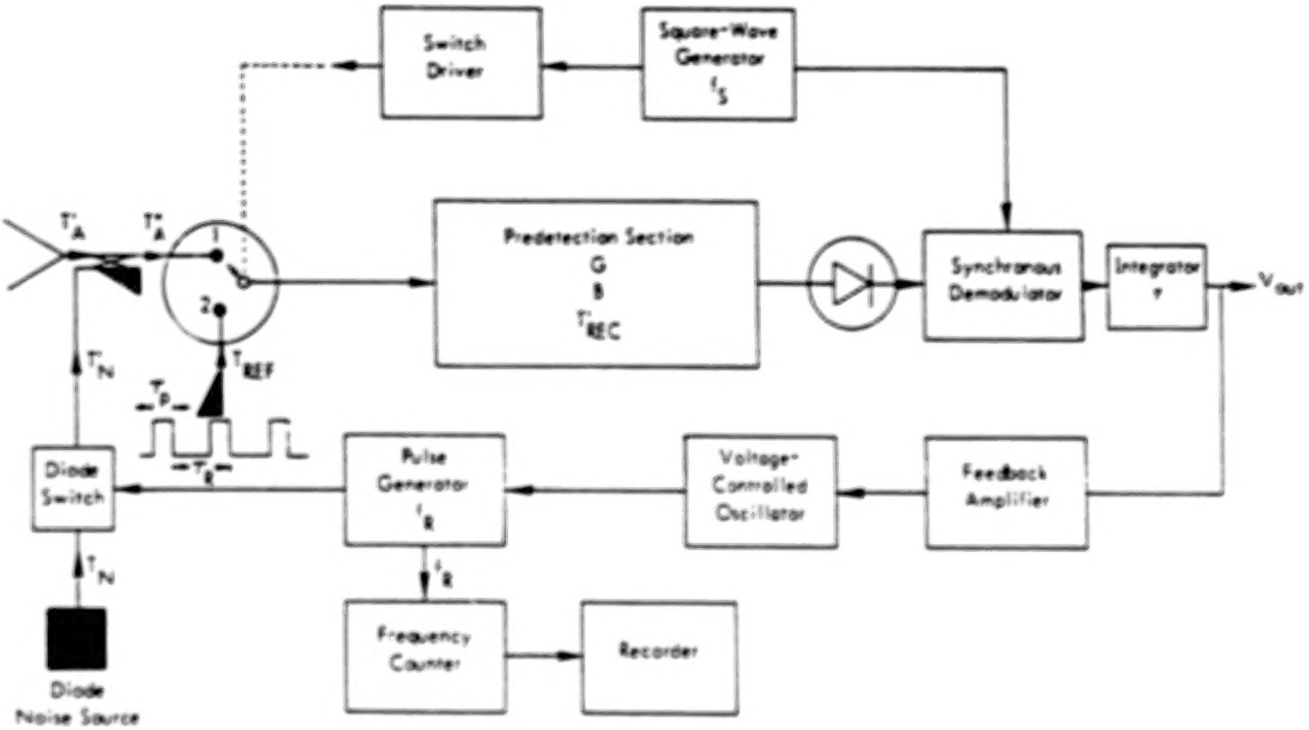
Switch Driver
Square-Wave Generator f_S
T'_A
T''_A
1
2
Predetection Section G B T_{REC}
Synchronous Demodulator
Integrator τ
V_{out}
T'_N
T_{REF}
τ_P
T_R
Diode Switch
Pulse Generator f_R
Voltage-Controlled Oscillator
Feedback Amplifier
T_N
f_R
Frequency Counter
Recorder
Diode Noise Source

Figure 3. Dicke radiometer (noise injection).

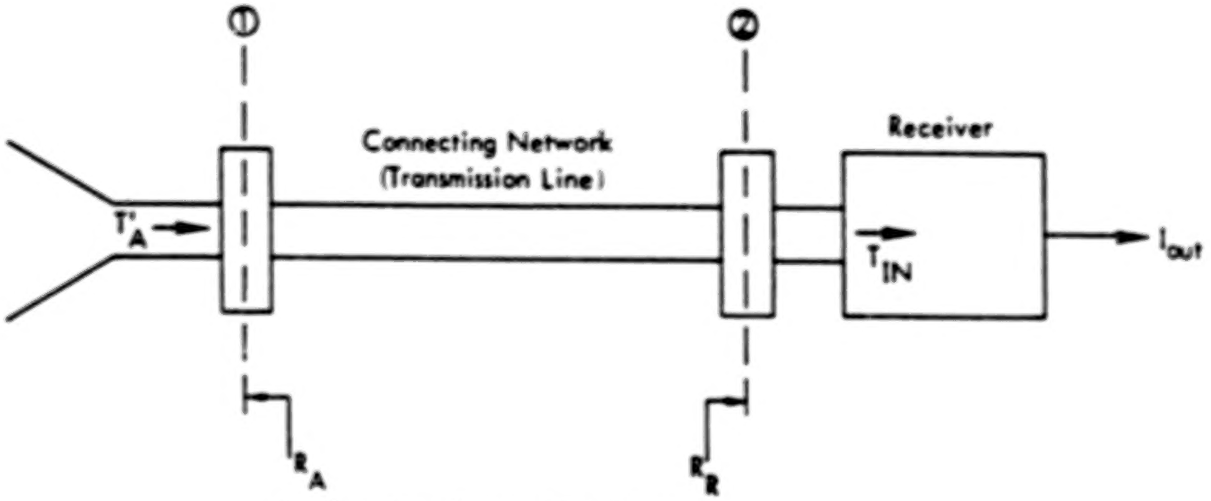
①
②
Connecting Network
(Transmission Line)
Receiver
T'A
TIN
Iout
RA
RR

(a) Receiver Connected to Antenna

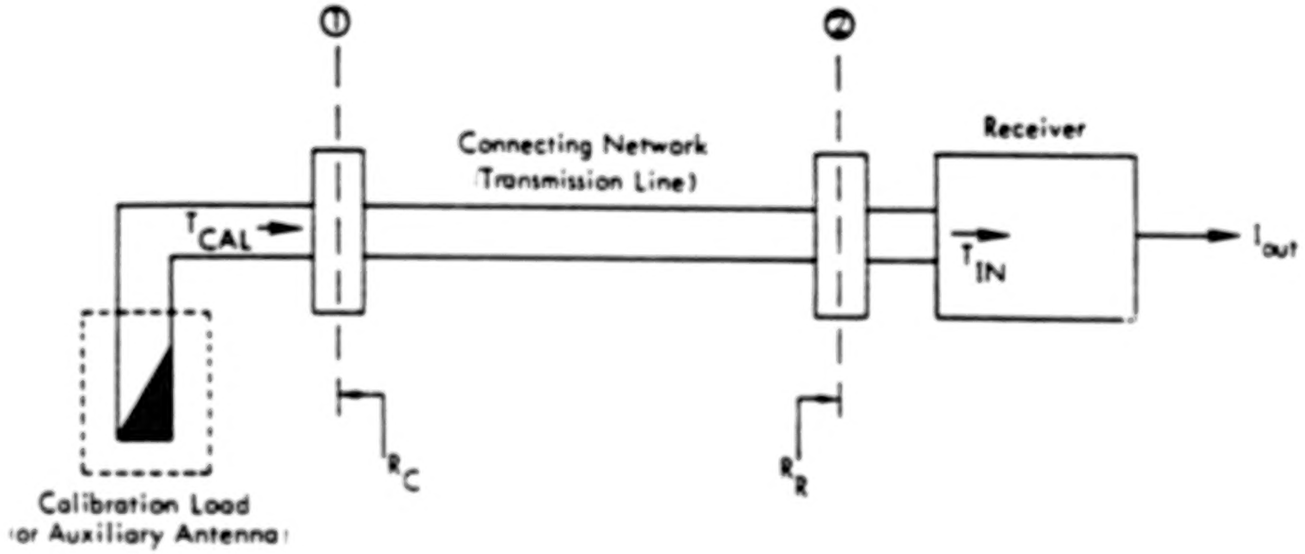
①
②
Connecting Network
(Transmission Line)
Receiver
TCAL
TIN
Iout
RC
RR
Calibration Load
(or Auxiliary Antenna)

Figure 4. Effects of impedance mismatch.

N90-27144

RADARS IN SPACE

Victor E. Delnore
Lockheed Engineering and Sciences Co.
Hampton, VA

I will discuss some of the capabilities of active microwave devices operating from space (typically, radar, scatterometers, interferometers, and altimeters, fig. 1). Figure 2 gives a brief outline of items to be covered in this discussion. General radar parameters and some basic radar principles are explained first, applications of these parameters and principles are explained next, and, finally, trends in space radar technology and where space radars and active microwave sensors in orbit are going are discussed. With any of these active microwave devices, you can control certain things, and I have listed those items in figure 3. These aspects include frequency, modulation, polarization, incidence angle, pulse repetition frequency, and pulse width. There are other aspects that you might be able to control on your own instrument, but if you are riding "piggyback" on somebody else's satellite, you can't control the orbit or the satellite's position. The best thing to do in a case like that is to record the position of the satellite so that you can back out your own data later on. Then you are in a good position to determine sigma-naught (σ^0), which is a measure of the facet scattering of the reflecting surface. The σ^0 quantity can be determined for your chosen or observed conditions, and, once you get that number as a function of whatever conditions you have, then you can try to relate that to conditions you are interested in.

An example of surface scattering is shown in figure 4. Look at the top row. If you have a really flat smooth surface, then you have a reflection whereby the angle of reflection is equal to the angle of incidence, shown in the figure as θ. But notice what happens if the surface gets a little rough. The rougher the surface becomes, the greater the likelihood you will have energy reflected in different directions. Where the surface becomes really rough, there is energy reflected in all directions. You can only hope that some energy comes back toward the source direction, so that you can make a measurement.

Let's now define this σ^0 quantity. Imagine there is a ray of energy coming toward you. Now, σ^0 is simply the measure of the energy scattered in the direction that you are interested in. Usually it's the direction that the incidence wave is coming from. σ^0 for any surface may vary with incidence angle, azimuth, frequency, and polarization. The rougher the surface, the more likely it is to get isotropic scatter (scatter in many directions). If I draw a dashed line around the amount of reflected energy to represent isotropic scatter, then σ^0 is defined as 1, or 0 dB. Other values of σ^0 would be represented by longer or shorter arrows (as shown in fig. 4). Shorter arrows would be a σ^0 of less than 1, or negative dB if you work in log space. Likewise, if you have more energy scattered in the direction you are interested in, then you have a σ^0 of greater than 1 in ratio space, or positive decibels. σ^0 values of terrestrial features as measured from space span a very wide range, and the measured value depends on the roughness and is much lower for flatter surfaces and higher for rougher surfaces.

The sampling scheme also can affect your measurement. There is a problem defining σ^0 for point sources. Figure 4 shows distributed targets. There are two common models for scattering. One of them is the specular, or optical, model and the other is the Bragg, or point scatterer model. Specular scattering is similar to what happens at the sides of a billiard table. Each reflecting surface is called a facet.

So, for example, if the incident energy is from a certain direction, and there is a facet tilted back toward the source, you get a lot of reflected power. Other facets, however, don't get very much power back. So specular scattering is good for near-nadir calculations.

The Bragg, or point scatterer, model has a surface that is represented as a summation of sinusoidal surfaces, each one with its own characteristic wavelength. In Bragg scattering, the surface component which has a wavelength approximately twice the size of the radar wavelength will be sifted out, or selected. That surface component is the one from which you get the most reflection. This concept was used extensively for the SEASAT wind-measuring scatterometer where the wavelength was approximately 2 cm. Even from orbit this 2-cm radar wavelength was very sensitive to the 1-cm capillary waves, the little "cat's paws" on the water surface, not to the general tilt of the ocean. Here the σ^0 in Bragg scattering is proportional to the energy spectrum of the little wind-induced ripples; that is how the wind measurement is made.

The upper graph of figure 5 represents both specular and Bragg scattering efficiencies as a function of incidence angle off of nadir. Notice the pronounced fall-off with incidence angle for the specular model. On the other hand, the Bragg scattering is flatter. What happens in the real world, of course, is a summation of those two as you move from nadir out to grazing. In the lower graph of figure 5, notice that as the surface gets rougher, the angular dependence decreases. If you have a very smooth surface and you try to measure σ^0 as a function of incidence angle, then you'll see that the amount of signal you get back is very sharply dependent on incidence angle. On the other hand, if the surface is very rough, then the amount of signal that returns is not going to be very dependent upon incidence angle. You can test this idea yourself if you're on the side of a lake in the evening, with a point source of light on the opposite shore. If the water is very calm, then any reflection you see on the surface of the water is going to be very angle-dependent; that is, the reflection occurs at only one spot on the lake surface. But, if the water gets rougher, then that single point source of light is reflected from a patch of water surface representing a spread of incidence angles.

Let us now discuss volume scattering. You get internal reflections (fig. 6) beneath the first surface, and energy gets scattered around inside. Some of this energy comes back toward you. Penetration depth is associated with this energy, and this penetration depth, like all good penetration depths, is the depth at which the intensity is e^{-1} of what it was at the surface. The penetration depth is given by this expression, where the ϵ's are simply the dielectric constants of the layered media traveling from one stratum down to the next. What we need to know about this expression is that at typical microwave wavelengths for dry soils, you might get approximately 1 meter penetration; for very dry sands in deserts, tens of meters; and for polar ice sheets, hundreds of meters. This allows all kinds of opportunities for looking at subsurface entities.

Now, we will review antenna patterns. Figure 7 is a representation of a beam with two side lobes. Beam width, β, is given by this expression where the beam width is approximately equal to the wavelength divided by some dimension of the antenna. This is an approximation to a numerical solution; it comes from a transcendental equation. The term λ is the wavelength involved, and there is a width and length for the antenna, unless it is circular; then, of course, you have a diameter. Width and length are being used here as two dimensions from a two-dimensional antenna. The antenna pattern that you generate from some test equipment might look something like the lower left part of the figure, where the side lobes are represented as little bumps. If the power at the peak, or center, is 0 dB, then 3 dB down is the half-power point. The beam width is defined as the angle between the two half-power points.

The radar equation is shown in figure 8. An antenna at altitude h, using wavelength λ, sends out a pulse, and a reflection then appears. P_i is just the power intensity incident on a scattering surface that measures X_a long by X_r wide. P_i equals the transmitted power multiplied by the antenna efficiency. There is an angular dependence and the inverse square law for the spreading of energy. P_c is returned power intensity back at the antenna (now acting as an energy collector for the receiver). If we multiply P_c by the dimensions W and L, then we get the amount of power that is incident on the antenna. P_r is the amount of power received, which is just P_c times the area of the antenna. So this (P_r) is the expression we want; this is really one form of the radar equation. The power received is P_r, but basically the expression includes the following: the transmitted power P_t (which you can control), the size of the antenna, the speed of light, σ^0, a few trigonometric functions, β (the beam width), the altitude of the orbit (distance above the ground), and the radar wavelength. Associated with this radar equation must be a signal-to-noise ratio (SNR), which is the power received, divided by the thermal noise in the antenna. Here, k is the Stefan-Boltzman constant, T is absolute temperature, and BW is bandwidth. You know many of these things, you have to keep track of others, and you measure P_r back at the antenna. Then you back out σ^0 and model it to whatever you are interested in (such as rain rate or surface roughness).

Figure 9 shows the formation of a resolution cell on the ground. For a sideways-looking sensor, we use two dimensions on the ground; one is azimuth and the other is range. Azimuth is the direction the spacecraft is moving, and range is crosstrack to that direction. We will use azimuth and range as our two ground dimensions. Imagine a spacecraft moving along in perspective view with the subtrack of the satellite on the ground underneath it. The beam is alongside looking in the crosstrack direction. (This is just for explanation purposes, because it eliminates the Doppler.) We will discuss Doppler later on; however, right now there's no radial component of velocity between the target area and the orbiting radar; therefore, there is no Doppler shift in the returned signal.

I want to explain how we get the cell size and shape on the ground based on the different radar and orbit parameters. These pulses radiating out along the beam are adjacent wavefronts. They can be as close together as $\frac{C\tau}{2}$. τ is the pulse width, which is equal to one over the bandwidth. You can set up a train of these pulses, but if you get them any closer together than the pulse width itself you really don't have a pulse train anymore. I assume that you would always want to get the finest resolution on the ground that you possibly could so this would be the minimum spacing in the range direction. If you project that onto the ground, the resolution in the range direction comes out to be, with the appropriate geometry, typically 20 m for microwave frequencies and bandwidths. Therefore, you have approximately 20 m in the range direction, which is pretty good. On the other hand, if you do the same calculations for the azimuth direction, you get an expression that gives typically 1 to 2 kilometers, which is not very good. If you are not trying to image some discrete object or shape, then 1 to 2 km might be acceptable. Notice one thing: the range resolution does not have an h in it. The term h, you may remember, is the altitude of the spacecraft. We have these two expressions, X_r for the resolution in range and X_a for resolution in azimuth. They are approximately 20 m and 1 or 2 km, respectively.

Let's now review ways to improve the ground resolution. Figure 10 illustrates how to do it. At the top of the figure is the expression that existed before for Δ_r, the change in range distance from 1 resolution cell to the next. In other words, this is the finest resolution you can see on the ground. This expression represents the speed of light divided by the bandwidth or the speed of light times the pulse width. To make Δ_r smaller, there is a constraint. The transmitted energy is equal to peak power multiplied by the pulse width. If the pulse width is too small, then there might not be enough energy in the returned pulse to be detected. There must be a reasonably sized pulse width. One solution is to try different methods of modulation, such as chirping, phase modulation, and various other techniques to improve that range resolution. Most scientists think 10 to 20 m is very useful for most geophysical studies.

Consider how to improve the azimuth resolution. In figure 10, you see that the minimum detectable spacing between adjacent things in the azimuth direction on the ground goes is the altitude times the radar wavelength divided by the size of the antenna. The obvious thing is to do something about either λ (the wavelength) or L (the size of the antenna). If you try to make λ smaller (in regard to microwave) and λ is already pretty small, you can go into millimeter-wavelength radar. The other possibility is to do something about L, the size of the antenna. We will explain this further when we discuss synthetic aperture radar later in this paper.

First, we will discuss Doppler processing. In figure 11, we swing the same radar beam forward. Again suppose that the spacecraft is moving along with the same geometry as we discussed before, only now, instead of this radar beam pointing straight out crosstrack, it's aimed somewhat forward. This was the arrangement used in the SEASAT scatterometer and various proposed scatterometers yet to be flown. On the left of figure 11 is a perspective view, and on the right is a plan view, both of the same thing. Notice the lines of equal Doppler shifts and the lines of equal range on the ground. Now let's consider one area in which we are interested. Look at the bottom portion of figure 11; we can see how we actually form this cell. The lines of equal Doppler are present because of the radar receiver's filter, specified by a Doppler filter response curve with a width equal to the noise bandwidth. There will be other similar ones laid out at different Doppler shifts. When you want to look at objects on the ground that lie between adjacent Doppler lines ("isodops"), you tune them in with the appropriate Doppler filter. Likewise, with time delays you are looking at ground or water between two adjacent range rings, and range is really equivalent to time. A third way to select what you want is to aim the antenna. The half power points might lie at the nulls on either side of the peak, seen also as bold lines at the bottom of figure 11, from the upper right drawing. Also consider that while all of this is happening, the spacecraft has progressed along its orbit so that this cell (which is the instantaneous field of view) becomes smeared. The result of the smeared cell is an irregular hexagonal shape, which is just one cell. There are other cells along the beam, and there might even be other beams. That is how we get Doppler cells on the ground for a real aperture radar.

The antenna beam arrangement for SEASAT's scatterometer was as shown in figure 11, with four beams spaced 90° apart. Each spot on the ocean was sampled twice. First, the forward beam on one side would hit a patch of water, and then the aft beam on the same side would hit it. Therefore, you got two different azimuthal looks at the same patch of water. It turned out that the model function between σ^0 and the geophysically interesting parameters (namely, wind speed, in this case) can give both wind speed and wind direction. Remember, it is the wind that sets up the capillary waves on the water, and that is what the scatterometer was looking at. It was using a 2-cm wavelength, which is related by Bragg scattering to the 1-cm capillary ripples on the water. The model function states that if you have at least two different azimuth looks, you can determine both wind speed and wind direction. It was highly successful even though there were only 3 months of data. Scientists are still analyzing that data 11 years later. Charts of the global distribution of wind vector have been published. Some of them have been on the covers of *Science* and *Aviation Week*. The radar gives you multiple looks at the same patch of water. With a second look, you get wind speed and an ambiguous direction, but the ambiguity is usually 180°, and you have other information that helps you eliminate the ambiguity. The proposal for the next scatterometer after SEASAT, which would have been the Navy Remote Ocean Sensing System (NROSS), was cancelled in 1980. This scatterometer would have had the same four beams, along with a science beam out front, which would have guaranteed that each patch of water that lay along the satellite's subtrack would be hit at all different incidence angles, so that a lot could have been learned concerning dependence on incidence angle.

Now let us consider synthetic aperture radars (SAR's). SAR's enable you to get extraordinarily fine resolution in the azimuth direction with an orbiting radar or even with an aircraft radar. The premise is that in a certain amount of time the beam width of the antenna is repeated along the ground, as shown at the top of figure 12. You can control the overlapping or gapping by regulating the duty cycle of the transmitter. If you set the overlapped distance to 0, then you move a distance in orbit that gives you a distance on the ground such that there is no overlap and there are no gaps. On the other hand, if you deliberately allow overlap, then you get multiple samplings of each small area on the ground. This turns out to be very useful for imaging radars. The real beam width (β) is equal to the wavelength divided by the linear dimension of the antenna. As you can see in the top portion of figure 12, you can get an expression for this script L, which is a synthesized antenna length. Now you can calculate a synthetic beam width (β_s), which is equal to λ divided by this script L instead of the normal L. As the antenna moves along its path in orbit, data must be recorded and the antenna has to be stabilized. The script L becomes the effective dimension of the antenna. If we combine the equations shown in figure 12, then we find that the x_a in the azimuth direction equals half the size of the real antenna, which is really exciting. Now we have an expression that shows that the resolution on the ground in the azimuth direction is down to a few meters. We have both the x_a and x_r down to a few meters. That is the basis of synthetic aperture radar, which affords us all kinds of opportunities for very fine resolution on the ground, in both dimensions!

In figure 13, we describe radar altimeters, which are technically radars. You send out a pulse, and you listen for the echo; it is an active microwave device. Imagine that a pulse is formed and sent to the ground, or to the ocean surface, and you listen for the return. This is just a simple radar or radio altimeter such as those that exist on an airliner or a military aircraft. Altitude is what you want to measure precisely, and it is simply the speed of light or the speed of electromagnetic waves multiplied by the time interval. Actually, you use the time between when you sent the pulse and when you heard the return, divided by two, because it is a complete trip. This measurement is accurate to delta h, which is c times the pulse width divided by 2, which is also c over twice the bandwidth. There are two ways to use radar altimeters. One way is the beam-limited method (shown here in the center); this is used for terrain that varies a lot on the ground. The other way is the pulse-limited method (shown here on the right); this is used for relatively smooth surfaces like the ocean. The question is, then: why don't you use it as beam limited all the time, and not as pulse limited, so that you will always get better resolution on the ground? The reason is, of course, that the beam width is related to the antenna size. Beam-limited requires a longer antenna than pulse-limited, and so if you want to use a smaller antenna and cut down your cost and your stability problems, you need to use pulse-limited. Beam limited is more useful, but pulse limited is cheaper to build and operate.

The altimeter used on SEASAT, flown in 1978, was a simple instrument with which a tremendous amount was learned. That particular instrument was optimized for ocean studies. What was learned about ocean dynamics was substantial because now we have accuracies down in the 50-centimeter range. We can now obtain data for testing all these theories about dynamic heights across the Gulf Stream, where there are just a few meters change in sea surface height across several hundred kilometers.

I've listed in figure 14 some geophysically interesting targets for active microwave; however, this list will never be complete. The SEASAT scatterometer dealt primarily with wind vector over the ocean. Other targets for active microwave are both the extent of ice (whether it's there or not) and the classification of ice into first year or multi-year. In regard to vegetation and snow (the extent and the wetness of the snow), it turns out that microwave radars are very sensitive to the wetness of the snow. These instruments are really good at discerning dry snow from wet snow.

Let's mention some of the advantages of active microwave. Since the target area need not be sunlit, radar is a day-night system. Microwave is also an all-weather (within certain limits) system, since it can, in many circumstances, penetrate clouds. By this statement I mean that if the rain cells are really heavy, then, of course, you have detected rain. But you can't really look through those rain cells; that is why a combined active/passive approach is useful. Another big advantage of active microwave over passive microwave is that you can control the illumination rather than depending upon what the surface emits.

In figure 15, I've listed some trends in space radars. Interferometers allow you to measure the phase difference detected at two different antenna locations that are fairly close together. Knowing the phase difference between the two antennas resolves detail and gives you added opportunity for finer resolution. The term bistatic radar is used when a transmitter is in one location and the receiver is in another. This radar can be two different satellites. We've even had cases in which the transmitter is on a satellite and the receiver is on an airplane that's underflying the satellite. This lets you measure σ^0 as a function of the two different angles, which provides even more information about the scattering surface than you have with just σ^0 of some incidence angle that was the same for both transmit and receive. Anthropologists and Egyptologists can study ancient drainage patterns that are discernible underneath the top layers of sand using active microwave sensors. Inferences are being made concerning ancient civilizations in the Sahara desert. The trend in subsurface sounding of geological formations is to go to even lower frequencies (greater wavelength). According to the formula, the greater the wavelength, of course, the deeper the penetration. Another trend in space radars is combined active/passive methods. This is especially useful in ice classification. NASA Langley Research Center personnel have worked with the Canadian Centre for Remote Sensing to develop in combined active-passive methods to classify ice.

Figure 16 lists technology breakthroughs anticipated in the next few years; these breakthroughs will result in more applications for active microwave. Improved onboard processing of the synthetic aperture radar will be necessary. I mentioned earlier in the definition of σ^0 that the definition for point targets is not really clear and that for calibration purposes it would be useful to have better definitions. In regard to the development of distributive transmitters for large array antennas, we have done quite a bit in distributive receivers and detectors, but we need to do more concerning distributed transmitters. It is also necessary to get more precise control of large antenna surfaces by using methods such as adaptive shaping. The larger the antenna, the more difficult it is to control the surface. Development of "smart" filters is needed to minimize the little smudging and speckling you get in the synthetic aperture radar data. We are extending microwave technology into the millimeter ranges for increased resolution, and taking advantage of certain atmospheric windows.

References

1. Charles Elachi, *Introduction to the Physics and Techniques of Remote Sensing.* Wiley, 1987 (Chapter 6).

2. F. T. Ulaby, R. K. Moore, and A. K. Fung, *Remote Sensing*, Vol. 3, Artech House Inc., 1986.

Radars in Space

Backscatter and Cross Section

- *Overview of capabilities of active microwave devices (radars, scatterometers, interferometers, and altimeters operating from Earth orbit).*
- *Basic concepts and definitions commonly used in radar work.*

Figure 1

Outline

- General radar parameters
- Some basic radar principles
  - Surface scattering
  - Volume scattering
  - Antenna patterns
  - Forming a cell on the ground
  - Real aperture radar & Doppler
  - The Radar Equation
  - How to improve ground resolution
- Applications
  - Synthetic aperture radar
  - Radar altimetry
  - Geophysically interesting targets
- Trends in Space radars
  - Anticipated breakthroughs
- References

Figure 2

Radars in General

You can control: Frequency
Modulation
Polarization
Incidence angle
PRF, Pulse width

You must record:
Position of radar
Look direction of radar
Range to target
Inc. angle at target

Also, other active microwave devices

Then you can figure out:
σ° of target for your chosen or observed conditions

And try to relate σ° to geophysically interesting phenomena
(Soil moisture, wind speed, etc.)

Figure 3

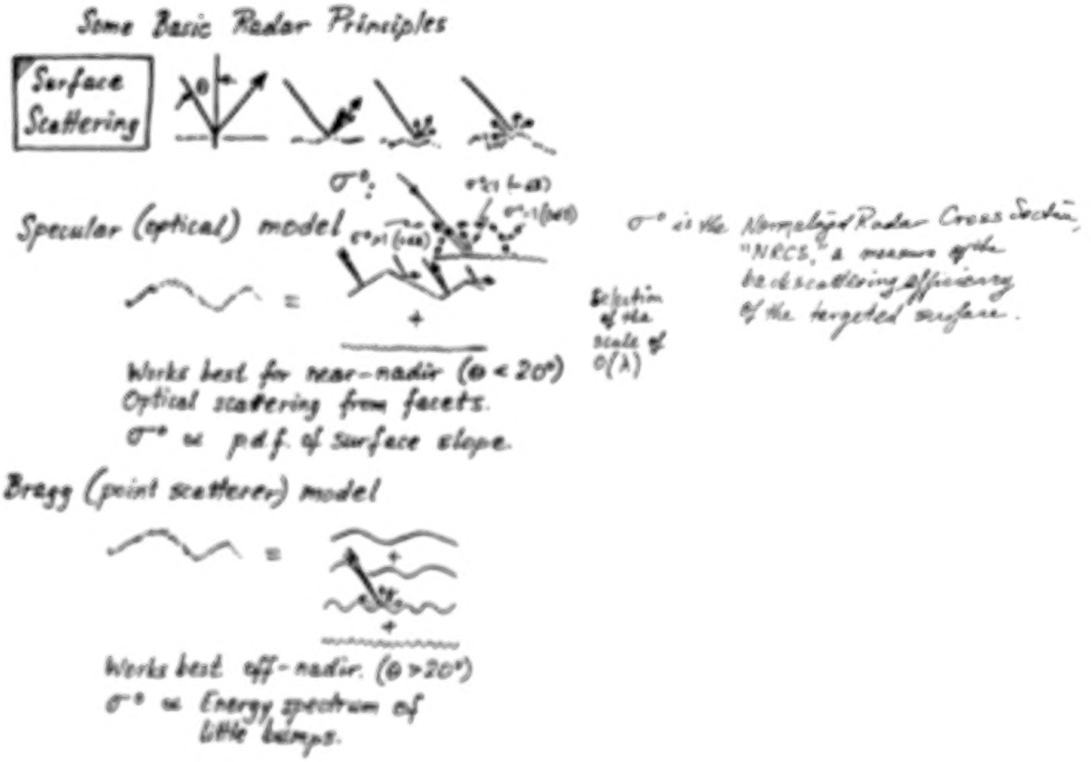

Some Basic Radar Principles

Specular (optical) model

σ° is the Normalized Radar Cross Section, "NRCS," a measure of the backscattering efficiency of the targeted surface.

Selection of the scale of $O(\lambda)$

Works best for near-nadir ($\theta < 20°$)
Optical scattering from facets.
$\sigma^\circ \propto$ p.d.f. of surface slope.

Bragg (point scatterer) model

Works best off-nadir. ($\theta > 20°$)
$\sigma^\circ \propto$ Energy spectrum of little bumps.

Figure 4

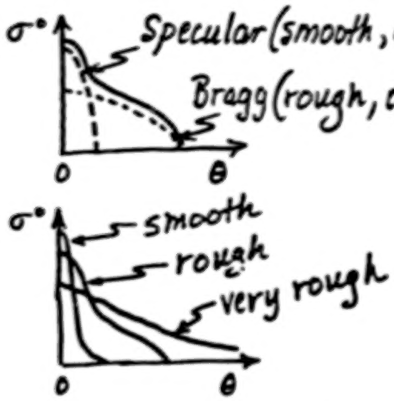

The rougher the surface,
the less the angular dependence.

In practical radar work, the scattering occurs at many angles (sometimes across a continuum of angles), so a mixture of Specular and Bragg scattering is observed.

Notice the moon's reflection on very calm water. It will appear at just 1 angle. But if the water gets rough, the moon's reflection will be smeared over a wide range of angles.

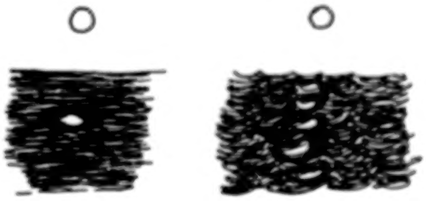

Figure 5

Volume Scattering

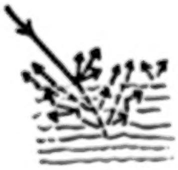

lots of internal reflections + the sfc scatter

Penetration Depth L_p (as in ϵ')

$$L_p = \frac{\lambda}{2\pi\sqrt{\epsilon'}\,\tan\frac{\epsilon''}{\epsilon'}}$$

at typical microwave λ's,

dry soils	1m
very dry sands	10 m
Polar ice sheets	100m

Can sound through:

snow cover (esp. "dry" snow)
tree canopies

Figure 6

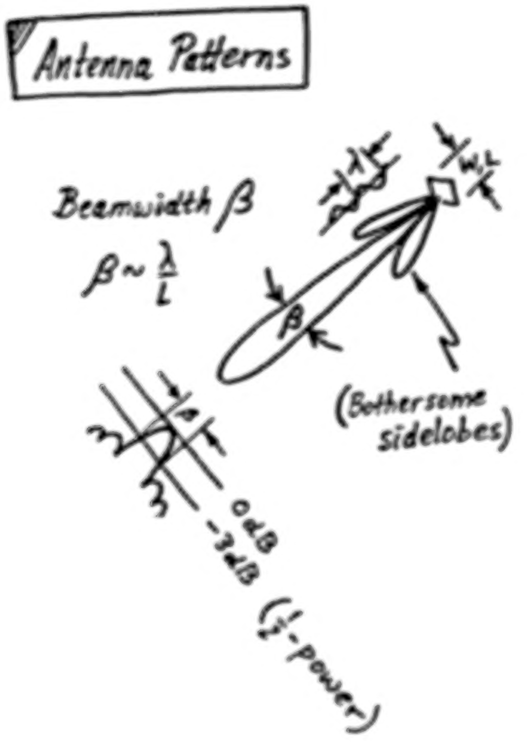
Antenna Patterns
Beamwidth β
$\beta \sim \frac{\lambda}{L}$
λ
W, L
β
(Bothersome sidelobes)
0 dB
-3 dB ($\frac{1}{2}$-power)

Figure 7

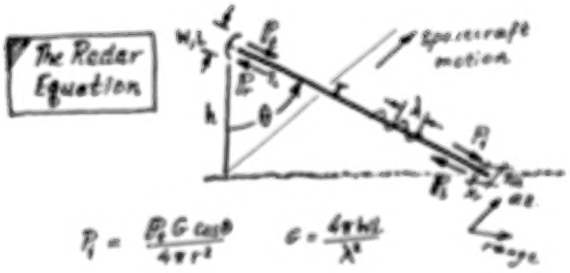
The Radar Equation
W, L
P_t
P_r
h
θ
r
Spacecraft motion
λ
P_1
P_3
X_a
X_r
range

$$P_1 = \frac{P_t G \cos\theta}{4\pi r^2} \qquad G = \frac{4\pi WL}{\lambda^2}$$

$$P_3 = P_1 X_a X_r \sigma^\circ$$

$$P_2 = \frac{P_3}{4\pi r^2}$$

$$P_r = WL P_2$$

$$= \frac{P_t W^2 L c \sigma^\circ \cos^4\theta}{8\pi \lambda h^3 \beta \sin\theta}$$

$$SNR = \frac{P_r}{P_N} = \frac{P_r}{kT\,BW}$$

You know P_t, W, L, c, λ, BW, + β

Keep track of h, θ

Measure P_r ⟶ This is the measurement made by a scatterometer

Solve for σ°

Then model σ° to terrain, water, whatever

Figure 8

Forming a Resolution Cell on the Ground

(No Doppler)

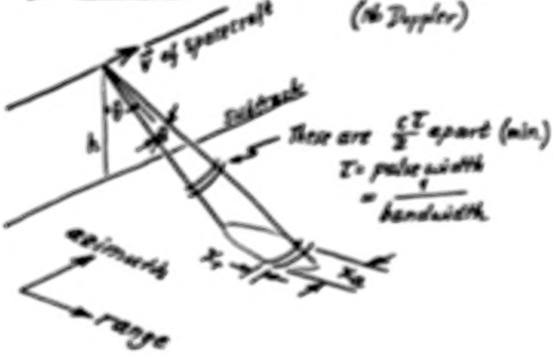
$\vec{v}$ of spacecraft
θ
h
subtrack
These are $\frac{c\tau}{2}$ apart (min)
τ = pulse width
$= \frac{1}{\text{bandwidth}}$
x_r
x_a
azimuth
range

x_r = resolution in range direction

$= \frac{c\tau}{2\sin\theta} = \frac{c}{2\,BW\sin\theta}$ typ. 20 m.

x_a = resolution in azm. direction

$\frac{h}{\cos\theta}$

$= \frac{h\lambda}{D\cos\theta}$ typ. 1-2 km (!)

Note x_r indep. of h.

Figure 9

How to improve ground resolution

x_r : $\Delta r \sim \frac{c}{BW} = c\tau$

$x_r = \frac{c\tau}{2\sin\theta}$

increase BW (decrease τ)
to make Δr smaller

but,
Energy = Peak Pwr × τ

10-20 m anyway

If Energy gets too low,
can't detect return pulse

Solution: Play tricks by
modulating pulse train
(chirping, phase mod, etc.)

1-2 km

x_a : $\Delta a \sim \frac{h\lambda}{L}$

$x_a = \frac{h\lambda}{D\cos\theta}$

Do something about L.

Can increase L by going to Synthetic Aperture Radar (SAR), but 1st let's finish up with real aperture radars.

Figure 10

Real Aperture Radar with Doppler Cells

(Example: Non-imaging Scatterometer)

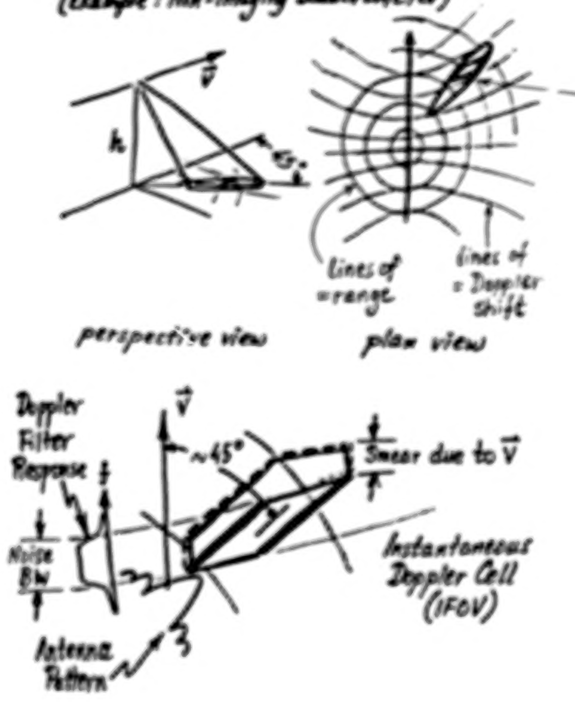
$\vec{v}$
h
x_r
lines of = range
lines of = Doppler shift
perspective view
plan view
Doppler Filter Response
$\vec{v}$
~45°
Smear due to $\vec{v}$
Noise BW
Instantaneous Doppler Cell (IFOV)
Antenna Pattern

This is one of 4 beams (spaced 90° apart in azimuth) used on SEASAT in 1978. A given patch of water would get "seen" by the 2 beams on that side of the spacecraft. The 2 looks would be 90° apart, allowing calculation of both wind speed and wind direction from the one patch of water.

For SEASAT, the IFOV was about 30 × 50 km, and there were about 14 of them in each beam.

Figure 11

Synthetic Aperture Radar (SAR)

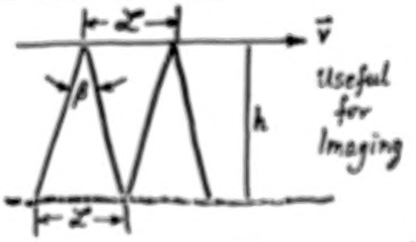
$\mathcal{L}$
$\vec{v}$
β
h
Useful for Imaging
$\mathcal{L}$

There was also a SAR aboard SEASAT. It imaged both terrestrial and oceanic features, down to about 20 m resolution.

Real BeamWidth $\beta = \frac{\lambda}{L}$ Also, $\beta = \frac{\mathcal{L}/2}{h} \Rightarrow \mathcal{L} = \frac{2\lambda h}{L} = 2\beta h$

Synth. BeamWidth $\beta_s = \frac{\lambda}{\mathcal{L}}$ $\mathcal{L}$ = effective ant. length

$\beta_s = \frac{\lambda}{\mathcal{L}} = \frac{L}{2h} \Rightarrow x_a = h\beta_s = \frac{L}{2}$ (Wow!!)

= SAR resolution in azm. direction

Now have $x_a \sim$ a few m, like x_r

SAR Processing: Focused & Unfocused
Focused — phase shift for varying r.
Unfocused — ignore phase shifts $< \frac{\lambda}{8}$

Figure 12

Radar Altimeter

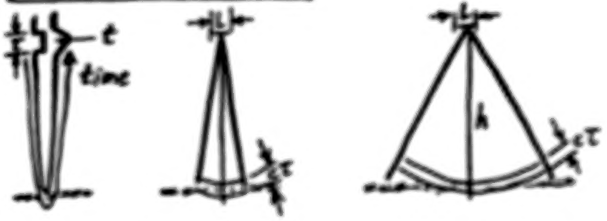

Beam-limited (for varying terrain)

Pulse limited (for smooth surface)

$$h = \frac{ct}{2},$$

accurate to $\Delta h = \frac{c\tau}{2} = \frac{c}{2BW}$

($\frac{1}{2}$m for SEASAT, 1978)

For an Imaging Altimeter,
Use a narrow beam, and
Scan it cross-track (PVO, 1978)

SEASAT also carried a radar altimeter.

Many investigations were conducted in which 2 or more of these active microwave devices were used in combination to extract geophysical parameters that had not been in the original plans for the instruments taken singly.

Also, various combinations of the active devices with the passive, radiometer-type instruments were useful.

Figure 13

Geophysically Interesting Targets for Active Microwave

Wave Structure — water, sand
Geological Faults & Folds
Soil Moisture
Precipitation
Wind Vector over the Ocean
Ice — Extent & Classification
Vegetation
Snow — Extent & Wetness

Advantages of Active Microwave
- Cloud penetration
- Day/Night
- All weather (within limits !!)
- Control of illumination

Figure 14

Trends in Space Radars

Interferometers —
resolve position ambiguities w. 2 antennas
1) range from 1 ant. to target
2) Doppler time series
3) Δrange betw the 2 ant's.
4) Δϕ at 2 ant's resolves detail

Bistatic radars —

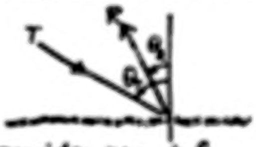

$\sigma^\circ(\theta_T, \theta_R)$ provides new info.
about scatt. surface

Subsurface Sounding — $L_p = \frac{\lambda}{2\pi\sqrt{\epsilon'}\tan\frac{\epsilon''}{\epsilon'}}$
Polar Ice
Ancient drainage patterns
Geologic formations
⇒ Go to lower frequencies (greater λ)

Combined Active/Passive
Ice Classification

Figure 15

Anticipated Technology Breakthroughs

Improved on-board processing for SAR's

Better definitions of σ° for point targets (for calibration)

Development of distributed transmitters for large array antennas

Precise control of large antenna surfaces (adaptive shaping)

Development of smart filters to minimize speckling in SAR's

Extension of microwave technology into millimeter ranges, for increased resolution and to take advantage of atmospheric windows.

Figure 16

N90-27145

LIDAR INSTRUMENTS PROPOSED FOR Eos

William B. Grant and Edward V. Browell
NASA Langley Research Center
Hampton, VA

Introduction

Lidar, an acronym for light detection and ranging, represents a class of instuments that utilize lasers to send probe beams into the atmosphere or onto the surface of the Earth and detect the backscattered return in order to measure properties of the atmosphere or surface. Lidar have been used since the early 1960s, shortly after the invention of the laser, and have become quite useful in a variety of applications. The associated technology has matured to the point where two lidar facilities, Geodynamics Laser Ranging System (GLRS) (Ref. 1) and Laser Atmospheric Wind Sensor (LAWS) (Ref. 2), have been accepted for Phase B studies for Eos. A third lidar facility, Laser Atmospheric Sounder and Altimeter (LASA) (Ref. 1), with the lidar experiment EAGLE (Eos Atmospheric Global Lidar Experiment)* was proposed for Eos. The EAGLE experiment for LASA was not accepted because of the weight and power requirements, and the tunable solid-state laser technology required for gaseous species such as water vapor was judged not yet ready for a long-term space mission.

The generic lidar system has a number of components (Ref. 3). They include controlling electronics, laser transmitters, collimating optics, a receiving telescope, spectral filters, detectors, signal chain electronics, and a data system. Lidar systems that measure atmospheric constituents or meteorological parameters record the signal versus time as the beam propagates through the atmosphere. The backscatter arises from molecular (Rayleigh) and aerosol (Mie) scattering, while attenuation arises from molecular and aerosol scattering and absorption. Lidar systems that measure distance to the Earth's surface or retroreflectors in a ranging mode record signals with high temporal resolution over a short time period.

The overall characteristics and measurements objectives of the three lidar systems proposed for Eos are given in Table 1.

Geodynamics Laser Ranging System (GLRS) (Ref. 1)

GLRS is a lidar system being designed to measure the position of retroreflectors to an accuracy of <1 cm and Earth surface height along the nadir ground track to an accuracy of <10 cm (see Table 2). The retroreflectors will be placed in regions of known seismic activity with easy access for ground teams. Each region, such as along the San Andreas Fault in California, will have a number of retroreflectors whose positions will be measured at regular intervals or during times of seismic activity. It is important to measure the distance to as many retroreflectors as possible at a given time to help reduce errors due to uncertainty in orbit knowledge and variations in the atmospheric index-of-refraction. Two wavelengths will be used to help reduce errors because of refractive index variations.

Topographical measurements will be made primarily over polar ice fields, where it is expected that the smaller ground spot size (60 m) compared to microwave systems will lead to more accurate determinations of snow and ice heights, and hence, the stored water amounts.

In both measurement programs, optically dense clouds between the platform and the target region will render it impossible to obtain signals from the surface. Although there is consideration being given to using GLRS to study cloud properties in addition to the other

---

* E. V. Browell, Eos Atmospheric Global Lidar Experiment (EAGLE) Proposal, submitted to NASA Headquarters, July 15, 1988.

PRECEDING PAGE BLANK NOT FILMED

measurements, when clouds do interfere, it would be better not to operate the lasers so as to prolong the instrument lifetime. The Principal Investigator of the GLRS instrument (S. Cohen, Goddard Space Flight Center) has expressed an interest in having the Information Sciences Experiment System (ISES) acquire and process cloud location data from any available source and relay to GLRS enough to allow GLRS to decide whether or not to attempt to make measurements.

Laser Atmospheric Wind Sensor (LAWS) (Ref. 2)

LAWS is a lidar system being designed to measure tropospheric wind fields (see Table 3). LAWS will use aerosol backscatter at 9.11 microns to determine the horizontal wind components. The lidar will be able to measure the Doppler frequency shift along the line-of-sight by measuring shifts from the local oscillator frequency and using surface returns to correct for the relative motion between the platform and the Earth. The lidar system will scan conically so that it samples a large swath around the ground track, and so that it can acquire returns in two pointing directions to provide enough information to calculate the horizontal wind components, assuming that the vertical component is zero or known. The vertical resolution of LAWS will be about 1 km, with very few photons being received in this interval. It would be useful for the analysis to add any information about the vertical and horizontal distribution of aerosols and clouds in the lower 20 km of the atmosphere in the region of the swath. Winds can change speed and direction with altitude, and regions with different winds may have different aerosol loading. In addition, it would be useful to have information concerning the existence of high-altitude cloud cover, because LAWS cannot penetrate clouds. This information could help extend the operational lifetime of LAWS, because it will probably be limited by the number of laser firings.

Eos Atmospheric Global Lidar Experiment (EAGLE) *

EAGLE was proposed to use the LASA facility for lidar measurements of water vapor, aerosol, and cloud profiles (see Table 4). It was not initially selected for Eos because of the weight and power requirements of the combined system and because the tunable, solid-state laser technology was deemed to be not sufficiently mature for an extended mission in space. However, EAGLE/LASA is discussed here for completeness. Eagle was proposed in a Differential Absorption lidar or DIAL mode for measuring water vapor. In this approach, one laser wavelength is tuned to an absorption line of the molecular species of interest, while the other is tuned nearby but away from absorption by that species. This generally ensures that the difference is due primarily to absorption by the species of interest, rather than to other species or changes in molecular and aerosol scattering with wavelength. A ratio of the backscattered radiation with range is used to determine the density of the species along the lidar line-of-sight. Of course, the non-absorbed wavelength can be used to measure aerosol properties, such as the aerosol vertical profile or cloud top and mixing layer height.

The lidar signal is received as photon counts versus time (range) for each wavelength. In processing the data, the background signal has to be subtracted, and corrections have to be made for range (the signal should decrease as $1/R^2$, where R represents the range to the scattering volume), for modeled atmospheric scattering and extinction. The data must also be checked for the cloud presence. These corrections can be made either on individual returns or on averages of a number of returns, depending on which leads to more accurate results. A number of signals have to be averaged in order to increase the number of measured photons and reduce the statistical error.

---

* E. V. Browell, Eos Atmospheric Global Lidar Experiment (EAGLE) Proposal, July 15, 1988.

References

1. LASA, Lidar Atmospheric Sounder and Altimeter, Eos Instrument Panel Report, Vol. IId, NASA, 1987.

2. LAWS, Laser Atmospheric Wind Sounder, Eos Instrument Panel Report, Vol. IIg, NASA, 1987.

3. R. M. Measures, Laser Remote Sensing: Fundamentals and Applications, J. Wiley & Sons, N.Y., 1984.

TABLE 1. Eos LIDAR* INSTRUMENTS

INSTRUMENT:	GEODYNAMIC LASER RANGING SYSTEM (GLRS)	LASER ATMOSPHERIC WIND SENSOR (LAWS)	Eos ATMOSPHERIC GLOBAL LIDAR EXPERIMENT (EAGLE) ATMOSPHERIC
PLATFORM:	NPOP-1	JPOP	TBD
WAVELENGTH REGION:	1.06 MICRONS 532 nm	9.11 MICRONS	725 nm
MEASUREMENT OBJECTIVE:	PLATE TECTONIC MOTION, EARTH SURFACE HEIGHT CLOUD-TOP HEIGHT	TROPOSPHERIC WINDS	WATER VAPOR, AEROSOLS
MEASUREMENT PRINCIPLE:	SIGNAL VS TIME OF FLIGHT	DOPPLER SHIFT	SIGNAL VS TIME-OF-FLIGHT, DIFFERENTIAL ABSORPTION
HERITAGE:	LAGEOS, MARS OBSERVER	GROUND, AIRCRAFT SYSTEMS	GROUND, LOW-ALTITUDE AIRCRAFT, LASE SYSTEMS

*LIDAR = LIGHT DETECTION AND RANGING

TABLE 2. GEODYNAMICS LASER RANGING SYSTEM (GLRS)

LIDAR SYSTEM PARAMETERS:

LASER:	Nd:YAG (1.06 MICRONS) FREQUENCY-DOUBLED Nd:YAG (532 nm)
PULSE ENERGY:	10 mJ
PULSE REPETITION FREQUENCY:	10 Hz
RECEIVER APERTURE:	30 cm
POINTING FLEXIBILITY:	+/ – 60 DEGREES
POINTING FOR SURFACE HEIGHTS:	NADIR

RETROREFLECTOR ACQUISITION ROUTINE:

INPUT PLATFORM POSITION, ATTITUDE

DIRECT LIDAR TOWARDS CALCULATED POSITION OF RETROREFLECTOR

FIRE LASER

SCAN LIDAR UNTIL RETROREFLECTOR RETURN SIGNAL FOUND

SCIENTIFIC OBJECTIVES:

PLATE TECTONIC MOTION

EARTH CRUSTAL DEFORMATION

POLAR ICE CAP THICKNESS, EXTENT

CLOUD-TOP HEIGHTS

ANCILLARY DATA REQUIRED:

CLOUD COVER

VOLCANIC, EARTHQUAKE ACTIVITY

SYNERGISM:

RADAR ALTIMETER

SAR

TABLE 3. LASER ATMOSPHERIC WIND SENSOR (LAWS)

SYSTEM PARAMETERS

LIDAR	
TELESCOPE APERTURE	1.25 m
FIXED NADIR LOOK ANGLE	45 DEGREES
WAVELENGTH	9.11 MICRONS
LASER	CO_2 WITH O-18 ISOTOPE
PULSE ENERGY	10 JOULES
PULSE REPETITION FREQUENCY	8 Hz
PULSE LENGTH	3-5 MICROSECONDS
TELESCOPE SCAN RATE	6 RPM
CROSS-TRACK REACH	700 km
WIND MEASUREMENT ACCURACY	1-3 m/SEC

USES OF DATA

IMPROVED NUMERICAL WEATHER PREDICTION

IMPROVED UNDERSTANDING OF MESOSCALE SYSTEMS

MORE ACCURATE DIAGNOSTICS OF LARGE-SCALE CIRCULATION AND CLIMATE DYNAMICS

IMPROVED UNDERSTANDING OF GLOBAL BIOGEOCHEMICAL AND HYDROLOGIC CYCLES

ANCILLARY DATA REQUIRED

LARGE REGIONS OBSCURED BY HIGH CLOUDS

AEROSOL VERTICAL DISTRIBUTION (FINE SCALE)

SYNERGISM

OCEAN SURFACE WINDS

STRATOSPHERIC WINDS

AEROSOL, MOLECULAR SPECIES TRANSPORT

TABLE 4. Eos ATMOSPHERIC GLOBAL LIDAR EXPERIMENT (EAGLE)

LIDAR SYSTEM PARAMETERS

LASER:	SOLID-STATE, DIODE-PUMPED
WAVELENGTH:	725 nm
PULSE ENERGY:	1 J
PULSE REPETITION FREQUENCY:	20 Hz
RECEIVER APERTURE:	1.25 m
POINTING:	NADIR

MEASUREMENTS:

AEROSOL VERTICAL PROFILE

MIXING LAYER, CLOUD-TOP HEIGHTS

WATER VAPOR VERTICAL PROFILE (1-km VERTICAL RESOLUTION BY 100–300 km HORIZONTAL RESOLUTION)

USEFUL INPUT DATA:

EXTENT OF CLOUD COVER

SYNERGISM:

MODIS, HIRIS - WATER VAPOR FOR CORRECTION OF SURFACE IMAGES

AIRS - WATER VAPOR VERTICAL PROFILE

LAWS - AEROSOL PROFILES, WIND FIELDS

STATUS:

AWAITING FURTHER TECHNOLOGICAL DEVELOPMENTS IN SOLID-STATE LASERS: LIFETIME, PULSE ENERGY, RELIABILITY, PULSE REPETITION FREQUENCY, BEFORE BEING CONSIDERED FOR A MISSION ON Eos.

N90-27146

Eos VISIBLE IMAGERS

W. L. Barnes
NASA Goddard Space Flight Center
Greenbelt, MD

I am head of the Sensor Concepts and Development Branch, Goddard Space Flight Center. I have been working with the Moderate Resolution Imaging Spectrometer, (MODIS) for nearly 5 years. Dr Wayne Esaias and I initiated the MODIS Instrument Panel in 1984. In the last year or two, the branch has expanded its Eos responsibilities to include the Geoscience Laser Ranging System (GLRS). We are monitoring dual Phase-B studies on both MODIS and GLRS. This paper, however, will examine some of the proposed Eos optical imagers. Table 1 is a list of the imagers and their acronyms. In addition to MODIS-N (Nadir) and -T (Tilt) in the class of facility imagers, there are the High Resolution Imaging Spectrometer (HIRIS) and the Intermediate Thermal Infrared Radiometer (ITIR). Principal Investigator (PI) instruments include the Multi-Angle Imaging Spectrometer (MISR), from JPL, the polarimeter (EOSP), and the Lightening Imaging Sensor (LIS). A summary of these sensors is given in Table 2. In the table, TL/PI refers to the Team Leader for facility instruments and PI is the Principal Investigator.

The spectral range of MODIS-N ranges from 0.4 to 14 microns in some 40 spectral bands. MODIS-T is a true spectrometer with 10-nanometer bandwidth spanning from 0.4 to 1 micron in 64 bands. The Instantaneous Field of View (IFOV) of MODIS-N ranges from 250 to 1000 m. That is not quite true in that the IFOV was 250 to 1000 m when the Eos altitude was 800 km. When it was reduced to 705 km, NASA Headquarters requested that we maintain the same angular IFOV. Therefore, the footprint on the ground is now 214, 428, and 856 m and the swath is 110°. We have maintained MODIS-T at a 1000-m IFOV and 90° swath. HIRIS has 192 spectral bands, 30-m spatial resolution, and approximately a 2° or 24-km swath. The MISR's swath is 200 km and has a 1.7-km IFOV. By cutting down on the swath, the MISR can go to a 200-m IFOV, so there is a way of getting high resolution on an occasional basis. More detail on some of these sensors will be given later. The Earth Observing Scanning Polarimeter (EOSP) has a 10-km IFOV and a 100° swath, which is the same as MODIS-N, and 12 spectral channels.

Marshall Space Flight Center's instrument, the LIS, is a single-channel, 10-km IFOV sensor with a 42° swath, which results in 550 km on the ground. The Japanese ITIR will have 11 bands between 0.9 and 12 microns. With 15- and 60-m resolution, this is the highest resolution imager on Eos. ITIR's swath is either 30 or 75 km and can be varied according to the mission requirements. Lines 8 and 9 of Table 2 show whether or not the instrument can point alongtrack or crosstrack.

MODIS-N is strictly nadir pointing but it scans 2300 km crosstrack so there is no need for crosstrack pointing. MODIS-T does point plus or minus 50° alongtrack. It has a wide swath so crosstrack pointing is not necessary. HIRIS points both crosstrack and alongtrack. This allows it to view any area within the MODIS-N and -T swath. By pointing side-to-side, it can pick out any spot on the Earth within a 2-day period. The MISR instrument does not move; instead, it has 8 cameras with fixed fore and aft pointing angles. None of the other sensors point except the ITIR, which has one fixed-angle pointing channel for stereo data. The data rates presented in the case of MODIS are buffered rates for daylight operation. During the daylight, MODIS-N is putting out about 15 megabits per second. Approximately 40 percent of the

PRECEDING PAGE BLANK NOT FILMED

orbit is in daylight. During the 60 percent that is night, only the thermal channels are output. MODIS-T also operates 100 percent of the daylight with an output of about 7 megabits per second and is shut off at night. There will be stored commands to go from daylight to dark on both instruments. We will also have stored commands on MODIS-T for pointing. That is about all of the commands needed except for turning various channels off in case something happens to them.

__Question__: Will the daylight channels of MODIS-N be turned off during the night portion of the orbit?

I suspect we will leave them on and just reconfigure the output buffer so that we only ingest the nighttime channels.

__Question__: Will the HIRIS channels be turned on only as they are needed?

I do not know about HIRIS, but my guess is that they will leave them on at all times and only select those channels that they want. HIRIS has data restrictions, but I believe they are strictly data volume. I do not believe there is a power problem. HIRIS is limited to about 3.4 megabits per second, long term average, and 10 megabits per second average in any one orbit, which is about a 3 percent duty cycle. The rest of the data rates in Figure 2 are small except for the ITIR, which will output 55 megabits per second due to its high spatial resolution. The PI sensor duty cycles are to be determined, depending on operational constraints.

__Question__: Is MODIS digitized to 10 bits?

No. MODIS-N is 12 bits and MODIS-T is 14 bits. Fourteen bits for MODIS-T is required because of the very high dynamic range needed for it to view both land and oceans, whereas MODIS-N contains separate ocean channels and land channels, each with their individual dynamic range. Therefore, not as much digitalization is needed as is required for MODIS-T. The 14-bit digitizer on MODIS-T could be replaced with a 12-bit digitizer and commandable gain changes, but that approach results in a considerable increase in complexity, and the slight increase in data rate resulting from a 14-bit digitizer was viewed as a small price to pay for the decrease in sensor and operational complexity.

MODIS-T is an imaging spectrometer consisting of a 64-by-64 detector array, a collecting telescope and mirror. A parametric summary, a system schematic, and an optical schematic are shown in Table 3 and Figures 1 and 2, respectively.

__Question__: What is the spectral range and bandpass of the 64 channels of MODIS-T?

They are nominally 10-ns wide and range from 0.4 to 1.04 micrometers. They probably will not be exactly 10 nm, but will be closer to 9.8 nm depending on the final design. It is very much like HIRIS, the spectrometer that spans the visible near infrared (NIR) and shortwave infrared (SWIR) spectrums.

__Question__: Will channels be selected on-board for transmission to the ground?

Earlier in the design phase, we decided that rather than trying to pick out channels and send them down, it would be easier to send them all and sort them out on the ground. The biggest requirement from the instrument panel was 17 channels for ocean bioproductivity. The ocean scientists had a reason for each of the 17 channels and at one time we considered a sensor with 17 maximum channels. With the spectrometer approach, it was deemed simpler to transmit all channels.

Question: Is the MODIS spatial resolution constant across the swath?

There is no attempt to make a constant IFOV cross-scan. We selected a whiskbroom scanner that expands the IFOV as we go crosstrack, resulting in 2 1/2-km pixels near the ends of the swath.

Question: What are the system drivers for MODIS-T?

The absolute accuracy of 2 percent is very tough; nobody has ever done that. We also have a very strong requirement that the instrument not polarize incoming, unpolarized radiance any more than 2 percent at all scan and tilt angles. That is equally tough.

MODIS-N is an imaging radiomonitor, not a spectrometer like MODIS-T, with 250-m spatial resolution in two channels, 500 m in 12 channels and 1000 m in 20 channels. We are also looking at expanding two of the channels' dynamic ranges so that we can look at fires. Ordinarily they would saturate, if there is any appreciable area of fire in the pixels. By looking at the amplitude, one can determine what part of the pixel is covered by the hot object. The range expansion will be attained using nonlinear digitalization. We keep a total of 12 bits but make the upper bits (higher temperatures) respond at a lower gain.

Question: Will MODIS be capable of measuring the thermal signature of power stations?

Probably, since the temperature resolutions are around 0.05°. If the power station outflow is spread over a 1-km pixel it will probably raise the temperature a tenth of a degree or more. It is difficult because it will integrate the output over the 1-km pixel.

Question: Does MODIS operate at night?

Yes, you can see a lot in the thermal bands at night. It is going to be the same or better than Advanced Very-High-Resolution Radiometer (AVHRR).

MODIS-T is basically an ocean color instrument because of its tilting capability. The primary goal of MODIS-T is to measure global ocean color. There are also eight ocean color channels in MODIS-N that allow it to pick up some of the data missed when MODIS-T is changing tilt angle. During that tilt maneuver, MODIS-T misses a large amount of data. MODIS-N will be able to acquire data from that side of the swath which is not contaminated by glint. MODIS-N also has most of HIRIS channels and will be able to gather data for moisture and temperature profiles. The sounding data will be at 1-km spatial resolution, which has never been done. This will allow the atmospheric scientists to examine severe storms at a spatial resolution unavailable previously.

Question: What is the major improvement in sounding when comparing HIRIS to MODIS-N?

HIRIS samples every 14 km, while MODIS-N will develop a 1-km resolution sounding image.

Question: At 1-km resolution, can the thermal channels detect hot spots such as forest fires?

There is going to be some confusion. That is, a warm city and a small fire may be indistinguishable. They average out and you won't be able to tell the difference.

Question: But, won't you be able to distinguish by location?

Yes, if you are out over the rain forest in Brazil and you see something hot, you can be pretty sure that somebody is burning forest. However, if you are over New York City, it could be someone burning New York City.

Table 4 lists HIRIS functional parameters. HIRIS is an imaging spectrometer that covers the spectral range from 0.4 to 2.5 micrometers in 192 bands, with 3 sets of 64 bands in each spectrometer. The spectral resolution will vary because they are using prisms, which change dispersion with wavelength. The pointing, as shown in Table 4, is +52 and -30° alongtrack, and crosstrack is ±26°. The 280-MBPS output rate is determined by the Tracking and Data Reply Satellite System (TDRSS) high data rate limitation of 300 MBPS. HIRIS will enable a variety of remote sensing sciences. The main reason is that in the 2- to 2-1/2 micrometer spectral region, there are numerous features that allow one to identify geological features. Dr. Goetz has been working in that area for a long time using aircraft instruments, including Infrared Imaging Spectrometer (IRIS) and Advanced Visible Infrared Imaging Spectrometer (AVIRIS) that are out of JPL. For accurate calibration, the scientists want the sensor to look at onboard solar diffuser targets, the Moon, onboard lamps, absolute detectors, and instrumented ground targets. One must use as many techniques as possible to get the absolute calibration to below 5 percent and, hopefully, as low as 2 percent.

Table 5 lists some of the attributes of the MISR, a PI instrument developed by JPL. Figure 3 shows a conceptual view of MISR. The system consists of 8 cameras with 4 pointing ahead and 4 pointing aft. The pointing angles are 25, 46, 60 and 72.5°. Each camera has 4 spectral bands with wavelengths from 0.4 to 0.86 micrometers. The main purpose of MISR is to develop atmospheric corrections for the Eos users.

Additional uses for MISR include cloud classification, cloud structure, etc. The spatial resolution is ordinarily 1.7 km, a bit coarser than MODIS.

Question: Will MISR be used mainly to support HIRIS?

No, because HIRIS has 30-m spatial resolution, and MISR a 1700-m resolution. MISR will be used to correct the wide field scanners, like MODIS using wide field atmospheric corrections. Nobody has been able to perform quality atmospheric corrections routinely except over the oceans for ocean color corrections. Atmospheric corrections over land are difficult.

The Eos photopolarimeter, shown in Figures 4, 5, and 6, is a low-risk instrument with 12 spectral bands going from 0.4 to 2.2 microns with 10-km spatial resolution. The scanner consists of two mirrors that cancel out the polarization caused by the scanner. The mirrors cross in such a way as to cancel the polarization from the scan system. Polarization caused by the scan mirror is a problem, and EosP has solved that problem. An instrument similar to EosP has flown to Mars. Two or three of these have flown on planetary probes. They are well developed and are, therefore, rather low risk. The problem with polarization measurements is that both the atmosphere and the ground polarizes, and the sensor is looking at both. The observer has to separate them, which is difficult. However, it may be possible to separate the two components by examining the spatial scale of the ground signal compared to that of the atmosphere.

The ITIR is interesting because it is a high-resolution thermal instrument (see Table 6). Dr. Anne Kahle of JPL has been working with an airborne sensor called TIMS and has proposed TIGER, which is the Eos version of TIMS. She has been selected to incorporate some of her thoughts and some of her results into the Japanese ITIR. She has gone to Japan to disuss this. It remains to be seen what ITIR will look like after incorporating some of the TIGER channels.

MODIS-T is basically finishing up Phase B. The Phase-B studies of MODIS-N with Perkin Elmer and SBRC will be completed in July 1989. The Phase-C/D RFP will be released in November and hopefully MODIS-N will be under contract within 10 months to 1 year after that, which would result in a start in October 1990, which coincides with the proposed Eos FY91 new start.

Question: Where will the Eos data be processed?

The ground rules under which we are operating are that all the processing through Level 1 will be done at the Eos Data Information System (EosDIS). In the case of MODIS, the 24 Science team members are supposed to supply Level 2 and 3 algorithms ready for use by EosDIS. However, we are working hardest on trying to calibrate and locate the data for Level 1 to make sure that it is the best it can be and then, if somebody wants to take Level 1 data and do their own Level 2 and/or Level 3 products at their own facility, fine. Our major concern is to get to Level 1.

Question: How will HIRIS limit their output to 280 MBPS?

They are going to do two things: channel selection and swath width selection. They will narrow the swath to less than the present 24 km. The swath is viewed by four butted detector arrays. On command, the outer arrays can be deleted, resulting in a 12-km swath. In some cases, all channels can be viewed over a narrow swath or in other cases, a few channels can be imaged over the full 24 km. The data from MODIS-N and -T are approximately 700 gigabits a day. MODIS generates more data than HIRIS because of its 100-percent duty cycle. The MODIS data volume is 600 computer tapes a day for 15 years. The HIRIS duty cycle is only about 3 percent. The total for all of Eos is a Terabit a day. MODIS is a big part of the total. An optical disk juke box holds 48 twelve-inch optical disks. MODIS fills up one of these each week. GSFC management has requested a building of 150,000 square feet for EosDIS, of which 50,000 square feet is to store data. A 150,000 square foot building will be one of the largest buildings at GSFC.

Question: Does MODIS process the data onboard?

We have been asked to packetize the data. In addition to packetization, we must buffer the data and send it to the data system on the platform. How we do that is left up to us, and we are trying to arrive at a design now. For instance, we would like for each packet to contain only one channel with an identifier so that the data stream on the ground can be examined and a given channel extracted.

Question: How do MODIS and HIRIS interact?

There has been some synergism studies. There is interest in the ground data systems as to what parts are common between HIRIS and MODIS, and whether there are possible savings. There probably are, and we have tried to look at this commonality. We have had some meetings between Dr. Goetz and the MODIS people, and he was on the MODIS Instrument Panel. If there is any onboard coordination it probably should be at the HIRIS end, since MODIS runs 100 percent of the time, and it will be up to HIRIS to grab the required data. Once the MODIS data gets to the platform, if HIRIS wants to route part of it through the LAN to HIRIS, this is possible. But I don't know if it has been requested.

Question: How would an instrument PI on Eos go about getting data from another sensor on the platform?

He would have to make a request to the Eos project, and I don't know of anyone who has done this at this time.

Question: How are the sensors controlled on the platform?

The platform has a large number of stored commands. How they distribute those commands is to be determined.

Question: How does an experimenter interact with the EosDIS data set?

The experimenter is supposed to be able to dial up the system, find out what data is available, and find where the data is. How the data will be distributed to the experimenter is to be determined. Possibly, they will distribute the data over the wire, or they will use the mail system. There will be a lot of routine data products and I think I will leave it to Dr. Esaias to talk to some of those. But, if you are looking for a weekly average of a parameter, EosDIS may be generating that and it may send it to you in a composite form once a month. You can ask for a routine distribution of that type of data and they will probably mail it to you. In some ways that is still to be determined. The Eos Project is in the middle of Phase-B studies for EosDIS and they have a structure review in the next month or two where they will start laying out what the hardware looks like and how they are going to use it.

Question: How long will it take for EosDIS to process the data?

They advertise 48 hours to Level 1 and 48 more hours to Level 2 and 3.

Question: Will all of the data be processed in these time periods?

It turns out that it is not very realistic if you need a second instrument's data to help generate it. In other words, if you need HIRIS data to make a data product from MODIS, you are going to have to wait 48 hours or 96 hours for the HIRIS Level 3 to come out and feed it back into the MODIS data. If all the data you need is from your instrument and you don't need outside data, even though it may be routinely available, then the 48- and 96-hour times are probably realistic.

Table 1. Eos Optical Imager Acronyms

Facility Imagers

MODIS-N	Moderate Resolution Imaging Spectrometer-Nadir
MODIS-T	Moderate Resolution Imaging Spectrometer-Tilt
HIRIS	High Resolution Imaging Spectrometer
ITIR	Itermediate Thermal Infrared Radiometer

Principal Investigator Imagers

MISR	Multi-angle Imaging Spectro-Radiometer
EOSP	Earth Observing Scanning Polarimeter
LIS	Lightning Imaging Sensor

Table 2. Summary of Eos Optical Imagers

	MODIS-N	MODIS-T	HIRIS	MISR	EOSP	LIS	ITIR
TL/PI	V. Salomonson	V. Salomonson	A. Goetz	D. Diner	L. Travis	H. Christian	A. Ono
Sponsor	GSFC	GSFC	JPL	JPL	GSFC	MSFC	Japan
Spectral Range (μm)	0.4-14	0.4-1.0	0.4-2.5	0.4-0.9	0.4-2.3	0.8	0.9-12
Bands	40	64	192	4	12	1	11
IFOV (m)	1000, 500, 250	1000	30	1730	1x10^4	1x10^4	15, 60
Swath (degrees)	110	90	2	30	110	42.4	2.5, 6
Swath (km)	2330	1500	24	210	2330	550	30, 75
Pointing							
Alongtrack	N	Y	Y	Y	N	N	Y
Crosstrack	N	N	Y	N	N	N	N
Data Rate (MBS)	15	7	280	2	0.08	0.003	55
Duty Cycle (%)	100	100	3	TBD	TBD	TBD	TBD

Table 3. MODIS-TILT (T) Summary

PARAMETERS	EXPECTED PERFORMANCE
PLATFORM ALTITUDE	705 KM
IFOV	1.4 MRAD (1KM)
SWATH	90 DEG/1500 KM
SPECTRAL BANDS (10 NM WIDTH)	64 (O.4-1.04 MIC.) (AREA ARRAY)
RADIOMETRIC ACCURACY (ABS) (GOAL)	+/- 2% MAX
POLARIZATION SENSITIVITY	2% MAX < 700 NM 4% MAX > 700 NM
MODULATION TRANSFER FUNCTION	0.3 AT NYQUIST (SPEC)
S/N PERFORMANCE (SPEC) (70 DEGREE SOLAR ZENITH)	500:1(405 NM) 300:1(625 NM) 150:1(825 NM)
QUANTIZATION	14 BIT
SCAN EFFICIENCY	50 %
INTEGRATION TIME	4 MSEC
COLLECTING APERTURE (DIA)	50 MM
OVERALL DIMENSIONS (APPROX)	TBD
WEIGHT	TBD

Table 4. HIRIS Functional Parameters

DESIGN ALTITUDE	705 KM
IFOV	30 M
SWATH WIDTH	24 KM
SPECTRAL COVERAGE	0.4 - 2.5 UM
AVERAGE SPECTRAL SAMPLE INTERVAL	
0.4 - 1 UM	9.4 NM
1 - 2.5 UM	11.7 NM
POINTING	
ALONG-TRACK	+52°/-30°
CROSS-TRACK	+26°/-26°
ENCODING	12 BITS/PIXEL
MAXIMUM INTERNAL DATA RATE	405 MBPS
MAXIMUM OUTPUT DATA RATE	280 MBPS
IMAGE MOTION COMPENSATION	GAIN STATES OF 1 (OFF), 2, 4 AND 8

Table 5. MISR Instrument Description

- **8 separate multispectral pushbroom cameras providing 8 different viewing geometries**
  - View angles: [illegible] and 72.5° both fore and aft of nadir
  - Spectral bands: (1) 443 nm (2) 550 nm (3) 670 nm (4) 860 nm
- **Refractive camera design**
- **High dynamic range and high signal-to-noise ratio obtained using a mosaicked 4 x 2048 pixel CCD detector array in each camera**
- **Redundant absolute calibration using**
  - Deployable solar diffuser panel (the only moving instrument part)
  - Stable self-calibrating [illegible] photodiodes

Mass: 75 kg Volume: 0.5 m³ Power: 77 W avg, 95 W peak

- **Scenes composed of 32 images**
  - [illegible]
  - Data frame [illegible] 210 km [illegible] x 134 km (downtrack)
- **Uniform ground sample spacing and cross-track resolution obtained at all view angles**
- **Continuous daylight observations of the entire Earth without coverage gaps accomplished every 16 days**
- **Instrument normally operated in Global Mode (222 kbps output)**
  - 1.73 km resolution
  - 60 contiguous frames from pole to pole
- **Selected targets observed in Local Mode (2 Mbps output)**
  - 216 m resolution
  - Normally a single frame interspersed among Global Mode frames
  - Approximately 6 targets observed per day
- **Calibration observations of deployable diffuser plate acquired near north and south poles about once per month**

Table 6. ITIR

Science Objectives

- Global observation of surface geology with spatially and spectrally high resolution.

Instrument Description

1) Multiple bands over wide spectral region

   1 NIR band
   5 SWIR bands
   5 TIR bands

2) Pushbroom scanning with linear array detectors.

3) Spatial Resolution

   15m (NIR & SWIR), 60m (TIR)

4) Stereoscopic viewing in the NIR.

Technical Parameters:

MASS:	290Kg
VOL:	0.96 m^3
POWER:	650W (peak)
DATA RATE:	52.2 Mb/s (peak)

Measurements:

- NIR - image and aerosol calibration.
- SWIR - mineral resources.
- TIR - mineral resources and water vapor calibration.
- Spectral Resolution: 0.5µm
- Swath: 30 or 75 km

NIR: 0.85 - 0.92µm
SWIR: 1.60 - 2.36µm
TIR: 3.53 - 11.70µm

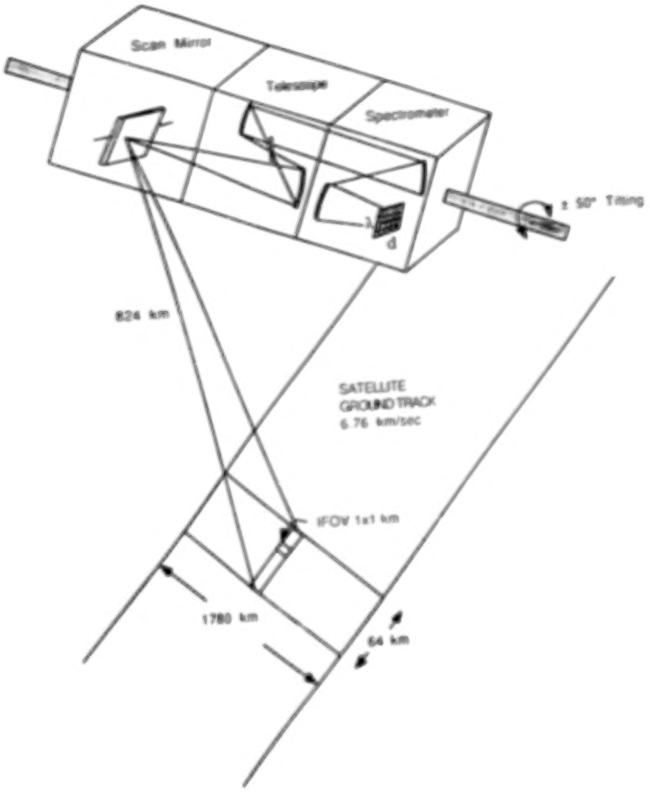
Scan Mirror
Telescope
Spectrometer
± 50° Tilting
λ
d
824 km
SATELLITE
GROUND TRACK
6.76 km/sec
IFOV 1x1 km
1780 km
64 km

Figure 1. MODIS-T Optical Concept.

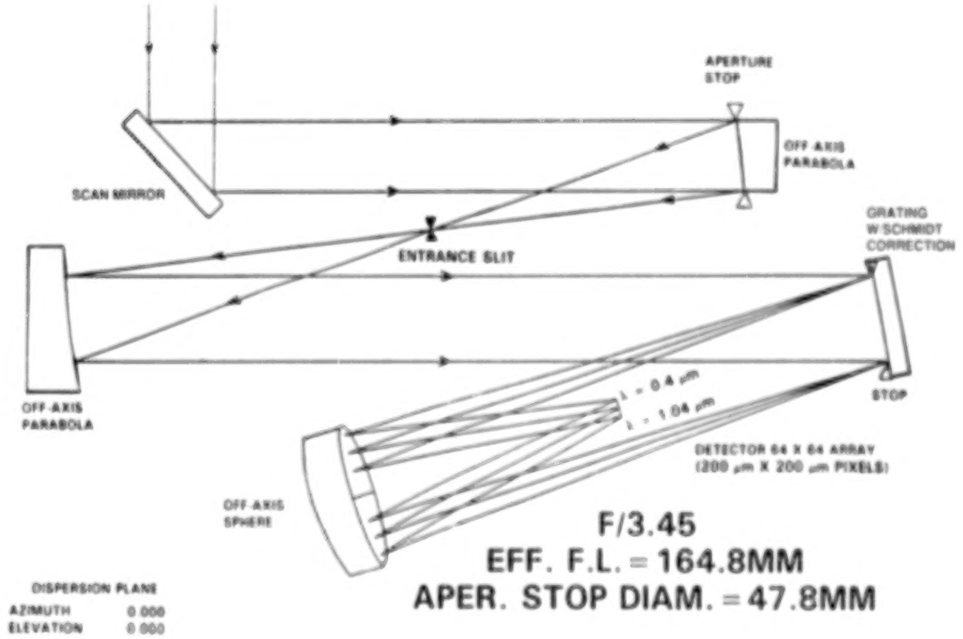
APERTURE
STOP
OFF-AXIS
PARABOLA
SCAN MIRROR
ENTRANCE SLIT
GRATING
W/SCHMIDT
CORRECTION
OFF-AXIS
PARABOLA
STOP
λ = 0.4 μm
λ = 1.04 μm
DETECTOR 64 X 64 ARRAY
(200 μm X 200 μm PIXELS)
OFF-AXIS
SPHERE
F/3.45
EFF. F.L. = 164.8MM
APER. STOP DIAM. = 47.8MM
DISPERSION PLANE
AZIMUTH 0.000
ELEVATION 0.000

Figure 2. MODIS-T Optical Design Grating-Type Reflecting Schmidt.

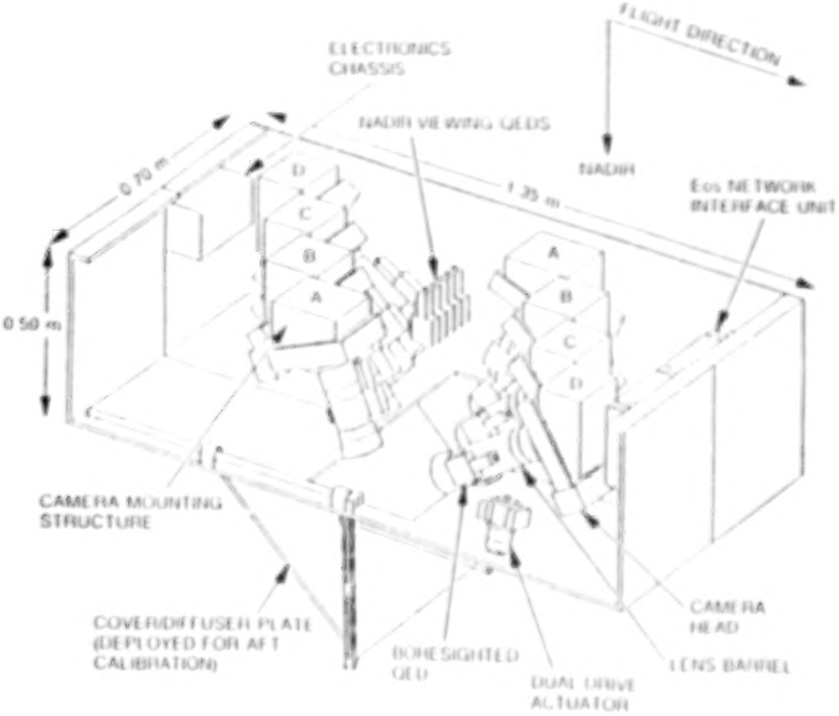
ELECTRONICS CHASSIS
FLIGHT DIRECTION
NADIR VIEWING QEDS
NADIR
0.70 m
1.35 m
Eos NETWORK INTERFACE UNIT
0.50 m
D
C
B
A
A
B
C
D
CAMERA MOUNTING STRUCTURE
COVER/DIFFUSER PLATE (DEPLOYED FOR AFT CALIBRATION)
BORESIGHTED QED
DUAL DRIVE ACTUATOR
CAMERA HEAD
LENS BARREL

Figure 3. MISR Instrument.

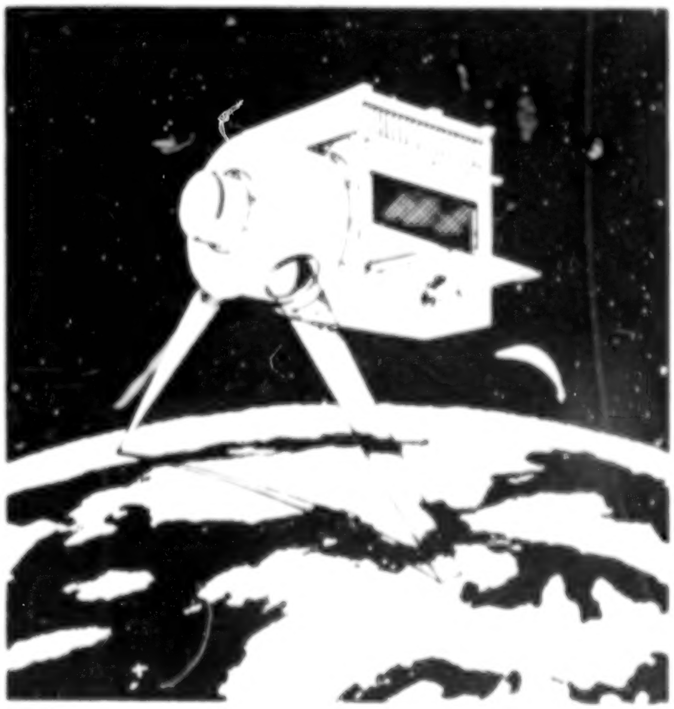

- **KEY MEASUREMENTS:**
  - CLOUD MAPS: OPTICAL THICKNESS, PARTICLE SIZE AND CLOUD TOP PRESSURE
  - AEROSOL MAPS: GLOBAL DISTRIBUTION AND OPTICAL THICKNESS
  - POLARIMETRY INFORMATION FOR VEGETATION AND OTHER LAND SURFACE RESEARCH
- **CORRECTION PARAMETERS FOR EOS**
  - MAPS KEY INPUTS FOR ATMOSPHERIC CORRECTION MODELS
    - SINGLE SCATTERING ALBEDO
    - MEAN PARTICLE SIZE
    - REFRACTIVE INDEX AEROSOL OPTICAL THICKNESS
  - COMPLETE ALGORITHMS USABLE DATA TO BE DEVELOPED FOR SCIENCE COMMUNITY
- **LOW-COST, LOW-RISK COMPLEMENT TO EOS FACILITY SENSORS**
  - 12 VISIBLE, NEAR AND SHORT IR BANDS
  - PROVEN TECHNOLOGY FROM PREVIOUS FLIGHT PROGRAMS
  - 0.03 m, 11 kg SENSOR ENVELOPE, 11W OPERATING POWER AND 88 kbps PEAK DATA RATE
  - 55 SCAN, 10 km IFOV

Figure 4. Earth Observing Scanning Photopolarimeter (EOSP) Offers Key Eos Measurements as Well as Correction Parameters for Other Sensors.

RELIABILITY BY DESIGN

- ± 0.1% POLARIMETRIC ERROR (SIMULTANEOUS 0°/90° AND 45°/135° POLARIZATION COMPONENTS MEASUREMENT)
- INSENSITIVITY TO DETECTOR DRIFT (INTERCHANGEABILITY OF DETECTORS FOR ORTHOGONAL COMPONENT MEASUREMENT)
- GLOBAL COVERAGE/WIDE PHASE ANGLE RANGE (LIMB-TO-LIMB SCAN)
- SMALL INSTRUMENT POLARIZATION (COMPENSATED TWO-MIRROR SCAN SYSTEM)
- < 3% ABSOLUTE CALIBRATION ERROR (INFLIGHT CALIBRATION)
- 12 BANDS SELECTED FOR MAXIMUM SENSITIVITY TO CLOUD AND AEROSOL FEATURES (410, 470, 555, 615, 675, 750, 880, 950, 1250, 1600, 2050, AND 2250 nm)

KEY COMPLEMENTARY MEASUREMENTS

- CLOUD PARTICLE SIZE MEASUREMENT (2.25 μm)

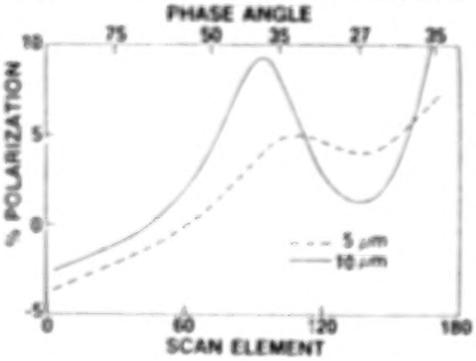

- AEROSOL OPTICAL THICKNESS IN CLOUD-FREE REGIONS
  - BASED ON INVERSE RELATION BETWEEN POLARIZATION DEGREE AND AEROSOL OPTICAL THICKNESS
  - ACCURACY RELATIVELY INSENSITIVE TO ABSOLUTE RADIOMETRIC ERROR

Figure 5. EOSP Offers a Highly Reliable Complement to Eos Facility Sensors.

- *SCAN-METHOD:* POLARIZATION COMPENSATED TWO-MIRROR OBJECT-SPACE SCAN
- *SCENE FLUX COLLECTION:* EIGHT BORE-SIGHTED 1 cm APERTURE, f/5 REFRACTIVE TELESCOPES
- *SPECTRAL SEPARATION:* DICHROIC BEAMSPLITTERS
- *POLARIZATION:* CALCITE WOLLASTON PRISMS IN EACH TELESCOPE ASSEMBLY
- *DETECTION:* SI PHOTODIODES AND 165K PV HgCdTe DETECTORS
- *COOLING:* PROVEN SINGLE-STAGE RADIATIVE COOLER

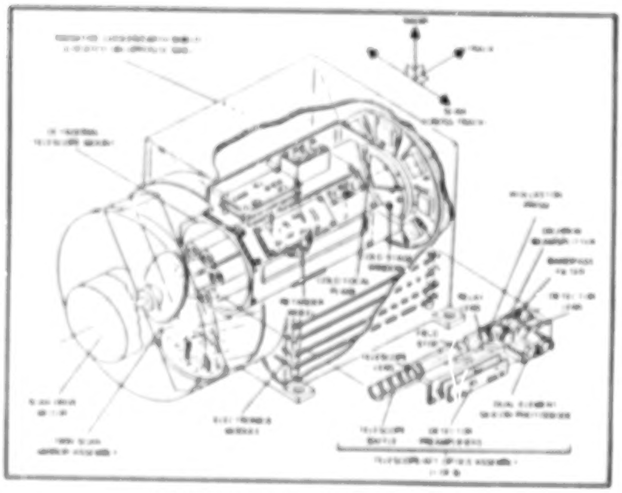

CUTAWAY VIEW OF EOSP

Figure 6. Low Cost and Risk Hardware Design Uses Flight-Proven Technology.

N90-27147

SAGE III: A VISIBLE WAVELENGTH LIMB SOUNDER

W. P. Chu, M. P. McCormick, J. Zawodny, and L. R. McMaster
Atmospheric Sciences Division
NASA Langley Research Center
Hampton, VA

ABSTRACT

This paper will present a brief description of the SAGE III (Stratospheric Aerosol and Gas Experiment III) instrument that has been selected to fly onboard the National Polar Platform I (NPOP I) for the Earth Observational System (Eos) in 1996. The SAGE III instrument will perform earth limb sounding with the solar occultation technique measuring the ultraviolet (UV), the visible, and the near infrared (IR) wavelength solar radiation. The instrument will produce atmospheric data for the vertical distribution of aerosol, ozone, nitrogen dioxide, water vapor, and oxygen. The details of the instrument design, data flow, and processing requirements will be discussed here.

INTRODUCTION

The SAGE III instrument is part of a long heritage of space flight instruments that performed solar occultation measurements for remotely sensing the earth's atmosphere. The simple SAM (Stratospheric Aerosol Measurement) instrument was flown onboard the Apollo capsule during the Appollo-Soyuz Test project in 1975 (Pepin et al., 1977). SAM II was launched onboard the Nimbus 7 platform in 1978 (McCormick et al., 1979) and has operated continuously ever since. SAGE I was launched on the AEM II spacecraft in 1979 and operated for almost three years until the spacecraft malfunctioned in 1981 (McCormick et al., 1979). SAGE II was launched in 1984 on the Earth Radiation Budget Satellite (ERBS) platform (Maudlin et al. 1985) and is still operating flawlessly. SAGE III is currently being proposed for the NPOP I and the space station attach payload missions during the Eos mission in 1996. The instrument design has evolved from the simple one-channel SAM instrument with a hand-held pointing system to the sophisticated seven-spectral-channels sun photometer with spectral grating optics, automatic sun acquisition electronics, and mechanical scanning capability of the SAGE II instrument. The SAGE III instrument will expand on the experience and technology advances gained from previous SAGE missions to perform earth limb sounding with the solar occultation approach.

MISSION OBJECTIVES

The scientific objectives of the SAGE III experiment are to produce geophysical data on the vertical distribution of the key species in the upper atmosphere such as ozone, aerosol, water vapor, nitrogen dioxide, and oxygen; and to provide a long-term data base on these species for trends monitoring. The remote sensing approach is solar occultation. The major advantage of solar occultation measurements is that the instrument can be made to be almost totally self-calibrating. Both the radiance throughput and the spectral radiance response of the instrument can be calibrated against the solar radiation immediately during each measurement event, be it a spacecraft sunrise or sunset measurement. The fundamental measurements from the SAGE III instrument will be the ratio of solar radiance. The ratio of solar radiance is attenuated by the earth's limb to the unattenuated solar radiance values. Therefore, only relative radiance measurements are required and the requirement for absolute radiance measurement is totally relaxed. The spectral locations of the nine channels of the SAGE III instrument are illustrated in figure 1 together with the relative contribution of extinction by the various atmospheric species at a height of 18 km. Of the nine channels of SAGE III located at 310, 385, 450, 525, 600, 760, 940, 1020, and 1550 nm, the channels at 310 and 600 nm are for ozone measurement extending the altitude range from 5 km up to 90 km height. The channel at 450 nm is for nitrogen dioxide measurements; the channel at 940 nm is for water vapor measurement; the channel at 760 nm centering at the oxygen A band is for oxygen measurement; and the rest of the seven channels are for aerosol remote sensing.

PRECEDING PAGE BLANK NOT FILMED

INSTRUMENT DESCRIPTION

The SAGE III instrument as currently envisioned will be similar in design as the other SAGE instruments. Figure 2 shows the schematic of the sensor part of the instrument consisting of the scan head, telescope, and the spectrometer and detector subsystem. The scan head is made up of an elevation scan mirror that can scan both in elevation and azimuth, together with a sun tracker sensor for pointing and solar tracking. Incoming solar radiation is reflected by the scan mirror into the F/2 telescope to form the scanned image of the solar disc on the focal plane. A circular aperture limiting the view angle to a circular cone of one arc minute full angle at the focal will define the instrument's field of view. The same aperture also serves as the entrance slit to the spectrometer and detector subsystem. The spectrometer and detector subsystem consists of a stigmatic imaging concave reflection grating which can form a flat field image of the earth's limb spectrum on the 512-element silicon CCD detector array. The CCD detector array, in combination with an order-sorting segmented interference filter, measures the disperse radiation in three separated orders. As illustrated in figure 3, the CCD detector array measures first-order diffracted light from 280 to 800 nm, and from 910 to 1070 nm; second-order diffracted light from 410 to 455 nm; and third-order diffracted light from 356 to 400 nm. The IR channel centered at 1550 nm is situated at the grating zero order diffraction with a separate interference filter and discrete InGaAs detector. Each CCD pixel in the first order can produce 2-nm spectral resolution. In the second order, it can produce 1-nm spectral resolution. The broadband channel output of such channels as 1, 2, 4, 5, and 8, is obtained by electronically summing the appropriate adjacent pixel output for the desired spectral bandwidths. The fine spectral resolution channel output for NO_2, H_2O, and O_2 at 450 nm, 940 nm, and 760 nm, respectively, are obtained from electronically addressing the 20 individual pixels in each of these spectral bands.

SAGE III DATA ACQUISITION AND PROCESSING

The data acquisition operation for the SAGE III instrument will be similar to the previous SAGE instruments described by Chu and McCormick (1979). During a spacecraft sunset event, the instrument will slew in azimuth to acquire the sun. As soon as the sun sensor indicates that the sun is in the instrument's field of view, the scan mirror will scan in elevation until a full sun scan is obtained. During this time, several full-up scans will be obtained for the unattenuated solar limb profiles, while the solar Fraunhofer line positions will be monitored for subsequent wavelength calibration. The scan mirror will continue the elevation scanning across the solar disk until the sun is set beyond the horizon. Then the instrument will automatically shut off. For a sunrise event, the reverse procedure will be followed.

The irradiance measurements performed by the SAGE III instrument can be converted to the slant path transmission profile for each of the wavelength channels (pixel) by ratioing the solar scans transversing the atmosphere to the extraterrestrial solar scans. The procedure will be similar to the algorithms developed for the SAGE I and SAGE II missions as described by Chu and McCormick (1979). The transmittance function of the ray tangent height h_t, according to the Bouguer law, is given by

$$\begin{aligned} T_\lambda(h_t) &= \exp\left[-\delta_\lambda(h_t)\right] \\ &= \exp\left[-\int \sigma_\lambda(h) d\rho_\lambda(h)\right] \end{aligned} \tag{1}$$

where $\delta_\lambda(h_t)$ is the total slant path optical depth at wavelength λ with ray tangent height h_t; σ_λ is the total extinction coefficient of the atmosphere as a function of altitude h and wavelength λ; and ρ is the geometric path length corrected for refraction. Denoting the slant path optical depths as the measurements, equation (1) becomes a Fredholm equation of the first kind relating the measurement $\delta_\lambda(h_t)$ to the integral with the unknown function $\sigma_\lambda(h)$ as the integrant. Using numerical quadrature with unity weights and assuming the atmosphere is spherical symmetry and homogeneous, the integral can be replaced with a numerical sum over the products of the total extinction coefficients in each layer with the corresponding geometric ray path length in the layer

Dividing the atmosphere into m homogeneous layers, equation (1) becomes

$$\delta_\lambda(h_i) = \sum_{j=1}^{m} P_{ij}\sigma_\lambda(h_j) \tag{2}$$

The total extinction coefficient at each tangent altitude is a linear combination of the extinctions of each of the species as given by

$$\sigma_\lambda = \sigma^{Ray}(\lambda) + \sigma^{O_3}(\lambda) + \sigma^{NO_2}(\lambda) + \sigma^{aero}(\lambda) \tag{3}$$

where $\sigma^{Ray}(\lambda)$ is the extinction coefficient for Rayleigh scattering; and $\sigma^{O_3}(\lambda)$, $\sigma^{NO_2}(\lambda)$, and $\sigma^{aero}(\lambda)$ are the extinction coefficients for ozone, nitrogen dioxide, and aerosol at wavelength λ, respectively. For ozone and nitrogen dioxide, the extinction coefficients are determined by the product of the species number density and their absorption cross section at the given wavelength. The aerosol extinction coefficient is a function of aerosol size distribution, shape, and index of refraction. For homogeneous, spherical particles, one has

$$\sigma^{aero}(\lambda) = \int_0^\infty Q(n, r, \lambda)N(r)dr \tag{4}$$

where $N(r)$ is the size distribution function and $Q(n, r, \lambda)$ is the extinction cross section for a particle with refractive index n and radius r, as computed from Mie theory.

Equations (2) and (3) represent the SAGE III measurements as a function of wavelengths and heights, while the solution is in the form of a function of different species in vertical altitudes. The wavelength-dependent part of the measurement solely represents the overlapping contributions from the different species, and is independent of the height variable. The inversion process would generally require a two-step procedure to separately handle the wavelength and height variables. One part of the inversion process decouples the different wavelength measurements into individual species contribution, while the other part of the procedure deconvolutes the slant path optical depth profiles into vertical extinction profiles. Two different approaches to the solutions of equations (2) and (3) have been discussed by Chu et al., (1989) for the study of the SAGE II inversion algorithm.

Figure 4 illustrates the data flow block diagram for SAGE III data processing. SAGE III data will consist of raw count radiance data as a function of time for the nine spectral channels sampling at 64 times per second, plus the accompanying engineering data. The data processing software will be modeled after the SAGE II data processing algorithms (Chu, et al., 1989). The algorithms can be separated into three main sections: the driver section, followed by the transmission section, and finally the inversion section. The driver section handles data screening and merges necessary ancillary data such as the spacecraft's ephemeris data and the instrument's engineering data. The transmission section performs calibration and normalization of scan data by properly localizing each radiance measurement. This is accomplished only after the extraterrestrial solar scans for each channel have been selected and screened, and individual solar radiance measurements have been located both on the solar limb and in the atmosphere as slant path tangent height. The inversion section performs the inversion by converting the transmission data into geophysical parameters describing the vertical distributions of the various species; aerosol, ozone, nitrogen dioxide, water vapor, and oxygen molecules. A detailed description of the various sections of this algorithm have been discussed elsewhere (Chu and McCormick, 1979; Chu et al., 1989).

The overall inversion procedure of calibrating raw scan data into optical depth profiles and the subsequent inversion technique are complex. The complete SAGE III measurements require significant computer storage and computation power for processing at all the spectral channels available. However, simplified processing approaches can be implemented for selected wavelength regions where a single species dominates the measured signal. For example, aerosol signature will dominate the measurements at the 1550-nm and 1020-nm channels with negligible contribution from Rayleigh scattering. Similarly, at the 600-nm wavelength channel, the ozone contribution will dominate the measurements with small aerosol contribution below 20-km altitude. For the cases considered above, quick-look aerosol and ozone profiles can be obtained from less sophisticated algorithms. These algorithms will use parameters interpolated from precalculated tables using standard atmospheric models. The tables could contain such information as sun shape changes caused by atmospheric refraction, Rayleigh extinction profiles, and other variables needed for quick-look data processing. The inversion procedure will be simpler because no separation of the different species contribution will be required. This kind of quick-look processing is ideally suited for the onboard processing unit being considered for the Eos system.

SUMMARY

A brief description of the SAGE III instrument and the anticipated data processing schemes have been presented here. The instrument design is still in the conceptual stage and is currently being finalized during the phase A-B activities of the Eos project. The anticipated data processing activities discussed here represent the cumulated experience acquired from processing the previous satellite missions such as SAM II, SAGE I, and SAGE II. It is anticipated that as the instrument design becomes mature, the data process scheme will necessarily be updated and modified.

REFERENCES

Pepin, T. J., M. P. McCormick, W. P. Chu, F. Simon, T. J. Swissler, R. R. Adams, K. H. Crumbly, and W. H. Fuller: *Stratospheric Aerosol Measurements*, NASA SP-421, pp. 127-136, 1977.

McCormick, M. P., P. Hamill, T. J. Pepin, W. P. Chu, T. J. Swissler, and L. R. McMaster: *Satellite studies of the stratospheric aerosol*, Bull. Amer. Meteor. Soc., 60, 1038-1046, 1979.

Mauldin III, L. E., N. H. Zaun, M. P. McCormick, J. H. Guy, and W. R. Vaughn: *Stratospheric Aerosol and Gas Experiment II instrument: a functional description*. Optical Eng., 24, 307-312, 1985.

Chu, W. P. and M. P. McCormick: *Inversion of stratospheric aerosol and gaseous constituents from spacecraft solar extinction data in the 0.38-1.0 μm wavelength region*, Appl. Opt. 18, 1404-1414, 1979.

Chu, W. P., M. P. McCormick, J. Lenoble, C. Brogniez, and P. Purvost: *SAGE II inversion algorithm*, J. Geophys. Res., 1989, 94, 8339-8352, 1989.

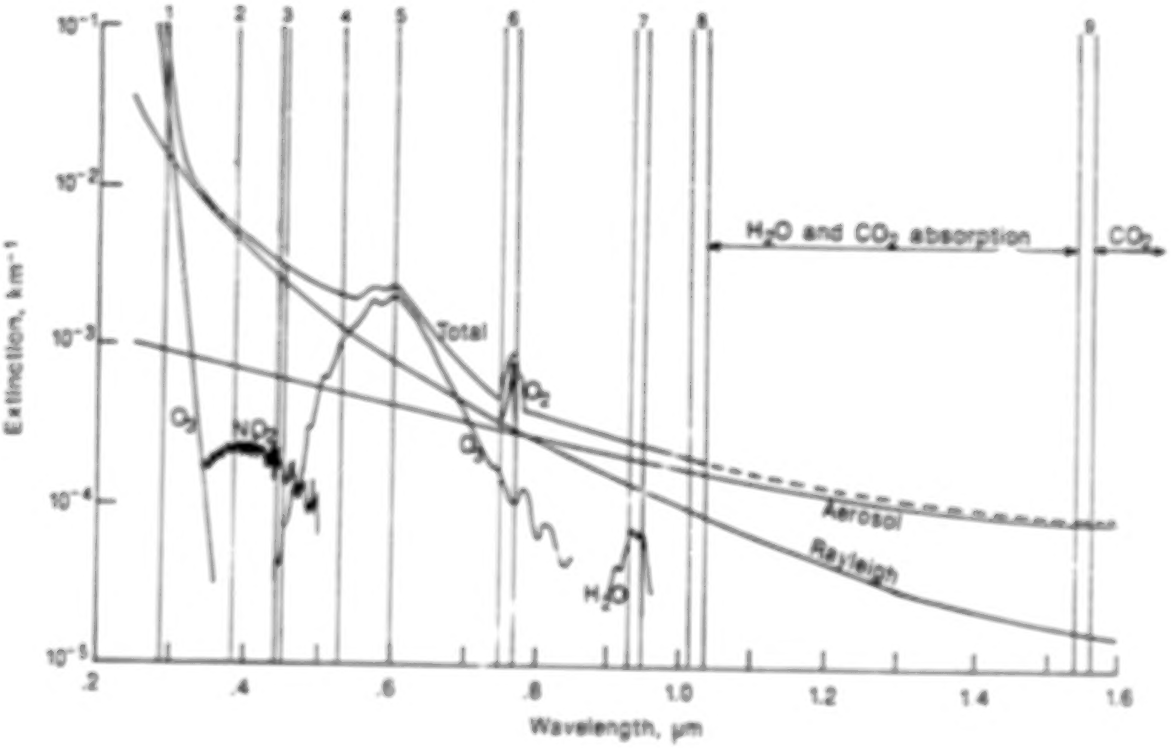

Figure 1. SAGE III channel locations.

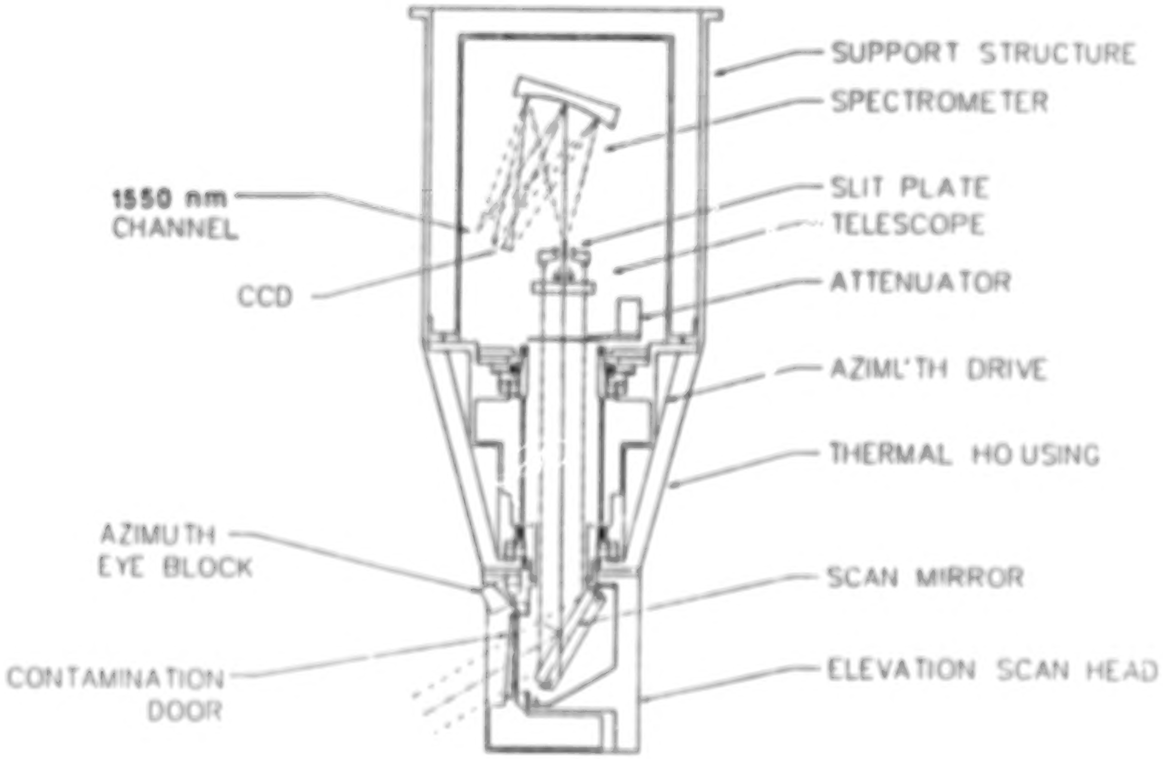
SUPPORT STRUCTURE
SPECTROMETER
1550 nm CHANNEL
SLIT PLATE
TELESCOPE
CCD
ATTENUATOR
AZIMUTH DRIVE
THERMAL HOUSING
AZIMUTH EYE BLOCK
SCAN MIRROR
CONTAMINATION DOOR
ELEVATION SCAN HEAD

Figure 2. Schematic of SAGE III instrument.

N90-27140
thru
N90-27161
Unclas

H1
E
43

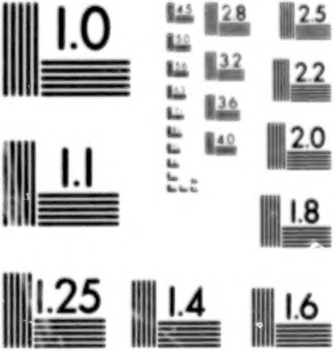
1.0
1.1
1.25
1.4
1.6
1.8
2.0
2.2
2.5
2.8
3.2
3.6
4.0
4.5
5.0

MICROCOPY RESOLUTION TEST CHART
NATIONAL BUREAU OF STANDARDS
STANDARD REFERENCE MATERIAL 1010a
(ANSI and ISO TEST CHART No. 2)

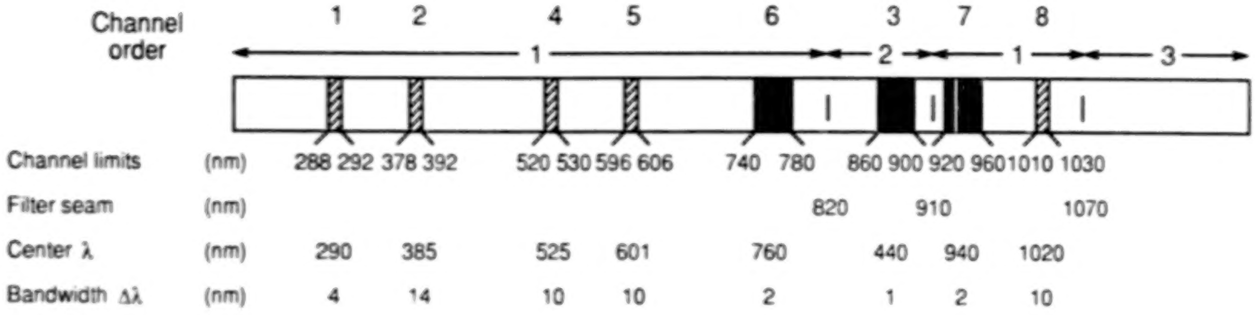
Channel order
1
2
4
5
6
3
7
8
1
2
1
3
Channel limits (nm) 288 292 378 392 520 530 596 606 740 780 860 900 920 960 1010 1030
Filter seam (nm) 820 910 1070
Center λ (nm) 290 385 525 601 760 440 940 1020
Bandwidth Δλ (nm) 4 14 10 10 2 1 2 10

Figure 3. CCD detector array with spectrum.

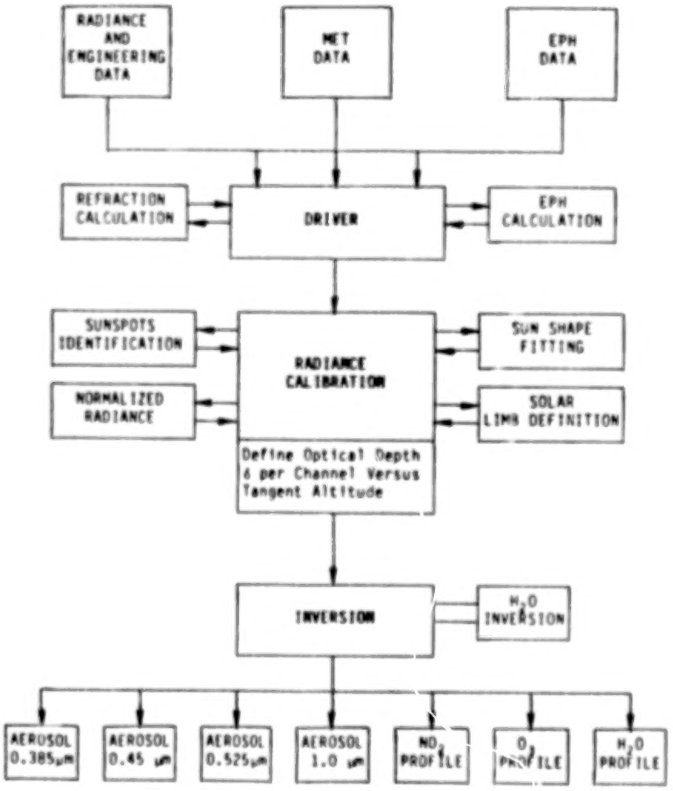
RADIANCE AND ENGINEERING DATA
MET DATA
EPH DATA
REFRACTION CALCULATION
DRIVER
EPH CALCULATION
SUNSPOTS IDENTIFICATION
RADIANCE CALIBRATION
SUN SHAPE FITTING
NORMALIZED RADIANCE
SOLAR LIMB DEFINITION
Define Optical Depth δ per Channel Versus Tangent Altitude
INVERSION
H2O INVERSION
AEROSOL 0.385μm
AEROSOL 0.45 μm
AEROSOL 0.525μm
AEROSOL 1.0 μm
NO2 PROFILE
O3 PROFILE
H2O PROFILE

Figure 4. Data flow block diagram for SAGE III data processing.

N90-27148

DESCRIPTION OF SAFIRE FOR ISES

Jae H. Park
Chemistry and Dynamics Branch
Atmospheric Sciences Division
NASA Langley Research Center
Hampton, Virginia

The SAFIRE (Spectroscopy of the Atmosphere using Far Infrared Emission) is a limb emission experiment using a far-IR Fourier transform spectrometer (FTS) and a mid-IR broadband multispectral radiometer covering the range 80–1600 cm^{-1}. The purpose of this experiment is to obtain vertical distributions of temperature and key constituents of O_y, HO_y, NO_y, ClO_y, and BrO_y families in the stratosphere, mesosphere, and thermosphere. The spectral channels and gases within each channel are summarized in Table I. The instrument includes a 48-element (6 × 8) Ge:GA detector array operating at 4K in the far-IR and a 105-element (7 × 15) HgCdTe array operating at 80K in the mid-IR.

The SAFIRE uses four different scan modes for vertical coverage and resolution to address various scientific requirements. The instrument has an Instantaneous Field of View (IFOV) of 1.5 km for the radiometer and 3.0 km for the FTS. With a proper selection of vertical step size, the range of altitude coverage can be varied. The Chemistry mode, for example, covers 10–110 km in 72 sec with a vertical step size of 1.5 km. The interferogram is sampled every 8 sec, with 1-sec mirror turn-around. The radiometer collects data during the same 8 sec at a 5-Hz rate. Therefore, the FTS data rates for the six 8-detector element arrays are 8.7 Mbs (83.5×10^9 bytes/day), and radiometer data rates for seven 15-detector element arrays are 8.4 Kbs (0.081×10^9 bytes/day).

The SAFIRE data reduction will start with the retrieval of temperature profile as a function of pressure using two CO_2 channel data. Constituent distributions then are obtained from other channel data using the retrieved temperature profile. The data reduction of a mid-IR radiometer is similar to the Limb Infrared Monitor of the Stratosphere (LIMS) procedure (Gille and Russell, 1984); i.e., the production of calibrated radiances from raw instrument counts and inversion of calibrated radiances to temperature and constituent distributions using a radiative transfer equation. The far-IR channel data reduction will require a more complicated procedure; i.e., production of a calibrated interferogram from raw instrument counts, phase correction on the interferogram, inverse Fourier transform of the interferogram to obtain emission spectrum, and nonlinear least-squares fit of the spectrum to retrieve constituent distribution (Park and Carli, 1986). The SAFIRE measurements are limited to the region above the tropopause because of radiance saturation by H_2O and clouds.

The computational capability necessary to process at the instrument data rate (from level 0 to level 1B) is estimated to be 19 MFLOPS for FTS data and 0.02 MFLOPS for radiometer data. It seems, therefore, that the real-time application of SAFIRE data using an onboard processing device is not feasible. Although a temperature anomaly may be detected from the two CO_2 radiometer channels using an onboard processor for the stratosphere, it is not possible to distinguish between CO_2 outflux and temperature anomaly. Temperature anomaly does not, therefore, offer tropospheric information useful for real-time application.

References

Gille, J. C. and J. M. Russell, III, The Limb Infrared Monitor of the Stratosphere: Experiment Description, Performance, and Results, J. Geophys. Res., vol. 89, 5125–5140, 1984.

Park, J. H. and B. Carli, Analysis of Far-Infrared Emission Fourier Transform Spectra, Appl. Optics, vol. 25, 3490–3501, 1986.

Table I. SAFIRE Spectral Channels and Measurement Gases
(interfering gases in parentheses)

Far-IR FTS

Channel	Measurement gas	90% pt. Filter (cm^{-1})
I	O_3 (OH HCl H_2O O_2)	82.0–84.4
II	H_2O_2 (HO_2 O_3 O_2)	94.0–96.0
III	HOCl (H_2O O_3 O_2 HBr)	98.5–100.0
IV	H_2O_2 (H_2O O_3)	111.8–112.6
V	OH (H_2O O_3 O_2 HBr)	116.4–118.6
VI a	H_2O	157.0–159.0
VI b	N_2O_5 (H_2O)	310.0–390.0

Mid-IR Radiometer

Channel	Measurement gas	5% pt. Filter (cm^{-1})
I	CO_2 (H_2O O_3) (for temperature and pressure)	630.0–670.0
II	CO_2 (H_2O O_3) (for temperature and pressure)	580.0–760.0
III	HNO_3 (H_2O CO_2 O_3)	850.0–920.0
IV	CH_4 (H_2O CO_2 N_2O)	1335.–1365.
V	NO_2 (H_2O N_2O CH_4)	1560.–1630.
VI	O_3 (H_2O CO_2)	926.–1141.
VII	N_2O_5 (H_2O CO_2 O_3 CH_4 N_2O)	1225.–1265.

N90-27149

ERBE AND CERES BROADBAND SCANNING RADIOMETERS

William L. Weaver and John E. Cooper
NASA Langley Research Center
Hampton, Virginia

INTRODUCTION

Broadband scanning radiometers have been used extensively on Earth-orbiting satellites to measure the Earth's outgoing radiation. The resulting estimates of longwave and shortwave fluxes have played an important role in helping to understand the Earth's radiant energy balance or budget. The Clouds and the Earth's Radiant Energy System (CERES) experiment is expected to include instruments with three broadband scanning radiometers. The design of the CERES instrument will draw heavily from the flight-proven Earth Radiation Budget Experiment (ERBE) scanner instrument technology and will benefit from the several years of ERBE experience in mission operations and data processing. The discussion in this paper starts with a description of the scientific objectives of ERBE and CERES. Next follows comparisons between the design and operational characteristics of the ERBE and CERES instruments and between the two ground-based data processing systems. Finally, aspects of the CERES data processing which might be performed in near real-time aboard a spacecraft platform are discussed, and the types of algorithms and input data requirements for the on-board processing system are identified.

SCIENTIFIC OBJECTIVES AND EARTH SATELLITE SYSTEMS OF ERBE AND CERES

The scientific objectives of the ERBE mission are listed in table 1, and these objectives and the overall ERBE mission concept are described in reference 1. ERBE scanner instruments are flying on three Earth-orbiting spacecraft, the ERBS, NOAA-9, and NOAA-10. The ERBS spacecraft and its on-board ERBE instruments are operated by NASA from the Goddard Space Flight Center, Greenbelt, Maryland; and the NOAA-9 and NOAA-10 TIROS weather satellites are operated by NOAA from Suitland, Maryland. ERBS is in a processing orbit with an inclination of 57° while NOAA-9 and NOAA-10 are in near-polar, Sun-synchronous orbits with different local times for their ascending nodes. ERBS and NOAA-9 have been operating since October and December 1984, respectively, and NOAA-10 has been operating since September 1986.

The CERES mission is expected to meet the scientific objectives of ERBE but also incorporates additional scientific objectives (see table 2). The satellite system currently being proposed for the Earth Observing System (Eos) is similar to that of ERBE and consists of the Space Station Freedom platform in a low-inclination processing orbit and the NASA and European Space Agency (ESA) platforms in near-polar, Sun-synchronous orbits.

DESIGN AND OPERATION OF THE ERBE AND CERES INSTRUMENTS

Figure 1 is a schematic of the ERBE scanner instrument, and table 3 lists some of the ERBE instrument's important design characteristics. Further details on the design of the ERBE scanner instrument can be found in reference 2. Two identical CERES instruments are proposed to be flown on each of the orbiting Eos platforms. Figure 2 is a drawing of the proposed CERES instrument, and table 4 lists preliminary design characteristics of the CERES instrument for comparison with those of ERBE. The ERBE and CERES instruments are controlled by their own microprocessors. Thus, each instrument can be directed to change its operational mode by sending real-time commands or by storing commands in the spacecraft computer memory for execution at specified times.

The most significant difference between the ERBE instrument and the proposed CERES instrument is the operation of the azimuth beam, which controls the plane in which the detectors scan. The entire instrument structure below the pedestal of both instruments (see figures 1 and 2) can rotate in azimuth between 0 and 180°. The ERBE instrument normally operates in a fixed cross-track position (azimuth = 0 or 180°), and the azimuth beam is rotated to the Sun azimuth only for solar calibrations or other special events. Both CERES instruments aboard a platform will be designed to rotate continually in azimuth between 0 and 180°. It is expected, however, that one of the CERES instruments will normally operate in the fixed cross-track mode to provide maximum spatial coverage and to provide continuity with measurements from the ERBE scanner instruments. The second CERES instrument will operate in the rotating-azimuth mode. The rotating-azimuth mode of operation will provide better angular sampling for improved Angular Distribution Model (ADM) development and reduction of flux errors from the ADM's.

The ERBE instrument can operate in four different scan modes. The scan modes include three Earth-viewing modes and a solar scan mode (used during solar calibrations). The CERES instrument is expected to have the same scan-mode capability. The instrument output in any of the four scan modes consists of 74 radiometric measurements per channel during a 4-second scan period. In the normal Earth scan mode, 8 measurements are made as the detectors view space 14° below the horizon (space look); 62 measurements are made as the detectors scan the Earth from horizon to horizon; and the final 4 measurements are made as the detectors view the internal calibration sources at a scan position inside the instrument housing on the opposite side of the instrument from the space look. The sampling rate for all measurements is 0.033 seconds. In the solar scan mode, the detectors view space and then scan directly to a position in the instrument housing where they view the attenuated output of the Sun which is incident on the two side-by-side apertures shown in the drawings of figures 1 and 2.

Two types of calibrations can be performed with the ERBE instruments: internal and solar. The CERES instrument calibration options are expected to be the same as those of ERBE. Both calibrations are performed using special preprogrammed sequences of microprocessor commands. Internal calibrations are performed while the instrument remains in the normal Earth-scan mode. The solar calibration sequence includes commands which rotate the azimuth beam to the required Sun azimuth angle and cause the instrument to change to the solar scan mode.

The field stop in front of the ERBE detectors is a 3.0°- × 4.5°-hexagonal aperture, chosen to offset aliasing effects caused by scan motion and data sampling rates. The design technology of the CERES radiometric detectors will be very similar to that of ERBE. To reduce the field of view of the CERES detectors significantly from that of ERBE would probably require changing to another type of detector technology. Comparing tables 2 and 3 shows that the currently proposed spectral characteristics of the three CERES radiometric detectors differ slightly from those of the ERBE detectors. Although the filters which will be used on CERES will be an improvement over those on ERBE, they will not be perfect filters. Some spectral corrections will still need to be made to the raw radiometric measurements.

The relatively low ERBE instrument data rate of 960 bits per second includes the radiometric measurements and instrument housekeeping measurements. The total ERBE instrument output during a 4-second scan period consists of 74 radiometric measurements for each channel, the corresponding elevation or scan angle, and 24 housekeeping measurements. The output of the CERES instruments will need, in addition to these data, azimuth position data corresponding to each of the 74 radiometric measurements. The total data output of a CERES instrument will, therefore, be moderately higher than that of ERBE.

GROUND-BASED DATA PROCESSING

The ERBE telemetry data which are provided to Langley by Goddard and NOAA consist of the entire raw output of the ERBE instruments and certain spacecraft housekeeping data. Goddard computes and provides the ephemeris data for all three spacecraft. A flow chart of the ERBE data processing system is shown in figure 3. The ground-based data processing system for CERES is expected to be an extension of the ERBE data processing system.

The circles in figure 3 represent processing tasks, and the rectangles represent algorithms or data input (arrows drawn into circles) or data output (arrows drawn out of circles). The processing down to the Merge circle (step 4.1) consists mostly of decommutation, screening and editing, and reformatting of the data. In the next two processing steps (steps 4.1 and 4.2), the telemetry and ephemeris data are merged, and the locations of the measurements on the Earth's surface are computed. The data products at this point (Earth-located raw measurements) are archived by the ERBE project at the National Space Sciences Data Center (NSSDC). This archival data product is called the Raw Archival Tape or the RAT. In the next step, the raw radiometric measurements are converted to radiances, using algorithms and calibration data obtained from preflight testing and in-flight calibrations. The conversion algorithms also make use of certain instrument housekeeping measurements. The converted radiances are edited before they are corrected spectrally and inverted to the top of the Earth's atmosphere (TOA). The raw radiance measurements are corrected for errors caused by spectral filtering using scene identification information derived from the measurements themselves. The corrected radiances (sometimes called inveterate radiances) are then inverted to radiant fluxes at the TOA using input angular models which have been derived from data obtained on previous missions. The models used on ERBE were derived from data obtained from NIMBUS 7.

The instantaneous longwave and shortwave fluxes at the top of the Earth's atmosphere represent the lowest level Earth radiation budget data useful in scientific investigations. The ERBE data product which includes the instantaneous fluxes is called the Processed Archival Tape (PAT) and is archived on 24-hour tapes by the ERBE project at the NSSDC. The corresponding data from CERES will be called the Standard Data Product and will also be archived. These data can be useful in a host of studies in which an investigator might want to perform his own spatial and temporal averaging. The instantaneous fluxes would also likely be the most useful data in real-time applications, and so the remaining discussion will focus on the processing required to produce this data product and the types of algorithms and input data required.

ON-BOARD PROCESSING REQUIREMENTS

Figure 4 is a simplified flow chart of the processing steps required to produce the instantaneous fluxes at the top of the Earth's atmosphere. The input telemetry data are assumed to include the output of the CERES instruments and all spacecraft data required, such as operational mode and attitude data. The ephemeris data are assumed to be available from on-board sources and to include accurate spacecraft and solar ephemeris data. Each bullet in figure 4 can be thought of as a process that requires a set of algorithms and/or data input. The lines marked with stars identify algorithms and/or data which are subject to changes during the mission.

Decommutation of the telemetry data and reformatting of the telemetry and ephemeris data are required before the two data streams can be merged. The on-board data screening algorithms could, perhaps, be simpler than those used in the ground-based processing system, but ERBE experience taught us that quality evaluation of the data is very important. Merging the telemetry and ephemeris data and computing the Earth locations of the measurements may be straightforward but require moderate numbers of vector transformations. The Earth location computations could be simplified by modeling the motions of the instruments azimuth and elevation beams, but such a modeling procedure would increase the risk of mislocating some of the measurements.

Algorithms for conversion of the housekeeping and radiometric data will require raw sensor output as well as other housekeeping measurements. Calibration coefficients used in the algorithms to convert the raw radiometric measurements to radiances will probably need to be updated with results from in-flight instrument calibration data. ERBE experience taught us that editing of the converted radiometric and housekeeping measurements increases the confidence level of the resulting science products; some editing algorithms would be desirable at this point in the processing.

Correcting the converted radiances for errors in spectral filtering can be done using stored correction factors whose values are a function of the specific scene over which the measurement is made. The radiances used to produce the CERES Standard Data Product will be corrected using scene identification information derived from the CERES measurements. An on-board processing system could probably improve the scene identification process by making use of the data output from other on-board instruments, such as MODIS.

The final step in the process to produce the CERES Standard Data Product is inversion of the corrected longwave and shortwave radiances to radiant fluxes at the top of the Earth's atmosphere. The primary data contained in the CERES Standard Data Product, which include the instantaneous radiances, shortwave and longwave fluxes, and the associated scene, are listed in table 5. In the inversion process, angular models of the Earth's radiant energy are applied to each radiance measurement to produce a value of the radiation field at a point on a reference surface above the Earth. The angular radiation models are usually stored in tables. The inversion of the longwave radiation component is relatively simple compared to that of the shortwave component, sometimes requiring no more than a limb darkening curve, which is a function of the measurement zenith angle relative to the instrument.

CONCLUDING REMARKS

The CERES mission is expected to incorporate essentially all the ERBE science objectives and will extend those objectives. The Eos Earth-satellite system is very similar to that of ERBE and consists of the low altitude, low inclination, processing orbit of the Space Station Freedom and the NASA and European Space Agency Sun-synchronous, polar-orbiting platforms. The CERES instrument design is expected to follow that of ERBE, but each CERES instrument package will consist of two scanners capable of rotating continuously in azimuth. One instrument is expected to operate in the fixed cross-track azimuth mode to provide maximum spatial coverage. The other instrument will operate in a bi-axial (rotating-azimuth) mode to provide more complete angular sampling. The data rates for the CERES instrument, like those of ERBE, are very low.

The Standard Data Product of the CERES mission, which consists of the instantaneous radiant fluxes at the top of the Earth's atmosphere, will be produced by the ground-based Eos Dis system within 72 hours. The Standard Data Product, which could have near-real-time applications, might also be produced through processing aboard the Eos platforms. Some of the algorithms and data input required for the on-board processing may have to be scaled down to decrease the on-board processing burden.

REFERENCES

(1) - Barkstrom, Bruce R., 1984: "The Earth Radiation Budget Experiment (ERBE)." Bulletin of the American Meteorological Society.

(2) - Kopia, L. P., 1986: "The Earth Radiation Budget Experiment Scanner Instrument." Rev. Geophys. and Space Physics, 24, 400-406.

TABLE 1

SCIENTIFIC OBJECTIVES OF ERBE

Determine monthly averages of Earth radiation budget components at top of atmosphere for various spatial scales

- 250-km to 1000-km regions
- 10-degree latitudinal zones
- Global
- Equator-to-pole transport gradient

Determine average diurnal variations in the Earth radiation budget on a regional and monthly scale

TABLE 2

SCIENTIFIC OBJECTIVES OF CERES

Produce consistent global data base of radiation and clouds
- Use broadband scanner for radiation budget
- Use spectral information for clouds

Contribute to Eos tasks in
- Biogeochemical cycles
- Climatological processes
- Atmospheric geophysical processes
- Oceanic geophysical processes

Provide input for multidisciplinary approaches to
- CO(2) induced climate changes
- El Nino-related weather perturbations

TABLE 3

ERBE SCANNER INSTRUMENT CHARACTERISTICS

COMPUTER-CONTROLLED OPERATIONAL MODES
  Any fixed azimuth position between 0 and 180°
  (normal crosstrack)

Four scan modes (3 Earth, 1 for solar calibration)
  Normal Earth scan - views space, Earth, internal
  calibration sources

Calibration sequences
  Internal - Views blackbodies, shortwave sources
  Solar - Views attenuated solar input

SPATIAL FIELD OF VIEW OF DETECTORS
  Approximately 3.5° circular aperture (Half power
  contour)

SPECTRAL CHARACTERISTICS OF DETECTORS

Total radiance	(0.2 to 50 microns)
Shortwave radiance	(0.2 to 5.0 microns)
Longwave radiance	(5.0 to 50 microns)

DATA RATES (EACH INSTRUMENT)
  960 bits/sec (Radiometric and housekeeping data)
  74 radiometric measurements per channel in 4-second
  scan cycle

TABLE 4

PRELIMINARY DESIGN CHARACTERISTICS OF CERES INSTRUMENT

TWO IDENTICAL INSTRUMENTS ON EACH ORBITING PLATFORM

COMPUTER-CONTROLLED OPERATION
- One instrument in fixed (crosstrack) azimuth position
- One instrument in rotating-azimuth mode (between 0 and 180°)

- Four scan modes (3 Earth, 1 for calibration)
  - Normal Earth scan - Views space, Earth, internal calibration sources

- Calibration sequences
  - Internal - Views blackbodies, shortwave sources
  - Solar - Views attenuated solar input

SPATIAL FIELD OF VIEW OF DETECTORS
- Approximately same as ERBE

SPECTRAL CHARACTERISTICS OF DETECTORS

Total radiance	(0.3 to 50.0 microns)
Shortwave radiance	(0.3 to 3.5 microns)
Longwave radiance	(5.0 to 50.0 microns)

DATA RATES (EACH INSTRUMENT)
- 2000 bits/sec (Radiometric and housekeeping data)
- Approximately 74 radiometric measurements per channel in 4-second scan cycle

TABLE 5

CONTENTS OF ERBE PROCESSED ARCHIVAL TAPE AND CERES STANDARD DATA PRODUCT

Times of measurements

Earth locations of measurements

Converted shortwave and longwave radiances (W/M**2.ST)

Derived shortwave and longwave top-of-atmosphere fluxes (W/M**2)

Scene identification (Clear, partly cloudy, mostly cloudy, overcast)

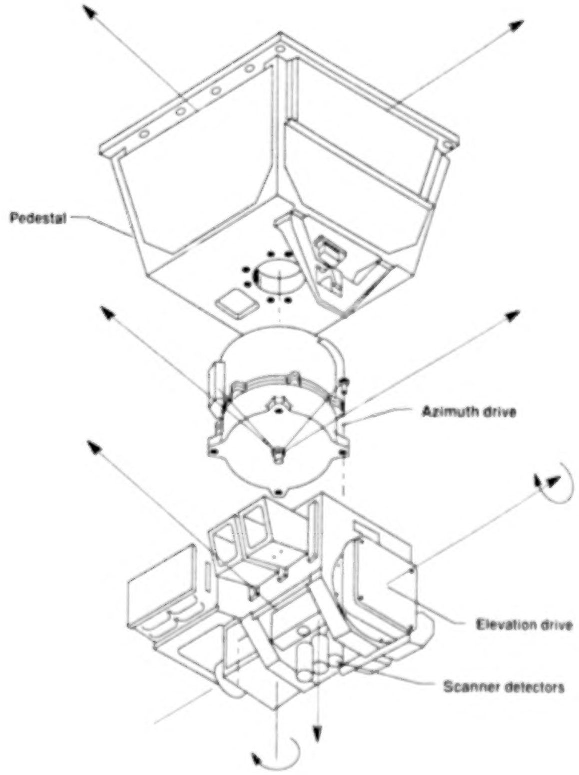
Pedestal
Azimuth drive
Elevation drive
Scanner detectors

FIGURE 1.- ERBE SCANNER INSTRUMENT

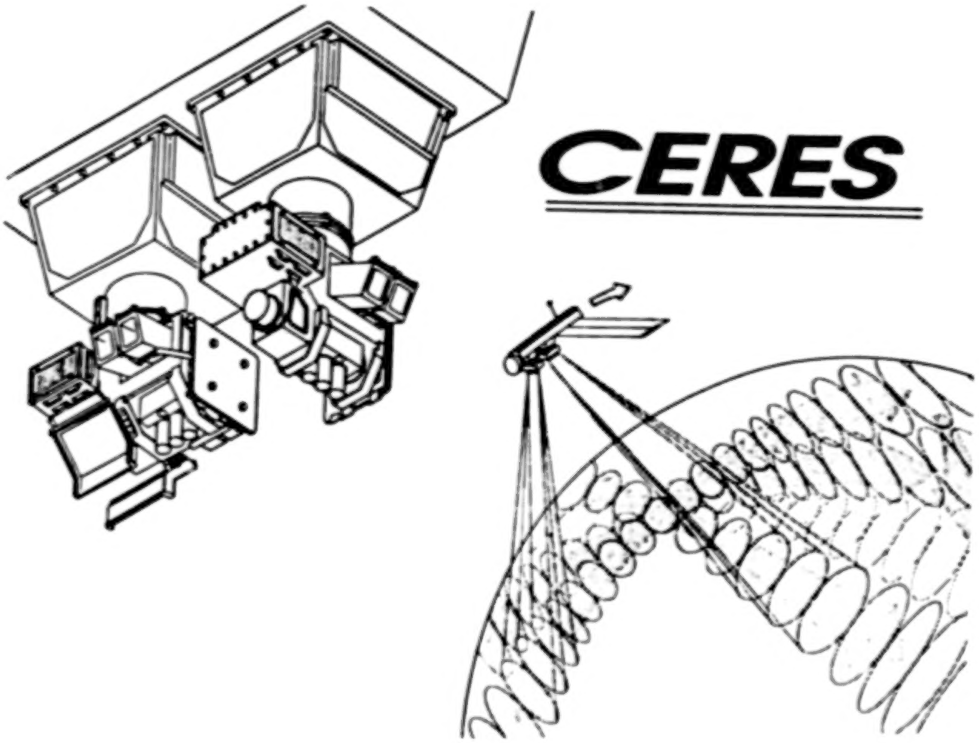

FIGURE 2.- CERES INSTRUMENT

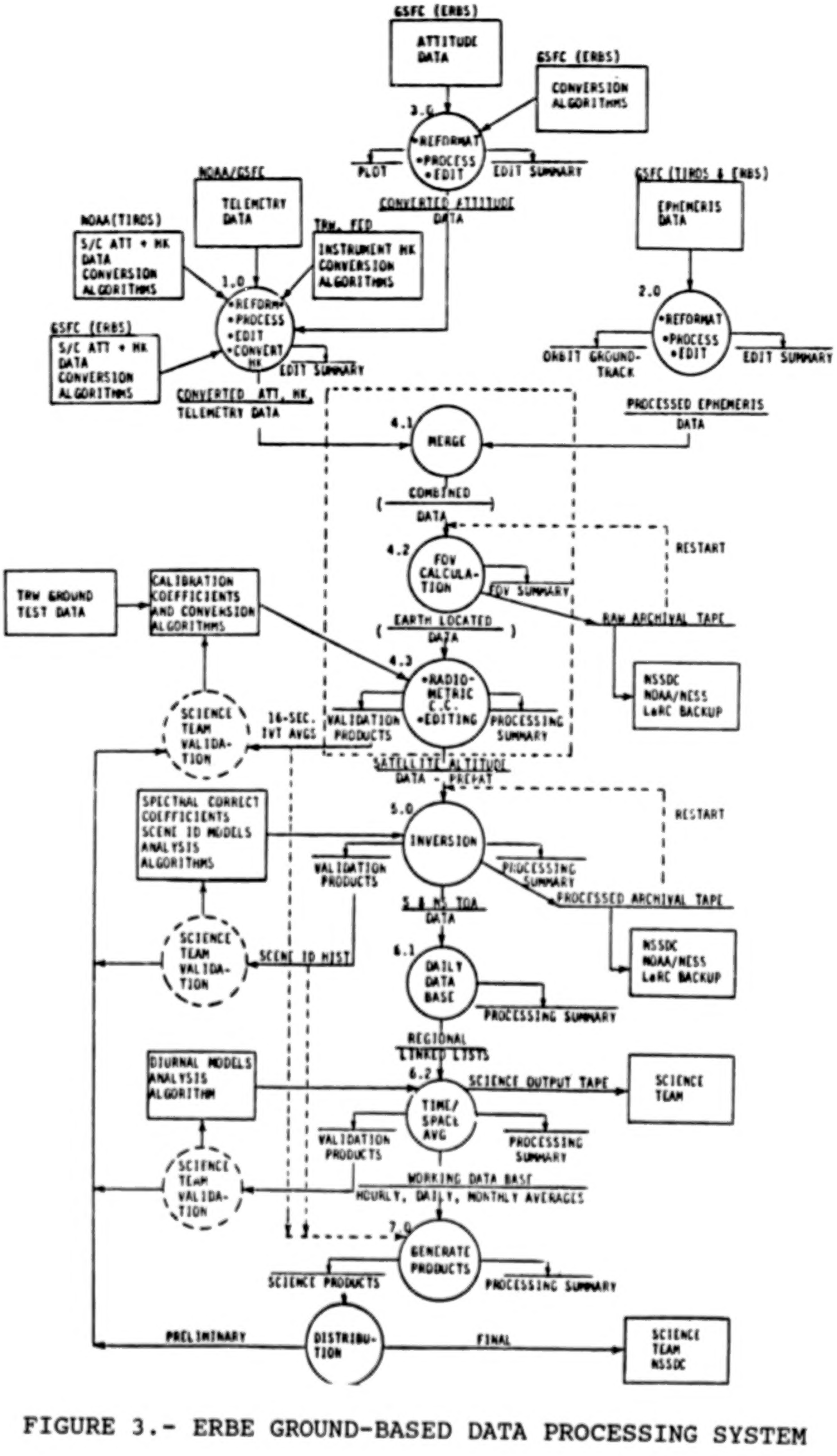
GSFC (ERBS)
ATTITUDE DATA
GSFC (ERBS)
CONVERSION ALGORITHMS
3.0
•REFORMAT
•PROCESS
•EDIT
PLOT
EDIT SUMMARY
NOAA/GSFC
TELEMETRY DATA
CONVERTED ATTITUDE DATA
GSFC (TIROS & ERBS)
EPHEMERIS DATA
NOAA(TIROS)
S/C ATT + HK DATA CONVERSION ALGORITHMS
TRW, FED
INSTRUMENT HK CONVERSION ALGORITHMS
1.0
•REFORM
•PROCESS
•EDIT
•CONVERT HK
GSFC (ERBS)
S/C ATT + HK DATA CONVERSION ALGORITHMS
EDIT SUMMARY
2.0
•REFORMAT
•PROCESS
•EDIT
ORBIT GROUND-TRACK
EDIT SUMMARY
CONVERTED ATT, HK, TELEMETRY DATA
PROCESSED EPHEMERIS DATA
4.1
MERGE
COMBINED DATA
RESTART
4.2
FOV CALCULATION
FOV SUMMARY
TRW GROUND TEST DATA
CALIBRATION COEFFICIENTS AND CONVERSION ALGORITHMS
RAW ARCHIVAL TAPE
EARTH LOCATED DATA
4.3
•RADIOMETRIC C.C.
•EDITING
NSSDC
NOAA/NESS
LaRC BACKUP
SCIENCE TEAM VALIDATION
16-SEC. IVT AVGS
VALIDATION PRODUCTS
PROCESSING SUMMARY
SATELLITE ALTITUDE DATA - PREPAT
RESTART
SPECTRAL CORRECT COEFFICIENTS SCENE ID MODELS ANALYSIS ALGORITHMS
5.0
INVERSION
VALIDATION PRODUCTS
PROCESSING SUMMARY
PROCESSED ARCHIVAL TAPE
S & NS TOA DATA
SCIENCE TEAM VALIDATION
SCENE ID HIST
6.1
DAILY DATA BASE
NSSDC
NOAA/NESS
LaRC BACKUP
PROCESSING SUMMARY
REGIONAL LINKED LISTS
DIURNAL MODELS ANALYSIS ALGORITHM
6.2
SCIENCE OUTPUT TAPE
SCIENCE TEAM
TIME/SPACE AVG
VALIDATION PRODUCTS
PROCESSING SUMMARY
SCIENCE TEAM VALIDATION
WORKING DATA BASE
HOURLY, DAILY, MONTHLY AVERAGES
7.0
GENERATE PRODUCTS
SCIENCE PRODUCTS
PROCESSING SUMMARY
PRELIMINARY
DISTRIBUTION
FINAL
SCIENCE TEAM NSSDC

FIGURE 3.- ERBE GROUND-BASED DATA PROCESSING SYSTEM

ORIGINAL PAGE IS
OF POOR QUALITY

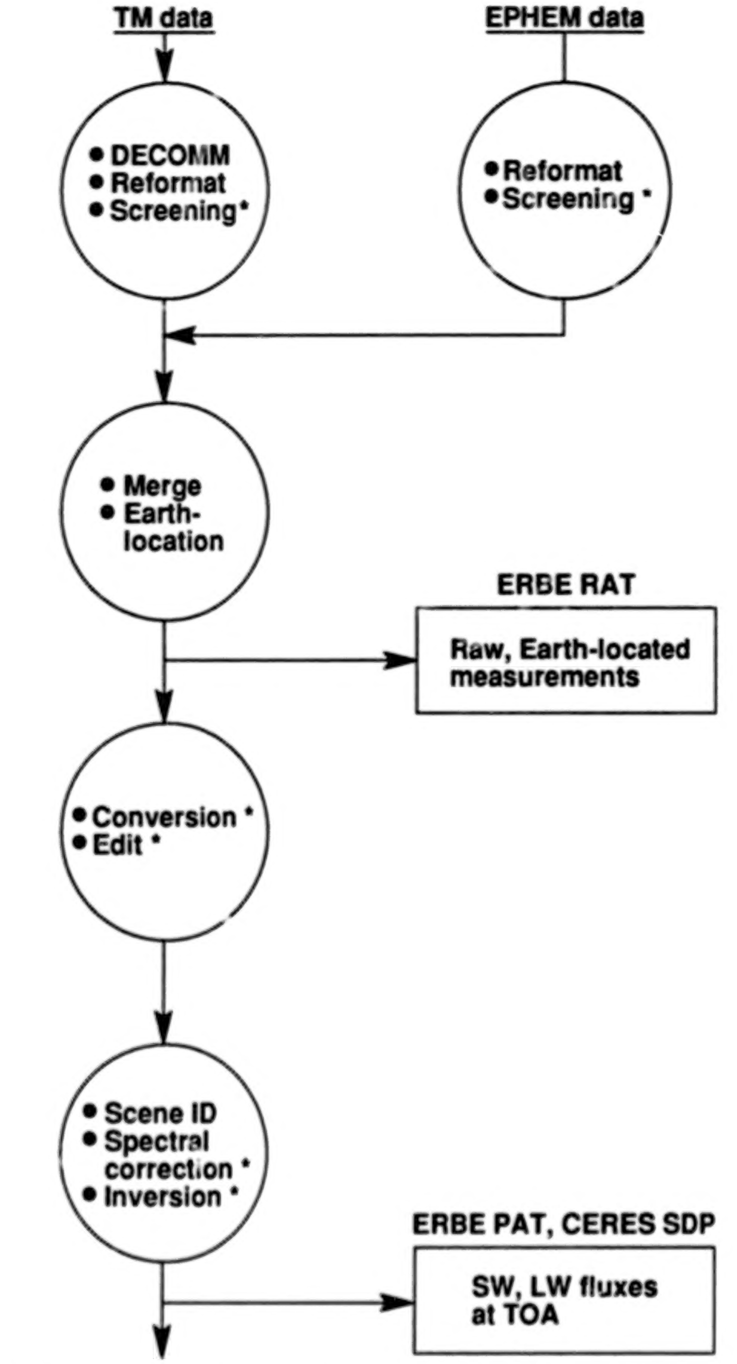
TM data
EPHEM data
• DECOMM
• Reformat
• Screening*
• Reformat
• Screening *
• Merge
• Earth-location
ERBE RAT
Raw, Earth-located measurements
• Conversion *
• Edit *
• Scene ID
• Spectral correction *
• Inversion *
ERBE PAT, CERES SDP
SW, LW fluxes at TOA

SDP - Standard data product
TOA - Top of Earth atmosphere
* - Algorithms and/or data subject to change with time

FIGURE 4.- PROCESSING TO PRODUCE RADIANT FLUXES AT TOP OF EARTH ATMOSPHERE

N90-27150

TROPOSPHERIC SOUNDERS

H. A. Wallio
NASA Langley Research Center
Hampton, VA

This presentation is a bit more specific in that the discussion of tropospheric sounders will be about passive, infrared, nadir-viewing sensors, and in particular, the MAPS and TRACER experiments. What is discussed in a general way is the gases measured, the output data products, the data rates, data flow, and data processing for this type of experiment.

The Measurement of Air Pollution Satellites (MAPS) experiment is a nadir-viewing gas correlation filter radiometer that has flown on the space shuttle in 1981 and 1984. The Tropospheric Radiometer for Atmospheric Chemistry and Environment Research (TRACER) is a proposed multi-level gas correlation filter radiometer experiment proposed for Eos and has received Phase I approval.

THE MAPS EXPERIMENT

The primary gas measured by MAPS is carbon monoxide (CO) which is photochemically active and represents the major sink for the hydroxyl (OH) radical in the troposphere. Since OH is the principal oxidizer for most reduced species in the atmosphere, changing levels of CO will alter the chemical processes in this region. Although there is uncertainty in the magnitudes, the sources and sinks of CO are thought to be well known. CO is naturally produced as a result of the oxidation of methane and other hydrocarbons and is destroyed principally as a result of photochemical processes. Man's contribution is thought to be nearly as large as natural sources. Some of the impacts of CO as a pollutant are listed in figure 1.

Some highlights of figure 1 are that the anthropogenic source consists primarily of technological sources (concentrated in the Northern Hemisphere) and biomass burning (concentrated in the tropics). One of the more important results of the first MAPS flight in 1981 was the measurement of large longitudinal gradients. Up until that time the few extrapolations of the measurements of CO had led to the interpretation of global latitudinal variations with the expectation of little or no longitudinal differences.

Figure 2 is a simplified pictorial schematic of a gas filter radiometer. Energy emitted by or reflected from the surface of the Earth propagates through the atmosphere and is gathered by the nadir-viewing instrument. As the radiation passes through the atmosphere, it undergoes selective absorption and reemission that varies depending on the composition, temperature, and pressure of the atmosphere. After entering the instrument, the radiation is divided and directed in parallel through a system of gas-filled cells. The energy transmitted through the cells then passes to a detection system. Because the gas in the cells acts as a highly selective filter, there is generally a difference in the energy transmitted to the detection system through the various cells. The difference in the signals is related to both the amount of gas in the atmosphere with absorption features that correlate with those of the gas in the cells and the height of that gas in the atmosphere. If one of the cells is evacuated, the energy passing directly through the vacuum cell is a measure

PRECEDING PAGE BLANK NOT FILMED

of the scene brightness. If none of the cells is evacuated, the scene brightness in the passband must be measured separately. Combining this scene brightness measurement (called L), a difference signal between the vacuum and gas cell paths (called ΔL) and knowledge of certain atmospheric parameters (such as the temperature profile) through a numerical radiative transfer program allows inference of the atmospheric mixing ratio of CO.

Figure 3 shows the normalized signal functions for the MAPS instrument as configured for the 1981 shuttle flights. These functions are similar to the weighting functions associated in temperature sounding. The peak of the signal function occurs in the troposphere and the signal goes to zero at the top of the atmosphere where the density decreases to zero. The signal function also goes to zero near the surface since the signal is a function of the temperature contrast between the boundary surface and the atmosphere. The integral of the signal function multiplied by the normalization constant results in the actual radiance measured by the instrument.

Figure 4 is a plot of the infrared CO mixing ratios from the 1981 shuttle flight. The CO mixing ratios have been averaged and plotted in a 5° × 5° box on a mercator projection. Because of shuttle cooling problems, this data is only a 3-hour portion of 12 hours of data that was taken between two reliable calibrations.

Figure 5 is the same type of plot for the 1984 shuttle flight. The CO mixing ratios here are an 8-day average CO mixing ratio averaged over a 5° × 5° box. Both figures 4 and 5 are one of the primary data output products and clearly show the large longitudinal variations in CO mixing ratios that had not been previously seen or predicted before these measurements. In particular, notice the high values over South America and South Africa due to biomass burning, and also over Europe and China due to industrialization. The longitudinal variations are larger than the latitudinal variations for this particular time of the year.

THE Eos TRACER EXPERIMENT

TRACER is a gas correlation filter radiometer proposed and accepted for Phase I definition studies in the Eos program. The Principal Investigator is Henry G. Reichle, Jr. of NASA LaRC. Table 1 shows the general science objectives for the experiment. The orbit and duration of the Eos platform offer a unique opportunity to measure the global and time-dependent distribution of CO. These same conditions mean that the data will be a unique set to be analyzed for transport and chemical studies and for the determination of source and sinks. Also listed in Table 1 is a synopsis of the instrument description.

The instrument is a passive nadir-viewing gas filter radiometer operating at wavelengths of 2.3 and 4.6 μm. The basic concept of the instrument is the same as was shown schematically in figure 2. The implementation of the instrument is different in that it will have a different electrical and optical method of detecting radiances and that the instrument control signal and data processing will be handled by an onboard digital computer. Table 2 lists the TRACER co-investigators, their affiliation, and their primary areas of interest. The co-investigators are divided into two groups: the science team and the experiment team. The science team is primarily outside of LaRC and members may be replaced over the long lifetime of this experiment. The experiment team are all from LaRC and are expected to remain with the project for its lifetime and thus provide a cohesive memory of the goals, design, and implementation of the experiment.

As stated previously, the TRACER concept is basically the same as MAPS in that they are both passive nadir-infrared gas filter radiometers with three major differences. The first is that TRACER has two wavelength regions: 4.6- and 2.3-μm. The second is that optics are different; TRACER will use rotating gas cells rather than choppers and beam splitting. The third is that signal differencing, signal processing, housekeeping, and instrument control will be handled by an onboard computer which is part of the instrument package. The inserts in figure 6 are the gas cell conditions that are used to determine the difference signal for plotted signal functions.

The normalized signal functions for the TRACER instrument are shown in figure 6. As can be seen from the figure, the instrument will measure CO mixing ratios at several levels of the atmosphere. The lower, mid, and upper tropospheric levels are all measured using the 4.6-μm channel. CO in the mixing layer of the atmosphere is measured using reflected sunlight at 2.3 μm. The signals for these measurements are achieved by rotating fixed-length, fixed-pressure gas cells through the optical beam. There are two additional gas cells on the rotating wheel. These cells are filled with nitrous oxide (N_2O) and methane (CH_4). These cells are used in an enhanced data correction technique, which allows the data inversion algorithms to be adjusted for variables such as the presence of clouds, common channel error, and to reduce the effects of false correlation from other gases in the atmosphere.

As part of the design, the TRACER instrument will incorporate the MAST 1750A computer. This computer will handle the data sampling, data digitization, signal differencing, data storage, data formatting, and data transfer. The computer will control the instrument operation and sequencing including internal calibration sequencing. Finally, the computer will perform preliminary data inversions to arrive at CO mixing ratios based on the spacecraft ephemeris and climatalogical atmospheric models. The results of this preliminary data reduction will be merged into the output data stream and can serve as an Eos level-2a data product. The computer will be capable of reprogramming from the ground on the data uplink. This will let the instrument and experiment evolve during the expected 5-year mission duration.

Figure 7 is from the TRACER proposal which shows the general data flow and dissemination plan. Notice on this figure the boxes with no shading on either edge. These are the functions and programs that are to be handled by EosDIS. All of the other boxes indicate software and production handled at LaRC at either pre- or post-launch. For the ISES concept, the unshaded boxes would be the only candidates available for processing onboard the spacecraft. Using an ISES onboard computer would be very redundant because these programs will be executed onboard by the TRACER MAST 1750A computer, on the ground by the EosDIS computer, and also executed at LaRC.

Table 3 is also from the TRACER proposal and shows the expected TRACER processing requirements from input through final output for the various experiment parameters for each of the Eos levels. The main point of this table is to show the low data rates for the TRACER experiment. The final output product will be four CO mixing ratios every second. The peak data rate for the experiment, including all housekeeping, is expected to be 10 kbs.

In summary, TRACER is a semi-autonomous package with very low data rates only requiring access to the platform data bus and platform power. The integral computer exceeds the present instrument design requirements and will probably be reprogrammed to meet future experiment and instrument design changes required as the experiment evolves over a 5-year lifetime.

Table I. TRACER Experiment Science Objectives and Instrument Description

P.I. SCIENCE INVESTIGATION

SCIENCE OBJECTIVES:

- TO DETERMINE THE LONG TERM, TIME-DEPENDENT, THREE DIMENSIONAL, GLOBAL DISTRIBUTION OF TROPOSPHERIC CARBON MONOXIDE
- TO APPLY THESE DATA TO THE DETERMINATION OF SOURCE STRENGTHS, TO THE ELUCIDATION OF VERTICAL AND HORIZONTAL TRANSPORT PROCESSES, AND TO THE DEVELOPMENT AND VERIFICATION OF GLOBAL CHEMICAL-TRANSPORT MODELS

INSTRUMENT DESCRIPTION:

- NADIR-VIEWING GAS FILTER RADIOMETER OPERATING AT 2.33 μm AND 4.67 μm
- SIGNAL DIFFERENCES ARE FORMED BY ROTATING FIXED-PRESSURE, FIXED-PATH LENGTH GAS CELLS THROUGH THE OPTICAL PATH
- ALL SIGNAL PROCESSING, INSTRUMENT CONTROL, AND DATA PROCESSING FUNCTIONS HANDLED VIA ONBOARD DIGITAL COMPUTER

Table II. TRACER Co-investigators

SCIENCE TEAM

Paul Fraser	CSIRO, CO Measurements
Michael Garstang	U. Va, Atmospheric Motions
Ivar Isaksen	U. Oslo, Chemical/Transport Modeling
Ralph Nicholls	York U., Instrument/Rad. Transfer
Wolfgang Seiler	Fraunhofer Inst., Co Measurements
Jennifer Logan	Harvard U, Chemical/Transport Modeling
Reginald Newell	MIT, Atmospheric Motions
Ronald Prinn	MIT, Chemical/Transport Modeling

EXPERIMENT TEAM

Vickie Connors	Atmospheric Motions
Jack Fishman	Chemical Modeling
Curtis Rinsland	CO Meas./Spectroscopy
H. Andrew Wallio	Radiative Transfer/Instrument

Table III. TRACER Input, Output, and Processing Requirements

(a) - Input Data

Input Data Description	Eos Level	Data Source	Peak Rate (Mbits/ sec)	Volume (Mbits/ day)	Temporal Resolution	Spatial Resolution
Raw telemetry data	0	Raw TM	0.01	864	1 sec	20 km Raw
Tracking data	0	TDRSS	Small	5.6	1 min	500 km
Calibrated engineering units	1a	Eos L0	0.01	864	1 sec	20 km
Ephemeris data	1a	Eos L0	Small	5.6	1 min	500 m
Calibrated radiances	1b	Eos L0	0.01	980	1 sec	20 km
Mixing ratio	2a	Eos L1b	0.01	1225	1 sec	20 km

(b) - Output Data Products

Output Data Description	Eos Level	Units	Volume (Mbits/ day)	Temporal Resolution	Spatial Resolution
Level 0 telemetry data	0	Counts	864	1 sec	20 km
Telemetry reports	0		small	Daily	
Calibrated engineering units	1a	Volts, temp	864	1 sec	20 km
Ephemeris data	1a	m, m/s	5.6	1 min	500 m
Ephemeris reports	1a		small	Weekly	
Level 1a reports	1a		small	Daily	
Calibrated radiances	1b	$w\ cm^{-2} sr^{-1}$	980	1 sec	20 km
Level 1b reports	1b		small	Daily	
Mixing ratios	2a	ppbv	980	1 sec	20 km
Level 2a reports	2a		small	Daily	
Correlative validated mixing ratios	2b	ppbv	980	1 sec	20 km
Level 2b reports	2b		small	1 year	Global

(c) - Data Processing Requirements

Processing Step	Level	Lines of Code	Operations Data Day	Frequency
Decommutation, reformatting	0	24,000	7×10^9	Daily
Location, calibration	1a	12,000	12×10^9	Daily
Radiance Measurements	1b	8,000	13×10^9	Daily
Mixing Ratios	2a	13,000	26×10^9	Daily
Data Validation	2b	8,000	4×10^9	Daily

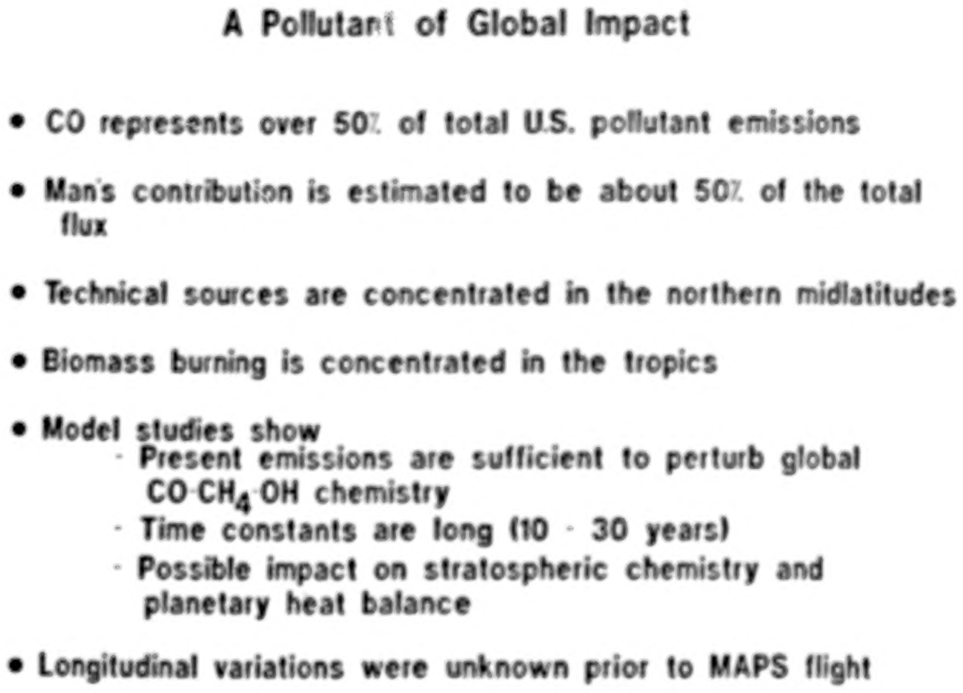

A Pollutant of Global Impact

- CO represents over 50% of total U.S. pollutant emissions
- Man's contribution is estimated to be about 50% of the total flux
- Technical sources are concentrated in the northern midlatitudes
- Biomass burning is concentrated in the tropics
- Model studies show
  - Present emissions are sufficient to perturb global CO-CH_4-OH chemistry
  - Time constants are long (10 - 30 years)
  - Possible impact on stratospheric chemistry and planetary heat balance
- Longitudinal variations were unknown prior to MAPS flight

Figure 1. Importance of trace gas carbon monoxide.

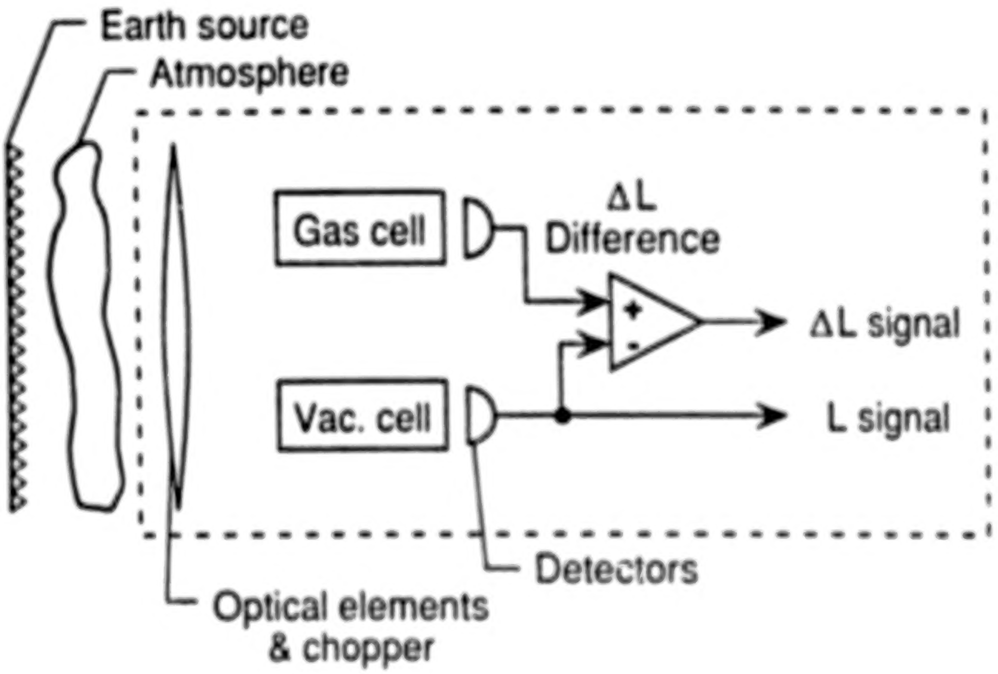
Earth source
Atmosphere
Gas cell
ΔL
Difference
+
-
ΔL signal
Vac. cell
L signal
Detectors
Optical elements
& chopper

Figure 2. Schematic diagram of the instrument.

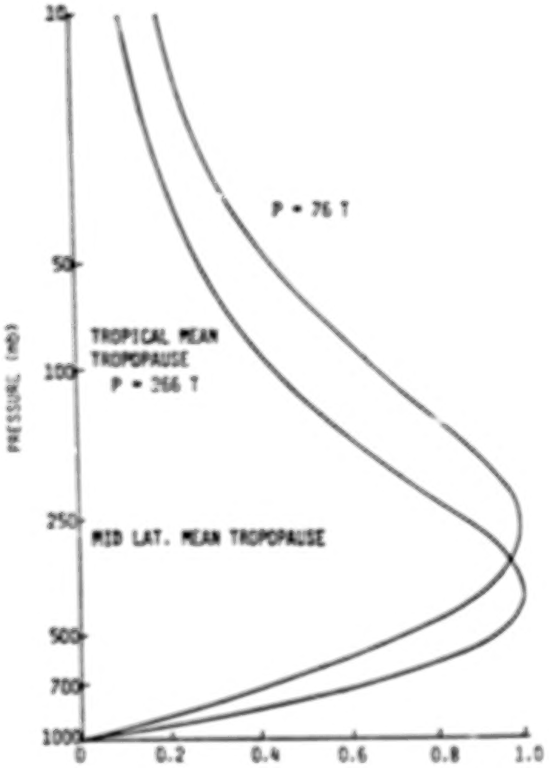

Figure 3. Normalized signal function for OSTA-1 MAPS Experiment.

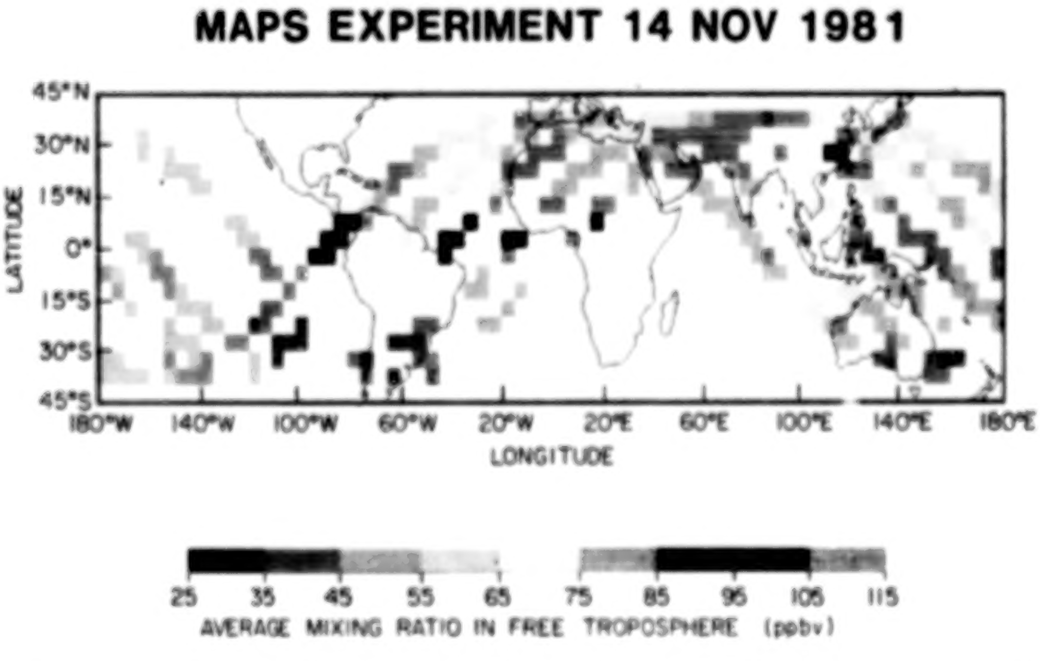
MAPS EXPERIMENT 14 NOV 1981
45°N
30°N
15°N
0°
15°S
30°S
45°S
LATITUDE
180°W
140°W
100°W
60°W
20°W
20°E
60°E
100°E
140°E
180°E
LONGITUDE
25
35
45
55
65
75
85
95
105
115
AVERAGE MIXING RATIO IN FREE TROPOSPHERE (ppbv)

Figure 4. Averaged tropospheric carbon monoxide ratios measured by MAPS instrument during OSTA-1 flight.

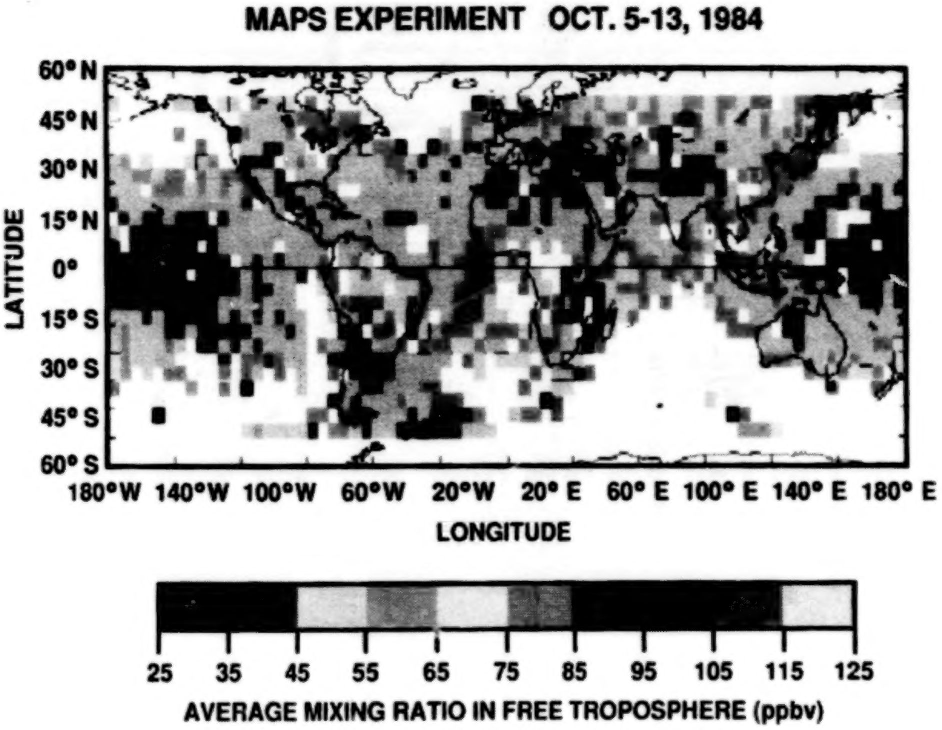

MAPS EXPERIMENT OCT. 5-13, 1984
LATITUDE
60° N
45° N
30° N
15° N
0°
15° S
30° S
45° S
60° S
180°W 140°W 100°W 60°W 20°W 20° E 60° E 100° E 140° E 180° E
LONGITUDE
25 35 45 55 65 75 85 95 105 115 125
AVERAGE MIXING RATIO IN FREE TROPOSPHERE (ppbv)

Figure 5. Average tropospheric carbon monoxide ratios measured by MAPS instrument during the OSTA-3 flight.

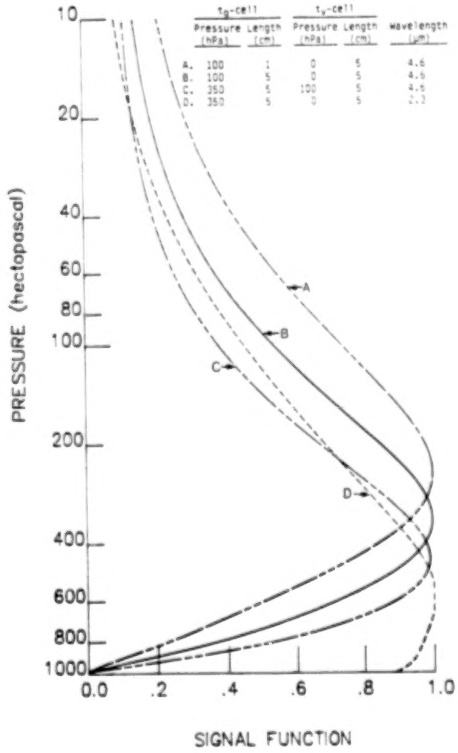

Figure 6. Normalized signal functions for the TRACER experiment.

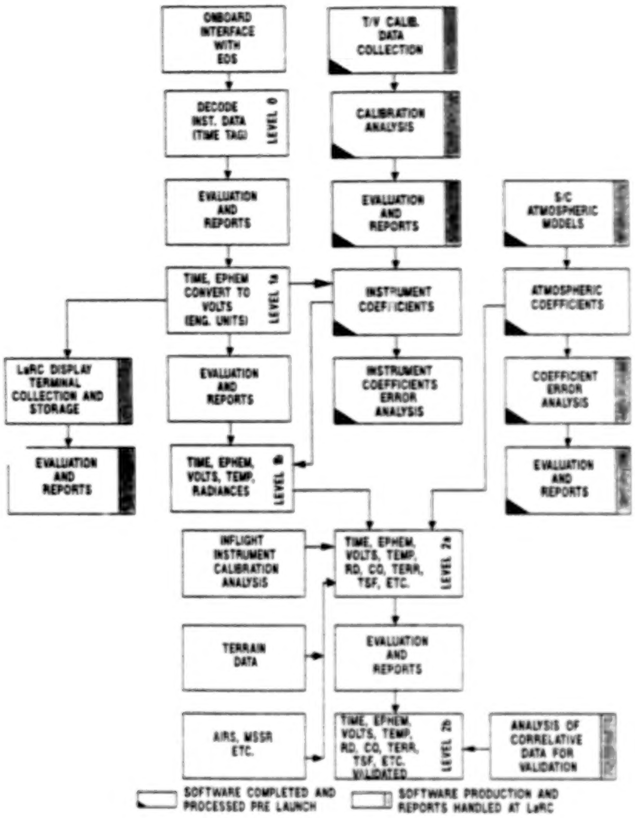
ONBOARD INTERFACE WITH EOS
T/V CALIB. DATA COLLECTION
DECODE INST. DATA (TIME TAG)
LEVEL 0
CALIBRATION ANALYSIS
EVALUATION AND REPORTS
EVALUATION AND REPORTS
S/C ATMOSPHERIC MODELS
TIME, EPHEM CONVERT TO VOLTS (ENG. UNITS)
LEVEL 1a
INSTRUMENT COEFFICIENTS
ATMOSPHERIC COEFFICIENTS
LaRC DISPLAY TERMINAL COLLECTION AND STORAGE
EVALUATION AND REPORTS
INSTRUMENT COEFFICIENTS ERROR ANALYSIS
COEFFICIENT ERROR ANALYSIS
EVALUATION AND REPORTS
TIME, EPHEM, VOLTS, TEMP, RADIANCES
LEVEL 1b
EVALUATION AND REPORTS
INFLIGHT INSTRUMENT CALIBRATION ANALYSIS
TIME, EPHEM, VOLTS, TEMP, RD, CO, TERR, TSF, ETC.
LEVEL 2a
TERRAIN DATA
EVALUATION AND REPORTS
AIRS, MSSR ETC.
TIME, EPHEM, VOLTS, TEMP, RD, CO, TERR, TSF, ETC. VALIDATED
LEVEL 2b
ANALYSIS OF CORRELATIVE DATA FOR VALIDATION
SOFTWARE COMPLETED AND PROCESSED PRE LAUNCH
SOFTWARE PRODUCTION AND REPORTS HANDLED AT LaRC

Figure 7. Data flow and dissemination plan for the TRACER experiment.

N90-27151

Data Analysis Techniques

Steve Park
Department of Computer Science
College of William and Mary
Williamsburg, VA

A large and diverse number of computational techniques are routinely used to process and analyze remotely sensed data. These techniques include:

- Univariate Statistics;
- Multivariate Statistics;
- Principal Component Analysis;
- Pattern Recognition and Classification;
- Other Multivariate Techniques;
- Geometric Correction;
- Registration and Resampling;
- Radiometric Correction;
- Enhancement;
- Restoration;
- Fourier Analysis;
- Filtering.

Each of these techniques will be considered, in order.

Univariate Statistics

The standard way to reduce a large amount of *homogeneous* remotely sensed data to a handful of representative numbers is to apply traditional elementary univariate statistical techniques. These include:

- measures of central tendency (mean, median, mode);
- measures of dispersion (variance, standard deviation);
- measures of distribution (percentiles, histograms).

These techniques are well understood and only require a modest computational capability, particularly if they are implementated as "one-pass" algorithms. That is, for example, the variance, s^2, (and the mean, $\overline{x}$) of n data points should be calculated in one pass as

$$s^2 = \frac{1}{n} \sum_{i=1}^{n} x_i^2 - \overline{x}^2$$

rather than in two passes as

$$s^2 = \frac{1}{n} \sum_{i=1}^{n} (x_i - \overline{x})^2.$$

Doing so minimizes memory requirements.

As an alternative, if the data is quantized as, say, 8-bit integers then a 256-bin histogram is easily computed and from it all other statistics can be calculated. For example, the mean is then

$$\overline{x} = \frac{1}{n} \sum_{l=0}^{255} l f[l]$$

where $f[l]$ is the histogram bin count corresponding to the data value l.

Multivariate Statistics

The standard way to compare several related sets of remotely sensed data (each of which is homogeneous)—for example, multi-spectral data—is to apply traditional multivariate statistical techniques. These include:

- measures of co-relation (covariance matrices, correlation matrices);
- measures of multivariate distribution (bivariate histograms).

As in the case of univariate statistics, these techniques are well understood and only require a modest computational capability, particularly if they are implemented as one-pass algorithms. Thus, for example, the covariance, c, (and the associated means) of two sets of n data points should be calculated in one pass as

$$c = \frac{1}{n} \sum_{i=1}^{n} x_i y_i - \overline{x}\,\overline{y}$$

rather than in two passes as

$$c = \frac{1}{n} \sum_{i=1}^{n} (x_i - \overline{x})(y_i - \overline{y}).$$

As an alternative, multivariate statistics can be calculated from bivariate histograms. For example

$$\sum_{i=1}^{n} x_i y_i = \sum_{l_1=0}^{255} \sum_{l_2=0}^{255} l_1 l_2 f[l_1, l_2]$$

where $f[l_1, l_2]$ is the bivariate histogram bin count corresponding to the data pair (l_1, l_2). However, the desirability of bivariate histograms as analysis tools for multivariate remotely sensed data is problematic. For example, a complete set of bivariate histograms for a 6-channel, 8-bit multispectral data set would involve the use of 15 arrays, each 256 × 256.

Principal Component Analysis

Multivariate remotely sensed data frequently exhibits inter-component correlation; e.g., adjacent spectral bands are highly correlated. For this reason the *principal component transformation* (PCT) is sometimes applied to "decorrelate" the data. The result is a new (uncorrelated) set of data. If the multivariate data is k dimensional, then the PCT is implemented as a $k \times k$ matrix which is applied on a (multivariate) data point-by-data point basis. The amount of computation per data point is typically modest, provided k is not large. However, the construction of the PCT matrix involves a significant amount of computation. Three steps are involved.

- Calculate the $k \times k$ covariance matrix (or an approximation thereof) for the original multivariate data set.
- Calculate the eigenvector - eigenvalue decomposition of the covariance matrix.
- Construct the PCT matrix from the k eigenvectors of the covariance matrix.

Since the data must be processed once to calculate the PCT matrix and then a second time to apply the transform, principal component analysis is an inherently two-pass algorithm with a corresponding potentially large memory requirement. To get around this problem, it is common to essentially "guess" the covariance matrix a priori thereby avoiding one of the two passes.

If T is the PCT matrix and $\mathbf{x}$ is a k-dimensional multivariate data sample, then the transformation

$$\mathbf{x}' = T\mathbf{x}$$

defines a new set of multivariate data. It is frequently the case that the (diagonal) correlation matrix for this new data set will have only a few significant diagonal elements indicating that the effective dimension k' of the new data set is less than that of the original, k. This dimensionality reduction is an important consideration in pattern recognition and classification.

Pattern Recognition and Classification

Pattern recognition and classification is a statistical technique frequently applied to multispectral, remotely sensed image data. The concept is easily understood, however a successful implementation is frequently difficult. The primary reason for this is the difficulty of providing a sufficiently accurate statistical characterization of the classes.

The computational requirements associated with pattern recognition and classification are similar to those associated with a principal component analysis. Indeed, the PCT is frequently advocated as a preprocessing dimensionality reduction step so that classification can then be accomplished in a new smaller and "more orthogonal" space in which patterns become better separated. The point is that classification is done on a sample-by-sample basis with the amount of computation per classification determined by the complexity of the classification algorithm. There is a classic accuracy versus time tradeoff involved—more accurate classification is typically associated with a more complex algorithm. The complexity is, in turn, usually determined by the amount of statistical data (assumptions) required to characterize the patterns.

Most classification techniques are based upon a *maximum likelihood* application of *Bayes' Rule*. That is, each possible k-dimensional measurement vector $\mathbf{x}$ is assumed to have a probability distribution $\Pr\{\mathbf{x} \mid c\}$ for each of a finite number of pattern classes, c. The a priori probability of each class, $\Pr\{c\}$ is also assumed to be known. The conditional probability that $\mathbf{x}$ belong to class c is then

$$\Pr\{c \mid \mathbf{x}\} = \frac{\Pr\{c\}\Pr\{\mathbf{x} \mid c\}}{\Pr\{\mathbf{x}\}}$$

where

$$\Pr\{\mathbf{x}\} = \sum_{c} \Pr\{c\} \Pr\{\mathbf{x} \mid c\}$$

and the sum is over all possible classes. A measurement vector $\mathbf{x}$ is then classified by finding (searching for) that class c for which $\Pr\{c \mid \mathbf{x}\}$ is largest.

Other Multivariate Techniques

There are an enormous number of largely empirical techniques which have been developed for specific types of multivariate remotely sensed data. Most of these techniques attempt to answer the same basic question . . . "given two sets of data which may be separated in time, space, or wavelength to what extent are the two *different*?" It is impossible to comprehensively summarize all these techniques. However, it is at least possible to demonstrate three classifications into which many of these techniques fall.

- Multispectral—two nearly simultaneous observations of the same spatial area but in different spectral bands; e.g., vegetation studies in the visual and near IR. In an attempt to correct for atmospheric effects, many techniques involve "ratioing"—the division of one data set by the other. Because multispectral operations are typically quite simple and are applied sample by sample, the computational requirements are usually modest.

- Multitemporal—two spectrally compatible observations of the same spatial area made at significantly different times; e.g., seasonal observations of crops. The basic issue here is *change-detection* and many techniques involve "differencing", which is the subtraction of one data set from the other. The operations here are also typically quite simple and are applied sample by sample. As a result, the computational requirments are usually modest.

- Multispatial—two nearly simultaneous and spectrally compatible observations of the same area but differing in orientation, spatial resolution, or both; e.g., two similar imaging systems viewing the same spatial area but from different points in space. This geometric process of mapping one data set onto another is called *spatial registration* and is a notoriously complex computational process, particularly for image data.

Many multivariate techniques are actually "multi-multi". For example, it is frequently the case that one wants to analyze two images of approximately the same spatial area taken at different times, by different instruments located at different points in space. This is always a non-trivial process.

Geometric Correction

A major concern in the processing and analysis of remotely sensed data is to ensure that the data has the correct geometric characteristics. This is particularly true for image data. The details of the application and the instrument determine the requirements and therefore the techniques. However, the following factors are all potentially important and their contribution to a lack of geometric fidelity must be understood:

- detector geometry—defines the sample (pixel) grid in the scene;

- analog filter and detector response delays—a lag in time (perhaps frequency dependent) which may produce a potentially significant spatial shift in the data;

- sensor scan rate and slew (if applicable)—the ground track corresponding to a scanning sensor is "curved" relative to the ground track of the instrument;

- spacecraft altitude and velocity—departures from nominal can produce potentially significant geometric effects;

- spacecraft attitude (roll, pitch, and yaw)—departures from nominal can produce potentially significant geometric distortion;

- earth rotation;

- perspective geometry.

Geometric correction *in real time* will be a computational challenge. This is particularly true for image data. Recognize that the "traditional" way to do a final geometrtic correction (if high geometric fidelity is required) is on the ground with a computer-aided, interactive system heavily reliant on ground control points.

Registration and Resampling

Multispatial problems of registration and resampling arise primarily with image data whenever pixel values are required at points where they don't exist. Spatial registration is the geometric process whereby one coordinate system is mapped onto another. In effect, an image is created on a rubber sheet which is then pulled and stretched onto a new coordinate (pixel) grid. New pixel values must then be generated—this interpolation process is called resampling. Many resampling techniques are available, however computational consideration virtually always dictates that only local, efficient techniques are used. Local methods typically require a knowledge of the 16 nearest neighboring pixels (on a 4 × 4 grid) and their associated pixel values. This presents a significant computational challenge if the image is not in fast, random access memory.

In practice, resampling is virtually always implemented using either

- bilinear interpolation—in which case only the 4 nearest neighboring pixels are involved, but the interpolation function is not "smooth", or

- parametric cubic convolution—a smooth interpolation process involving the 16 nearest neighboring pixels.

The application (spatial resolution) determines which of these techniques should be used. If high spatial resolution is the requirement, cubic convolution is the choice.

Multispectral problems of registration and resampling can also arise. They are much less commonly discussed in the (image processing type) literature. In this case, the problem is really a restoration or inversion problem because spectral bands are frequently not sufficiently narrow enough to permit multispectral data to be analyzed as "point" (wavelength) samples. However, although the mathematics here may be involved, the implementation typically requires only a modest computational capability, unless the number of spectral bands is large.

Radiometric Correction

Another major concern in the processing and analysis of remotely sensed data is to ensure that the data is radiometrically correct. The following factors are all potentially important and their contribution to a lack of radiometric fidelity must be understood:

- detector response—the conversion of sensed radiance into voltage, typically modeled as an I/O transfer function with multiple parameters (gain, offset, etc.) whose values are estimated via extensive extensive pre-flight and in-flight calibration tests;

- analog-to-digital (A/D) conversion—the conversion always causes a quantization error; this error is negligible only if the number of bits per sample is sufficiently large enough and the "dynamic range" of the converter is properly matched to the detector response;

- atmospheric effects—the atmosphere acts as a (stochastic) filter to modulate the "signal" as it passes from the scene to the detector.

Correction for the first two factors is typically straightforward with only a modest computational effort required—unless extremely high radiometric fidelity is required; in which case, the detector response model may be quite complex (e.g., a Kalman filter). Even in this case, however, the correction is applied sample by sample and so the memory requirements are modest.

Atmospheric corrections *in real time* will be a computational challenge primarily because of the need to combine data from a variety of sensors and apply a significant amount of "engineering judgement" when these data do not all agree.

Enhancement

Enhancement is any *empirical* technique applied to data (typically image data) to increase the "information content" (visually or otherwise) of the data. This is the stuff of image processing and includes a variety of techniques which are usually applied pixel by pixel. That is, if $g(m,n) = l$ represents the value (gray level) of pixel (m,n) and if $l' = T[l]$ represents a gray level transformation (typically stored as a look-up-table) then the transformation

$$g'(m,n) = T[g(m,n)]$$

applied for all pixels (m,n) defines a new (enhanced) image, g'. The choice of $T[\cdot]$ defines the enhancement and includes the following standard techniques:

- linear contrast stretching—linearly stretch all values in the primary range of interest and clip the others;

- histogram equalization—redistribute gray levels so as to maximize the entropy of the enhanced image;

- histogram specification—redistribute gray levels in accordance with a specified (desired) histogram;

- gray level slicing—selected gray levels are unchanged; all others are clipped.

Pseudocolor enhancement is an extension of gray level enhancement in which scalar data is mapped to a color display by the pseudo (false) assignment of colors to gray levels. This is an increasingly popular technique in remote sensing (with limited scientific merit) whereby even the most benign data set can be manipulated to produce a quite dramatic appearance.

Restoration

Radiometric correction is really just a special case of the *restoration* (or inversion) problem. For example, an image of a scene is only an imperfect copy of that ideal image which would be produced if it were possible to geometrically project the scene through the optical system with no degradation. The traditional discrete 2-d *linear* model of this process is

$$g(m,n) = \sum_{m'} \sum_{n'} h(m,n;m',n')f(m',n') + e(m,n)$$

where f represents the ideal image of the scene, h represents the system impulse response (point spread function), e is an (additive) noise term, g is the actual measured image, and the summation is over all space. Both g and h are assumed to be known and it is presumed that the noise, e, can be characterized statistically. The problem then is to solve for f. Equivalently, remove the effects of the instrument (h) and the noise (e) from the data (g) to determine the object (f) which was remotely sensed.

In many applications the instrument is so well designed (h is effectively a delta function) and the noise is so small ($e \approx 0$) that the subtle difference between f and g can be ignored. When this is not the case, the restoration problem must be solved. Doing so is a mathematically and computationally challenging activity which is usually facilitated by the additional assumption that the linear process which relates f to g is also *shift-invariant*. In this case, the previous equation simplifies to a *convolution*

$$g(m,n) = \sum_{m'} \sum_{n'} h(m-m',n-n')f(m',n') + e(m,n)$$

and the problem can be analyzed and solved (at least in theory) by using Fourier methods.

Fourier Analysis

If g is a 2-d array (e.g., an image) of size $M \times N$, then the corresponding *discrete Fourier transform* (DFT) of g is the $M \times N$ array $\hat{g}$ defined by

$$\hat{g}(\mu,\nu) = \frac{1}{MN} \sum_{m} \sum_{n} g(m,n) \exp\left(-2\pi i \left(\frac{m\mu}{M} + \frac{n\nu}{N}\right)\right).$$

The definition in 1-d is analogous and the continuous form of this transform involves little more than replacing $\sum$'s with $\int$'s.

There are several good reasons why the Fourier transform enjoys such popularity:

- the convolution theorem—convolution in the spatial (m,n) domain is equivalent to multiplication in the frequency (μ,ν) domain;
- many remote sensing instruments are built to specifications (resolution, response, etc.) which are formulated in the frequency domain;
- the DFT lends itself to the analysis of periodic data;

- there is a compelling "duality" between space (or time) and frequency; e.g., the array g can be recovered from the $\hat{g}$ array by a second (inverse) Fourier transform

$$g(m,n) = \sum_{\mu} \sum_{\nu} \hat{g}(\mu,\nu) \exp\left(2\pi i \left(\frac{m\mu}{M} + \frac{n\nu}{N}\right)\right);$$

- for most values of M and N there is a *fast* implementation of the DFT—the fabled *fast Fourier transform* (FFT).

All of this must be balanced against the observation that, for large values of M and N the FFT is a computational resource hog—memory requirements are proportional to MN and the operations count is proportional to $MN \log_2(MN)$.

Filtering

Filtering is the process of modifying sample values using a weighted linear combination of sample values in a neighborhood of the value in question. For example, if g is a 2-d array of data and h is a 2-d array of weights then the (convolution) equation

$$g'(m,n) = \sum_{m'} \sum_{n'} h(m-m', n-n') g(m',n')$$

defines a new, filtered, array g'. In 1-d and 2-d, this is the stuff of signal and image processing.

Filtering is typically used for:

- noise suppression—a "low-pass" filter designed to suppress high-frequency noise;
- high frequency enhancement—a "high-pass" filter designed to empirically boost high frequencies thought to be previously suppressed during data acquisition;
- high frequency restoration—typically, some form of a Wiener filter derived based upon a convolutional model of the data acquisition process.

In most cases, filters are designed (or derived) in the frequency domain and then transformed to the spatial domain. The design of a filter is always a challenging process. If (and perhaps, only if) it is done right, then the spatial domain implementation in 1-d requires only a modest computational capability. In 2-d, however, there is likely to be a data-management problem associated with maintaining a data list for the nearest neighbors of the point being filtered.

References

For those interested in acquiring a better background in data analysis techniques as they relate to remote sensing, I recommend beginning with the

- *Manual Of Remote Sensing*, 2nd edition, (ISBN 0-937294-41-1) chapters 17, 18, and 21

and the many references contained therein. Although this manual is now 6 years old, much of the material in these three chapters remain state-of-the-art. Chapter 17 (edited by Fred Billingsley) is particularly recommended. However, be aware that the computational view in each of these chapters is the traditional one—do all the processing on the ground, take as much time as necessary, and use all the horsepower you can muster.

N90-27152

ONBOARD PROCESSOR TECHNOLOGY REVIEW

Harry F. Benz
NASA Langley Research Center
Hampton VA

Abstract

In this short review paper, I discuss the general need and requirements for the onboard embedded processors necessary to control and manipulate data in spacecraft systems. I review the current known requirements from a user perspective, based on current practices in the spacecraft development process. I then discuss the current capabilities of available processor technologies, and project these to the generation of spacecraft computers currently under identified, funded development. I provide an appraisal of the current national developmental effort.

Introduction

By nature of an introduction, I will recite a number of assumptions that are embedded in the NASA practices of implementing missions. I will then bring some practical realities of implementing new embeddable computer resources into these missions.

A good reference for backup material for this paper is the "NASA Space Systems Technology Model" Volume IIB, Chapter 11. More current material is included in the GAO Report "Space Operations, NASA Efforts to Develop and Deploy Advanced Spacecraft Computers."

For NASA to "sell" a mission project, the program manager must assure NASA senior management that the technology to implement the mission is "in hand." The Office of Aeronautics and Space Technology in its "NASA Space Systems Technology Model" has embedded a seven-layer description of technology readiness for implementation. For those readers with experience with the military description of the process of technology development, these generally correspond to the levels of 6.1, 6.2, etc. Readiness level seven implies that the technology has been used successfully in the relevant environment, and it is essentially "off the shelf." The goal of every NASA program manager is to use this "off the shelf" technology in his mission to simultaneously minimize risk, minimize cost, and meet mission goals. To gain performance or short-term cost advantage, a mission project manager may use a technology that is a little less mature and incur a little risk. This use of technology at the level six, or engineering model tested implies that the technology is mature but has not been used successfully in the relevant environment. A typical flight program takes five years from inception or proposal to flight. A year is taken for mission definition and technology tradeoff studies, three years for subsystem or payload development and test, and a final year for system integration and flight vehicle integration and test.

Most researchers and technology developers within NASA, especially those supported by the Office of Aeronautics and Space Technology, perform basic research at level one, where the basic physical phenomenon is discovered; or at applied research at levels two through four, or five, where the physical phenomenon is engineered into a conceptual design, the conceptual design is tested, the critical functions are tested, and major components are tested. With increasing levels of complexity, there is an exponential increase in associated developmental cost, and an increasing level of committment required by the OAST program management from the project user program office to keep the expensive technology development from "withering on the vine." In the processor development area, there has never been sufficient resources made available from the OAST program to carry computer development to level seven. The computers that NASA uses have been primarily adapted from military or militarized commercial computers. An example of such a computer is the NASA Standard Spacecraft Computer that was repackaged for the space environment by the NASA Standard Parts Program, run by the NASA Chief Engineer's Office. The most recent example is the Gallileo computer, the Harris 80C86, which is a redesigned gate level copy of the Intel 8086 with a radiation hard fabrication and a limited amount of single-event upset immunity.

Within the commercial semiconductor industry, there is a rule of thumb that the capability of a technology will double every three years. In order to maintain a product market in this rapidly expanding technology area, the semiconductor manufacturers must have an overlapping developmental program. The time necessary to develop each next generation manufacturing capability is two or three years. The time necessary to design the next generation component technology is three years. The time to win market share for a new processor is a year, and the useful manufacturing lifetime is about three years.

To build a processor in the current environment, there is a fifty-million-dollar engineering investment to design, to manufacture, to integrate hardware, and to develop software operating systems and higher level language compilers. This cost must be recoverable from sales and does not include the component production facility. The facility costs are roughly one hundred million to capitalize and forty million per year to operate. Every three to five years, with increasing complexity, this facility must be recapitalized.

This has brought about an apparent paradox. To propose and build in mission hardware, the hardware must be mature in the marketplace. With a five-year mission development cycle, by the time the hardware is launchable, it is no longer available in the marketplace. It has become obsolete. Thus, we are building systems of obsolete hardware. The components must be delivered from warehouses of obsolete parts. Since they are no longer manufactured, it is impossible to acquire more should the warehouse become depleted without significant capital and manufacturing costs, which are beyond the scope of the mission. Both the DoD and NASA have recognized this for years, but there appears to be no long-term solution. This is a characteristic of a growth technology.

The military and space semiconductor manufacturers are almost wholly captive to the military and space industries and thus the government. The system operating environments and requirements are significantly different; there is somewhat of a carryover of manufacturing methods and practices; and there is a higher cost at almost an exclusively government-subsidized marketplace. The government recognizes this and is attempting to help through sponsorship of the Very High Speed Integrated Circuit (VHSIC) program, the MMIC program, the GaAs pilot line facility, and most recently with Semitech. The industry recognizes this and has been attempting to remedy it through Microelectronics and Computing Corporation (MCC) and Semiconductor Research Corporation (SRC).

Thus there are fundamental differences in the requirements, cost, marketplace, schedules, and readiness that confound the use of current or next-generation commercial processing technology in the space mission environment.

Requirements of the Natural Space Environment on Processors

The space environment imposes a number of physical constraints on the hardware to be used in spacecraft payloads. The physical constraints which must be met are the vacuum of space which imposes the constraint that all the electronics must be conduction cooled to maintain junction temperatures and thus long time reliability. This is normally done at the subsystem level into a heat rejection system. This conduction cooling forces a mass penalty onto the launch vehicle. The more power there is to dissipate, the more massive the thermal distribution and dissipation. Power is also much more expensive to generate. This has traditionally forced acceptance of low power complementary logic families to reduce the static dissipation of power.

In the Complementary Metal Oxide Semiconductor (CMOS) logic, standby power is near zero, and all power is dissipated dynamically by changes of logic state. This implies that the processor hardware can be powered down by reducing the system clock, a simple concept that allows operational phase tradeoff between tasks to be processed and the available power. Thus the speed power product is of critical importance to optimize functionality. The spacecraft orbit for the particular spacecraft also is important. Low earth equatorial orbits are relatively inexpensive to reach, and the natural radiation is reduced by the earth's shadow and magnetosphere. High geostationary orbit is expensive because of the energy required to launch and the higher radiation environment. Polar orbit is more expensive to launch because the launch vehicle cannot take advantage of the earth's motion, and the radiation environment is much more severe because of the lack of shielding by the magnetosphere at the poles, and the low polar altitude of the Van Allen belts, which are encountered twice each orbital period for the life of the mission.

The natural radiation environment is not so severe as the military strategic weapons environment, but several constraints are similar. The hardware must be designed at the cell within the chip level to be total dose tolerant to the level of the expected mission orbital life. It must be latch-up free. With the development of logic at the 1.25 micrometer minimum feature size, the amount of charge that retains the logic level within the cells of the devices is less than that deposited by a cosmic ray passing through the cells of the device. Parasitic devices inadvertantly designed into the devices by following best commercial packing rules allow virtual Silicon Controlled Rectifier devices to exist within the wells of a CMOS device. There is no gate to allow these devices to turn on, and there is no means to turn them off. These cosmic rays in traversing the whole spacecraft pass through these devices on a statistical basis and turn on the SCR devices. This causes catastrophic device failure. The cosmic rays also can upset the logic by simply overwriting memory cells in conventional memory or within registers in a CPU. The logic must be designed to be "bullet proof." This additional design constraint costs design specialization, design time, and chip area. This is in direct opposition to the marketplace drivers of the commercial chip developer.

The commercial chip developer is interested in maximizing the number of gates on a chip whose parameters are centered within the commercial, market-driven manufacturing production facility. With the incorporation of 1.25-micrometer technology into digital flight control systems on military and commercial aircraft which fly at higher altitudes, cosmic ray latch-up and upset will likely become significant drivers in the cost and system complexity of such systems. Conventional passenger aircraft normally fly significantly above the protection that the atmosphere provides for cosmic rays. In a normal transcontinental flight, the typical radiation dose to a passenger is equivalent to a chest x-ray, primarily caused by other charged particles, but with a cosmic ray component. When these systems are finally flown, there will likely be many unexplained upsets identified in the fault tolerant architectures. Whether these fault tolerant control systems can recover their system integrity and state between single event upsets is yet to be determined. Thus in the current integrated circuit technology epoch, there should be a merging of aeronautics and space requirements in the cosmic ray area.

The remoteness of the environment imposes additional constraints. The hardware must be testable on orbit to allow operational validation. Except for Shuttle-reachable satellites, the hardware cannot be repaired during its operational life; therefore, it must include a level of fault tolerance and must have carefully predicted failure statistical models.

Mission cost is a primary driver. Individual NASA space missions simply cannot afford to develop their own hardware as one-time developments. Another primary driver is performance. No mission can accept performance that is unable to meet its needs. The commercial sector has made great progress in its marketplace. The adaptation of commercially manufactured products for the space environment is very costly and involves significant redesign. Only few commercial vendors see this government-only space marketplace as a place for long-term profitability.

Desirable Attributes of a Spaceborne Processor

The attached requirements and targets should be achievable by the mid 90's for technology levels six and seven from a variety of sources. The Generic VHSIC Spaceborne Computer, developed by IBM and Honeywell through the SDIO/AFSTC SAT 144 program for use in their BSTS currently offers the most short term promise over the 80C86 used in Gallileo. On the technology horizon, the Rad Hard -32 bit processor, under development by a variety of consortia through the SDIO/AFRADC SAT 143 program SSTS, offers the next most promising processor epoch. The short term targets and goals are centered on a GVSC multiprocessor specification.

Current Spaceborne Processor Capabilities

I have collected from various sources, including commercial product offerings, spacecraft mission documents and developmental planning documents, a representative collection of the currently available processors. I have included this collection in Table 1 as Processor Characteristics. By best estimates, I have attempted to categorize its suitability and readiness. I will discuss the characteristics that I have identified as columns in the table. I have categorized these columns as: performance, using standard instruction set mixes where available (including the DAIS, and Whetstone which, primarily, have suitability for control-type algorithms with some arithmetic); the power of the CPU chipset; the radiation hardness and mechanisms; the self-testability; sponsors; and other remarks. In Table 2, I have followed the same format, and have identified when the implementing CPU chipset was or is planned to be ready for use in the radiation hard space environment, when the memory management unit is ready, when a bus interface unit is ready, and when a gate array for use in "glue logic" is ready. I must note here that a chipset and a fabrication technology do not make a spacecraft computer. Also in columns are the CPU-ALU width for performance, the size of the memory space directly addressable, and the high level software tools available for the user programmer. An additional survey was published in the June, 1989, issue of "Defense Science," in an article entitled, "Radiation Hardness--The New Requirement" by J. S. Tirado and the accompanying chart entitled "4th Annual Directory of Radiation Tolerant IC's."

Conclusions

The technology is sufficiently mature to build an experimental ISES. If EOS NPOP-1 holds schedule, the SDIO/AFSTC-sponsored Generic VHSIC Spaceborne Computer hardware will be ready and "off the shelf." If the EOS NPOP-1 schedule slips, the SDIO/AFRADC-sponsored Radiation Hard 32-bit processor, a RISC-MIPS-based chipset, will then be sufficiently mature for "off the shelf" use.

DESCRIPTION OF REQUIREMENTS FOR EMBEDDED PROCEDURES

- PERFORMANCE - INSTRUCTION RATE FOR STD MIX, DAIS, WHETSTONE, DHRYSTONE, ETC.
- POWER - CMOS TO SMALLEST FEATURE SIZE - PRIMARY IMPACT ON WEIGHT
- WEIGHT - LEO, EQUATORIAL IS EXPENSIVE; POLAR IS VERY EXPENSIVE, GEO EVEN MORE
- SIZE - TO MEET MOUNTING/THERMAL INTERFACE
- ENVIRONMENT
  - TEMPERATURE - MIL STD TEMPERATURE RANGES
  - VACUUM - OUTGASSING, HEAT FLOW
  - VIB - LAUNCH
  - EMI/RFI INTERNAL/EXTERNAL - CANNOT INTERFERE WITH SENSORS, CANNOT BE INTERFERED WITH IN PRESENCE OF HIGH POWER XMTRS, SAR
  - RAD HARD CMOS - SINGLE EVENT LATCH UP FROM COSMIC RAYS
    - TOTAL DOSE - BENIGN ENVIRONMENT WITH POTENTIAL BELT CHARGING
    - SINGLE EVENT UPSET FROM COSMIC RAYS
- TESTABILITY - VALIDATION ON ORBIT
- FAULT TOLERANCE - FAIL OPERATIONAL, FAIL SAFE, CANNOT CONTRIBUTE TO MISSION FAILURE
- MTBF/MTBCF - CONSISTENT WITH MISSION LIFE
- "SECURITY"/INTEGRITY - PROTECTION FROM INTRUDERS, ACCIDENTS

ISES REQUIREMENTS (R)/TARGETS (T)

- PERFORMANCE: 25 MIPS AGGREGATE DAIS MULTIPROCESSOR (T)
- POWER: 200 W (T)
- WEIGHT: 40 KG (T)
- SIZE: 1/2 ATR, 6" X 10 " x 20" (T)
- ENVIRONMENT:
  - TEMPERATURE - MIL SPEC -55°C TO +125°C OPERATING (INTERNAL)(R)
  - VACUUM - HERMETIC DURING STORAGE/ALL CONDUCTION COOLING (R)
  - VIB - LAUNCH ENVIRONMENT (R)
  - EMI/RFI - NON INTERFERING WITH MISSION/SCIENCE SENSORS (R)
  - RAD HARD CMOS - NO SINGLE EVENT LATCH UP (R)
    - TOTAL DOSE: 3E5 RADS/S; (R FOR POLAR, GEO)
    - SINGLE EVENT UPSET, LET > 42, IE-10 UPSETS/BIT-DAY (T)(R FOR CONTROL)
  - TESTABILITY - 100% (T)
- FAULT TOLERANCE - FAIL OPERATIONAL, FAIL SAFE, REDUNDANCY TECHNIQUES ONLY (R)
- MTBF/MTCF - 60K HR/300K HR (T)
- "SECURITY"/INTEGRITY TO MEET MISSION REQUIREMENTS (R)

(KEY R = REQUIREMENT)
T = TARGET

TABLE 1. PROCESSOR CHARACTERISTICS

PROCESSORS (CHIPSET ONLY)	PERFORMANCE	POWER	RAD HARD	TESTABLE	SPONSOR	REMARKS
1802	100 KIPS	0.5 W	YES BULKCMOS 2M	NO	MATURE	MAGELLAN (COMMONLY USED)
80C86	?	0.5 W	BULK CMOS YES - LIMITED AND LATCH UP	NO	MANY	GALILEO PECULIAR SEU UPSET SPEC
SA3300	750 KIPS	1.5 W	YES BULKCMOS	NO	DOE	CRAF CANDIDATE
469R^{2}	3 MIPS	3 W	CMOS-SOS YES	NO	CDC-IRAD/SDIO	MOST VERSATILE
RI-RCA 1750	500 KIPS	2 W	YES CMOS-SOS	NO	MIDGETMAN ICBM	PROPRIETARY
GVSC (2)	4 MIPS	5 W	YES BULK-CMOS	100%	VHSIC-AFSTC/ SDIO	SDIO-BSTS
80386	4 MIPS	3 W	NO (?) BULK-CMOS	NO	NASA-SSF	NASA SS INTEREST IN REVERSE ENGINEERING FOR RAD HARD
MDC281	630 KIPS	3 W	NO ? BULK-CMOS	NO	MDAC-IRAD	COFS
RH-32 (4-2)	25 MIPS	3 W	YES BULK-CMOS	100%	DARPA-ORD-SDIO	MIPS R-3000 JIAWG CAP32 - SDIO - SSTS
GaAs MIPS (2)	200 MIPS	15W (CPU)	YES GaAs	NO	DARPA-ORD	CURRENTLY 25 MIPS

TABLE 2. PROCESSOR CHARACTERISTICS (CONCLUDED)

PROCESSORS	CHIPSET READY	MMU READY	BIU READY	GA READY	ALU WIDTH	MEMORY SPACE	HIGH LEVEL SOFTWARE
1802 - (RCA)	75	N/R	N/R	1980	8	384K x 86	1802 ASS'Y
H80C86 (HARRIS)	1985	NO	YES	1985	16	?	BASIC, FORTRAN, PASCAL, -C
SA3300 (32032)/(SANDIA)	1988	90	90	1988	32	2^{32} x 16B	ADA
469R2 (CDC/1750)	1987	N/R	N/R	1987	16	64K x 16B	JOVIAL/1750
RI-RCA 1750	1988	N/R	N/R	1985	16	64K x 16B	JOVIAL/1750
GVSC (2) (1750A)/ (IBM-HONEY)	1989	1989	1989	1988	16	64K x 16B/ 256K x 16B	ADA/1750
80386	YES	YES	YES	1989	32	2^{32} x 16B	ADA-C-PASCAL FORTRAN
MDC 281 MDAC/MARCONI	87/89	NO PLANS	(SCI) 88	(H-)87	16	64K x 16 256K x 16	TARTAN ADA
RH-32 (4-2) (CORE MIPS) UNISYS/UTMC-IBM-TRW/MDAC-HONEY/WEST	90	91	91	90	32	2x2^{32}x32B	RISC-ADA/TLD ADA/CSALI-CORE MIPS
GaAs MIPS (2) TI-MDAC	88	90	90	88	32	2x2^{32}x32B	ADA/CORE MIPS

CONCLUSIONS

THE CURRENT STATE OF THE ART FOR SPACECRAFT ON-BOARD COMPUTING IS LIMITED.

EXPERIMENTS EMBODIED AS PROGRAMS MUST BE RELATIVELY UNSOPHISTICATED.

N90-27153

BRIEF STATE-OF-THE-ART REVIEW ON OPTICAL COMMUNICATIONS FOR THE NASA ISES WORKSHOP

Herbert D. Hendricks
NASA Langley Research Center
Hampton, Virginia

Abstract

This is a brief review of the current state of the art of optical communications. This review covers NASA programs, DOD and other government agency programs, commercial aerospace programs, and foreign programs. Included is a brief summary of a recent NASA workshop on optical communications. The basic conclusions from all the program reviews is that optical communications is a technology ready to be accepted but needed to be demonstrated. Probably the most advanced and sophisticated optical communications system is the Laser Intersatellite Transmission Experiment (LITE) system developed for flight on the Advanced Communications Technology Satellite (ACTS). Optical communications technology is available for the applications of data communications at data rates in the under 300 MBits/sec for nearly all applications under 2 times GEO distances. Applications for low-Earth orbiter (LEO) to ground will allow data rates in the multi-GBits/sec range. Higher data rates are limited by currently available laser power. Phased array lasers offer technology which should eliminate this problem. The major problem of cloud coverage can probably be eliminated by look ahead pointing, multiple ground stations, and knowledge of weather conditions to control the pointing. Most certainly, optical communications offer a new spectral region to relieve the RF bands and very high data communications rates that will be required in less than 10 years to solve the communications problems on Earth.

Introduction

NASA interest in optical communications has centered around a number of advantages that optical communications offers. These advantages range from a factor of 10 reduction in antenna size to reduced antenna weight (which also helps improve spacecraft stability and pointing problems), reduced power requirements, a new spectral region to help elevate RF band crowding, higher data transmission rates, and more secure data transmission. Shown in figure 1 is an LEO to telecommunications data relay satellite (TDRS) link comparison of laser communications vs. Ku band communication. From this data it is obvious that optical communications offer some very major advantages over RF communications.

Even though NASA, DOD, Europeans, and the Japanese have planned experiments, very little has been flown in space to demonstrate the technology. A number of aircraft-to-ground demonstrations have been performed. Probably the most sophisticated experimental system to date was planned as the LITE project to fly on the ACTS. However the LITE project has been scratched from ACTS. The good news is that the technology development is continuing. The remainder of this paper will be directed toward the identification of some of the ongoing programs and what organizations are involved as well as a summary of where optical communications stand today and what needs to be developed for the future.

NASA Programs

The major efforts in the development, fabrication, and demonstration of optical communications components and systems have been focused at the NASA Goddard Space Flight Center, Langley Research Center, and the Jet Propulsion Laboratory.

Jet Propulsion Laboratory

Research and development in this area has been directed toward the Deep Space Missions. Current work has been aimed toward the development of coherent communications systems based on diode pumping of Nd:YAG and the development of external modulation techniques. JPL is looking to the future for a 10-year lifetime device with a 2-Watt laser requirement with an external modulator for a 20 MBits/s data rate.

Goddard Space Flight Center

Research and development at this center has been directed toward Direct Detection Light Technology (DDLT) component and system development for the LITE experiment aboard ACTS. The DDLT system would share the Air Force/Massachusetts Institute of Technology/Lincoln Laboratory (MIT/LL) coherent experiment optics and would function when the coherent experiment was in the off mode. Optical communications experiments would be performed between ACTS and the Goldstone, AZ site and the GSFC Greenbelt, MD site as well as to an experimental module called Light Technology Experimental Facility (LTEF) aboard the Shuttle. This DDLT system will utilize the 20-cm optics of LITE, a multiple laser power summer with 200-300 milliwatts power output, and provide direct modulation of the lasers at a 220 MBits/s data rate. GSFC has performed a number of pointing, tracking, and acquisitions systems studies and development programs. GSFC has also addressed the problem of developing long life and stable semiconductor lasers.

Future missions requirements at GSFC are seen to require laser power in the 1-5 watts range and communication data rates to 4 GBits/s to provide communications for all of the upcoming NASA missions. These laser power level and modulation rates will require further development of high power semiconductor lasers.

Langley Research Center

Research and development programs at Langley have centered on the development of laser technology, optical transceivers, and lately the possible use of optical communications with ISES.

Langley has developed and demonstrated a number of semiconductor lasers for applications to optical communications. This technology has mainly centered on AlGaAs semiconductor lasers with emission in the 50-100 mW range and direct modulation demonstrations to 2 GBits/s. Recent developments have been aimed toward the utilization of phased array lasers to demonstrate multiple watt devices capable of modulation to 5 GBits/s. Other recent efforts have centered on the development and demonstration of a narrow linewidth semiconductor laser in InGaAsP for coherent communication applications.

A joint program with the Air Force has been completed in the area of optical transceivers. This development provided a military family of transceivers up to 1 GBits/s. A second phase of the program currently underway is addressing a high speed transceiver which will operate up to 4 GBits/s.

Langley Research Center has proposed an ISES which utilizes optical communications to downlink data to interactive users of Eos or Space Station data. This system design could utilize existing 20-cm optics, tracking, pointing, and acquisition systems. Implementation of a simple 30-mW laser would easily provide communications rates in the 100 to 1000 MBits/s communications rates. Look ahead and smart pointing systems to alleviate cloud coverage problems and a network of recieving stations interlinked with high speed fiber optic systems would make it a very useful system.

Other Government Agency Programs

The Air Force and Navy support most technology developments in the way of components, subsystems, and systems. Only the coherent optical communications research and development, by MIT/Lincoln Laboratory, part of the LITE experimental system for flight on the ACTS, will be discussed. This project provides the most information available for general use and does not impact DOD restrictions or provide proprietary contractor information.

The original approach for the coherent communications experiment was to downlink to Goldstone, AZ and GSFC at Greenbelt, MD. By utilizing coherent communications, which should have 15 dB better sensitivity than Direct Detection Light Wave Technology (DDLT) there would be a direct comparison of the two optical communications techniques. The coherent design consisted of a 30-mW laser which could be modulated to 220 MBits/s. The laser system was quadruple redundant with an analysis and tuning system. The overall weight was 200 pounds and needed 200 electrical watts. The parts were to be radiation hardened and flight qualified. Perkin Elmer supplied part of the optics and Ball Aerospace part of the point system. No current plans exist for flight. However, a flight version of the system will be available in 1992. This particular system has the best design information available for comparison to other system designs. In addition to the flight system, there was also a ground system design which used 30-cm optics.

Commerical Aerospace Programs

The major commercial companies involved in optical communications component, subsystem, and system development are Martin Marietta, TRW, McDonnell Douglas, Ball Aerospace, Perkin Elmer, Hughes Aircraft Company, GE Aerospace, Spectra Diode Laboratory, David Sarnoff Research Center, and Stanford Telecommunications, Inc. None of these company projects will be discussed because of the many and varied proprietary restrictions. There are a number of government-funded (DOD) projects connected to each company. They range from crosslinks, uplinks, and downlinks systems to a variety of subsystems and component developments. The main conclusion is that there are few major program efforts of such size as the LITE experiment for ACTS.

Foreign Programs

Research and development by foreign countries of which knowledge is available is based on the major efforts of a European project and a Japanese project.

European Program

The European project, called the Semiconductor Laser Intersatellite Link Experiment (SILEX), consists of a contractor team made up of Matra(prime) of France, Dornier of West Germany, Bertin of France, ANT of West Germany, Telespazio of Italy, Selenia of Italy, and Spazio of Italy. The SILEX project consists of two GEO laser communications packages for a '92-'93 launch. This system uses wavelength multiplexed AlGaAs semiconductors with a data relay capability of 480 MBits/s.

Japanese Program

The Japanese project is being put together by a team from the National Space Development Agency of Japan, the Radio Research Laboratory, and the Ministry of Posts and Telecommunications. The project is a GEO-Ground experiment with a 1992 launch and a GEO-GEO experiment for 1996 launch. The project is built for the ETS-6 satellite and utilizes AlGaAs Semiconductor lasers.

NASA Optical Communications Workshop

A NASA optical communications workshop, sponsored by Code RC (Dr. M. M. Sokoloski), was held at Annapolis, Md. on March 28-29, 1989. The major purpose of the worshop was to review optical communications technology with a view toward satisfying future communications needs of the Global Change Technology Initiative (GCTI). A review of the "Mission to Earth" communications requirements was presented along with a view of potential science applications of optical communications technology. A government and industry briefing on optical communications was presented before the workshop sessions.

The workshops were split into three sessions: Laser Technology, Systems Technology, and Science Benefits. The laser technology working group concluded that semiconductor lasers with good lifetime existed with power outputs up to 35 mW. Semiconductor lasers with power outputs up to 100 mW are available but with questionable limits on their lifetime. By power multiplexing a system of lasers with reasonable life, 200 mW power output was achievable with modulation capability to GBit/sec data rates. Within the next 3-5 years phased array lasers, Nd:YAG lasers, and Master Oscillator Power Amplifier lasers should offer in excess of 1-watt power ouput at high modulation rates.

The Systems Technology Working Group foresaw that optical communications systems at 1 MBits/s at 2 times GEO and that 220 MBit/s systems at 1 times GEO were currently available. Technology needs were high power lasers/amplifiers, modular highly integrated packaging, better acquisition and tracking systems, and novel approaches to reducing the weight of the optical systems. Reasonable systems are available by 1991 whereas higher data rate systems will be available for deployment in the 1996-98 timeframe with technology fixed by 1991-93.

The Science Benefits workshop concluded that global wind sensing, water vapor measurements, gravity field mapping, planetary sciences and fundamental theories such as gravitational wave detection would be possible through the use of optical communications systems and associated technology.

ISES Optical Communications

The ISES optical communications system could be easily achievable on an LEO mission such as Eos or Space Station Freedom. The optical communications system could implement a direct detection systems approach and utilize a 20-cm optic system with a 30-mW AlGaAs laser which could be modulated up to a multi-Gibits/sec data rate while maintaining a signal margin. Pointing, acquisition, and tracking systems of the type developed by Ball Aerospace would satisfy the system's needs. Electronics of the LITE type developed by MIT/LL would be a model for the systems. For GEO-GEO and GEO-Ground communications, either a coherent communications system such as that built by MIT/LL or a DDLT type design such as that built by GSFC would provide a 200-300 MBits/sec data rate. Any higher data rate requirements would require a higher power laser which requires greater lifetime than is currently available. These types of laser devices should be available in the 1991-92 timeframe. A ground station design could utilize 20- to 30-cm optics depending upon data rate for communications and be of the type being developed by MIT/LL.

The item that will mean most to the success of optical communications is the ability to communicate to a variety of ground stations located throughout the United States. Therefore a point ahead capability to direct the optical beam to a clear cloud free location is imperative. This will require a computer with knowledge of the weather pattern and a selection alogrithm to assure a clear communications path. With the advent of expanding high data rate fiber optics communications routes by a number of communications companies, the problem of directing data to the user is no longer a problem.

Summary

Optical communications systems can do the job at higher data rates than achievable in the RF domain. Near-Earth systems requirments are ready. What needs to be done is to qualify the optical communication system for use in space. A satellite for proof of demonstration of optical communications needs to be available.

Optical communications systems require longer ranges such as those from GEO orbits, and data rates higher than 200 MBits/s require higher laser power. This technology is advancing more rapidly in the past four years than previously thanks to DOD funding. Multi-GBits/s data rates for communications are a reality for optical communications systems. The electronics to drive and sense the signals are available.

What needs to be done is to utilize more systems development such as in the ACTS - LITE optical communications to drive out and develop optimized systems. Lighter weight hardware with further reduction in system power would be the major goals. System packaging and space qualification of the hardware are also major requirements. Adequate funding has not been directed toward solving needed flight hardware systems demonstrations.

Optical communications is a super data rate channel for the transfer of data and informations. It is past ready for experiments and demonstrations. What needs to be done is to properly implement the available technolgy into an acceptable demonstration to prove the viability of optical communications.

Acknowledgments

The author would like to acknowledge many helpful discussions, literature and copies of talks supplied by the following who have made this brief summary of optical communications technology possible:

Dr. M. M. Sokoloski, NASA Headquaters, Code RC
Dr. M. Fitzmaurice, GSFC
Mr. L. Caudill, NASA Headquaters, Code EC
Dr. Vincent Chan, MIT Lincoln Laboratory
Dr. Jim Lesh, Jet Propulsion Laboratory
Dr. Don Carlin, David Sarnoff Research Center
Dr. Don Chanin, David Sarnoff Research Center
Dr. Mike Ettenberg, David Sarnoff Research Center
Dr. William Streiffer, Spectra Diode Laboratory
Dr. David Welch, Spectra Diode Laboratory
Dr. Joe Weller, Naval Research Laboratory
Dr. Michael Gordinier, McDonnell Douglas Astronautics, Co.
Dr. Nick Pchelkin, Kirtland AFB
Dr. Vernon Heinen, NASA Headquaters, Code RC
Mr. Robert Marshalek, Ball Aerospace Systems Group
Dr. Dan Botez, TRW
Mr. Steve Mecherle, TRW
Mr. Dale Mikelson, Martin Marietta Astronautics Group
Dr. Chandrasekhar Roychoudhuri, Perkin Elmer
Dr. James Sparkman, NOAA
Mr. Alan Wissinger, Perkin Elmer Corp.
Mr. Brian Hendrickson, Griffis AFB
Dr. Tom Giallorenzi, Naval Research Laboratory
Dr. L. Goldberg, Naval Research Laboratory
Dr. Steve Katzberg, Langley Research Center
Dr. Harry F. Benz, Langley Research Center
Dr. Roger Breckenridge, Langley Research Center

LINK COMPARISON

LASER VS. Ku BAND

LINK CHARACTERISTICS

- o 300 MBPS DATA RATE
- o 10E-5 BIT ERROR PROBABILITY (UNCODED)

	LASER	Ku BAND *
LEO TRANSMITTER POWER	0.25 WATTS	10 WATTS
LEO ANTENNA DIAMETER	7 INCHES	12 FEET
TDRS ANTENNA DIAMETER	10 INCHES	16 FEET
LINK MARGIN	6 DB	6 DB

*FROM TDRSS USER'S GUIDE, REVISION 4, JANUARY 1980

Figure 1. Low Earth orbiter to TDRS link comparison of laser communication versus Ku band communication.

N90-27154

Applications of ISES for Geology

David E. Bowker
Langley Research Center
Hampton, Virginia

Many geological investigations do not require real-time remote sensing data insofar as the scenes are not very dynamic. However, there are times when rapid data acquisition can be very appealing, such as when directing a field operation or assessing the extent of environmental damage following a natural event. Before discussing these potential applications, it would be meaningful to define what is meant by real-time data.

For the most part real-time means that the data is being sent directly to the user as soon as it is collected and put on the spacecraft local area network (LAN). However, several things could delay this. If the Information Sciences Experiment System (ISES) onboard data processing is significant, or if data must be accumulated for several minutes or even orbits, then there could be a significant delay and the term "near real-time" is perhaps more appropriate. Thus the time between data acquisition and transmission is dependent on the application.

The data requirement will depend on the sensors involved and the ground station capabilities. ISES will be able to perform such operations as calibration, registration, geometric correction, grid referencing, resampling, applying algorithms, feature extraction, and the merging of multiple sensor output products. The data transmitted could vary from a simple set of statistics for a given area to a continuous stream of raw data from several sensors. Small portable ground stations will require highly processed data and probably low data rates.

Table 1 lists a variety of occasions where real-time remote sensing capability would be beneficial. This list is not intended to be complete but should be representative of the needs in the geological sciences. A discussion of these topics follows.

Table 1. - Areas of Interest for Real-time Data Transmission

1. Remote Sensing Verification During Field Sampling Programs

2. Remote Sensing Support for Field Investigations

3. Mass Movement:
    - A. Rock Slides
    - B. Mud and Debris Slides or Flows
    - C. Wind and Sand Storms

4. Earthquakes:
    - A. Surface Destruction
    - B. Fires

PRECEDING PAGE BLANK NOT FILMED

C. Flooding and Mud Flows

D. Tsunamis

5. Volcanics:

A. Gas and Smoke Venting

B. Lava Flows

C. Lahars

D. Pyroclastic Flows

E. Major Pyroclastic and Gas Eruptions

Remote Sensing Verification

Many remote sensing programs require the collection of surface samples during the overpass of a satellite, primarily for the purpose of scene calibration. At such times it is desirable to have verification that the satellite data was satisfactory over the area of interest. This is not always apparent from the ground, so a real-time data link could reveal such parameters as percent cloud cover, average aerosol index, and condition of the satellite data. If certain conditions are not met the investigators may wish to repeat the sampling during a following satellite overpass rather than chance having to return to the field at a later date. When aircraft are used as the primary remote sensing platform, the regional view of the satellite is still a valuable asset for making decisions affecting the program activities.

Remote Sensing Support

Geological investigations that are not remote sensing oriented may still benefit from the real-time transmission of satellite data. During the preparation for the field work geologists will consult pertinent maps and remote sensing data, but once in the field it may become apparent that conditions have changed since the last data were collected. Many surface features could have changed due to erosion or deposition, or vegetation might obscure much of the geologic structure. The ability to receive satellite imagery would be an asset at such times. There is also the possibility of making new discoveries, such as the location of faults or potential ore deposits, whereby satellite data might confirm the significance of the information. In most of these cases high resolution visible or microwave imagery will be desired, but the capability to receive such data may be limited by the receiving station. Access to adequate ground facilities may be the limiting factor under these conditions.

Mass Movement

Mass movement involves the transport of some portion of the land surface, such as in creep, landslide, or slip. With the exception of rain- or snow-induced slides, most mass movements do not have precursors. The more dramatic slides can be induced by such factors as stress relief, earth tremors, surface loading, weathering, etc. Although these events can be quite extensive and life threatening, the best that can be done is to quickly assess the magnitude of the damage. Near real-time satellite data would certainly be an aid to achieving this end. In these cases, an existing facility near the incident could process the data and generate the desired end products.

Wind storms, which include hurricanes, tornadoes, and sand storms are generally associated with meteorological phenomena, but they can result in major alterations of the land's surface. The poor atmospheric conditions at such times implies the need for microwave data during the event with visible imaging data at the nearest available time. In all events that involve making estimates of surface change it will be essential to have a data base for making comparisons of scene imagery. The storage of such a data base on the satellite would probably not be feasible, except under limited conditions, and therefore the data base would have to be kept at the local ground facility.

Earthquakes

Major earthquakes are predominately confined to well known areas and zones of the earth's surface. Since most result from the build up and release of stress along extensive fault systems, there is some periodicity to their occurrence. However, with the exception of foreshocks, which are not reliable indicators, there is little or no immediate warning of an impending major earthquake. The role of remote sensing, then, as in the mass movement episodes discussed above, is primarily one of damage and impact assessment. Both day and night high resolution coverage is desired at the disaster site. Fires may also accompany a major surface disturbance in urban areas and this will require the monitoring of atmospheric conditions as well. When reservoirs, lakes, and rivers are affected there is the additional problem of flooding and resulting mud flows. This puts an additional emphasis on continuous monitoring since aftershocks are still a consideration.

When earthquakes occur on the seafloor along the continental shorelines there is the potential for the generation of a tsunami. It is not possible to predict when a life threatening tsunami will occur, even when the location and magnitude of the quake is known. An international early warning network issues predictions of arrival times of potential tsunamis at major seaports around the world as a precautionary measure. At the present time it is doubtful that real-time satellite data would be a benefit other than to monitor coastal regions for damage.

Volcanoes

Volcanic activity is basically confined to the earth's major plate boundaries, the ocean ridges, and isolated hot spots. Unlike earthquake activity, however, volcanic upheavals often display a number of warning signs that may be monitored routinely by satellite. The sighting of smoke plumes and hot spots on or near the earth's surface, and/or volcanic gases in the troposphere or stratosphere, may portend a more serious event.

Data from the thermal bands of any imaging instrument could be examined on a regular basis over the known volcanic regions of the earth and the output used to alert investigators when temperatures above a given level are found. A similar approach could be taken with the atmospheric instruments, whereby the detection of a known volcanic gas above a certain magnitude could be used to activate a more dedicated search for its source. The primary magmatic gases emitted from lavas are water vapor, hydrogen, oxygen, nitrogen, hydrogen sulfide, sulphur dioxide, sulphur trioxide, carbon dioxide, carbon monoxide, hydrochloric acid, chlorine, methane, hydrogen fluoride, argon, and helium. Only one or two of these need to be monitored on a systematic basis.

Once a volcanic event has been detected there is the need for frequent monitoring of surface and atmospheric conditions. Lava flows can be observed both day and night with thermal imagery while lahars, a more common volcanic occurrence, can be surveyed with conventional multispectral data. As a volcano becomes more active pyroclastic flows and gases become more prevalent. During a major explosive event pyroclastic material and gases can be ejected into the stratosphere and dispersed worldwide. Mapping of surface activity may be hampered by poor visibility at such times, but the aerosol plumes may be a threat to both surface and aerial transportation and will require continuous monitoring.

Eos Instruments

Many of the instruments scheduled for NPOP-1 and NPOP-2 (see Appendix A at the end of this publication for a complete list) are useful in supporting the applications discussed above. The High Resolution Imaging Spectrometer (HIRIS) and Synthetic Aperture Radar (SAR) are the two most desired instruments because of their high resolutions and all weather coverage (SAR only) but cannot be considered at this time because of their limited on-time (about 3% and 7%, respectively) and command and control problems. The microwave instruments (AMSU, AMSR, NSCAT/SCANSCAT, SWIRLS and MLS) may be very useful for monitoring snow and ice fields and specific surface and atmospheric parameters, but should not be considered as prime candidates for geologic applications. MISR, a four-band, eight-direction, pushbroom scanner could be important also, but is best utilized here as a support for the other instruments.

The major sensor requirements for the geologic area include visible-near-IR thermal imaging, surface measurements, and gas and aerosol detection and mapping. Table 2 lists eleven instruments in these three categories and shows their desired use in five primary areas of application: quicklook, field support, early warning, rapid assessment, and continuous monitoring.

Table 2. - Selected NPOP-1 and NPOP-2 Instruments and Their Areas of Application

	Quicklook	Field Support	Early Warning	Rapid Assessment	Cont Monitoring
MODIS N+T	X	X	X	X	X
ITIR			X	X	X
GLRS				X	
HIRRLS/DLS			X	X	X
SAGE III			X	X	X
MOPITT/TRACER			X	X	X
SAFIRE			X	X	X
TES			X	X	X

The MODIS instruments are the most useful because of their continuous operation and wide field of view. However, the spatial resolution is not adequate for most detailed investigations and HIRIS and SAR data will have to be requested for follow-on examinations. The Intermediate Thermal Infrared Radiometer (ITIR) has the highest resolution (15m) and will be very useful for thermal imaging.

The Geodynamics Laser Ranging System (GLRS) will be needed to establish surface elevation and horizontal distances following major upheavals. It is shown here only in the rapid assessment application because of the laser's limited lifetime. However, due to poor atmospheric conditions following some events, there may be a substantial delay in obtaining new data.

One or more of the atmospheric instruments can be used to monitor gases and aerosols for early warning detection. Because of the wide variety of gases and the different vertical and horizontal monitoring modes, perhaps all of them will be needed for continuous monitoring following a major volcanic event.

Concluding Remarks

The principal applications for onboard data processing and real-time data transmission in the geological sciences area are 1) the detection of early warning signs of potential catastrophic events and 2) the rapid assessment of impact and damage following major events. Also, the opportunity for quicklook and supporting data during field investigations should not be disregarded.

The Eos platforms are ideal for these applications because of the variety of earth sensing instruments and their differing modes of operation. Further study is required to define the role for each instrument and to assess how they can aid each other in establishing an improved output product.

N90-27155

APPLICATIONS OF ISES FOR THE ATMOSPHERIC SCIENCES

James M. Hoell, Jr.
NASA Langley Research Center
Hampton, VA

Introduction

The proposed Information Sciences Experiment System (ISES) (Katzberg et al., paper in this CP) will offer the opportunity for real-time access to measurements acquired aboard the Earth Observation System (Eos) satellite. These measurements can then be transmitted to remotely located ground based stations. The purpose of this paper is to summarize a report on the application of such measurements to issues related to atmospheric science which was presented to a workshop convened to review possible application of the ISES in Earth sciences. It is noted that the initial report at the workshop and the present discussion are limited in scope and are not intended to be all inclusive of the applications that might benefit from ISES. Rather, the examples noted herein serve primarily to highlight that real-time access to some of the measurements currently proposed for the Eos could, indeed, benefit certain areas in atmospheric science.

The proposed protocol for Eos instruments requires that measurement results be available in a central data archive within 72 hours of acquiring data. Such a turnaround of raw satellite data to the final product will clearly enhance the timeliness of the results. Compared to the time that results from many current satellite programs, the 72-hour turnaround may be considered "real time". Nevertheless, the examples discussed below will emphasize applications in which a more rapid access to results will be required.

The need for rapid access to Eos results implies that there will be a real-time response to direct or change the course of an ongoing activity. An obvious and common example of the use of real-time data is meteorological data which is used directly (images) and indirectly (temperature and water vapor profiles) in daily forecasting. Data, such as visible and IR images from the various weather satellites (GOES, METOSAT, Polar Orbiter, etc.) are, in fact, often used as real-time data. This type of data is used for post mission and for flight and mission planning of many atmospheric chemistry experiments conducted today. It is difficult to imagine weather forecasting or field programs without real-time satellite data. There is, however, a limited experience base for applications of other types of real-time data from satellite platforms. This is a direct consequence of the lack of such data.

Examples of Current Atmospheric Chemistry Experiments

In this section, examples will be discussed showing how real-time measurements from one or more of the proposed Eos instruments could have been applied to the study of certain issues important to global atmospheric chemistry. Each of the examples discussed is based upon a field mission conducted during the past five years. Each of these examples will emphasize how real-time data could have been used to alter the course of a field experiment, thereby enhancing the scientific output. The centerpiece of each experiment was an aircraft instrumented to meet one or more specific objectives. For the examples, brief overviews of the scientific rationale and objectives(s), the region of operation, the measurements aboard the aircraft, and finally how one or more of the proposed Eos instruments could have provided data to enhance the productivity of the mission are discussed.

The first mission discussed here is the Amazon Boundary Layer Experiment (ABLE 2), which was conducted as part of NASA's Tropospheric Chemistry Program. It is of interest to note here that the initial impetus for this mission was based upon the global measurements of tropospheric carbon monoxide (CO) obtained from the first flight of the MAPS instrument aboard the shuttle (Reichle et al., 1986) in 1981. Figure 1 shows the global distribution of CO resulting from this shuttle flight. Note in particular, the enhanced CO mixing ratios appearing off the eastern coast of South America. The broad objectives of the ABLE 2 mission were to study the origin of this enhanced CO and the role of the Amazon Rain Forest in global chemistry/climate.

PRECEDING PAGE BLANK NOT FILMED

The Amazon Rain Forest is the world's largest remaining tropical rain forest. Figure 2 illustrates many of the processes that occur throughout the vast regions of the Amazon Basin. Both theoretical and available data support hypotheses that (1) tropical rain forest environments are characterized by relatively intense sources of certain biogenic gases (e.g., methane and nitrogen oxides) and aerosols; (2) the Amazon Basin is a region of frequent atmospheric instability with intense convective activity, resulting in the potential for rapid mixing of biogenic gases and aerosols to high altitudes where they impact global tropospheric chemistry; and (3) the tropical troposphere is a region of intense photochemical activity where oxidation of certain biogenic traces gases (e.g., isoprene (C_5H_8)) produces gaseous products, such as CO, that may be significant to global budgets.

The scientific objectives of ABLE 2 were accomplished through a coordinate program of measurements by U. S. and Brazilian scientists from ground, balloon, and airborne platforms. The centerpiece of the mission was instrumentation aboard the NASA Wallops Flight Facility Electra aircraft. During the mission, the Electra was based in Manaus, Brazil near the center of the Amazon Forest. The mission was conducted in two phases, the first at the beginning of the 1985 dry season during the June/July time period and the second at the close of the 1987 wet season during the April/May time period. The field operations during the 1987 rainy season were more extensive and are illustrated in Figure 3. Table 1 lists the investigators measurements during the 1987 missions. Similar measurements were also obtained during the 1985 mission. Figure 4 shows the study areas during the 1985 and 1987 operations. During both phases of ABLE 2, extensive airborne measurements were obtained over the rain forest including focused studies coordinated with the ground based instruments located approximately 50 km northwest of Manaus, basin scale surveys to characterize the source/sinks and photochemical transformation of trace species, and long range transport of primary and secondary tropospheric species.

As noted above, meteorological forecasting is a familiar example of the use of real-time satellite data. During ABLE 2 GOES, visible and IR images, received in Manaus via a communication link to the Langley Research Center Meteorological Center, proved invaluable for daily flight planning particularly during the convectively active rainy season. Frequently, images showing the meteorological conditions within a proposed study area several hours before initiating the particular flight plan were used for go/no-go decisions or for a change in flight plans. Similarly, real-time results from several of the proposed Eos instruments would have undoubtedly proved as useful for daily and long range flight planning. The availability of the large scale, upper tropospheric CO distributions, such as illustrated in Figure 1, would clearly have provided valuable insight into the temporal and spacial variability of large scale processes. Such CO data can be anticipated from the TRACER and/or MOPITT instruments proposed for Eos. During the 1985 dry season mission, dramatic increases in the background concentration of ozone (O_3), CO, and aerosols were observed. Highly structured layers containing enhanced concentrations of these species were frequently observed during several survey flights. The general increase in the background mixing ratios and the layers of air were attributed to long range transport of emission products associated with biomass burning occurring on the periphery of the forest several thousand kilometers from the ABLE 2 study regions. Real-time CO measurements from the TRACER or MOPITT instruments, O_3, aerosol measurements from the SAGE III instrument, and winds from the LAWS instrument would have provided advanced warning of the extent of these plumbs. Flight operations could have been re-structured to avoid these regions or to enhance the study within these regions. Furthermore, high resolution images from the IHRSS to provide information on the number and spacial extent of burning within or near the ABLE 2 study area would have also been useful.

The field deployment phase of another airborne study conducted by NASA's Tropospheric Chemistry Program was completed in September of 1989. This mission, denoted as CITE 3 (Chemical Instrument Test and Evaluation), focused on the study of the sulfur species in the marine environment. Unlike the ABLE 2 mission just discussed, the CITE 3 mission was totally airborne and conducted aboard the Wallops Flight Facility Electra. The primary objective of this mission was to evaluate the performance of instrumentation for measuring the sulfur compounds sulfur dioxide (SO_2), dimethelsulfide (DMS), hydrogen sulfide (H_2S), carbon disulfide (CS_2), and carbonyl sulfide (COS). A secondary objective of the mission was to determine, in a predominantly marine environment, the abundance and distribution of the above sulfur species which comprise the bulk of the gaseous global sulfur.

Atmospheric sulfur gas and aerosol species are involved in chemical processes which influence both air quality and climate. The primary sulfur species released into the atmosphere from anthropogenic, biogenic, and volcanic activity are the five compounds just noted above. Sulfur dioxide has both a large primary source in the form of fossil fuel combustion and a significant secondary source derived from the atmospheric oxidation of the sulfur precursor species CS_2, COS, H_2S, and DMS. Anthropogenic sources of SO_2 are currently estimated to account for approximately one half of the total global sulfur emissions.

Figure 5 illustrates what is currently thought to be the budget and important cycles for atmospheric sulfur. While the current budget estimates of the global sulfur budget are uncertain in part because of uncertainties associated with the measurement techniques, the most significant natural source of sulfur is thought to be associated with biogenic production of DMS by ocean phytoplankton. The lifetime of DMS is several hours It is oxidized to SO_2 followed by further oxidation to sulfate aerosols which are a major source of cloud condensation nuclei in the marine environment. A particular relevant question associated with global sulfur is formation of Cloud Condensation Nuclei (CCN) and their role in climate control. It has been postulated that an increase in global temperature will initiate increased DMS emission leading to an increase in CCN's available for formation of clouds. This would act as a negative feedback on climate warming. An alternate argument is that there has been no evidence to suggest that the increases in ambient SO_2 during the last several decades associated with anthropogenic sources have not led to increased cloudiness and, therefore, the sulfur connection to global climate change should not be viewed as one which would reduce climate change.

The areas of operation during CITE 3 are shown on Figure 6. Tables 2a and 2b list the measurements aboard the aircraft during CITE 3. Integration and approximately half of the tests flights were conducted with the Electra aircraft based at the Wallops Flight Facility followed by a three week deployment to Natal, Brazil. Operations over the mid-Atlantic off the U.S. coast and over the tropical Atlantic ocean off the coast of Brazil provided a wide range of environmental conditions to test instrumentation and to study the sulfur budget. Note that in addition to the sulfur instrumentation under test (Table 2a), selected measurements of other species important for understanding the performance of the various sulfur instruments and/or the sulfur photochemistry were also included in the CITE 3 payload. (Table 2b).

The real-time output from three Eos instruments would have been particularly valuable during the CITE 3 mission. The MIRS and MODIS instruments would have provided a map of the phytoplankton concentration in upper layers of the ocean surface; and the LAWS instrument would have provided measurement of winds. As noted above, the biological output from certain phytoplankton species is the major source of DMS. Location of ocean regions that might have higher productivity of DMS would have provided for the first time a direct correlation of the emissions of DMS and its subsequent oxidation to SO_2. A direct measurement of tropospheric winds would have offered the opportunity to track a given air parcel and therefore study the photochemistry of DMS over at least one diurnal cycle. Attempts to study the photochemical history of a given air mass through the use of forward trajectory analysis have not met with a great deal of success, particularly in such data sparse regions as over the ocean. Real-time measurements of winds via LAWS should greatly improve the ability to repeat measurements in a given air parcel.

The Airborne Antarctic Ozone Hole Experiment (AAOE) and the Airborne Arctic Stratospheric Expedition (AASE), sponsored by NASA and NOAA to study the cause of the depletion of O_3 over the Antarctic continent and to evaluate the possibility of a similar phenomena over the Arctic regions, represent two airborne missions focused on stratospheric chemistry. Both missions utilized the NASA DC-8 and ER-2 aircrafts instrumented for measurements of a range of species (Table 3) pertinent to the chemistry of stratospheric O_3. The scientific rationales for these missions have been well publicized in the press and scientific literature and therefore will not be discussed here. It is only noted here that these expeditions were also based upon satellite observations from TOMS O_3 first showing the reduction in O_3 over the Antarctic continent. A number of the instruments proposed for Eos would have provided valuable inputs to the operation of these missions. In particular, upper tropospheric and stratospheric measurements of O_3, temperature, water vapor, nitrogen dioxide, and stratospheric winds via proposed Eos instruments such as the Dynamic Limb Sounder (DLS), High Resolution Research Limb Sounder (HIRRLS), Microwave Limb Sounder (MLS), Spectroscopy Atmosphere Far-IR (SAFIRE), and Stratospheric Wind Infrar Limb Sounder (SWIRLS).

Examples of Future Field Studies in Atmospheric Chemistry

In this section several specific examples of airborne atmospheric chemistry experiments that are currently in the planning stages are briefly discussed. Here again, it is recognized that these examples are a rather limited subset of the field experiments that are in various stages of planning by U.S. and foreign agencies. The intent here is primarily to emphasize the obvious - namely, that future airborne atmospheric science missions will exist, and that as they grow in size and complexity, the availability of real-time Eos measurements can be expected to become an integral part of each mission.

A particularly relevant mission for consideration here is, like several of the missions discussed above, based upon global measurements of an important trace atmospheric species from a satellite platform. This proposed mission will study the chemical and dynamic processes that contribute to the formation of a large scale O_3 enhancement over the tropical Atlantic Ocean west of central Africa (Figure 7). This feature was derived from analysis of TOMS and SAGE II observations (Fishman, 1990). This feature, seasonal in nature with its maxima occurring during the September to November time period, represents a significant enhancement to the tropical ozone climatology and is undoubtedly important to understanding the current global O_3 budget and the global distribution of the hydroxyl radical, the most important species in tropospheric photochemistry.

The proposed mission (e.g., TRACE-A) will focus on the origin of this O_3 enhancement which has been identified in satellite observations as a common but variable feature during this period. Ozonesonde measurements from Natal, Brazil have also noted a similar O_3 enhancement during this same time period. It is hypothesized that regional scale dynamic and chemical conditions result in photochemical production of O_3 in mid-tropospheric air which has been enriched in nitrogen oxides from continental surfaces sources such as biomass burning in central Africa.

A series of aircraft flight, satellite observations, and ground-based support measurements have been proposed to elucidate the dynamical and chemical factors determining the origin of this newly discovered component in the global tropospheric O_3 budget. It is anticipated that measurement capabilities will be required for N_xO_y, HNO_3, PAN, NMHC, CO, O_3 , and aerosol composition and distribution. The current planning for the operational area for the TRACE-A mission is shown in Figure 6. The O_3 enhancements appear to be predominately in the free troposphere and to extend over a vast area of the tropical Atlantic and will therefore require the use of NASA's newly acquired DC-8 aircraft.

It is anticipated that the aircraft measurements during the TRACE-A mission will be coordinated with real-time satellite measurements of O_3 from current satellite instruments such as the TOMS and SAGE II whenever possible. The availability of real-time profiles of O_3 from the Eos SAGE III instrument would clearly make a valuable contribution during the proposed study. Similarly, real-time data on the distribution of CO from the TRACER and/or MOPITT instruments, and upper tropospheric profiles of H_2O and aerosols from SAGE III would enhance the ability to conduct this mission. Such measurements would define the temporal and spacial extent of the O_3, thereby providing real-time input to the flight planning to enhance the scientific output from this mission. Finally, a particularly valuable Eos measurement would be real-time upper tropospheric winds from the LAWS instrument. As noted above, these data would provide the unique ability to track an air parcel and study the photochemical formation of O_3 within the same parcel over a period of several days. Such measurements would be useful in determining if the enhanced O_3, indeed originates from the photochemistry of biomass emissions.

A series of airborne missions that will focus on studying transport and photochemistry of key trace tropospheric species over the Pacific Ocean is also under consideration. (See Fig. 6.) It is anticipated that these missions will begin in the early 1990's with perhaps three to four major field operations over a period of four to five years. Satellite measurements over the vast expanse of the Pacific Basin can provide invaluable support to these missions. Particularly useful would be measurements of upper tropospheric winds via the LAWS instrument since this region is almost devoid of rawinsonde measurements. Real-time winds along with measurements of other trace species such as CO and O_3 would also be valuable for defining the transport of effluent to the Pacific basin from the Asian continent. Measurement of CO, O_3 and H_2O would be important in assessing the origin of the air masses. Volumes of air having low CO and

H_2O and high O_3, for example, are likely to have a significant contribution from stratospheric regions. Air masses having high CO and H_2O are likely to have a significant contribution from the marine boundary contaminated by an anthropogenic source.

Concluding Remarks

The examples discussed above illustrate possible applications of real-time Eos data that could be made available through the ISES. Each example was based upon a field mission in which aircraft flight planning would actively respond to global/regional satellite observations. In each case, it was assumed that Eos observations provided a large scale map of the spacial and temporal distributions of one or more key atmospheric parameters of species. This map was then used to direct a more detailed study via an instrumented aircraft.

As the International Geosphere Biosphere Program (IGBP) gains momentum in the 1990's, multi-nation field experiments employing ground- and aircraft-based measurement platforms can be expected. These field programs will be global in scope and, undoubtedly, will be designed to take advantage of the global coverage offered by satellite observations. It seems clear that, as with real-time meteorological data, real-time observations of trace atmospheric species will become an invaluable tool for these missions in the 1990's and beyond.

References

1 Reichle, H. G., V. S. Connors, J. A. Holland, W. D. Hypes, H. A. Walleo, J. C. Casas, B. B. Gormsen, M. S. Saylor, and W. D. Hesketh: "Middle and Upper Tropospheric Carbon Monoxide Mixing-Ratios as Measured by a Satellite-Borne Remote Sensor During November 1981," J.G.R., vol. 91, 1986, pp. 10865–10887.

2. Toon, Owen B., James F. Kasting, Richard P. Turco, and May S. Liu: "The Sulfur Cycle in the Marine Atmospheric," J.G.R., vol. 92, 1987, pp. 943-963.

3. Fishman, Jack, Catherine E. Watson, Jack C. Larsen, and Jennifer A. Logan: "Distribution of Tropospheric Ozone Determined From Satellite Data," J.G.R., vol. 95, March 20, 1990, pp. 3599–3617.

Table 1. Principal Investigators in ABLE-2B Field Expedition
April–May 1987

INVESTIGATOR	INSTITUTION	INVESTIGATION
	UNITED STATES PRINCIPAL INVESTIGATORS	
Meinrat O. Andreae	Florida State University	Sulfur measurements (a,s)
Sherwin M. Beck	NASA Langley Research Center	Airborne meteorological data (a)
Edward V. Browell	NASA Langley Research Center	Aerosols, ozone profiles (a)
David R. Fitzjarrald	State University of New York at Albany	Meteorological studies (s)
Michael Garstang	University of Virginia	Meteorological studies (s)
Gerald L. Gregory	NASA Langley Research Center	Ozone (a)
Robert C. Harriss *	NASA Langley Research Center	Methane (s), carbon dioxide (a)
Charles L. Martin	Simpson Weather Associates	Meteorological studies (s)
Pamela A. Matson ‡	NASA Ames Research Center	Nitrous oxide (s)
Reinhold A. Rasmussen	Oregon Graduate Center	Isoprene/other trace gases (a,s)
John A. Ritter	NASA Langley Research Center	Flux of carbon monoxide, ozone, water vapor (a)
Jeffrey E. Richey ‡	University of Washington	Methane, carbon dioxide (r)
Glen W. Sachse	NASA Langley Research Center	Carbon monoxide (a)
Hanwant B. Singh	NASA Ames Research Center	PAN (a)
Robert W. Talbot	NASA Langley Research Center	Aerosols (a)
Arnold L. Torres	NASA GSFC Wallops Flight Facility	Nitric oxide (a)
Peter Vitousek ‡	Stanford University	Nitrous oxide (s)
Steven C. Wofsy	Harvard University	Nitric oxide (s), carbon dioxide (a,s)
	BRAZILIAN PRINCIPAL INVESTIGATORS	
Elen M. C. Cutrim	Federal University of Para	Rainfall studies (s)
Pedro L. S. Dias	University of Sao Paulo	Meteorological studies (s)
Volker W. J. H. Kirchhoff	Instituto de Pesquisas Espaciais	Ozone, Carbon monoxide (s)
Luiz C. B. Molion	Instituto de Pesquisas Espaciais	Project Scientist - Brazil (s)
Paulo Artaxo Netto	University of Sao Paulo	Aerosols (a, s)
Carlos A. Nobre	Instituto de Pesquisas Espaciais	Meteorological studies (s)
Daniel Nordeman	Instituto de Pesquisas Espaciais	Radon (a)
Lycia M. Moreira-Nordemann	Instituto de Pesquisas Espaciais	Precipitation chemistry (s)
Alberto W. Setzer	University of Sao Paulo	Satellite imagery (s)

* ABLE 2B and AGE Program ‡ AGE Program (a) Airborne (s) Surface (r) River

Table 2a. Sulfur Measurements During CITE-3 Field Expedition, August–September 1989

TECHNIQUE		ANALYSIS[1]	SPECIES					ORGANIZATION	INVESTIGATOR
CT/GC/FPD	Analysis Opt. 1	IFA	SO_2	—	—	—	—	Drexel University	D. C. Thornton
	Analysis Opt. 2	IFA	—	—	H_2S	—	OCS		
	Analysis Opt. 3	IFA	—	DMS	—	—	—		
	Analysis Opt. 4	IFA	—	—	—	CS_2	—		
CT/GC/MS/ILS	Analysis Opt. 1	IFA	SO_2	DMS	—	CS_2	—	Drexel University	A. R. Bandy
	Analysis Opt. 2	IFA	—	—	—	—	OCS		
GC/IF/ECD (w/scrubber)		IFA	—	DMS	—	—	—	National Oceanic and Atmospheric Administration/ Pacific Marine Environmental Laboratory	J. E. Johnson
GC/IF/ECD (w/out scrubber)			—	—	—	CS_2	OCS		
GWA/GC/FPD		PFA	—	DMS	—	—	—	Max Planck Institute for Chemistry	M. O. Andreae
NATUSCH		PFA	—	—	H_2S	—	—		
CT/GC/FPD		IFA	—	DMS	—	—	—	University of Miami	E. S. Saltzman
NATUSCH		PFA	—	—	H_2S	—	—		
GWA/GC/FPD		PMA	—	DMS	—	—	—	University of Washington	R. J. Ferek
FC/IC		PMA	SO_2	—	—	—	—		
CHEMILUMINESCENCE (Filter)		PFA	SO_2	—	—	—	—	Institut fur Meteorologie und Geophysik	H.-W. Georgii
(Continuous)		IFA	SO_2	—	—	—	—		

[1] IFA - In-Flight Analysis
PFA - Post-Flight Analysis
PMA - Post-Mission Analysis

Table 2b. Ancillary Measurements During CITE-3 Mission

PRINCIPAL INVESTIGATOR	INSTITUTION	SPECIES
Enio Periera	Instituto de Pesquisas Espaciais	Radon
Paulo Artaxo	University of Sao Paulo	Aerosol Trace Elements
Gerald Gregory	NASA/Langley	O_3, Aerosol Size Distribution
Glen Sachse	NASA/Langley	CO
Sherry Farwell	University of Idaho	Total Sulfur
John Bradshaw	Georgia Institute of Technology	NO, NO_2, NO_y
Ronald Ferek	University of Washington	Aerosol Composition, MSA, CN
Patricia Matrai	University of Miami	Ocean Productivity
GTE Project	NASA/Langley	Aircraft Met./ Position/ Met. Forecasting/UV Flux/ Sea State

Table 3. Measurements and Platforms During Antarctic Ozone Hole Experiment

Investigator and Affiliation *	Species	Type of Measurement
Anderson (Harvard)	ClO, BrO	local ER-2
Wahner (NOAA AL)	$OClO$, BrO, O_3, NO_2	column DC-8
Farmer (JPL)	$ClONO_2$, HCl, O_3, NO, NO_2, HNO_3, H_2O	column DC-8
Mankin/Coffey (NCAR)	O_3, NO, NO_2, HNO_3, H_2O	column DC-8
Browell (NASA Langley)	O_3, Aerosols	profile DC-8
Gregory (NASA Langley)	O_3	local DC-8
Proffitt (NOAA AL)	O_3	local ER-2
Starr (NASA Ames)	O_3	local ER-2
Fahey (NOAA AL)	NO or NO_y	local ER-2
Wilson (DU)	aerosol, condensation, nuclei	local ER-2
Ferry (NASA Ames)	aerosol	local ER-2
Gandrud (NCAR)	NO_3	local ER-2
Kelly (NOAA AL)	H_2O vapor or total H_2O	local ER-2
Oberbeck/Pueschel (NASA Ames)	chemical composition vertical profile ~ 1μm	profile DC-8
Loewenstein (NASA Ames)	N_2O	local ER-2
Heidt/Vedder (NCAR/ NASA Ames)	whole air CH_4, N_2O, CO, CFCs	local ER-2/DC-8
Chan (NASA Ames)	U, V, W, T, p †	local ER-2
Gary (JPL)	$\delta T/\delta p$ †	local ER-2
Loewenstein (NASA Ames)	N_2O	local ER-2

* AL, Aeronomy Laboratory; JPL, Jet Propulsion Laboratory; NCAR, National Center for Atmospheric Research; DU, Denver University.

† U, eastward wind; V, northward wind; W, vertical wind; T, temperature; p, pressure

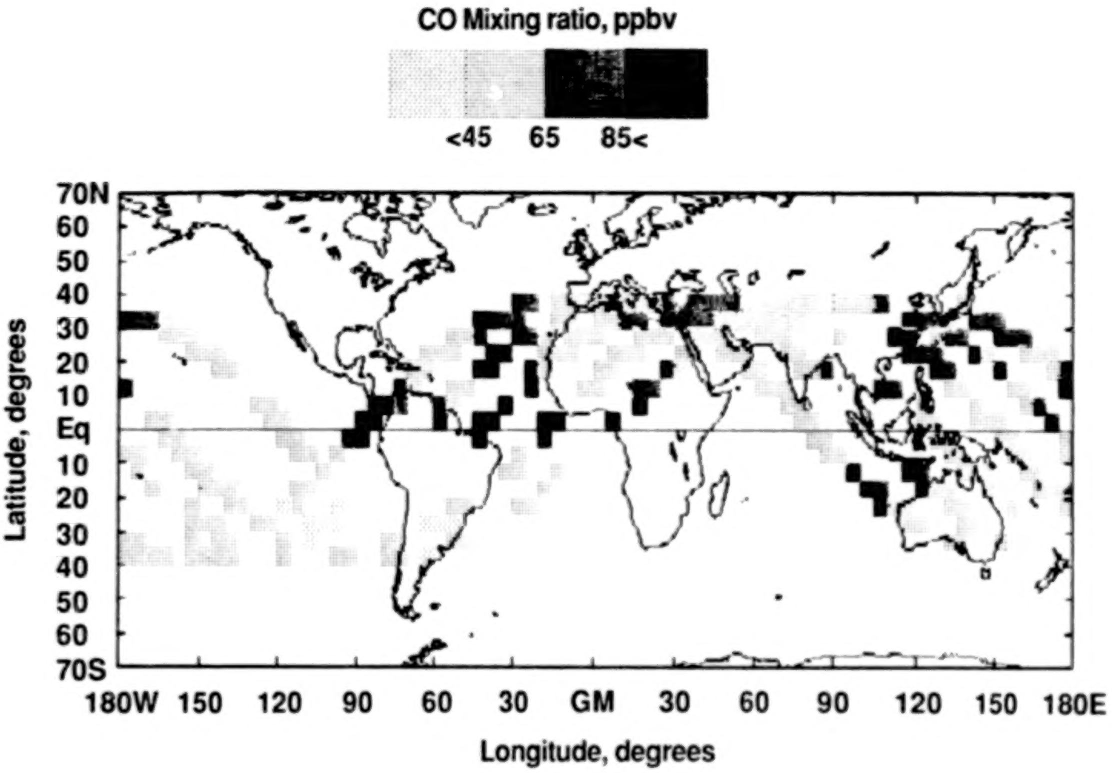
CO Mixing ratio, ppbv
<45
65
85<
70N
60
50
40
30
20
10
Eq
10
20
30
40
50
60
70S
Latitude, degrees
180W
150
120
90
60
30
GM
30
60
90
120
150
180E
Longitude, degrees

Figure 1. Tropospheric carbon monoxide mixing ratio MAPS experiment, 14 November 1981.

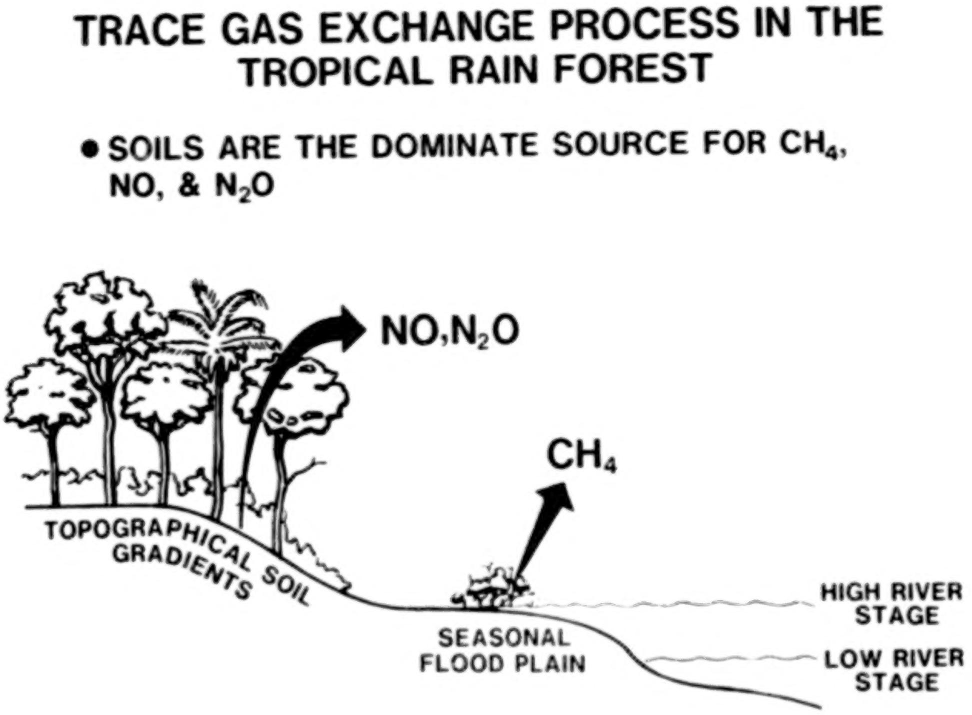

TRACE GAS EXCHANGE PROCESS IN THE TROPICAL RAIN FOREST

- SOILS ARE THE DOMINATE SOURCE FOR CH_4, NO, & N_2O

NO,N_2O
CH_4
TOPOGRAPHICAL SOIL GRADIENTS
SEASONAL FLOOD PLAIN
HIGH RIVER STAGE
LOW RIVER STAGE

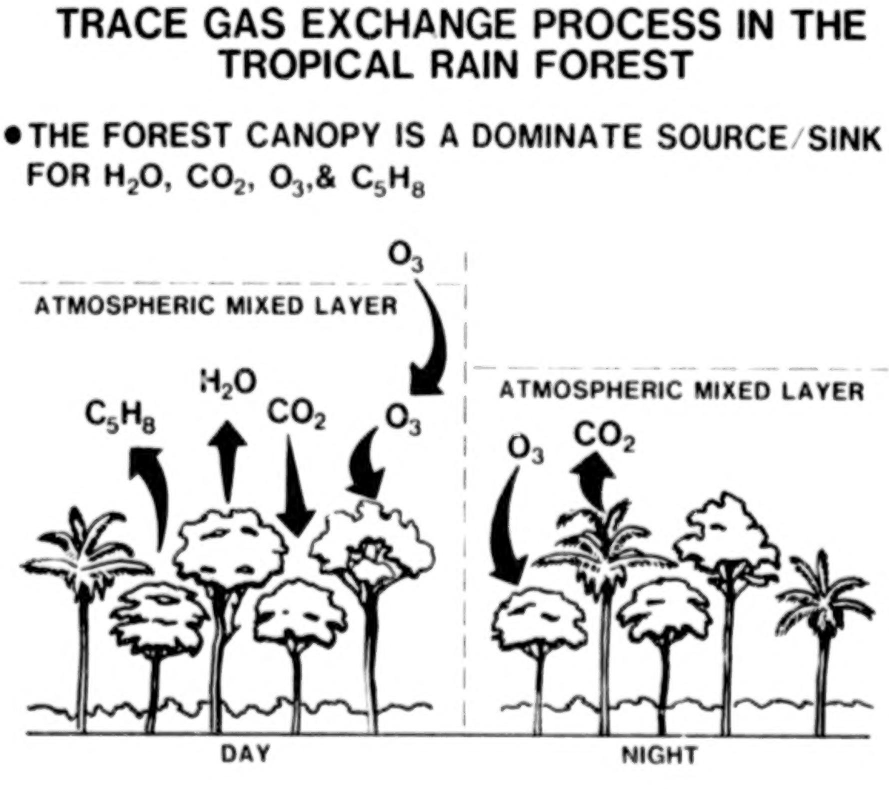

TRACE GAS EXCHANGE PROCESS IN THE TROPICAL RAIN FOREST

- THE FOREST CANOPY IS A DOMINATE SOURCE/SINK FOR H_2O, CO_2, O_3,& C_5H_8

O_3
ATMOSPHERIC MIXED LAYER
C_5H_8
H_2O
CO_2
O_3
ATMOSPHERIC MIXED LAYER
O_3
CO_2
DAY
NIGHT

Figure 2. Trace gas exchange processes in the tropical rain forest. (a) Tropical soils are a significant source of methane (CH_4), nitric oxide (NO), and nitrous oxide (N_2O). (b) The forest canopy is a dominant source/sink for water (H_2O), carbon dioxide (CO_2), ozone (O_3), and isoprene (C_5H_8).

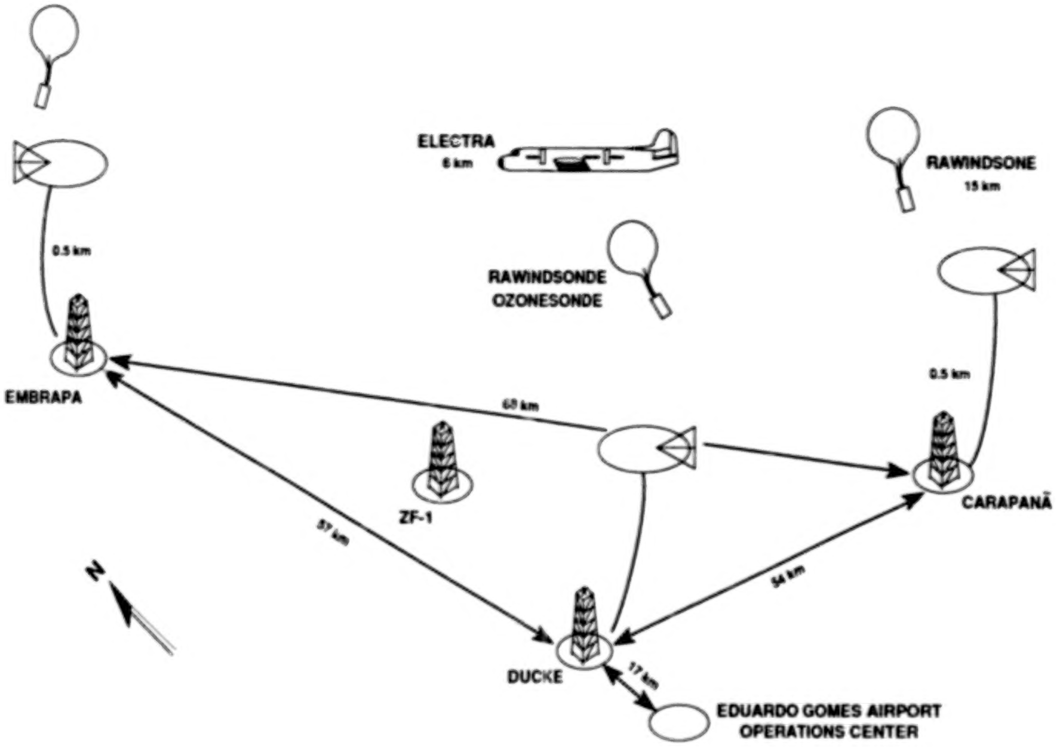
ELECTRA
6 km
RAWINDSONE
15 km
0.5 km
RAWINDSONDE
OZONESONDE
0.5 km
EMBRAPA
68 km
ZF-1
CARAPANÃ
57 km
N
54 km
DUCKE
17 km
EDUARDO GOMES AIRPORT
OPERATIONS CENTER

Figure 3. Mesoscale Convective Complex Triangle (MCCT) with ground and airborne sensor platforms deployed during the ABLE-2, 1987 Wet Season Mission. During the 1985 dry season, ground measurements were concentrated at the Ducke site.

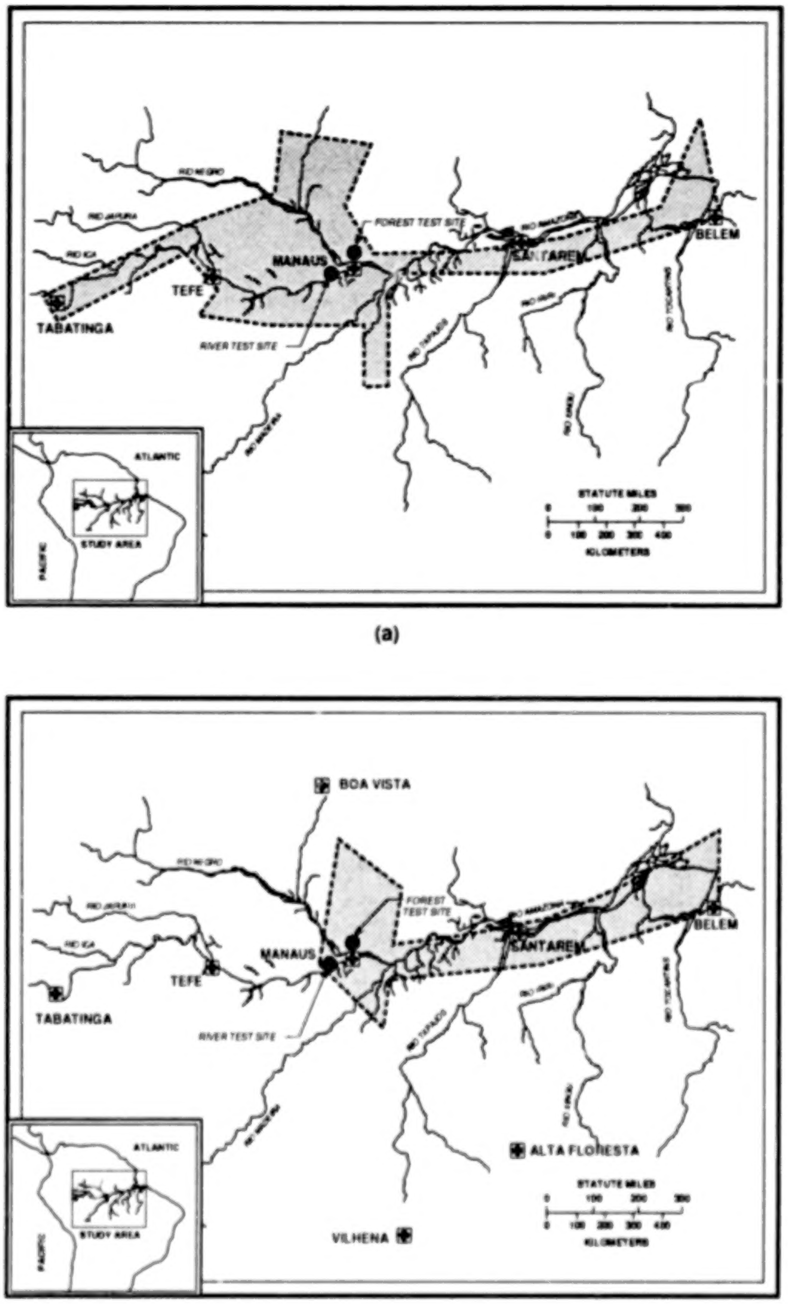
RIO NEGRO
RIO JAPURA
RIO ICA
FOREST TEST SITE
RIO AMAZONAS
MANAUS
SANTAREM
BELEM
TEFE
TABATINGA
RIVER TEST SITE
RIO TAPAJOS
RIO XINGU
RIO TOCANTINS
RIO MADEIRA
ATLANTIC
PACIFIC
STUDY AREA
STATUTE MILES
0 100 200 300
0 100 200 300 400
KILOMETERS
BOA VISTA
ALTA FLORESTA
VILHENA

(a)

(b)

Figure 4. Map of research areas for (a) ABLE-2A and (b) ABLE-2B.

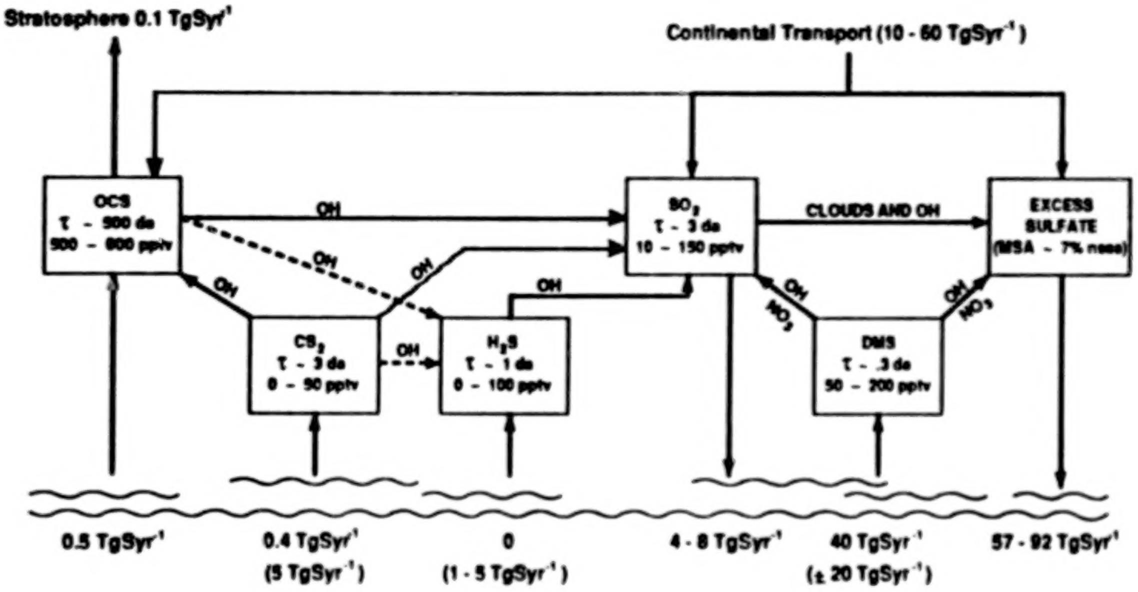
Stratosphere 0.1 TgSyr⁻¹
Continental Transport (10 - 60 TgSyr⁻¹)
OCS
τ - 500 da
500 - 600 pptv
OH
SO2
τ - 3 da
10 - 150 pptv
CLOUDS AND OH
EXCESS SULFATE
(MSA - 7% nss)
OH
OH
OH
OH
CS2
τ - 3 da
0 - 90 pptv
OH
H2S
τ - 1 da
0 - 100 pptv
OH
NO3
DMS
τ - .3 da
50 - 200 pptv
OH
NO3
0.5 TgSyr⁻¹
0.4 TgSyr⁻¹
(5 TgSyr⁻¹)
0
(1 - 5 TgSyr⁻¹)
4 - 8 TgSyr⁻¹
40 TgSyr⁻¹
(± 20 TgSyr⁻¹)
57 - 92 TgSyr⁻¹

Figure 5. Schematic of marine sulfur cycle (modified from Toon et al., JGR, 92, 1987).

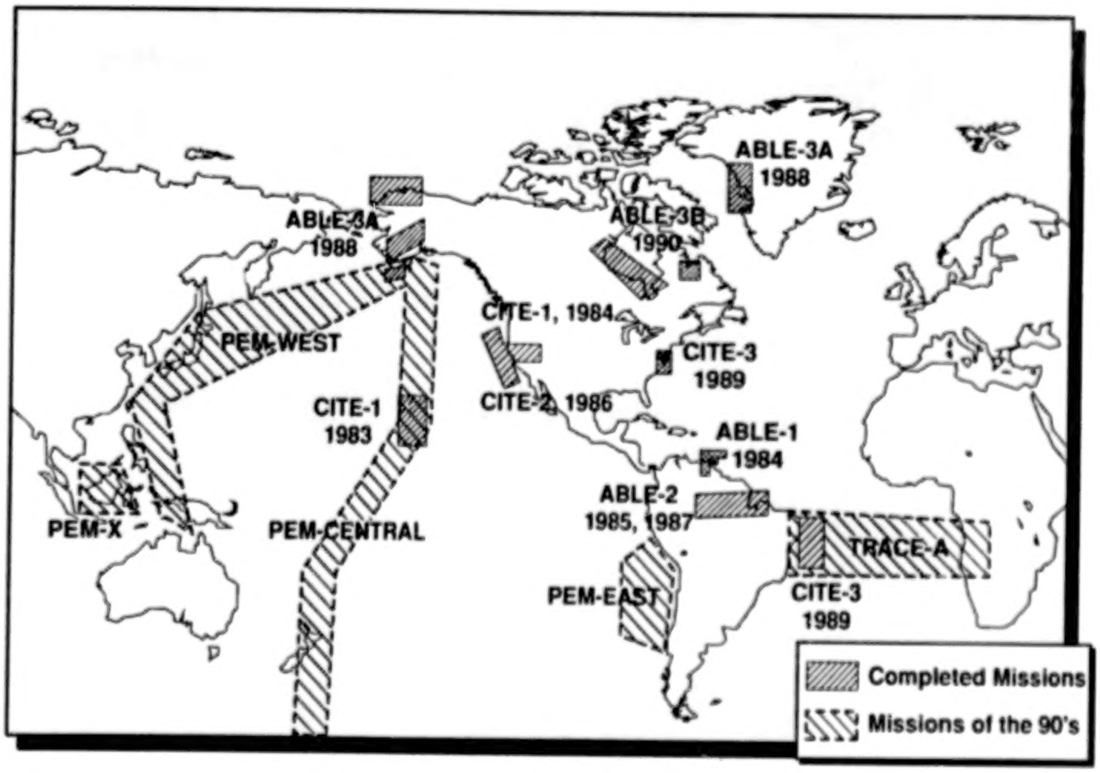
ABLE-3A
1988
ABLE-3A
1988
ABLE-3B
1990
PEM-WEST
CITE-1, 1984
CITE-3
1989
CITE-2, 1986
CITE-1
1983
ABLE-1
1984
ABLE-2
1985, 1987
PEM-X
PEM-CENTRAL
TRACE-A
CITE-3
1989
PEM-EAST
▨ Completed Missions
▧ Missions of the 90's

Figure 6. Completed and potential mission sites of the Global Tropospheric Experiment. The completed missions include CITE-1, -2, -3 and ABLE-1, -2, -3. Missions that may be conducted in the 1990's include TRACE-A, PEM-West, -Central, -East, and -X.

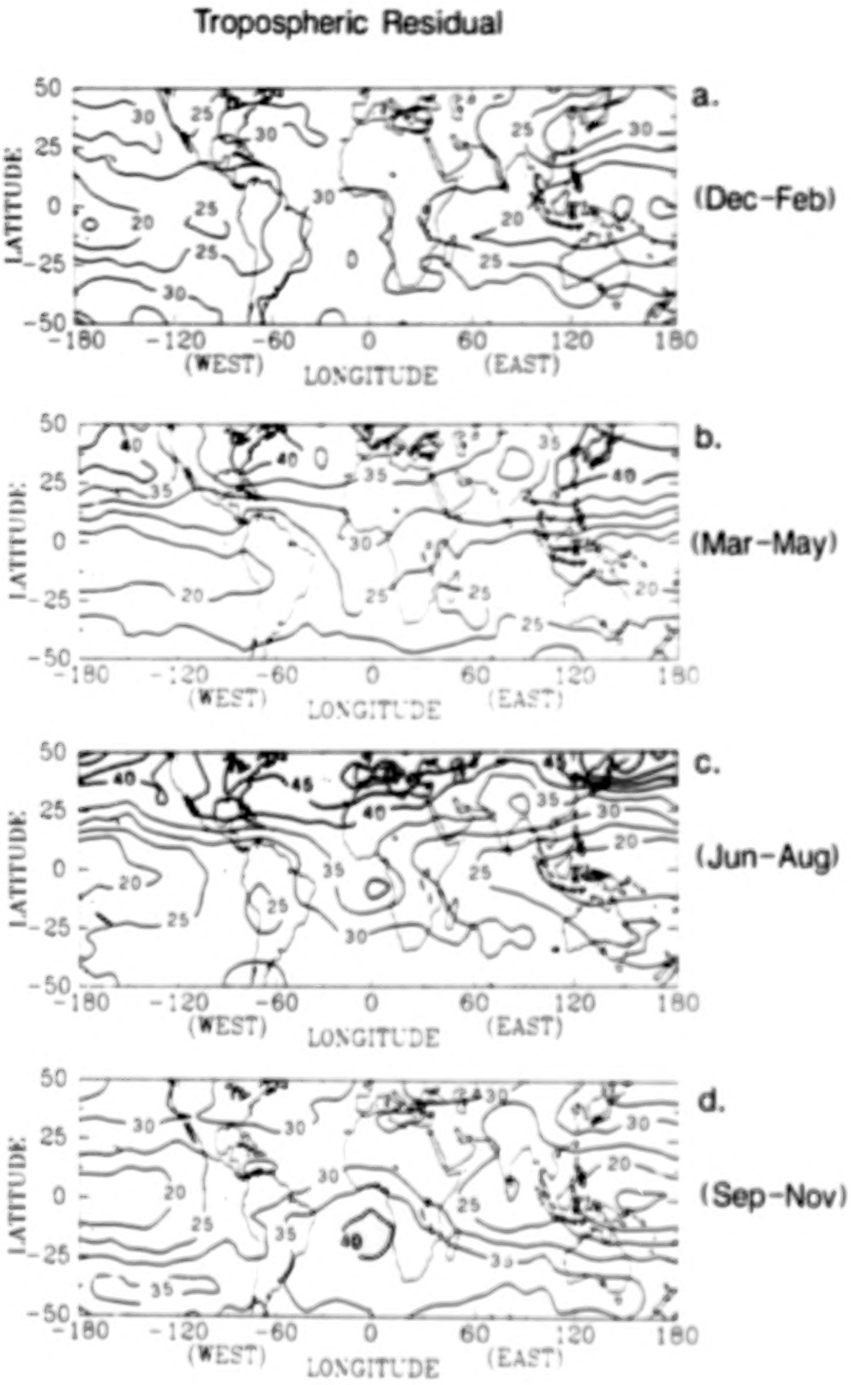
Tropospheric Residual
a.
(Dec-Feb)
b.
(Mar-May)
c.
(Jun-Aug)
d.
(Sep-Nov)
LATITUDE
50
25
0
-25
-50
-180
-120
-60
0
60
120
180
(WEST)
LONGITUDE
(EAST)

Figure 7. Seasonal contours of global tropospheric ozone derived from satellite observations. Note ozone enhancement in south Atlantic Ocean off coast of Africa in September–November time period. (Figure provided by Jack Fishman, Langley Research Center.)

N90-27156

APPLICATIONS OF ISES FOR THE OCEANS*

W. E. Esaias
NASA Goddard Space Flight Center
Greenbelt, MD

I will discuss my interests in oceanography and acquaint you with how some oceanographers feel concerning the need for direct broadcast, why, and what type.

I am particularly interested in the role of the ocean in carbon storage in sequestering. Through fossil fuel burning, approximately 5 to 6 gigatons of carbon are emitted into the atmosphere each year. Half of that amount stays in the atmosphere, and it is thought that about half of the remaining carbon goes into the oceans. The ocean biota represent a small pool, but they overturn very rapidly. In fact, this very small pool of carbon represents a mechanism that has sequestered over geological time 99.99 percent of the carbon on Earth. If you have read any of the Earth Observing System (Eos) literature, you have seen a figure of the carbon cycle. Most of the carbon reservoir is in sediments of marine origin, and our main interest is the ocean phytoplankton that is typically studied through ocean color. Phytoplankton represent a small biomass, but through eons of fixing carbon particles and sinking in the deep ocean, most of the carbon on Earth has ended up in marine sediments. Although the annual input is very large because of such processes as dissolution of carbon and deep water formation, the signal that represents this deep carbon storage is very small. We are looking at a very small signal difference between very large signals. To determine this difference really requires time series and comprehensive observation, as well as a great deal of in situ work understanding these processes; this entails ships out in the ocean and moored instruments. Many magnifiers of global processes exist, such as enhanced production in deep ocean due to aerosols (i.e., continental aerosols, Asian dust, and Saharan dust, which has a lot of iron). These magnifiers fulfill some nutrient limitations. A particular species or a group of species of phytoplankton called coccolithophores produce dimethyl sulfide, and it is thought this parameter might play a role in cloud formation. Due to eutrophication of estuaries and rivers, we are seeing enhanced production in coastal regions, which again affects or magnifies anthropogenic effects and carbon cycling. This observation is especially interesting because ocean colors are flow visualizers and signify mixing changes.

We have been processing Coastal Zone Color Scanner (CZCS) data and were able to generate a composite representation of 32 months of observations. We can see upwelling at the equatorial region, high productivity in the Northern latitudes, large production in the Southern oceans due to mixing, upwelling along the coasts of Africa, Peru, and the Western U.S., Amazon river outflows, and monsoonal areas. This composite basically represents the general picture that we had before satellite data. Things become interesting when we look at interannual variability. By transforming data like these, we can estimate the total zonal production and how much carbon is fixed (as a function of latitude). From this we calculate how much carbon is going into the ocean biomass, with time. The data set contains 32 months of data beginning when Nimbus 7 was launched; from this we can estimate a total carbon fix per day, which is equivalent to approximately 60 gigatons of carbon per year. The anthropogenic output is one-tenth of that amount. If one-tenth of this gets fixed by phytoplankton and ends up in the deep ocean, then all the fossil fuel CO_2 is used up and there is nothing to worry about. But it is unlikely that the number is that high; it is probably closer to 1 percent. Notice that there is a hint of a secular trend.

What we measure with the satellite is radiance in four spectral bands, and from that we look at color shift in an empirical relationship between the water-leaving radiance and the amount of chlorophyll pigment. Chlorophyll pigment is used as a measure of biomass. It is also the primary photosynthetic pigment, and these chlorophyll concentrations are a good indication of how fast the plants are growing. Plants in the ocean are not like plants on land. If you look at plants in the forest, you see only carbon trunks. The carbon stays around for a long time. But, the plants in the ocean are unicellular; they have no support structure. They divide once a day so the biomass is a good measure of how strong they are growing. If they are not growing, they are sinking to the bottom or they are being eaten. There is a very simple relationship therefore between the chlorophyll concentration and the total carbon fix.

---

*Paper taken from workshop recordings.

We can see trends, and for the first time, we can look at interannual variability. For example, we see the difference in CZCS data between winter and spring. In spring you get more sunlight, plants grow faster, the water column stabilizes, and the nutrients are fixed. Between winter and spring there is a tremendous increase in biomass and phytoplankton in the ocean, and a substantial fraction of that will sink in the deep ocean, be removed from contact with the atmosphere, and represent a short-term repository for carbon. One-tenth to one percent will get incorporated into the sediments and then enter a pool that is on a geological time scale. It is apparent from 1979 data that there is a spring bloom and a fall bloom (we see a much smaller spring bloom in 1980, a much larger fall bloom in 1981, and a spring bloom in 1981). This delineates some of the interannual variability that we see, which represents anthropogenic carbon input. So the variability in the ocean is large with respect to how much anthropogenic carbon is going in. The southern oceans receive outflow from rivers, where the winds are more constant and show very little interannual variability. The name of the game is how variable is the ocean, and for the first time, with satellite data sets, we can look at interannual variability. We have never been able to do that on these scales before from ship data.

In summary, our ocean estimate is 61 gigatons of carbon; compare that to 6 gigatons of carbon output by fossil fuel. The new production, which is the production that is due to nutrients coming up from underneath the ocean due to upwelling, is approximately 23 gigatons. We would expect that an equivalent amount of carbon gets sunk with residence times on the order of decades to centuries, and if 10 percent of that gets buried, then we have essentially solved the missing carbon problem. I don't believe any of the carbon budgets, but understanding the process of what you see in the satellite image and relating it to what happens to the carbon inside the ocean are the subjects of a major international effort called the Global Ocean Flux Program. Currently, there are field pilot studies occupying a transect from Iceland down past the Azores. If you understand the onset of the spring bloom and how much carbon goes deep into the ocean, you understand that the winter nitrate concentration is the primary limiting nutrient of phytoplankton production. Another issue is how deep the water mixes, because this is a prime forcing function. We are interested in wind stress and mixed layer calculations and running physical models in order to set up a physical regime with which to determine the biology. To give you an idea of the scale of this, consider the area that is occupied by this field experiment. The bloom starts first in the south. The U.S. was there in April, and now as time goes on, the bloom progresses north so the activity shifts toward the north. The Germans are there, our P3 aircraft is there, along with one Canadian vessel and the British who come and go. A Netherlands ship was also involved. My point is that this occupies a very large area of the world, and right now we have no way of determining what is happening on a regional basis. To look at some of the historical data, we need to know where to put stations. These stations were chosen because they were close to the European support and because they had past moorings there. One might move those stations if real-time information were available.

Since I was first asked to consider direct broadcasting, we have had follow-on studies for ocean color sensors to look at, some of which include direct broadcast and some not. I can see four reasons for support. 1) We need to back up single point failures, such as the Tracking and Data Relay Satellite (TDRSS), EosDIS, and a central data handling facility. 2) Obviously, we need real-time observations in support of field studies. The ocean does not stay fixed, and the name of the game is to get a ship to one of the bloom areas or plumes. We need data within a day. It is not obvious that the EosDIS will be able to deliver that. 3) We would like to experiment with onboard processing and selection of data for direct broadcast. 4) We need to develop future operational NOAA systems.

I'm concerned about all these areas. It seems we have a choice of three data rates. High data rate, X-band (I call high data rate anything above 20 megabits per second) will require a large ground station (there are going to be a few of them), lots of dollars, and some screening of data, because you still can't handle all of Eos and therefore must select which data and what day you put it out. It is going to require on-site processing at the ground station, and this will be a major effort. You still have a problem of how to get it out to the ships at sea. Oceanographic Principal Investigators (PI's) tend to go to sea: they take their act with them. For medium data rate (such as the L-band for the High-Resolution

Picture Transmission (HRPT) or S-band), there are lots of ground stations. Screening or selection of data (that is, which bands from which sensors) is needed. Many of these HRPT stations are within the PI domain, but you still have the problem of distribution to the field sites. There is also low data rate, in which you experiment with onboard data processing and produce a geophysical product.

There are potentially a large number of ground stations, and it is very foreseeable to have a station on every major or even minor oceanographic research ship with a PC to do processing. It really requires a selection of data. Which data do you send? For the most part, the PI would rather have the raw data, not a geophysical unit. The field party gets the data directly (that is, there are no problems in uplinking again to a satellite to get it out to a ship).

Concern about research for operational use is based on my own point of view, which is mostly for research needs. Does a scientist have a VAX or access to a supercomputer or does he just want information to show where to take a dory? We have considered the high- and low-data rate reception capability, but we should not forget the regional "value added" processing and routing. I mention this because commercially there is a great deal of interest in fisheries' broadcasting, in which a number of businesses have been set up to take ocean color and sea surface temperature data, process it (based on their previous knowledge of ocean conditions and topography), and forecast where the mackerel, squid, or other fish will be. That procedure requires that you get data to the fisheries and that they distribute a product to the ultimate user.

Another topic is cruise activity and planing for algorithm development. We hope to have more sophisticated algorithms making use of the multi-bands than were possible with CZCS. When you are at sea trying to validate a model, it is nice to know what the ocean is doing rather than use pigment as a predictor of some other species or pollution event and make your correlative measurements. It is nice to have that data in hand to find where the hot spot is. A hot spot in a general pigment measurement is not necessarily the hot spot of a coccolithophore bloom; they have different spectral signatures. This area is intended for tailored algorithm development and validation studies. The instrument scientists have a real need to get the data down to look at it to find out if their sensor is working right, i.e., sensor performance.

We use an ozone product to atmospherically correct our data in the final processing. Currently we have the Total Ozone Measurement Satellite (TOMS) data because we are doing it retrospectively now. With TOMS, we get approximately a 25-percent improvement in the results. With the present scenario we are going to have to wait approximately 5 days in order to get an ozone product unless it is from MODIS itself. You can read in wind speed because there will be glint corrections. The point is, there is a need for ancillary data. If it were possible to get that data on the ground quickly, to a first approximation (even though the people studying the ozone might not be satisfied, it could be a preliminary product for them), then all we need is a 90-percent-accurate ozone number to form a crude correction because it doesn't affect the CZCS data by more than one-third count. You will never see it using a correction term. I think there are other analogies in which quick data could be very useful in routine data processing.

Concerning timeliness, for research cruise planning, approximately a 12-hour response will be needed to be useful. The ocean community has been over this time and time again with no justifying need for real-time data distribution, and they have settled on 12 hours as a satisfactory number. We would like it sooner, but 12 hours is enough time to set up next day activities on the vessel.

It is certainly possible to consider doing the sea surface temperature (SST) processing onboard the satellite even though that method would have pluses and minuses. Currently it is done in a hands-off mode; it takes a bit of "number crunching," approximately 2 minutes on a micro-VAX 3 size instrument. Doing the CZCS pigment type algorithm onboard Eos might be feasible. It is not trivial; it takes on the order of 20 minutes on a micro-VAX 2 to process a 2-minute scene. It is an intensive task even with nearly optimized code. You have to know the ephemeris, calculate the Sun sensor geometry, store large look-up tables for the Rayleigh correction, make some assumptions concerning an ozone field, use a red color pixel to estimate aerosols and assume a default aerosol type, and use one of the channels to identify clouds, land, and glint.

One scene is approximately one-fourth of a megabit. The look-up tables for the atmosphere correction, where you have already solved the multi-scatter radiative transfer model, are typically done on every 32 pixels. You then interpolate within the look-up table. All of the data we have generated was essentially done in a hands-off mode. A number of us looked at the output to determine if it worked or didn't, and threw out what didn't work. It is not interactive in the sense that we are refining a coefficient. We know there are errors when you change from a marine to a continental aerosol model around Africa. Some of the errors can be estimated, and that is what we do. We don't have the information within the CZCS to make decisions as to what their corrections should be; therefore, MODIS final products certainly would be much better for quick results. People who are in favor of onboard processes would be delighted with something like that.

What I'm suggesting is that the way we process CZCS data today requires none of those corrections. There will be an ozone channel on MODIS. As for the research algorithms that people expect to have developed and ready to do MODIS ocean color, they are at the same stage that ISES is right now. We must answer these questions: what can we correct for, where do we get the data, and how do we code an algorithm? I think it is unrealistic to expect to come up with a consensus in time to help with the present algorithms and processing methodology that can be done. It's going to take a good deal of onboard storage and encoding software. There is no way that I would recommend that you get into the next-generation algorithm development for onboard processing. There are applications that haven't even used real-time wind speeds to do a good glint correction, for example. Atmospheric pressure is needed to recompute and solve the Rayleigh scattering model on a regional basis each time, because with the expected precision of MODIS, which we presently just ignore with CZCS, the atmospheric effect will be very evident in the research data product. Even the sea surface temperature, the multi-channel SST that NOAA does routinely, is not perfect. Many people find it has problems, but it is extremely useful for fishermen or setting up regional field studies. If it were available in real-time over a simple data link, that would be good. To me, one of the real challenges would be to control the selection of data from the various instrument types and output that through several channels of the HRPT.

The SST is a lot simpler than ocean color because it is just a simple difference or ratio between two channels; you multiply it by some coefficients to get approximately a degree and one-half accuracy. The atmospheric correction is extremely simple. You don't require people to use look-up tables or make extensive calculations. It can be done with a microprocessor by using a couple of channels and putting out a product of known performance. People are used to it and it is available in real-time. You don't have to go through Goddard and wait 3 days. You don't have to wait for the NOAA satellite. Suppose the NOAA satellite fails, we still have the data.

I see a couple of ways to handle the process for chlorophyll. You could have the ability to select MODIS visible channels. You could select up to 8 or 10 channels, maybe have a switch to select which ones are useful for oceanographers and land scientists, put them into a HRPT format, and direct broadcast to any current NOAA HRPT station. The Navy and universities will then have that data. It won't be all the data they will ultimately want, but it will be enough to tell them what to do tomorrow.

One of the main problems I see is that you still have to do onboard selection to choose what data to put into the data stream unit; you may be sending down the wrong data. Who gets to decide what and when would be a key issue. If I'm planning an experiment, how much lead time will I have to get a commitment from NASA that my data will be there when needed? It would not be good if I planned a multi-national effort and found that SAR data was scheduled to be taken that week; that does me no good at all. So the important thing is who controls the sensor outputs. If we have several selectable channels, such as an ocean channel, a land channel, a vegetation channel, a desert channel, and an atmospheric channel, which could be relied on, then it would make planning for field efforts much easier.

In conclusion, it would certainly be desirable to have a direct broadcast capability to support research ships at sea, as well as other activities. The format may include a selected number of raw data channels from some of the instruments, or it may contain fully processed geophysical parameters. The selection would be dependent upon the application, however, and a guarantee of availability when needed would be essential. Because the algorithm development for the MODIS data products is still an active issue, it is perhaps too early to state exactly what real-time products are needed and what mix of onboard and ground data processing is desirable.

N90-27157

APPLICATIONS OF ISES FOR COASTAL ZONE STUDIES

D. S. Bartlett
NASA Langley Research Center
Hampton, VA*

Introduction

In contrast to the discipline- and process-oriented topics addressed by many workshop participants, coastal zone studies are defined geographically by the special circumstances inherent in the interface between land and water. The unique characteristics of coastal zones which make them worthy of separate consideration are (1) the dynamic nature of natural and anthropogenic processes taking place, (2) the relatively restricted spatial domain of the narrow land/water interface, and (3) the large proportion of the Earth's population living within coastal zones, and the resulting extreme pressure on natural and human resources. These characteristics place special constraints and priorities on remote sensing applications, even though the applications themselves bear close relation to those addressed by other elements of this report (e.g., oceans, ice, vegetation/land use). The discussion which follows will first describe the suite of remote sensing activities relevant to coastal zone studies. Potential ISES experiments will then be addressed within two general categories: (1) applications of real-time data transmission and (2) applications of onboard data acquisition and processing. The discussion will conclude with a short summary.

Remote Sensing for Coastal Studies

A number of generic research and monitoring tasks are associated with important coastal zone processes, as follows:

1- Water circulation: The dynamics of coastal water circulation impact virtually every physical, chemical, and biological process in the coastal zone. Because of the smaller areas involved, current velocities and changes in those velocities tend to be much more rapid than in the open ocean. This is particularly true of tidally driven circulation which changes both speed and direction at time scales less than one day. This makes conventional shipboard measurement extremely difficult. Remote sensing studies of circulation generally make use of water turbidity or some other reasonably conservative, visible tracer within the surface water column to develop a synoptic picture of water mass distributions at a particular point in time. In order to follow the important changes taking place on time scales of hours and minutes, repeated imaging over hourly-daily temporal frequencies is required. Because of the characteristic spatial scales of most coastal water bodies, high spatial resolution, on the order of 50-250-m ground instantaneous field of view (GIFOV), is also frequently required although

---

*Now employed with the Institute for the Study of Earth, Oceans, and Space, University of New Hampshire.

PRECEDING PAGE BLANK NOT FILMED

coarser resolution has been used under certain circumstances. Related physical parameters such as waves and surface winds have been addressed using microwave sensors such as scatterometers.

2- Pollution: The combination of dynamic physical systems and intense human use make monitoring of pollution in coastal waters a difficult task which has benefitted from remote sensing techniques. Most such work has been analogous to the water circulation studies described above in which a known pollutant is monitored through its visible impact on water color, and the distrbution of the affected water mass is monitored through time. Some attempts to identify the type and concentration of selected pollutants through multispectral analysis have been made but such applications have not been conclusively demonstrated. Thermal effluents can be effectively monitored and their temperature estimated using imaging in the thermal infrared spectral region. Oil spills can also frequently be detected by their impact on the thermal rather than visible spectral signature of the water surface.

3- Biology: Water color can be used to map the distribution and, in many instances, the concentration of surface chlorophyll and thereby the density of phytoplankton in coastal waters. In most respects the methodology is the same as that used in the extensive studies of ocean productivity described in the workshop contribution on oceans. In the coastal zone, spectral signatures of phytoplankton are influenced by the presence of large amounts of inorganic material suspended in the water column and this can complicate analysis. Spatial and temporal dynamics of the system require higher resolution with respect to both of these parameters than is needed for ocean studies. The so-called "Coastal Zone Color Scanner" (CZCS) is, in fact, optimized for large-scale productivity studies in the deep oceans and on continental shelves. Applications in estuaries and other smaller-scale coastal environments would benefit from finer spatial resolution and, possibly, modifications to the spectral bands used.

4- Hazards: A number of hazards in the coastal zone have been addressed at one time or another through remote sensing technology. Shoreline erosion over large areas can be monitored if imagery of sufficient spatial fidelity is available. Short-term catastrophic erosion from storms is frequently documented using aerial photography and, in some cases, by orbital imagery. Ice is a hazard to shoreline communities and to navigation and extensive use of remote sensors, particularly microwave instruments, has been made for monitoring ice distribution (see contribution on snow and ice in this report). The location of toxic algal blooms, known as "red tides," has been monitored by NOAA using orbital imagery, including AVHRR data having 1-km GIFOV. In general, as with other applications, high spatial and/or temporal resolution sensors are required for coastal applications.

5- Vegetation and Land Use: Remote sensing applications in mapping land use and monitoring natural and agricultural vegetation are common and are similar to those described in the relevant contribution in this report. In this area spatial and temporal resolution requirements are not greatly different from those in non-coastal regions.

Potential Applications of ISES Real-Time Data Handling Capabilities

The dynamic nature of many important coastal zone processes make the prospect of real-time imagery from ISES extremely appealing. On the other hand, the need in many cases for high spatial resolution is not compatible with the sensors, such as MODIS, which obtain data at appropriate temporal frequencies (i.e., daily) and which are envisioned as the core of the Eos environmental monitoring system. Data from higher resolution sensors such as HIRIS and SAR would be of great interest but the narrow swaths of these instruments also lengthen the interval between data collections. In addition, the high data rates produced by these instruments restrict the amount of data which can be screened, particularly by the limited onboard capabilities of ISES. This means that coastal applications such as early warnings of pollution events, oil spills, and red tides, while technically feasible, will probably have to be limited to particular high-priority times and regions. The moderate-to-low resolution sensors collecting imagery on a daily basis will be useful for identifying large scale distributions of suspended material, for example, and directing field sampling parties to targets of interest before large changes have occurred.

There is an important trade-off in real-time applications between the efficiency and synoptic coverage of orbital remote sensing versus the higher information content which is usually associated with more conventional methods. For example, documentation of erosion in densely populated coastal regions almost always requires detailed surveys which are accurate to at least several meters. In such areas the issues of shoreline change and protection of valuable property are so important that even small events are quickly noticed and extensive local resources are devoted to in situ mapping and other detailed monitoring methods. ISES-generated real-time detection of erosion amounting to several tens of meters, the minimum detectable even with HIRIS, would be of questionable value under these circumstances, even if the information arrived a few hours or days before conventional methods could be deployed. It seems likely that similar circumstances will be encountered in a variety of instances (such as pollution detection, storm damage assessment, oil spill detection) in which orbital data may have some utility but in which the density of local observers and the importance of detailed data sets ultimately demand in situ study. In remote coastal areas where such conventional resources may not be available, the importance attached to short-term events is also likely to be much reduced, making the potential contribution of real-time orbital data problematical. One must be careful to select real-time ISES experiments which are likely to make a contribution that is not attainable using available conventional resources.

The most promising areas for real-time ISES experiments in the coastal zone will be in supporting scientific investigations through the siting of field parties and documentation of large scale environmental conditions. Some applications in early hazard warning or other environmental monitoring efforts are possible but must be selected carefully to avoid demonstrating capabilities which are already present through more conventional, information-rich means. Daily, quick-look visible and thermal IR images from MODIS of coastal regions in which field or high-resolution remote sensing studies are taking place would be very valuable. If ISES can access and transmit SAR data this could be applied to a variety of problems such as ice distributions, oil spills, and marine traffic control. The all-weather capability and pointability of SAR increases its effective coverage frequency for preselected sites and would be especially advantageous when local weather conditions make application of conventional field methods impossible.

Potential Applications of ISES Onboard Data Handling Capabilities

The massive data stream produced by the planned sensor package has the potential to overwhelm the storage and data transmission capabilities of Eos, and losses of data, particularly from high-data-rate sensors such as HIRIS and SAR, will occur when resources are required for higher priority uses. ISES could be used to alleviate this problem by recording and transmitting selected data streams outside of the allocated data system constraints. For example, planned interruptions in HIRIS data transmission might compromise a study of a coastal oil spill or of the distribution of suspended sediment, whether or not the data are required in real-time. ISES could potentially provide this data either directly to the user or to ground stations with facilities for recording the data for later use. Cloud detection algorithms within ISES, utilizing the greater coverage area and frequency of MODIS, could be used to filter requests for coverage by higher resolution sensors and direct those sensors to cloud-free areas. Capturing data which might otherwise be lost should be an important part of the rationale for ISES and, in particular, for placing the ISES capability on the Eos platform. Many real-time data requirements could be fulfilled by systems monitoring and transmitting selected portions of the Eos data stream on the ground. This will not be possible for data which never enters the Eos data system and ISES would make a valuable contribution to virtually every conceivable kind of application, coastal or not, by providing a means to acquire a selected data stream for a high-priority experiment or monitoring task.

Summary

The dynamics and intense human usage of coastal zones argue for extensive use of current and future remote sensing capabilities in environmental monitoring, enforcement, and scientific inquiry. However, coastal requirements for both high spatial resolution and frequent data collection often restrict the utility of orbital systems such as those planned for Eos. Highest priority for experiments utilizing the real-time data handling capabilities of ISES should be given to applications in which high spatial resolution is of lesser importance, such as the use of quick-look MODIS data to direct field sampling activities to transient large-scale features, or to unique capabilities, such as that of SAR to provide all-weather coastal images, which are not accessible to more conventional methodologies. ISES can also contribute to coastal, and other studies by collecting and transmitting data which would otherwise be lost because of the need to conserve Eos data handling resources. Such data would be valuable whether or not it was provided in real-time.

N90-27158

APPLICATIONS OF ISES FOR VEGETATION AND LAND USE

R. Gale Wilson
NASA Langley Research Center
Hampton, VA

Summary

Remote sensing relative to applications involving vegetation cover and land use is reviewed to consider the potential benefits to the Earth Observing System (Eos) of a proposed Information Sciences Experiment System (ISES). The ISES concept has been proposed as an onboard experiment and computational resource to support advanced experiments and demonstrations in the information and Earth sciences. Embedded in the concept is potential for relieving the "data glut" problem, enhancing capabilities to meet real-time needs of data users and in situ researchers, and introducing emerging technology to Eos as the technology matures. These potential benefits are examined in the context of state-of-the-art research activities in image/data processing and management.

Introduction

The capabilities and quality of remote sensing data acquisition systems continue to improve, but data acquisition technology has outpaced the technology to process, analyze, and interrelate the voluminous data sets that are produced. The complexity of the latter technology is so great that heavy reliance continues to be placed on human interpretation of data. The state-of-the-art in digital image interpretation seems to be well summarized by Hubaux (in ref. 1, p. 127):

> Remote sensing data processing is always a fight against an excess of information; in the jungle of data through which we try to find our way, we have to use an intellectual machete to chop away most information, so as to keep only that part (most often a tiny part) which is really relevant to our problem, and find the most convincing manner to present it.
>
> The present trend consists in considering remote sensing data as part only of the total information needed to solve most problems, and to incorporate them in Geographical Integrated Systems (GIS). This must, of course, be done with data in their digital format, and the use of the computer will certainly grow in the coming years. But whether the role of the human interpreter is declining, and whether completely automatic procedures will be found to solve most problems, remains to be seen.

An ISES has been proposed (refs. 2 and 3) to evaluate the role of onboard (ground-station-coupled) information extraction in space flight systems. The ISES concept has been initiated as a proposed Eos onboard experimental, computational, and communications resource to support advanced experiments and demonstrations in the information and Earth sciences. Such a resource could be an important element in addressing the overall data reduction and management problem.

The purpose of this paper is to review the current operational and Eos-planned research programs relevant to two applications areas; i.e., vegetation (including forests) and land cover/use, and to relate the needs in these programs to the ISES concept. While the paper focuses on these two remote sensing applications, many of the considerations on data requirements are not limited to just these applications. The remote sensing applications are first discussed, along with data management and processing techniques. In these discussions the primary difficulties and challenges in remote sensing research are examined to place the proposed ISES concept in proper perspective. The ISES role is then projected in terms of users' specific needs, the need for in-orbit intelligent data-taking to reduce the quantity and rate requirements for downlinked data, the state-of-the-art in data processing technology, and the long-term objectives of the Eos program.

Remote Sensing Systems

This paper is primarily concerned with satellite remote sensing systems. Ground-based and airborne sensor platforms will continue in roles of providing primary data collection, as well as ancillary and reference or calibration data to complement data from satellite systems and will continue to be important in the development of new and improved satellite systems. There exists a variety of instrumentation for collecting the Earth's reflected, emitted, or scattered radiation onboard satellite platforms. The primary instruments include photographic cameras, television cameras, visible and infrared scanning (imaging) radiometers, multi-linear arrays, and microwave radiometers (ref. 4). Each of these instrumental methods is briefly reviewed in the Appendix.

Remote Sensing Applications

A number of recent introductory and comprehensive reference books is available on remote sensing principles, applications, and instrumentation (e.g., refs. 5-7). These books provide in-depth treatments for different applications, including separate discussions for forest resource assessments, agricultural applications, rangeland applications, and urban/suburban land-use analysis. Only a brief summary will be presented here for these applications, focused on characterizing the associated types of measurement and data, to assist in considering real-time or near-real-time needs of users. For purposes of the discussions here, the vegetation category includes man-cultivated regions, as well as natural grassland, shrub-covered terrain, and forests.

Vegetation

Agricultural remote sensing involving cultivated crops, natural vegetative cover, and soil, is a very complex research subject because of the dynamic and cyclic processes and the interactions of reflection, absorption, transmission, and scattering of electromagnetic radiation by vegetation canopies. Vegetative remote sensing makes use of much of the total electromagnetic spectrum; i.e., that from the short-wavelength ultraviolet, visible, near infrared, and thermal infrared, through the longer-wavelength active radar and passive microwave regions. Microwave sensing offers the advantages of atmospheric and cloud penetration, day/night operation, and all-weather operations. For many applications, data from several wavelength regions are used synergistically. Very important use is made, too, of simultaneous ancillary weather and temperature data (e.g., National Oceanic and Atmospheric Administration (NOAA) weather satellites). Both human visual photointerpretation and computer image processing and classification play important coordinated roles in the data interpretation process.

The reflectance signature of green vegetation in the visible and infrared spectral regions is determined primarily by the chlorophyll absorption bands in the visible and water absorption bands in the infrared. As a result, there are some straightforward relationships; e.g., healthy leaves have high infrared reflectance, while unhealthy leaves have lowered infrared reflectance. Similarly, wilt (moisture stress) has long been recognized through decreased reflectance in the reflective part of the infrared spectrum. Generally, though, seasonal changes or state-of-health changes in plant canopies are not very simply related to changes in leaf chlorophyll and/or moisture content, because changes are distributed over the spectrum and there are many geometrical factors to consider in addition to the leaf reflectance: leaf transmittance into the canopy layers; the three-dimensional character of the canopy substructure; presence of stems, limbs, and other non-leaf structure; characteristics of the background, such as soil and leaf clutter; solar zenith angle; atmospheric conditions; and the observation geometry (look angle, azimuth angle). Therefore, it is not surprising to encounter numerous vegetation (and background) indices and coefficients that attempt to relate some of these influences and to account for spectral changes, which may be interrelated with spatial and temporal changes. Because of these complexities, the major problem encountered in photointerpretation and imagery analysis of crops, for estimating crop acreage, yield, and stress, is to develop techniques that are both fast and accurate in field/crop mapping. The United States Department of Agriculture, particularly, has urgent needs for better and more timely information, in the form of early warning of changes affecting production and quality, and in the form of crop-production forecasts. The USDA also has high interest in land use classification, renewable resources inventories, assessment of conservation practices, and pollution detection and impact evaluation.

Radar return signals are affected by the electrical characteristics of Earth features coupled with their geometry. The complex dielectric constant of an object is a measure of its reflectivity and conductivity. At microwave wavelengths most natural (dry) materials have a relatively low dielectric constant, whereas water is about an order of magnitude greater in its value. Therefore, water in soil or vegetation enhances the radar return signal. Plant canopies in general, with inherent high water content, provide strong signals for microwave radiometric measurements. Consequently, Side-Looking Airborne Radar (SLAR) and Synthetic Aperture Radar (SAR) applications to mapping natural vegetation; e.g., forests and crops, have been useful. Other uses of particular value to undeveloped regions of the world, are the delineation of boundaries; inventory information on forests, ranges, and water supplies; flood-inundation mapping; and determination of acreages in crop distributions. Possibilities exist for large-scale crop yield estimates. Research continues on the potentially valuable use of passive microwave imaging systems to provide regional soil moisture surveys over large inaccessible areas. Soil temperature measurements are also obtainable. With microwave sensing, burning forests, swamps, and peat piles can be efficiently detected even when covered by a heavy smoke layer.

Forest classification, inventory, and management are presently done through a combination of field activities and aerial or space imagery analysis. The eventual goal is to meet managing and planning objectives through maximum use of aerial or space imagery and to minimize the amount of field work. Classification of forest types by visual interpretative techniques makes use of highly skilled and trained imagery analysts, stereogrammetry, color and color IR photography, and scanning microdensitometry, along with sets of spectrogrammetric (e.g., Landsat) reference plots from ground sampling, orthophoto maps, SLAR data, and computer-based digital image processing.

Land Cover and Land Use

Reference 5 describes a multilevel land-use and land-cover classification system, developed by the U.S. Geological Survey, which incorporates four categories (scales) of images and/or photographs. The scales range from 1:250,000 and smaller to 1:20,000 and larger, representing 1) Landsat MSS image, 2) Landsat TM images and high-altitude aerial photographs, 3) medium-altitude aerial photographs, and 4) low-altitude aerial photographs. The coarsest levels of classification include urban or built-up areas, agriculture, rangeland, forest land, water, wetlands, barren land, tundra, and perennial snow and ice. The other levels of classification are subcategories of the more coarse levels, providing increasing details of land cover and use. Such a classification system can serve many needs in land-use planning and can accommodate the best existing techniques of both visual interpretation and digital image classification. The majority of urban applications require data collection in cycles from one to 10 years.

Reference 8 discusses the present status and future expectations regarding remote sensing technology for urban planning. Spatial resolution of civilian satellites is too coarse to provide good definition of complex urban-type scenery, because the average size of objects forming the urban landscape is usually less than satellite resolution. Consequently, a large percentage of pixels is comprised of more than one type of land cover. In addition, any one land use does not correspond to a specific spectral signature. Therefore, classification of land uses cannot be obtained directly from spectral radiometric information, but must also make use of morphological and topological data. It is not surprising, then, that for this application much reliance is still placed on visual photo-interpretation, in which dependence is not so much on spectral radiometric information as on shape, size, elevation, and the general structure of the image. The standard method for preparation of urban land-use/-cover maps in most countries is based on visual interpretation of high-resolution image data, primarily from aerial photogrammetric camera systems. Analysis of land use requires recording high-frequency, low-contrast detail with resolutions from about 0.5 to 10 m. Instantaneous fields of view better than 5 m are needed for visual interpretation. The high-resolution requirements for urban planning generally contrast with those for reconnaissance-level planning applicable to agricultural resources.

The trained interpreter relies heavily upon personal knowledge and experience, and the approach in visual interpretation is still far too complex to be completely computerized. Expert systems compete effectively only in the less intuitive tasks. The author of ref. 9 concludes, from work with image-differencing techniques, that visual interpretation of imagery is the most accurate technique for detecting urban change. At the same time, the author recognizes that at county, regional, and national scales, automated techniques are needed to provide unified records of spatial and temporal distributions of urban change. According to ref. 10 (p. 96), color IR video data, suitably digitized and processed, and superimposed with Geographic Information System (GIS) data, could provide a near-real-time update to land use/land cover types and conditions of vegetation.

Microwave instrumentation does not record in any simple way the spectral nature of urban and suburban features. Signatures are the result of complex interactions between terrain features and actively produced microwave energy. The signatures are dependent on the interrelationships among wavelength, polarization, and depression angle of the microwave beam and on the dielectric constant and surface roughness of the terrain features. Resolution requirements vary greatly with varying cultural developments.

Quick-Look and Other Operational Satellite Programs

Real-time and near-real-time data applications are highly relevant to the ultimate potential of a dedicated onboard data handling system for Eos. A Quick-Look program has been in operation with Landsat since the early 1980's (refs. 11-13). This program provides quick availability of raw or pre-processed data to users, meeting needs that would not be met if data access depended on large receiving and processing systems focused on central government agencies requiring high-volume and high-precision image products. Such users benefit from partially corrected (radiometrically and geometrically) full-resolution film or computer-compatible tape imagery. Quick-look systems are well suited for groups that have access to a receiving station and simple computer facilities for further data/image processing. The data can be viewed in image form on a display screen during the real-time pass while the raw data are stored on magnetic disks. The stored data are processed by selected enhancement and enlargement algorithms to best satisfy individual customer requirements. Photographic products based on data enhanced to individual specifications can be distributed to customers within hours of the satellite pass. The user may arrange in advance for the coverage of an area and time period to satisfy particular needs, or may choose to examine the data retrospectively.

Applications for quick-look data include natural resource surveys, analysis of land-use patterns, routine surveillance of navigation hazards, flood-damage assessments, forest fire studies, monitoring volcanic eruption damage, and crop-yield forecasts based on the variability of the weather, tillage, and seeding activities. The Quick-Look program has proved to be of much value to agencies responsible for informing the public of impending or occurring hazardous events and for reducing the impact of such events.

Although not designated as a quick-look program, the NOAA operational satellite system provides much data of high temporal resolution (refs. 14 and 15). The NOAA system was initially justified for meeting weather forecasting needs, and the meteorologist is the primary customer today, but it has many important applications in oceanography, hydrology, and agriculture. Some of the agricultural data derived from NOAA's satellite observations include precipitation measures and predictions, daily temperature extremes, canopy temperatures, insolation, and snow cover. Weather, actually, is the most important variable in determining year-to-year changes in agricultural production. The weather observations are used in numerical models that incorporate daily increments to provide estimates of soil moisture, crop yields, crop stress, crop calendars, winterkill, vegetation areal extent, and early warning of drought or freeze.

Reference 15 presents interesting observations of the U.S. Department of Agriculture's use of NOAA Advanced Very High Resolution Radiometer (AVHRR) data for monitoring and assessing crop conditions in selected countries. Before the satellite images are observed by analysts, each scene is processed to calculate vegetation indices that are averaged over pixels in geographically referenced grid cells, and the cell averages are entered into a database. But analysts make little use of this database, depending primarily on visual interpretation of computer-displayed images, weather data, and supporting crop and soil information. In the environment of limited time and personnel, visual analysis has been found satisfactory for assessing general crop conditions. However, the authors recognize additional potential dormant in the database and propose some methods of obtaining information that is not accessible through visual interpretation. Apparently, one of the fundamental problems to be dealt with is the matter of mixed pixels; i.e., pixels filled by more than one class of land cover; this matter continues to be an area of research. This problem is not completely solvable by very high resolution instrumentation, even if the large quantity of data and the data rates could be accommodated (refs. 16 and 1).

Data Management Considerations

Multitemporal and Multisensoral Data Requirements

An attempt will be made here to summarize general data handling and interpretation needs for vegetation and land-use applications of remote sensing and the current progress toward meeting those needs. Of particular value in this assessment was reference 1, which is a current treatment based on lectures of well-known specialists, representing universities and institutes in Europe and the United States.

Generally, applications of remote sensing involving vegetation or land-use classification require multitemporal and multisensoral data to obtain the maximum information from the measurements. As more advanced remote sensing systems evolve, the temporal resolution has been improved through polar-orbit configurations such as NOAA's and the planned Eos, as well as through scanning flexibility such as the forward- and backward-look capabilities of Systemé Probatoire d'Observation de la Terre (SPOT) and the planned Eos. Multi-instrument coordination and measurement, too, emphasize Eos.

For research in agriculture or forestry, the goal is often a classification algorithm, applicable to many examples of the type of scene of interest, and to future scenes that have similar characteristics. Similarly, in land-use inventory applications, classification methods are desirable. For example, it may be of interest to obtain (preferably autonomously) a map giving the land-cover distribution on a certain date. The difficulties to be overcome to achieve autonomous classification of an image can best be appreciated by considering the process of human visual image or photographic interpretation. In fact, the present trend in computer (machine) classification research is toward emulating more and more the processes of human visualization (ref. 17). The human interpreter does not recognize features and distinguish classes through pixel-by-pixel classification or by algorithmic processes. Local feature judgments are made in the context of surrounding pixels and larger units, such as fields, forest regions, water bodies, etc. In addition, human judgments are based on time history, with variations averaged in some sense over time and over spatial variety. External information, especially ground truth, is factored into the pattern recognition process. Analogously, digital classification methods are finding more success through use of supervised (ground truth use) rather than through unsupervised classification methods, and through texture and boundary evaluations, as opposed to pixel-by-pixel analyses. Statistical pattern recognition techniques that have been a focus of recent research activity have become recognized as inadequate in many respects, since it is difficult to include ancillary information in the classification procedure (ref. 17, p. 300).

Generally, for successful digital classification or recognition, a single-time image is not adequate. Often, it may be necessary to have an image of the same scene obtained by the same satellite on another date, an image from another satellite, topographical data, or ground truth data from direct observations. It is often more important for many people who make decisions to know where and when a change has taken place than to have a detailed land-cover map about an area at each of one or two times (ref. 10, p. 426). Changes in spectral reflectivity in registered, time sequential, remotely sensed images can convey more information to natural resource managers, environmental impact monitors, and urban planners than raw, enhanced, or classified images that cover the same geographic areas of interest. Dynamic areas require attention, whereas static areas do not. Then, for the multi-temporal or multi-instrument images to be useful for digital classification, the images must be precisely co-registered.

Geographic Information Systems (GIS's)

Methods and Applications.- Geographic information (integrated) systems (GIS's) are emerging as the major spatial data handling tools for solving complex natural planning problems (ref. 10, p. 270). A GIS is a computer hardware and software system designed to collect, store, retrieve, update, analyze, and display spatially referenced data. The thrust is to combine remotely sensed or directly sensed spatial data with geographical non-spatial map data. For example, the relief (magnitude and orientation of the slope) is important in environmental studies, particularly regarding problems in forestry and mountain agriculture. In many countries, good-quality, large-scale topographical maps exist, on which relief is represented by level curves or isolines. European and American cartographic institutes during the last two decades have devoted much effort to computerizing the map-making process. Digital mapping and systems built on that technology are one of the most effective methods of making massive amounts of information understandable.

Currently there is a trend towards database design of information systems. An information system must be based on a database if users expect timely answers and want to update the system as they learn about changes (ref. 18, pp. 16-17). The GIS technology has provided the vehicle for the merger of remotely sensed data with mapped data, allowing resource managers to combine both spatial and tabular data from many sources and preserve their geographic location. The various layers of data stored in the mainframe computer are registered to one another by a grid referencing system such as the Universal Transverse Mercator (UTM) system (U.S. Army, 1969). Such systems are a primary tool for many government agencies. For example, the Bureau of Land Management, to make its database more versatile, has incorporated terrain derivatives, roads, land ownership, water, land use, and other information digitized from USGS maps or from field annotation (ref. 10, pp. 404-406). The BLM resource specialists still use these primitive databases to identify areas for particular favored uses, such as firewood cutting or transplanting of endangered wildlife. Another practicable application is the wildfire attack system to deal with lightning-initiated fires in national forests. An interactive system of digital fire-related information, including spectral imagery and weather information via the Geostationary Operational Environmental Satellite, permits local attack managers to make almost instantaneous assessment of wildfire potential and critical decisions needed for appropriate action.

Present Research Status and Future Projections. Presently, most GIS databases are produced by digitizing map products. A goal of the scientific community of cartographers and remote sensing scientists is to be able to create sophisticated intelligent spatial databases, in which the user through a friendly interface can query interactively about map, terrain, or associated imagery, and obtain help in day-to-day decision-making processes. In present GIS systems it is not possible to perform complex queries that require dynamic computation of geometric and factual properties. Research on such systems, according to McKeown (ref. 19), "requires the integration of ideas and techniques from many disciplines such as computer graphics, computational geometry, database methodology, image analysis, photogrammetry, and artificial intelligence." Although automatic integration of remote sensing data with GIS's is not yet possible, since human interpretation and assistance are still necessary, AI/expert systems are expected to eventually play a significant role in the integration of remote sensing data with GIS's (e.g., see refs. 19-23). Reference 24 reports on the design of an expert system based on Landsat imagery. In that paper it is pointed out that the traditional approach to the analysis of remotely sensed imagery based on image processing techniques, such as segmentation and statistical classification, is basically limited by the lack of integration with geocoded databases and by the difficulty of handling contextual information. However, expert systems are likely over the near term, to remain largely research, or experimental systems. Prototypes based on formal AI languages will play a very important role in the future toward development of practical systems (ref. 10, p. 517). In reference 25 it is observed that problems known to require much commonsense knowledge, English-language understanding, complicated geometric/spatial models, complex causal/temporal relations, or the understanding of human intentions are not good candidates for current state-of-the-art expert systems. Such problems are seen as central to the development of practical geographic expert systems, and therefore, the need for much basic research is anticipated before practical geographic expert systems become a reality.

The digital terrain model (DTM) or digital elevation model (DEM) is an important data representation for some geographic information system applications. The importance of such a model is emphasized by the fact that high-precision image rectification for high-resolution land-use satellites such as Thematic Mapper and SPOT is possible only if a DTM is used as the master image (Dejace, in ref. 1, p. 140). In such use, the DTM becomes the primary data set, with the remotely sensed satellite data being supplementary to it. A DTM may be regarded as a data table giving the altitude above sea level of the nodes of a two-dimensional grid, generally with a square cell. The DTM is similar to a digital image and can be organized in computer memory in raster format. Construction of a DTM is a difficult process. Building a DTM either from stereo pairs of aerial photographs or from a topographical map involves specialized photogrammetric or complicated mathematical operations. Once such a model is generated, however, it is straightforward to calculate other associated models; e.g., the slope and azimuth of the maximum slope direction at every point of the grid, from which sun incidence angle, shadowing, and other phenomena may be calculated for each pixel. Possibilities such as the number of sunshine hours at each pixel corrected for incidence angle are envisioned.

There are significant problems to overcome in transforming digital map data into a DTM that can be integrated with satellite imagery. Part of the problem is the question of appropriate digital representation of the spatial geographical data. There are two distinct ways in common use for storing spatial information for computer use; i.e., "raster" format and "vector" format (Dejace, in ref. 1, pp. 136-137).

The raster format is analogous to the format in which digital images are stored. The coordinates of points are not written explicitly, but are easily retrieved for each pixel from the order in which the data are stored. Such a format is possible only when the data are organized in such a system as the nodes of a regular grid. The way in which the data are ordered in storage must be defined explicitly.

The vector format for storing data is used primarily in computer-aided cartography. A point is represented by its explicitly written spatial coordinates. A line is represented by an ordered sequence of pairs of coordinates defining points; i.e., the line is approximated by straight segments linking these points. A code is included to indicate what the line represents; e.g., a road, railroad track, or river. A surface is represented by its contour line and a code.

Both the raster and vector formats are used as intermediate data storage formats, thus creating a dilemma in the development of GIS's. Maps created by specialized hardware by using the vector format are of high cartographic quality, similar to conventional hand-drawn maps. However, algorithms for processing vector formatted data are more complicated than those for the raster format. When there is need to compare several thematic maps or images, the raster format provides more straightforward procedures than the vector format. In addition, recently developed software and specialized hardware for image processing are directly usable with the raster format. Resource managers have to combine the analytic capabilities of the best raster systems with the superior storage handling and output capabilities of the best vector systems, and at the same time allocate attributes spatially by means of an integral database management system. Such capability for interacting many data themes, for alternate options, requires a format which can present data in different combinations, interact them repetitively, and update and correct them easily. Development of specialized software is required and must be transportable from one computer system to another.

Most geographical data must be obtained from maps, and is usually digitized manually by use of a digitizing table involving vector formatting or by a raster scanner. Neither method is straightforward, however. Manual digitizing is tedious and susceptible to human error, and is considered a bottleneck in geographical data processing. On the other hand, most geographical paper documents are not suited to raster scanning because they contain too much information requiring pre-scanning, editing, and post-scanning steps. Therefore, manual digitizing, with the human eye, brain, and hand selecting what to digitize, is often the only current practicable method of digitizing. After the digitizing of several sets of data, geometrical processing is necessary to co-register them and to properly align them with satellite digital imagery.

Potential Role for Proposed Information Sciences Experiment System (ISES)

Recent papers (refs. 2 and 3) have characterized several needs for an Eos onboard computational resource:

To permit experiments and demonstrations in onboard information extraction, in support of both Earth science and information science technology advancement

To provide direct-to-user data products

To provide real-time response to events

To operate as an interactive experiment on a non-interference basis relative to other on-board instrumentation

To directly address the "data glut" problem

To provide capability for growth of Eos into evolving technology without adversely affecting standardization and reliability of the operational space system

These needs are discussed further.

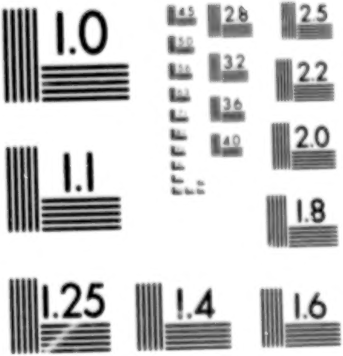
1.0
4.5
2.8
2.5
5.0
3.2
2.2
5.6
3.6
6.3
4.0
2.0
1.1
1.8
1.25
1.4
1.6

MICROCOPY RESOLUTION TEST CHART
NATIONAL BUREAU OF STANDARDS
STANDARD REFERENCE MATERIAL 1010a
(ANSI and ISO TEST CHART No. 2)

Quick-Look Needs for Eos

Some aspects of the ISES concept have been partially introduced into the design of the Eos (refs. 26 and 27), at least relative to the MODIS and HIRIS instrument operations and the coordination of their data outputs through the Eos Data Information System (DIS). These two instruments are designed to be complementary in terms of data outputs and coverages, but the instruments differ markedly in their modes of operation and their data rates. Some on-board processing is necessary to reduce the instantaneous transfer from the HIRIS instrument, with concommitant planning and command support for spectral and spatial editing. The HIRIS instrument will only take data in response to user requests, while the MODIS-N and MODIS-T instruments will operate on a full-time duty cycle (different spectral channels for day and night). The MODIS-T pointing operations require planning and control support as well. Both the HIRIS and MODIS allow for updates of schedules and commands for targets of opportunity and instrument emergencies. To accommodate requirements for real-time and near-real-time availability of the science data for field-experiment support and instrument health monitoring, both MODIS and HIRIS will produce low-rate data streams from their science data.

Basic limitations on real-time and near-real-time data transfer exist because of limited Eos access to the Tracking and Data Relay Satellite System (TDRSS), the primary medium of data communications from space to ground. The onboard processing capabilities of the Eos polar platforms relative to MODIS and HIRIS are still to be completely defined. The desirability of a number of onboard processing functions is recognized in the Eos community (ref. 27): buffering complete scans of data to sort measurements by channel before packetization; data compression; generation of products that could be used for instrument control, e.g., setting detector gains for land or sea, or altering sensing routine based on cloud cover; priority packet addressing to support real-time monitoring and near-real-time support of field experiments; building data packets from several instruments for ancillary and engineering/housekeeping use or for the ground data system use; and command and scenario storage and execution functions; e.g., sunglint avoidance, automatic gain changes for high solar zenith angles, and internal calibration sequences.

A very conspicuous need for onboard data sensing/processing is cloud-cover assessment as a preface to some instrument data takes, particularly in view of the continuous global coverage of some instruments, and the certainty of obtaining and transmitting large quantities of useless data to be filtered out at one of the ground-processing data output levels. This need is emphasized by the fact that on any single day, about half of the Earth's surface is obscured by clouds (ref. 28). Conversely, some instruments look for clouds, only, and could similarly benefit from cloud-cover (pattern) "knowledge" through a look-ahead sensor or knowledge base formed from sensing on immediately preceding orbits.

It appears that possibilities exist for significant enhancement of quick-look capabilities of the Eos via an onboard general processing system such as proposed in the ISES. Significant needs are presently being met in near-real-time and quick-look applications through Landsat and NOAA operational satellites, as discussed earlier. However, the fact that extensive ground processing is necessary to create a usable database from the quick-look data indicates opportunity for eventually improving the timeliness and efficiency of use of the data through onboard pre-processing activities and more extensive direct-to-user capabilities.

Table 1 lists a variety of experiments under consideration for Eos payloads that have potential applications to vegetation and land-use and represent opportunities both individually and in groups for enhanced data return through the ISES. Tables 2 and 3 present some examples of applications (needs) for which near-real-time data access might be enabled through the ISES.

Support of In Situ Experiments and Research

The Eos concept puts heavy emphasis on field measurements and ground-based analytical work, to complement the extensive satellite instrument measurements. In some cases, field measurements or ground-based database constructions may be the primary database, with the satellite measurements providing supplementary information; and in other cases, the converse relationship applies. In either case, close and timely coordination of the Earth-based and satellite-based data sets is very important to the full accomplishment of Eos objectives. The EosDIS and associated systems provide means to address some of these needs, particularly with respect to HIRIS and MODIS. However, since it may be up to 24 hours before Level-0 data is available for Level-1 processing, some timeliness may be missing in the coordination of field experiment work and satellite data. A dedicated onboard processor and communications package has potential for improving information exchange and synergism between field measurements and satellite measurements, particularly when communications among several experiments may be necessary.

Experiment Base for Evolving Technology

A computational and communications package on Eos would provide real-time in-space inputs to support prototype developments; i.e., an onboard experiment base for testing and evaluating emerging remote sensing technologies. As stated by Katzberg, et al. (ref. 2), "New technology is rarely used because it is not mature; and by the time it gets mature, it is no longer new." Use of relatively new technology in spacecraft operational systems seems unlikely to happen until an onboard experimental base is first established in an opportune (e.g., Eos) environment to test new technology in parallel with and in conjunction with operational systems. Flight simulations and extensive ground testing before introduction into flight application has an important role in early development of new systems, but there appears to be a beneficial role, too, for onboard testing and evaluation, to accelerate introduction of newer technology into dedicated flight systems and to provide information and insights that cannot be gained from ground tests and simulations alone.

Concluding Remarks

It is clear from a review of the current state-of-the-art of remote sensing that the term remote sensing connotes a much broader scientific field than the name literally covers. Smart sensors have served to broaden the concept, but to think smartly about remote sensing now, one has to think about sophisticated image processing; human vision modeling; computer (machine) vision; artificial intelligence; expert and knowledge-based systems; databases; GIS's; learning (neural) systems; advanced communications; and the most modern technology in sensors, cameras, scanners, radiometers, interferometers, and spectrometers. It seems accurate to say that a technological revolution is occurring in remote sensing. Pre-occupation with the data volume and complexities of image/data processing may largely account for the relatively modest current efforts toward application of onboard processing technology.

This paper was written to report the results of re-examining the needs for onboard processing and communications and direct-to-user data communications in remote sensing, relative particularly to applications involving the sensing of vegetation/forest cover and land-use assessment and planning. The evaluation is general to the field, but is focused on the Eos program and a proposed experiment for Eos, the ISES. To assess needs for onboard computer/communication resources for Eos, it was necessary to look at the state-of-the-art activity in these applications of remote sensing and to consider the problems being addressed and the trends in relevant ground-based research.

Particularly prominent in current remote sensing research is the emphasis on further advancements in GIS's, incorporating versatile database management systems for manipulating both spatial information, and the thematic attributes of that information. Through these systems, improvements are possible over traditional methods of capturing, storing, updating, analyzing, and displaying mapped natural resource data. It is well recognized now that the construction and maintenance of a GIS is an essential tool in any information or intelligence analyzing program dependent upon the acquisition, storage, and quick retrieval of large amounts of data relative to any portion of the Earth's surface. GIS technology allows the scientist to process and interrelate many more kinds of data than was previously feasible and opens opportunities for possibly providing new scientific understandings of a variety of topics (problems); e.g., assessment of a country's energy and mineral potential and assessment of hazards due to natural and man-made occurrences (ref. 10, p. 270).

The need is well recognized for eventual application of artificial and neural-type intelligence and expert system technology to database manipulation, and a significant amount of research is being so directed. Until more progress is made in such systems, much reliance will continue to be made upon human intelligent interaction to cope with the complexity of the data management processes. It has been recently proposed by some researchers that in lieu of the goal of completely autonomous systems, semi-automated systems in which humans interact with expert systems, may be the practical approach (refs. 29-31). Consistent with this thinking, it seems that a next logical development, concurrent with reasonable progress in such ground-based semi-automated systems, would be the introduction of semi-automated expert systems and smart sensors for onboard instrument control, data editing, and pre-processing. Such developments would also reinforce the long-term methodology of development of the Eos Data Information System, as presented in reference 32. The need is expressed there for incorporating within the EosDIS an "iterative learning process that is directed toward evolutionary modular or 'test bed' information system concept development." Such strategy "provides a reasonable environment to implement and evaluate concepts and advanced technologies with minimal risk of impairing system performance, integrity, maintainability, and security." The proposed ISES appears to be timed and tailored to serve as the onboard complement to such a ground-based EosDIS test-bed. At the same time, the ISES concept incorporates enhanced quick-look capabilities for Eos instrumentation, addresses direct-to-user data and communications needs, and includes support for coordinating field experiments with satellite experiments.

Appendix

Remote Sensing Instrumentation

Photogrammetric Cameras

Photographic systems have evolved from ground-based ones to aerial systems and then to a long sequence of spacecraft-based systems. Photographic data products played a very significant role in stimulating further interest and advancements in remote sensing, and they have continued into the 1980's era in Space Shuttle and Spacelab experiments. Photogrammetric systems have several advantages (ref. 1): very high geometric resolution for large formats; relatively simple instrumentation and geometric data evaluation; very high geometric accuracy; and possibilities for topographic information generation through stereographic imaging. At the same time, such systems have many limitations, compared with some of the more recently developed remote sensing systems. For example, photographic systems provide only information on the visible and near infrared reflecting properties of the Earth's surface, since they are limited to the spectral region from 0.3 to 0.9 micrometer. In addition, they are characterized by limited spectral resolution, non-linear radiometric effects, and use of film recording media with limited physical recovery capability.

Television Cameras

The Return Beam Vidicon (RBV) cameras used on Landsats 1-3 are well known uses of TV cameras on satellites. This type of sensor was used earlier on some weather satellites. RBV's were troublesome because of power problems that resulted in early failure. They provided high topographic detail, but radiometric resolution limitations reduced the usefulness of the data. Video systems can provide users with near-real-time imagery that is useful in applications requiring rapid turn-around-time, while not requiring high resolution. In addition, the electronic format of video data is compatible with computer image processing techniques, and it provides improved spectral resolution and extended spectral range, as compared with photographic systems. Recently, color IR video systems, designed around video tubes, have been used in remote sensing applications, at least in aerial and ground vehicles (ref. 33). Solid-state cameras (CCD's) have also been used in space remote sensing applications (e.g. ref. 34).

Ultraviolet, Visible, and Infrared Multispectral Radiometers and Imaging Spectrometers

The scanning radiometer is now the most commonly used type of instrument for satellite remote sensing in the visible and infrared spectral regions, covering the spectral range 0.3 to about 14 micrometers. The radiation sensed is either reflected solar radiation or radiation emitted from the Earth's surface, spectrally selected by filters, prisms, or grating systems. The basic design of the instrument involves a mirror system to focus radiation from the Earth's surface onto a detector and a mirror scanning mechanism to scan the instantaneous field of view along a line perpendicular to the satellite's orbit. The satellite image is constructed from a series of adjacent scan lines which result from the orbital motion of the satellite.

There is a trend toward replacing scanning systems in radiometers by solid-state multilinear arrays (MLA) detectors. Scanners inherently are susceptible to mechanical wear and failure. The MLA is a linear array of sensors, each of which creates a pixel of data along a line perpendicular to the direction of the satellite motion in its orbit. Present systems, also referred to as pushbroom scanner systems, are limited to wavelengths out to the near infrared.

Lidar, or laser radar, is an active (provides its own target irradiation) sensing system similar to microwave radar, operating in the UV to near IR regions. Such a system uses a laser to emit radiation in pulsed or continuous mode through a collimating system (ref. 35). The radiation that is returned is collected by a second optical system that focuses it onto a detector. Both the backscattered signal intensity and delay can be measured. The delay provides range measurement, while the backscattered intensity provides information about the size and the physical and chemical composition of the target.

Microwave Radiometers

Microwave radiometry is based on the spectral region from one to 300 micrometers (refs. 35 and 36) and is categorized as active, passive, imaging, or non-imaging (profiling). Radar is the most well known subdivision of active microwave radiometry. Pulses of microwave power are transmitted from an instrument toward a target and measurements are made of the reflections or scatterings returned to the same instrument from the different regions of the target. A radar scatterometer is a non-imaging active system for measuring the radar backscatter of terrain as a function of incidence angle (ref. 5).

Geometrical and electrical characteristics are the principal factors that influence the magnitude of the radar return signal for active systems. Geometrical effects include the relative orientation of the object and sensor, as well as the surface roughness and its magnitude relative to the wavelength (wavelength is also important in determining atmospheric penetration). At any chosen wavelength, radar signals may be transmitted and returned in various combinations of polarization, as empirically determined to be most useful. Smooth (relative to wavelength) surfaces in general reflect the signal away from the sensor, whereas rough surfaces return more of the signal, but a smooth target may be so oriented to cause a strong return. Objects or combinations of object surfaces may create the special case of an effective corner cube reflector, which results in multiple reflections and high signal return.

The basic configuration for aircraft active microwave radiometry is side-looking radar (SLR) or side-looking airborne radar (SLAR), so called because the antenna is fixed below the aircraft and pointed to one (or both) side(s), producing continuous strips of imagery parallel to the flight line. Conventional (real aperture) SLAR systems are relatively simple in design and in data processing requirements, but are rather limited in resolution and are constrained to relatively short-range, low-altitude, and short-wavelength operations. Associated with these limitations are limited aerial coverage and increased atmospheric attenuation and dispersion. These limitations are overcome in synthetic aperture radar (SAR), or coherent radar systems, more suitable in resolution capability for satellite applications. While these systems use a short physical antenna, they synthesize the effect of a very long antenna via the aircraft motion and special doppler data processing. SAR is more practical than SLAR for spacecraft operations, as well as for most aircraft applications. The disadvantage trade-off is much more complicated data processing.

With passive microwave sensing, the target's naturally occurring radiation is sensed. The emittance of the target varies with observation angle, polarization state, wavelength (frequency), and surface roughness (relative to wavelength). Brightness temperature is a commonly measured physical parameter; i.e., the temperature of a blackbody with the same emissive power as that of the target sensed by the microwave radiometer or scanner. The temperature and temperature distribution in the target body (surface feature), as well as its electrical and thermal properties, affect the quantity and spectral nature of the radiation received by the microwave measuring system. For a given target, the passive microwave signal may involve these components: 1) emitted radiation due to the material characteristics and temperature; 2) atmospheric radiation; 3) surface reflection originating with the sun or sky; and 4) radiation transmission from the subsurface region of the target. Therefore, for passive microwave signals, the signal strength and character over a given object depend on the object's temperature, emittance, reflectance, transmittance and the incident radiation. These dependencies, in turn, are affected by the object's electrical, chemical, textural, and shape characteristics, and by the angle from which they are viewed. Only very low radiation levels are available from passive microwave sources; therefore, a relatively large antenna beam width is required to collect sufficient power to provide a detectable signal.

References

1. Toselli, F., ed.: *Applications of Remote Sensing to Agrometeorology*. Kluwer Academic Publishers, 1989.

2. Katzberg, Stephen J.; Murray, Nicholas D.; Benz, Harry F.; Bowker, David E.; and Hendricks, Herbert D.: The Information Sciences Experiment System. *IEEE Proceedings-1989 Southeastcon*, 1989, pp. 511-516.

3. Foudriat, Edwin C; and Husson, Charles: Information Science Experiment System. *IEEE Proceedings-1989 Southeastcon*, 1989, pp. 527-531.

4. Harris, Ray: *Satellite Remote Sensing, An Introduction*. Routledge & Kegan Paul, 1987.

5. Sabins, Floyd F., Jr.: *Remote Sensing Principles and Interpretation*. W. H. Freeman and Company, 1987.

6. Swain, Philip H.; and Davis, Shirley M.; eds.: *Remote Sensing: The Quantitative Approach*. McGraw-Hill, Inc., 1978.

7. Colwell, Robert N., ed.: *Manual of Remote Sensing*, 2nd Ed., Vols. I and II, AMERSOC of Photogrammetry, 1983.

8. Baudot, Y.; Nadasdi, I.; and Donnay, J-P: Towards An Urban Land-Use Classification Using Textural and Morphological Criteria. *Proceedings of IGARSS '88 Symposium, 1988*, pp. 211-212.

9. Griffiths, G. H.: Monitoring Urban Change from Landsat TM and SPOT Satellite Imagery by Image Differencing. *Proceedings of IGARSS '88 Symposium*, 1988, pp. 493-497.

10. Opitz, Bruce K., ed.: *Geographic Information Systems in Government, Volume 1*. A. Deepak Publishing, 1986.

11. Miller, John M.; and Campbell, Norman: An Experimental Landsat Quick-Look System for Alaska. *Proceedings of Machine Processing of Remotely Sensed Data Symposium*, 1981, pp. 639-545.

12. George, Thomas H.; Miller, John M.; and Zender-Romick, Janis: The First Year of Operation of the Alaskan Landsat Quick-Look System. *Proceedings of Seventh International Symposium on Remote Sensing of Environment*, 1983, pp. 1253-1263.

13. Burger, G. J.; and Miller, J. M.: Custom-Enhanced Landsat Imagery in Near Real-Time. *Proceedings of the 10th Canadian Symposium on Remote Sensing*, 1986, pp. 699-703.

14. Yates, H.; Strong, A.; McGinnis, D., Jr.; and Tarpley, D.: Terrestrial Observations from NOAA Operational Satellites. *Science*, vol. 231, January 31, 1986, pp. 463-470.

15. Philipson, Warren R.; and Teng, William L.: Operational Interpretation of AVHRR Vegetation Indices for World Crop Information. *Photogrammetric Engineering and Remote Sensing*, vol. 54, no. 1, January 1988, pp. 55-59.

16. Gurney, Charlotte M.; and Townshend, John R. G.: The Use of Contextual Information in the Classification of Remotely Sensed Data. *Photogrammetric Engineering and Remote Sensing*, vol. 49, no. 1, January 1983, pp. 55-64.

17. Estes, John E.; Friedl, Mark A.; and Star, Jeffrey L.: Advanced Feature Extraction in Remote Sensing Using Artificial Intelligence and Geographic Information Systems. *SPIE Vol. 294 Recent Advances in Sensors, Radiometry, and Data Processing for Remote Sensing*, 1988, pp. 297-304.

18. Frank, Andrew U.: Overlay Processing in Spatial Information Systems. *Proceedings Eighth International Symposium on Computer-Assisted Cartography*, Nicholas R. Chrisman, ed., 1987, pp. 16-31.

19. McKeown, David M., Jr.: The Role of Artificial Intelligence in the Integration of Remotely Sensed Data with Geographic Information Systems. *IEEE Transactions on Geoscience and Remote Sensing*, vol. GE-25, no. 3, May 1987, pp. 330-348.

20. Ripple, William J.; and Ulshoefer, Veit S.: Expert Systems and Spatial Data Models for Efficient Geographic Data Handling. *Photogrammetric Engineering and Remote Sensing*, vol. 53, no. 10, October 1987, pp. 1431-1433.

21. Robinson, Vincent B.; and Frank, Andrew U.: Expert Systems for Geographic Information Systems. *Photogrammetric Engineering and Remote Sensing*, vol. 53, no. 10, October 1987, pp. 1435-1441.

22. Hogg, J.: Modelling Land Resources Within a Pilot Geographical Information System. *Proceedings of IGARSS '88 Symposium*, 1988, pp. 101-105.

23. Goodenough, David G.; Goldberg, Morris; Plunkett, Gordon; and Zelek, John: An Expert System for Remote Sensing. *IEEE Transactions on Geoscience and Remote Sensing*, vol. GE-25, no. 3, May 1987, pp. 349-359.

24. Goldberg, Morris; Goodenough, David G.; Alvo, Mayer; and Karam, Gerald M.: A Hierarchical Expert System for Updating Forestry Maps with Landsat Data. *Proceedings of the IEEE*, vol. 73, no. 6, June 1985, pp. 1054-1063.

25. Bobrow, Daniel G.; Mittal, Sanjay; and Stefik, Mark J.: Expert Systems: Perils and Promise. *Communications of the ACM*, vol. 29, no. 9, September 1986, pp. 880-894.

26. Han, D.; Ramapriyan, H.; Salomonson, V.; Ormsby, J.; Anderson, B.; Bothwell, G.; Wenkert, D.; Ardanuy, P.; McKay, A; Hoyt, D.; Jaffin, S.; Vallette, B.; Sharts, B.; Folta, D.; Hurley, E.; and MacMillan, D.: *MODIS-HIRIS Ground Data Systems Commonality Report*. NASA TM-100718, 1988.

27. Han, D.; Salomonson, V.; Ormsby, J.; Ardanuy, P.; McKay, A.; Hoyt, D.; Jaffin, S.; Vallette, B.; Sharts, B.; Folta, D.; Hurley, E.; and MacMillan, D.: *MODIS-Information, Data, and Control System (MIDACS) System Specifications and Conceptual Design*. NASA TM-100721, 1988.

28. Tarpley, J. D.; Schneider, S. R.; and Money, R. L.: Global Vegetation Indices from NOAA-7 Meteorological Satellite. *Journ. of Climate and Applied Meteorology*, vol. 23, March 1984, pp. 491-494.

29. Goodenough, David G.: Thematic Mapper and SPOT Integration with a Geographic Information System. *Photogrammetric Engineering and Remote Sensing*, vol. 54, no. 2, February 1988, pp. 167-176.

30. Wharton, Stephen W.; and Newcomer, Jeffrey A.: Land Image Data Processing Requirements for the EOS Era. *IEEE Trans. on Geoscience and Remote Sensing*, vol. 27, no. 2, March 1989, pp. 236-242.

31. Schowengerdt, Robert A.; and Pries, Richard A.: Interactive Image Feature Compilation for Geographic Information Systems. *SPIE Vol. 924 Recent Advances in Sensors, Radiometry, and Data Processing for Remote Sensing (1988)*, 1988, pp. 305-310.

32. Chase, Robert R. P.: Toward a Complete EOS Data and Information System. *IEEE Trans. on Geoscience and Remote Sensing*, vol. 27, no. 2, March 1989.

33. Meisner, Douglas E.; and Lindstrom, Orville M: Design and Operation of a Color Infrared Aerial Video System. *Photogrammetric Engineering and Remote Sensing*, vol. 51, no. 5, May 1985, pp. 555-560.

34. Wilson, R. Gale; Davis, Richard E.; Wright, Robert E., Jr.; Sivertson, W. E., Jr.; and Bullock, Gordon F.: *Radiometric Responsivity Determination for Feature Identification and Location Experiment (FILE) Flown on Space Shuttle Mission 41-G*. NASA TM-89017, 1986.

35. Barrett, E. C.; and Curtis, L. F.: *Introduction to Environmental Remote Sensing*. Chapman and Hall, 1976.

36. Lillesand, Thomas M.; and Kiefer, Ralph W.: *Remote Sensing and Image Interpretation*. John Wiley & Sons, 1979.

Table 1. NASA Eos Instruments Supporting Vegetation and Land-Use Research Applications

Clouds and the Earth's Radiant Energy System	CERES
Thermal Infrared Ground Emission Radiometer	TIGER
Stratospheric Aerosol and Gas Experiment III	SAGE III
GPS Geoscience Instrument	GGI
Earth Observing Scanning Polarimeter	EOSP
Moderate Resolution Imaging Spectrometer	MODIS
High Resolution Imaging Spectrometer	HIRIS
Synthetic Aperture Radar	SAR
Geoscience Laser Ranging System	GLRS

Table 2. Quick-Look Applications in Forestry

Drought indices measurement

Fire-danger monitoring

Fire-progress/control monitoring

Infestation/mortality detection and monitoring

Acid rain/pollution assessments

Volcanic effects on timber measurement

Forest inventories maintenance/updating

Air pollution impact on forest ecosystems measurement

Table 3. Quick-Look Applications for Vegetation

Drought indices and adequacy of irrigation sources measurements

Rangelands fire-danger monitoring

Wheat belt growth progress and crop yield estimations

Infested areas isolation for treatment

Pollution damage assessment

Growth cycle in major crop belts--monitoring

Vegetation stress assessment

Biomass measurements in deserts/dust-storm assessment

Storm-damage/soil-erosion/flood-inundation assessment

Herbicide drift-damage determinations

World-crop information gathering

Crop production and quality--early forecasts

N90-27159

APPLICATIONS OF ISES FOR SNOW, ICE, AND SEA STATE*

Alfred T. C. Chang
NASA Goddard Space Flight Center
Greenbelt, MD

Victor E. Delnore
Planning Research Corporation
Hampton, VA

Snow and Ice

There will be six facility instruments on the NASA NPOP-1 and NPOP-2 and additional instruments on the Japanese and European satellites. Also, there are the 24 selected NASA instruments that may be flown on one of the platforms. Many of these instruments can provide data that could be very useful for real-time data studies in the snow and ice area. This paper will not address any one instrument in particular, but will be concerned about what is potentially possible using the capabilities of some of these instruments.

In the snow area, we are mainly concerned with detecting seasonal snow and glaciers, while in the ice area we are concerned with sea ice, river and lake ice and also ice sheets. Over the years, the seasonal snow covering has averaged about 40 million square kilometers. Figure 1 shows one of the snow maps produced using Defense Meterology Satellite Program Special Sensor Microwave Imager (DMSP) SSM/I data. The SSM/I is a passive microwave radiometer with 19-, 22-, 37- and 85-GHz channels. It was launched in 1987, and the image shown here is a false color plot constructed from 19- and 37-GHz data. The resolution of the 19-GHz channel is about 60 km and that of the 37-GHz channel is about 30 km.

With this resolution we have a low data rate, and it is certainly reasonable to consider doing this in real time. We are using kilobit data rates, and there should be no problem at all doing any global type of study.

To arrive at the algorithm used here we mounted a radiometer on top of a truck and measured brightness temperatures over various snow fields. By combining these measurements with snow field and climatology data in a modeling program, we were able to generate this simple relationship between snow depth and brightness temperature. This algorithm depends on the radiative transfer in layers of snow crystals. In Figure 2 we show the effect of varying the snow crystal radius. One curve is for 0.3-mm crystal size data and the other is for the 0.5-mm size. The dominant effect of crystal size variation is in the 37-GHz data. Since the 18-GHz radiation basically does not scatter by snow crystal at all, it serves as a reference point to normalize the physical temperature.

This algorithm has worked pretty well over open areas like the prairies of Russia, but we know that in mountainous areas or regions with trees this simple algorithm is not going to work. The United States Geological Survey (USGS), United States Department of Agriculture (USDA) and NASA initiated a cooperative program over the Colorado River basin following the 1983 flood, and we are still working on these problems and getting close to a solution. We probably will not be using a simple relation like the one just given. Different regions of the world may require different algorithms. That will complicate the data retrieval a little, but it still shouldn't be too difficult.

Historically, horizontally (H) polarized data have been used in these applications because the H channel of a similar instrument on Nimbus 7 was better behaved than the vertical (V) channel. Although the H polarized data from the DMSP satellite was used above, both V and H polarization were available and they should give about the same results for future applications.

The only microwave radiometer that has been currently selected for the Eos project is the AMSR, a Japanese instrument that weighs around 900 kgm. This may be too heavy for inclusion on NPOP-1 or

---

*The snow and ice section is by Dr. Chang and the sea state section is by Dr. Delnore.

PRECEDING PAGE BLANK NOT FILMED

-2, so it is still not definite what the final channel selections will be or which instrument will be flown. However, it is reasonably certain that an 18- or 19-GHz channel and a 37-GHz channel will be available.

Using the given algorithm we can retrieve two parameters (the snow cover area and the amount of snow storage). The snow coverage has been derived by NOAA and the Air Force for a long time. NOAA is using visible data to come up with a weekly product. The Air Force uses ground measurements and models and comes up with a daily product. These two products do not always match each other; they sometimes differ by millions of square kilometers in area. We thought that more things could be done in this area; therefore, we are using microwave data for the snow depth estimates because that's the only sensor that can provide this information. Of course, we will probably use visible sensors for the area coverage because of the higher resolution, but there is still the cloud cover problem.

Radar altimeters can penetrate snow and give a different altitude than optical altimeters; thus, it is possible to get the snow depth in this manner. However, the dielectric constants of snow and ice are quite different, so when the temperature rises, microwave instruments can tell right away whether the snow is melting or not. Whereas snow storage will be more of a long-term type of measurement, snow melting will have more real-time importance.

In the Colorado River basin incident of 1983 there was an unusually hot week in May. Under normal conditions snow generally melts from the valleys toward the mountain peaks, but in this case it suddenly melted everywhere, from the bottom of the mountains all the way to the top, generating the big flood. This kind of event can probably be detected quickly in real time, and will be extremely important to the resource manager responsible for dams and reservoirs.

Now, water vapor is usually not a major factor. When it's cold there is not much water vapor in the air. It becomes a factor in the temperate regions, however, because sometimes there can be snow and rain mixed together. Since only the 37-GHz data are responding to the snow, it should be possible to determine the snow/rain mix during a storm. This will definitely be a real-time problem since it will affect traffic and snow removal. Another problem can be winter kill; this can be a big factor in the plains area if you don't have enough snow. Usually snow is a good insulator and can help prevent winter wheat kills. Real-time monitoring of conditions can help predict next year's crop conditions.

Another thing to consider is glacier movement. Glacier motion is on the order of about 70 meters per year. Although this is slow, according to Mark Myer's study the melting or receding of glaciers contributes significantly to the increase of the water level globally. This is obviously important for global change studies.

Sea ice has been extensively studied. In Figure 3 we see a large area in the northern hemisphere over Greenland and in the southern hemisphere over the boundary of Antarctica. What we can do now is determine its concentration. Figure 3 also shows the concentration and location of the sea ice. Global sea ice covers about 20 million square km. This large an area has an impact on the global energy balance, but the real-time usage of this data will be more for shipping. The traffic patterns are the important factor; where there is ice the ships cannot go through. The microwave instruments can tell the difference between frozen sea water and compacted snow over the land masses. Icebergs are a related problem but they must be detected using Synthetic Specture Radar (SAR) data.

At this moment, lake ice and river ice are not being studied with these same sensors because of the 25 to 50 km resolution. With improved resolution, however, it should be possible to monitor the beginning of melting and foresee the possibility of ice jams. These kinds of problems will obviously need real-time data.

It may be possible to use Geodynamics Laser Ranging System (GLRS) data or laser altimeter data to determine snow depths from year to year. These kinds of data will be very important in global energy models, hydrological cycles, and so on. Even though most of the global data is important, the real-time problems are not a sensitive issue in this area.

Figure 4 demonstrates some of the research we are currently doing with comparisons of aircraft and satellite data. The aircraft sensor was the same as that on the DMSP so that aircraft data could be used to interpret or validate the spacecraft data. In the future we will have to repeat these experiments because of different frequencies, resolutions, and other instrument parameters. Coverage is probably fairly easy to do, but determining the areal extent of leads is more difficult. Because the energy exchange between the atmosphere and the water surface is several orders of magnitude higher than when the water is covered with ice, if you have 20-percent open water, the energy exchange is quite different from solidly packed ice. That's why we need to understand the data better to make sure the retrieval is reasonable. It is very difficult to measure the ice concentration accurately except by using aircraft.

The distinguishing of water and ice on a daily monitoring basis in areas such as the Arctic Ocean is very important. This is a very dynamic region. There is the continual opening of pack ice and then within hours the ice sheets close up again, and some sheets wrap over other ice sheets. The ice edge is a part of this process also because the advancing and receding of the boundary has a significant effect on the energy exchange. Ships at sea want to know where the ice edge is to determine how far north they can go when taking a great circle route. Meteorologists want this information for their modeling programs.

This constant activity profoundly affects the climate in the Northern regions, which of course makes its way down to us in the Canadian Arctic front or polar express. What is happening at the poles then influences global climate and weather and needs to be monitored in real time. Right now SAR is the only instrument that can be used to determine the areal extent of leads in the ice packs. However, the large amount of data required is not practical. Visible sensors can help in the summer, but they are not very useful in the winter because of the low Sun angles in the polar regions. The Canadians and Norwegians have extensive aircraft programs to collect this vital information.

In summary, there are several areas in which real-time microwave radiometer data are needed, or would certainly be beneficial. They include the determination of the sea/ice boundary for ships at sea and for meteorological modeling; the determination of snow/rain mix in a storm as an aid to transportation, directing clean-up activities, and in crop management; and the determination of snow and ice melting locations and rates for flooding and reservoir management.

Sea State

We have already touched on this subject in the active microwave paper "Radars in Space" presented in this document. Let's say you have an aircraft or spacecraft moving in a fixed direction. The wind is blowing in a certain direction, and a radar is looking in some arbitrary direction. The radar return depends upon the small-scale roughness of the surface of the ocean, which in turn depends upon the wind stress on the water. Also, the radar cross section is further influenced by the incidence angle with which the radar beam strikes and is reflected from the sea surface. Figure 5 shows the dependence of radar cross section on incidence angle. Now, for a given incidence angle, suppose you look at the ocean at different azimuths with respect to the upwind direction. It turns out that there is an additional modulation, a biharmonic function, and this is shown in Figure 6. We measure the roughness and know the incidence angles at two or more azimuths, but there is still an ambiguity, so we have to know something else to resolve the actual wind direction. The something else that is needed is an algorithm, or model function, to get from the radar measurements to the wind vector. This is the basis of scatterometry and how it is used to determine wind speed and wind direction; we have to make measurements of each surface area (or resolution cell) from two or more directions to resolve ambiguities in specifying the wind.

The accuracy in determining wind speed with a scatterometer is about 2 meters per second. As far as the wind direction goes, we are generally within 20 degrees. Both of these accuracies are usually much better than the in situ measurements. Now I don't know if you have spent any time on ships, but when the crew gets around to recording wind speed and direction, they are really very sloppy about it. We had some simultaneous reports from ships that were within a mile of each other, and they showed wildly different wind directions. For instance, there are anemometers, one on each side of the mast. You're supposed to use the reading from the windward one to avoid the lee of the mast, but often the crew forgets to do that and reports the wrong one.

In Figure 7 we see a comparison of satellite wind measurements with surface observations. Hundreds of readings went into this, and what we have is the wind speed from the scatterometer backed out through the algorithm versus what surface observations there were. It turned out that after this big verification program of Seasat data there was much more confidence in the scatterometer data than there was in the so-called ground truth that had been obtained from the ships and buoys at sea.

It is clear from the experience we had with the Seasat instrument that sea state can be determined probably more accurately from space than by surface measurements. This kind of information is certainly desired in near real time, and with recent improvements in signal processing and data reduction, real-time global wind field and sea state calculations are certainly feasible.

The next generation of spaceborne scatterometers and radar altimeters will make direct measurements of ocean wave spectra; then we'll get sea state statistics without recourse to a wind algorithm.

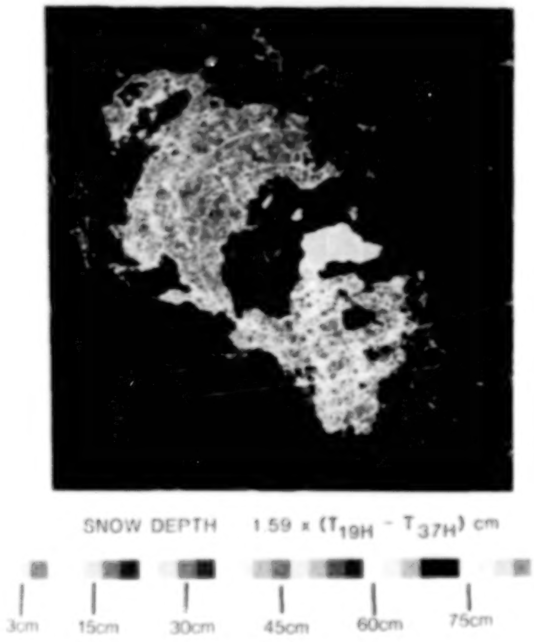
SNOW DEPTH 1.59 x (T19H - T37H) cm
3cm
15cm
30cm
45cm
60cm
75cm

Figure 1. DMSP SSM/1 derived snow depth map, January 1988.

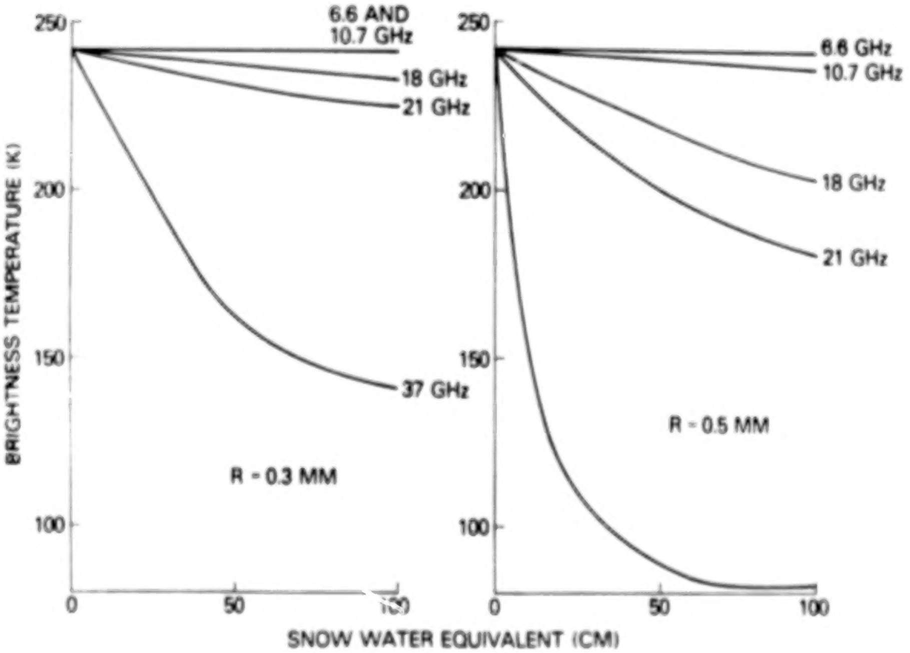

Figure 2. Calculated brightness temperature as function of snow water equivalent (horizontal polarization, $\theta = 50°$, frozen ground).

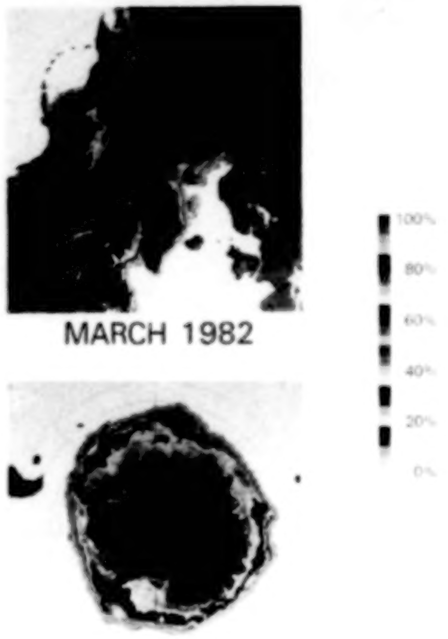
100%
80%
60%
40%
20%
0%

MARCH 1982

SEPTEMBER 1982

Figure 3. Winter sea-ice concentration from DMSP/1.

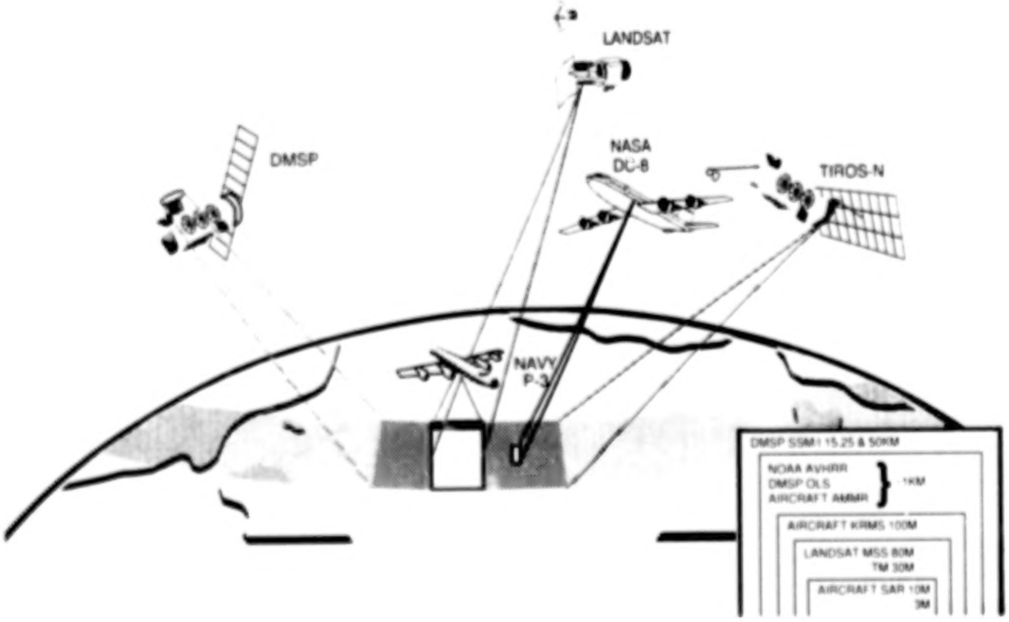
LANDSAT
DMSP
NASA
DC-8
TIROS-N
NAVY
P-3
DMSP SSM/I 15,25 & 50KM
NOAA AVHRR
DMSP OLS
AIRCRAFT AMMR
1KM
AIRCRAFT KRMS 100M
LANDSAT MSS 80M
TM 30M
AIRCRAFT SAR 10M
3M

Figure 4. Multisensor/multispatial validation of sea-ice parameters.

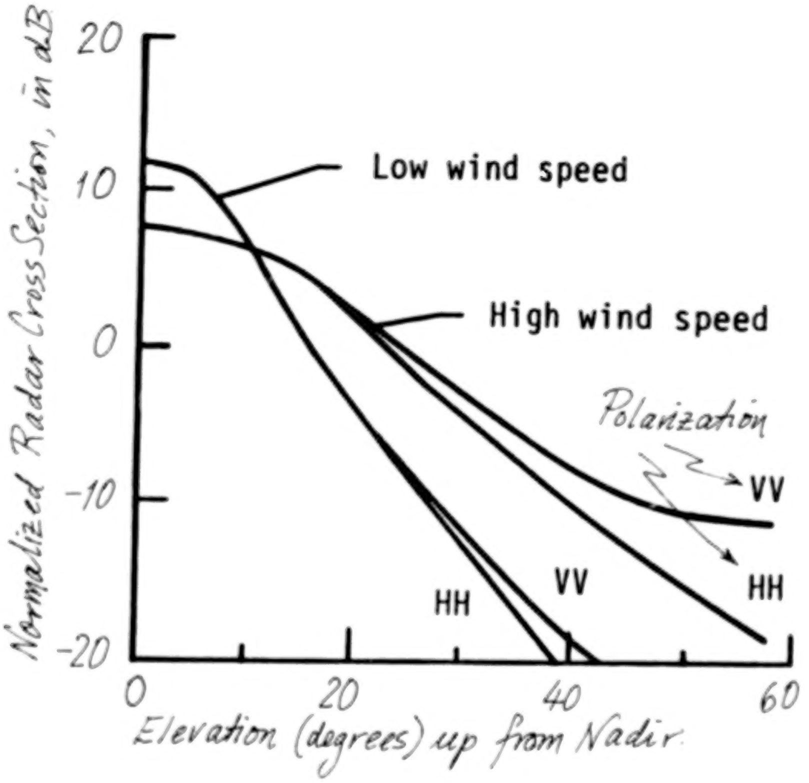

Figure 5. Dependence of normalized radar cross section on incidence angle for constant azimuth with respect to wind direction.

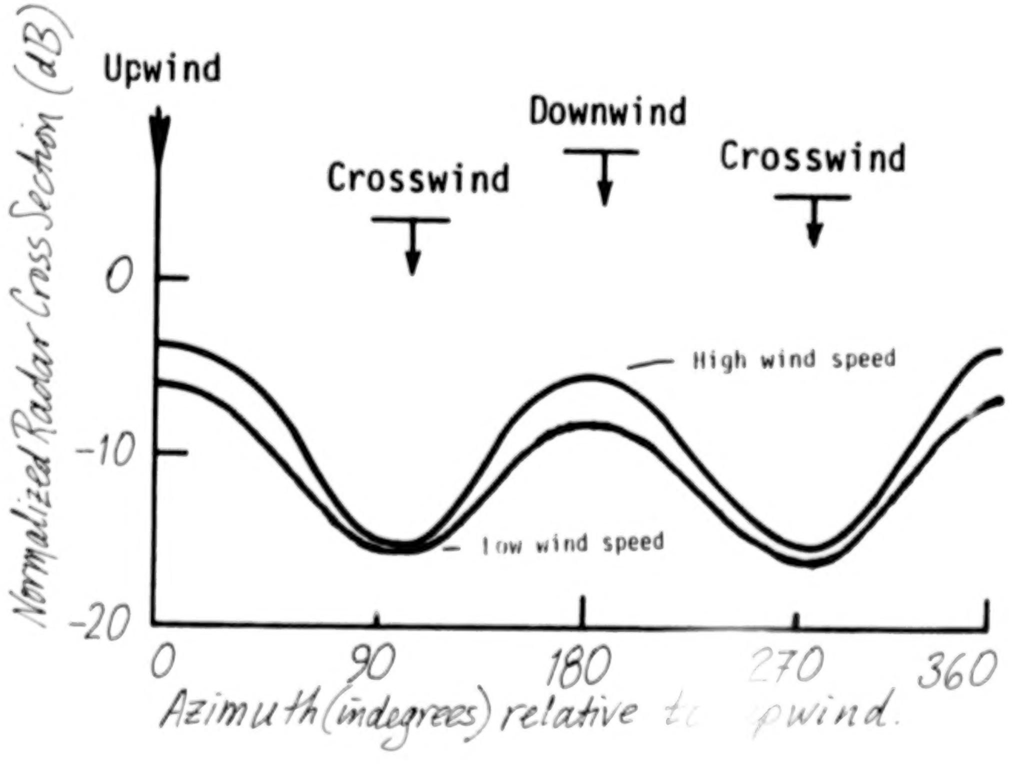

Figure 6. Biharmonic dependence of normalized radar cross section of sea surface on wind aspect for constant incidence angle.

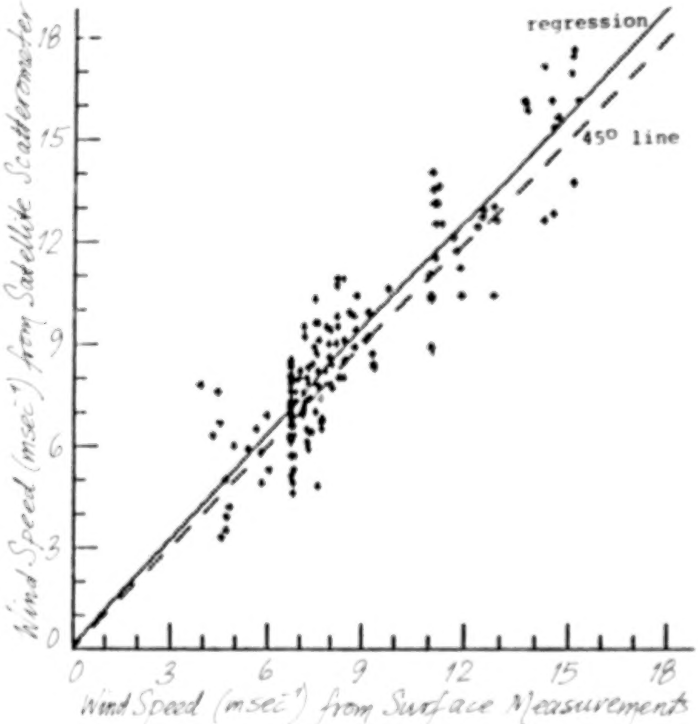

Figure 7. Comparison of satellite scatterometer (SEASAT) wind measurements with simultaneous sea surface wind measurements.

N90-27160

APPLICATIONS OF ISES FOR METEOROLOGY

Paul D. Try
Science and Technology Corporation
Hampton, VA

ABSTRACT

This presentation summarizes the results from an initial assessment of the potential real-time meteorological requirements for the data from Eos systems. Eos research scientists associated with facility instruments, investigator instruments, and interdisciplinary groups with data related to meteorological support were contacted, along with those from the normal operational user and technique development groups. Two types of activities indicated the greatest need for real-time Eos data: 1)technology transfer groups (e.g., NOAA's Forecasting Systems Laboratory and the DOD development laboratories), and 2) field testing groups with airborne operations. A special concern was expressed by several non-US participants who desire a direct downlink to be sure of rapid receipt of the data for their area of interest. Several potential experiments or demonstrations are recommended for ISES which include support for hurricane/typhoon forecasting, space shuttle reentry, severe weather forecasting (using microphysical cloud classification techniques), field testing, and quick reaction of instrumented aircraft to measure such events as polar stratospheric clouds and volcanic eruptions.

INTRODUCTION:

For the Information Sciences Experiment System (ISES) Meteorology Panel, the areas addressed included synoptic and mesoscale meteorological situations, considering clouds, temperature and humidity profiles, severe weather conditions, limits to visibility, and winds. The following contains a synopsis of the presentation given on 3 May 1989, with text material expanding on the content of the figures which were shown as part of the presentation.

BACKGROUND:

Over 40 scientists associated with various Eos instruments and NASA, NOAA, and DOD laboratories were contacted to discuss requirements for real-time meteorological data (see below). This broad spectrum of potential users provided a perspective which not only reflected current perceived needs, but also highlighted the need to better define the total capabilities envisioned by ISES.

CONTACTS (40+)

FACILITY INSTRUMENTS:

- MODIS - 3
- AIRS - 4
- AMSR - 2
- LAWS - 3
- GLRS - 2

PI INSTRUMENTS:

- HIMSS - 1
- CERES - 2
- SAGE III - 2
- LIS - 1

INTERDISCIPLINARY:

- 4D - 2
- OCEAN CLIMATE - 1
- AEROX - 2
- CERES - 1

ORGANIZATIONS:

- NASA:
  - HQ - 1
  - LaRC - 5
  - MSFC - 3
  - GSFC - 4
  - JPL - 1
  - JSC - 1
- NOAA:
  - NMC - 2
  - NESDIS - 3
  - PROFS - 2
- DOD:
  - OSD - 2
  - AF - 1
    - DMSP - 1
    - AWS - 1
    - AFGL - 2
  - USN -
    - ONR - 1
    - NEPRF - 2
    - NPS - 1
  - ARMY - ASL - 3
- UNIVERSITIES:
  - WISCONSIN - 2
  - CSU - 2
  - WASHINGTON - 2
- PRIVATE - TV/RADIO - 1
  - OTHERS - 1

The results of this informal community-wide survey (see below) indicated the groups which perceived the greatest need for real-time data. The theoretical meteorological research community and the operational meteorological organizations did not see the need for real-time data from Eos polar platforms, but for very different reasons. Most researchers see later receipt of the data as sufficient, while the operational community, whose mission performance depends upon real-time data, felt the limited spatial and temporal coverage negated the potential benefit for day-to-day operational use. It was the experimentalists and scientists involved in field testing who, along with the technique developers for the operational meteorological organizations, expressed the greatest interest and need for ISES real-time data. An additional community of users of state-of-the-art (SOA) meteorological data, which is often ignored, is the value-added professional group composed of the radio/TV meteorologists and the private consulting firms. Both groups require the latest technology available for real-time data when the data produce the appropriate commercial benefits. The extensive use of Doppler radars and use of merged satellite and radar animated presentations by TV stations (well before the National Weather Service and DOD operational forecasters have access to the technology) are just two examples of their interest in SOA real-time data. However, this group usually requires demonstration of the capability first, before committing resources.

TRENDS

SCIENTISTS: OPERATIONAL PROFESSIONALS:

NASA > < NOAA
UNIVERSITY > "NOT NEEDED" < DOD

"LATER OK" "COVERAGE TOO LIMITED"
(time and space)

FIELD TESTERS > "YES - NEEDED" < TECHNIQUE DEVELOPERS
AIRBORNE OPS NOAA - PROFS
CAL/VAL DOD - 6.2 LABS
AFGL/NEPRF/ASL

VALUE-ADDED PROFESSIONALS:

TV/RADIO >
PRIVATE CCM > "MAYBE - AWAIT PROVEN RESULTS"

DISCUSSION:

The potential uses of the ISES-derived Eos meteorological data can be divided into four primary areas (shown below) for further investigation.

PRIMARY USES OF REAL-TIME Eos DATA

1. COMPLEMENTARY REAL-TIME FORECASTING SUPPORT:
   (High Spatial/Spectral, Low Temporal Resolution)
   A. ENHANCEMENT (Known Results)
   B. IMPROVEMENT (Unknown Results)
   C. VALUE-ADDED (Proven Results)
2. FIELD TESTING:
   A. AIRBORNE OPERATIONS
      1) Find & Correlate
      2) Validate Satellite Algorithms
   B. QUICK RESPONSE TO EVENTS
      1) Fires & Dust Storm Plumes
      2) Volcanoes
3. RAPID ADJUSTMENTS TO RESEARCH APPROACHES:

   (Quick look, adjustment, and ancillary data requirements)
4. POSITIVE RECEIPT AND CONTROL OF DATA:

   (Non-US and US)

1. COMPLEMENTARY REAL-TIME FORECASTING: Because of the inherent advantages (high spatial and spectral resolution) and disadvantages (low temporal resolution/limited coverage) of Eos data, the primary utility for real-time Eos data lies in in its complementary impact on operational forecasting. While the operational GOES, GMS, and METEOSAT satellites provide the routine, real-time high temporal and spatial coverage, the Eos sensors can provide the multispectral, high resolution data which can periodically complement the operational data with previously undetected characteristics of a meteorological situation. For example, an Eos pass over a known mesoscale convective complex (MCC), could provide the ice/water determination, accurate cloud top and temperature data, droplet size distribution, rainfall/liquid water content (LWC) estimates, and surrounding wind field data needed to more accurately predict the development stage, movement, and severity of the MCC. The continued use of these

complementary data should also provide unexpected improvements in the forecasts based on operational experience, and the proven results will then create a greater demand on ISES.

2. FIELD TESTING: The greatest perceived need of the research community is in the execution of planned field testing, with the most urgent requirement coming from those with mobile measurement platforms, aircraft, or ships. The ability to direct, in real-time, the mobile platforms to the specific area requiring in-situ data collection, and to provide immediate validation of satellite-aircraft data correlation is significant. The latter is of particular importance in the validation of satellite data processing algorithms for such detailed measurements as aerosol/droplet size distributions. Also, real-time or near real-time data are needed to meet the rapid response requirements for episodic events such as fires, dust storms, and volcanic eruptions. Not only general location and plume movement data are needed, but detailed information concerning the most dense or most complex areas is often required for direction of the aircraft.

3. RAPID ADJUSTMENT OF RESEARCH APPROACHES: This is the "quick look" requirement that is used to calibrate instruments, adjust collection methods and areas, add additional measurements to the data collection program, etc. While most data collection, analysis, and field programs have been planned over a long time, seldom does one expect to have anticipated all the questions which will arise during data analysis. The value here is the ability to correct for unforeseen circumstances during data collection.

4. POSITIVE RECEIPT AND CONTROL: Although the Eos program has provided for world-wide access to the data, there has been concern expressed by non-US investigators over the communications and handling necessary for them to receive the data. A direct real-time downlink for some of the data would be desired to ensure receipt of certain critical data and allow for immediate use in their local area.

POTENTIAL EXPERIMENTS:

This leads us to a discussion of a set of potential meteorological experiments which would depend upon and make use of real-time Eos data. A series of six complementary real-time forecasting and seven field test experiments are proposed as the type which could make use of ISES data and should be investigated further.

1. COMPLEMENTARY REAL-TIME FORECASTING SUPPORT:

A) integrated cloud classification and evaluation

B) improved profiles of temperature, water vapor, and winds

C) characteristics and occurrence of cirrus, subvisual cirrus, and noctilucent clouds

D) improvements in tropical storm observation and forecasting

E) increased accuracy in surface visibility from data sparse areas

F) greater information for value-added professionals

A. INTEGRATED CLOUD CLASSIFICATION AND EVALUATION: The increasing resolution and coverage of the meteorological satellite sensors and the extensive data requirements of the many meteorological analysis and forecasting models have established the need for computerized handling of satellite data. This process requires a significant number of algorithms (Wielicki, 1989; Arking and Childs, 1985) beginning with the basic (but certainly not simple) cloud/no cloud algorithm. Whatever the wavelength (visual, IR, microwave), the definitive identification of cloud and precipitation areas is not trivial and often requires multispectral data analysis to successfully present the situation to the meteorologist. Shown are examples of the specific wavelengths which could be required to be cross correlated on-board and the resulting product (image) downlinked by ISES for real-time use. The ability of a meteorologist to accurately forecast the sensible weather parameters also may depend upon the knowledge of microphysical features of the meteorological situation. The ice/water cloud content, droplet size distribution, liquid-water content (LWC), and precipitation spatial distribution, and detailed cloud top and temperature data are all elements derivable from Eos ISES real-time data, and can influence real-time operational forecasting. The integration of the spatial and microphysical cloud data could provide the key complementary data set needed to enhance the forecast accuracy for many meteorological situations. The suggestion for ISES is the downlink of the individual bands referred to (priority of need is indicated) and the onboard processing results from three algorithms (to be modified by command) which merge the data from several sensors and provide the cloud classification and analysis results needed. The first algorithm would be an agreed-to standard to be maintained for consistency and comparison purposes, while the two others would be used on a trial basis and be modified as analysis and application dictate.

1 - COMPLEMENTARY REAL-TIME FORECASTING

A - INTEGRATED CLOUD CLASSIFICATION & EVALUATION:

PARAMETER	BAND	PRIORITY
1. CLOUD/NO CLOUD (over land, water, snow & ice)	.6u & Algorithm	4
	3.7u Black stratus (night)	2
	1.6u snow/cloud (day)	3
	18/37Ghz	
Coverage (fraction) & Size (cells)	Algorithm	
2. TYPE (ci/cu/st)		
Ice/Water (stage of development)	1.6u/.75u	3
3. TOP/BASE (Temp or bkscat)	11u & 14u / Lidar*	1&7/+

(* indicates Lidar data from GLRS, LAWS or ATLID)

PARAMETER	BAND	PRIORITY
4. OPTICAL DEPTH (Brightness)	.75u	4
Droplet Size Dist	2.1u/.75u	
Aerosol Size Dist/Correction	.5u/.7u/Lidar	5
5. LWC & Precipitation	37&90Ghz/.75u/LIS	
6. WATER VAPOR	6.7u	6

- SUMMARY DOWNLOAD: 8-12 BANDS PLUS 3 MERGED ALGORITHM RESULTS (1stnd/2trial)

(MODIS, AIRS, HIMSS, GLRS/LAWS/ATLID, and LIS)

B. IMPROVED PROFILES OF TEMPERATURE, WATER VAPOR, AND WINDS: A key factor in the accuracy of both the longer range (6 - 96 hrs)and shorter range (0-6 hrs) forecasting models and methods is the accuracy of the vertical profile data. Satellite-derived profile data (see below), while providing broad spatial coverage, have been unable to match the accuracy of the rawinsonde balloon (RAOB) data. Eos offers the opportunity to approach the accuracy of the RAOB by using sensors with greater spectral resolution and by merging the data from several sensors. For example, in addition to using higher resolution IR/MW sounders, by using lidar to pinpoint the planetary boundary layer (PBL) and the tropopause heights, a significantly more accurate profile (Westwater, et al., 1983) of temperature and moisture could be obtained for real-time application to short range severe weather, visibility, pollution, and surface wind forecasting. Also, the LAWS system offers the ability to greatly increase the coverage of wind profile data providing greater short range forecast accuracy as well as improved longer range forecast model accuracies. The downlink suggestion for ISES would be a standardized profile from a merged data set and two trial algorithms for research application.

1 - COMPLEMENTARY REAL-TIME FORECASTING

B - PROFILES (Temperature, Water Vapor, Winds)

(Est 50% improvement in profiles)

MERGED -- Lidar PBL & Tropopause Data with high resolution
AIRS (8-14u) and HIMSS (50-60Ghz) sounders.

-SUMMARY: DOWNLINK 3 profile sets, 1 stnd & 2 trial sets.

C. CHARACTERISTICS AND OCCURRENCE OF CIRRUS, SUBVISUAL CIRRUS, AND NOCTILUCENT CLOUDS: From a real-time perspective, the characteristics and probability of occurrence of particulates at high altitudes are parameters of considerable interest for the reentry of the Space Transportation System (STS) and the National Aerospace Plane (NASP). Since these particles provide the potential for structural damage as well as forced deviation from a planned reentry path (Corvault, 1988), the ISES requirement is for near-real time broad area measurements along and near the proposed reentry path. Ground-based lidar measurements of subvisual cirrus clouds have indicated that this upper air feature occurs routinely. With the normal 25-35% probability of occurrence for cirrus clouds and added effects of noctilucent clouds, the potential probability of ice crystal cloud particulate interaction with the STS/NASP vehicles on reentry appears to be significant (Wylie, 1989). While more detailed analyses by recovery location and further investigation into the aerosol interactions with the STS/NASP airframes will size the problem better, there is an area of potential real-time observational need associated with these high altitude features. The merging of lidar measurements with visual/IR imagery and apparent cloud top temperature data may be able to identify the features needed for real-time decisions related to reentry. The suggested downlink information would be the lidar high altitude return along with three algorithm products for continuing analysis.

1 - COMPLEMENTARY REAL-TIME FORECASTING

C - CIRRUS, SUBVISUAL CIRRUS & NOCTILUCENT CLOUDS

(STS and NASP real-time reentry decisions)

MERGED -- Lidar with MODIS (10.5u/.65u) & AIRS (CO2 slicing)
(New .4-.7u algorithms)

-SUMMARY: DOWNLINK - Lidar DATA & 3 ALGORITHM (1stnd/2trial)

D. IMPROVEMENTS IN TROPICAL STORM OBSERVATION AND FORECASTING: Since the lack of surfaced based observations in the tropics makes the satellite the dominant observational platform for tropical meteorology, there is considerable information concerning tropical storm development and movement which could be obtained from Eos data. Hurricanes/typhoons are relatively slow moving and can be easily tracked by geostationary and operational polar orbiting satellites; however, it is the detailed characteristics of the mass of the storm and the surrounding pressure, wind, temperature, and moisture fields which govern the all important forecast track. ISES can provide these data. Since actions required to protect from storm damage take many hours of preparation, adequate warning lead-time is required, and there is a need for real-time updates of the detailed storm environment. For example, the subsidence in the storm eye produces a warm core measurable from satellite and can be used to estimate the minimum pressure, maximum winds, and overall storm intensity (Kidder, et al., 1978). The surrounding cold cloud tops from overshooting cumulnimbus clouds also help define the intensity and locations of the more severe weather. Infrared sounder data with <15-km resolution coupled with lidar cloud top measurements should be able to provide these estimates. The precipitation areas, which are visually obscured, are particularly important since flooding is often the most significant consequence of a tropical storm. Microwave imager and lightning detector data should outline the areas and intensity of the precipitation. Finally, the dominant impact of the surrounding wind and pressure fields on the forecast track makes the satellite-derived surface wind measurements vital for real-time forecasting of storm movement. Both the scatterometer and microwave imager have capabilities in this area. Many of the sounder and imager algorithms are well known and viable for onboard processing; however, the interpretative nature of the microwave image and other requirements for spatial analyses will probably require significant level-2 data to be downlinked.

1 - COMPLEMENTARY REAL-TIME FORECASTING

D - TROPICAL STORM OBSERVATION AND FORECASTING IMPROVEMENTS

A. EYE TEMPERATURE (PRESS/WINDS) -- AIRS (15-km res)

B. COLD CLOUD TOPS -- AIRS/LIDAR

C. PRECIP -- HIMSS & LIS

D. WINDS (STORM & AREA) -- HIMSS & SCANSAT

-SUMMARY: DOWNLINK - LEVEL 2 & MERGED ALGORITHM DATA central pressure/max winds (1stnd/2trial)

E. INCREASE ACCURACY OF SURFACE VISIBILITY FROM DATA SPARSE AREAS: The real-time requirement for surface visibility (as impacted by the aerosol, water vapor, and related temperature profile) is primarily from DOD. This requirement is for support to operations which would take place in areas without ground-based observations. Many military missions are affected by low altitude restrictions to visibility. The detailed spectral data from visual/IR imagery coupled with lidar data of the aerosols in the boundary layer should provide much of the information needed for immediate direct mission support and short range forecasting (see below). The multispectral data from MODIS can provide some of the needed visibility information through extraction of optical depth data. Also, the lidar data should significantly improve the overall accuracy of the concentration and vertical distribution of aerosol by more accurate measurements of the planetary boundary layer (PBL).

1 - COMPLEMENTARY REAL-TIME FORECASTING

E - DERIVED SURFACE VISIBLILITY
(DOD Requirement -- Data Denied/Data Sparse Areas)

A. MODIS image data
(background catalog)

B. MERGED LIDAR data (PBL/profiles)

F. GREATER INFORMATION FOR VALUE-ADDED PROFESSIONALS: The commercial value of meteorological data when used in tailored forecasts for industry can be significant. This proven economic value and the competitive desire of TV meteorologists to show the latest SOA data provide an additional category of users who will show greater interest as the data become available. An example of the commercial value of meteorological support to a small segment of the population is illustrated by the data presented here (Carlson, 1989). A survey of agricultural users in Michigan indicated their priority for information and the potential savings they perceived was available from accurate meteorological support. The fruit and vegetable growers indicated the greatest impact from their small and concentrated operations. With the potential of $10-20,000/yr savings for individual farmers, this commercial application of Eos real-time data should be considered. While the ability to use the higher resolution data from Eos to improve short range forecasts of the key agricultural parameters may not prove to be feasible for the individual farmer, it should be for the several private forecast services which support the larger US-wide agricultural and other commercial communities.

1 - COMPLEMENTARY REAL-TIME FORECASTING

F - VALUE-ADDED PROFESSIONALS

(RADIO/TV, PRIVATE CCM, AND DIRECT USERS; E.G., AGRICULTURE)

EXAMPLE -- AGRICULTURE IN MICHIGAN

PRIORITY - 1 PRECIP

2 MAX/MIN TEMP

3 FREEZING DATA

4 DEGREE DAYS

5 SOIL MOISTURE

50 % $1-10,000/YR SAVINGS

20 % > $10,000/YR SAVINGS

FRUIT & VEG -- SMALL CONCENTRATED -- BIGGEST IMPACT --
25 % > $10,000 SAV

2. FIELD TESTING:

Field testing with mobile platforms, especially aircraft, is the most apparent research requirement for ISES meteorological data. There are seven types of experimental field tests (shown below) for which investigators have indicated a need or expressed desire for real-time data. The first group of experiments involves aerosol transport and relates to the improved ability to rapidly find the plume and be directed into the appropriate area of the plume. This allows the possibility for Lagrangian-type measurements over long distances, directing the aircraft from day-to-day to the appropriate altitude and location within the plume to follow the same parcel of air. For large meteorological features such as areas of Arctic haze or polar stratospheric clouds, accurate vectoring of the aircraft is needed to rapidly find and traverse the cloud area. Another field test with special interest in real-time data is the Global Atmospheric Sampling Program (GASP) supporting the testing of laminar flow control for airfoils. Cirrus and subvisual cloud crystals are of particular concern since they break up the laminar flow across the aircraft wing (Davis, et al., 1989); therefore, successful tests must be flown in perfectly clear air (undetectable from normal meteorological satellite images) and ISES data can identify the appropriate test areas in real-time. The final category for ISES data is that based on the need for quick reaction and detailed vectoring of instrumented aircraft to episodic events. Forest fires and volcanic eruptions are two examples of events where complex airborne sampling is needed with a rapid reaction capability.

2 - FIELD TESTING

A - DIRECT FIELD TESTING AIRBORNE OPERATIONS

- 1. AEROSOL TRANSPORT
  - a) FIND PLUMES & CORRELATION WITH ALGORITHMS
  - b) LAGRANGIAN CAPABILITIES FOR LONG DISTANCE TRANSPORT
- 2. CLOUD/AEROSOL LOCATION
  - a) ARCTIC HAZE
  - b) POLAR STRATOSPHERIC CLOUDS
  - c) GASP/ LAMINAR FLOW CONTROL

B - QUICK REACTION TO EVENTS

- 1. FOREST FIRE PLUMES
- 2. VOLCANOES

3. RAPID ADJUSTMENT OF RESEARCH APPROACHES:

The third category of requirements for ISES meteorological data relates to the value of seeing the Eos research quality data and its relationship to all other available information in a time perspective which allows the adjustment of the data collection program. Using the ISES-derived data for "quick look" analyses, adjustments to algorithms, sampling rates, spectral band selection, and addition of new data types are just a few of the actions which could be of significant benefit when unforeseen circumstances arise. Also, in the meteorological community, the "book binding" effect can occur and restrict the access to ancillary relevant data. This effect occurs when real-time meteorological data are not immediately extracted and must be retrieved (usually a long process) from a climatological/archival center, which may or may not have saved the data required or retained the data in the form needed. This has been a particular problem in the past for high resolution meteorological satellite data, much of which has not been archived or saved at all. For some types of investigations, especially those using multispectral imagery, this benefit from ISES should be thoroughly considered.

3 - RAPID ADJUSTMENT OF RESEARCH APPROACHES

"QUICK LOOKS"

4. POSITIVE RECEIPT AND CONTROL OF DATA:

The last category of use is one which relates to the previous categories, but adds the concern from those where communications and other data handling problems related to overseas access are involved. Also, some of the concern is over the ability of the Eos system to handle their needs. Some of the many international participants have expressed a strong interest in having access to Eos real-time data with the coverage and capability to immediately use the data in their local areas of interest.

4 - POSITIVE RECEIPT AND CONTROL OF DATA

INTEREST SHOWN BY NON-US PARTICIPANTS FOR LOCAL RECEIPT OF DATA

CONCLUSIONS:

As summarized below, there appear to be two categories of primary users and two key types of uses for real-time meteorological data from ISES. First, the technique developers responsible for improving the real-time forecasting capabilities of our civil and military weather services and, second, the experimental research scientists involved in field tests with mobile platforms, especially those with instrumented aircraft. From within these groups, ISES will have its greatest requirements for meteorological data and the potential specific uses of ISES capability, discussed earlier, can be a starting point for further investigation.

SUMMARY

-- TWO PRIMARY USERS:

1 - COMPLEMENTARY REAL-TIME FORECASTING (MESOSCALE)

Level 2 Enhancement data at 3-hr increments

2 - FIELD TESTING

(Find, correlate, validate & quick reaction)

Level 1A/B & 2 Data

** VALUE ADDED USERS EXIST **

(must prove worth and provide level 3 data)

-- EXPERIMENT DETAILS STILL TO BE WORKED OUT

1 - ALGORITHM SELECTION

2 - DATA INTEGRATION SCHEMES

3 - ONBOARD SIZING REQUIREMENTS

4 - RECEIPT FORMAT

****

*** NEED IS RECOGNIZED

BUT BY FEW TECHNOLOGY TRANSITION GROUPS

THEREFORE;

SOME IDEAS WILL NEED IMPETUS PROVIDED (CONCEPTS AND SOME FUNDING)

Many details have yet to be worked out; however, the need for ISES is recognized by those involved with meteorology. Any current reluctance in support is mostly due to the outyear nature of the program and the usual concern over funding. Therefore, with the appropriate maturing and better definition of the ISES program, greater direct support should develop from the meteorological research and support community.

BIBLIOGRAPHY:

Arking, A. and J.D. Childs, 1985: Retrieval of Cloud Cover Parameters from Multispectral Satellite Images. J. Climate and Appl. Meteor., 24, 322-333.

Carlson, J.D., 1989: The Importance of Agricultural Weather Information: A Michigan Survey. Bull. Amer. Meteor. Soc., 70, 366-372.

Covault, C., 1988: Ice Clouds Could Threaten Space Shuttle Reentry Safety, Aviation Week and Space Technology, 26 Aug 1988, pg 83.

Davis, R.E., D.V. Maddalon, R.D. Wagner, D.F. Fisher, and R. Young, 1989: Evaluation of Cloud Detection Instruments and Performance of Laminar-Flow Leading-Edge Test Articles During NASA Leading-Edge Flight-Test Program. NASA TP 2888.

Kidder, S.Q., W.M. Gray, and T.H. VonderHaar, 1978: Estimating Tropical Cyclone Central Pressure and Outer Winds from Satellite Microwave Data. Mon. Wea. Rev., 10,106, pp 1458-1464.

Westwater, E.R., M.T. Decker, and A. Zacks, 1983: Ground-based Remote-sensing of Temperature Profiles by a Combination of Microwave Radiometry and Radar. J. Climate and Appl. Meteor., 22, 126-133.

Wielicki, B.A., 1989: Satellite Cloud Retrieval: Past, Present, Future. AMS Symposium on the Role of Clouds in Atmospheric Chemistry and Global Climate.

Wylie, D., 1989: Cirrus Clouds and Their Relationship to Atmospheric Dynamics. AMS Symposium on the Role of Clouds in Atmospheric Chemistry and Global Climate.

N90-27161

Applications of ISES for Instrument Science

William B. Grant
NASA Langley Research Center
Hampton, VA

Introduction

It is often the case that some instruments being used for geophysical measurements cannot measure some parameters that are important for processing the data obtained using the instrument. However, the parameters of interest may be measured by other instruments and these data made available to the operators of the first instrument. One example is that the Total Ozone Mapping Spectrometer (TOMS) measures radiance in several ultraviolet channels to determine ozone column content while scanning large regions of the Earth's surface. It uses the longer wavelengths to detect the presence of clouds, so that the ozone values are determined above cloud height only. However, snow can mimic cloud reflectance, so it is important to have daily maps of global snow cover in order to distinguish snow from clouds (Ref. 1). Another example is provided from the Amazon Boundary Layer Experiment (ABLE). A number of instruments are placed on a DC-8, and it is flown over large regions of the Amazon forest. Most of the instruments are point sensors or in situ instruments, measuring only in the atmosphere that comes in contact with the airplane. Remote sensing lidar has also been included to measure aerosols and ozone from the aircraft height to the ground. In doing so, it provides data that are invaluable to the other instruments in determining the nature and history of the air sampled at flight altitude (Refs. 2 to 5).

For this paper, the following working definition of "instrument science" is defined:

"The on-board processing of data to the advantage of the instrument, the data stream, and near real-time users." In other words, processing the data immediately after it is acquired is useful in directing the operation of the same or different instrument or in providing a quick-look data set to users on the ground. The four applications which are also considered in this paper are:

1. The decision to acquire data due to some important occurrence detected by Eos instruments;
2. The decision not to acquire data at a scheduled time and/or location;
3. The decision to acquire additional data to improve data quality;
4. Combining data from several sources to enhance data quality.

In this paper, general examples will be presented, which may or may not apply directly to Eos instruments on the various platforms.

1. The Decision to Acquire Data Due to Some Important Occurrence Detected by Eos Instruments

This is the case where quick looks at portions of the data streams could be useful in determining the existence of and location of a natural or man-made occurrence of sufficient importance and extent that it could and should be studied further by a suite of Eos instruments. While many of these ideas were presented in other papers, they are presented here for completeness.

A. Volcanic eruption – located by an SO2 plume (TES, AIRS, SAGE III) or an aerosol plume (GLRS, MISR, SAGE III, HIRIS, etc.), then studied using HIRIS, SAR, GLRS. See Appendix A for a list of Eos instruments and their meanings.

B. Large fire – located from the thermal emission of the fire (MODIS, Lightning Imaging Sensor (LIS), or from the aerosol plume, then studied using SAR, TES, AIRS, TRACER/MOPITT.

C. Severe storm or preconditions for adverse weather – located from the clouds, water vapor, winds, etc., similar to what is currently done using meteorological satellites. However, the research instruments on Eos may have improved capabilities for identifying and studying storms.

D. Break up of Arctic polar vortex in spring. A recent NASA expedition to the Arctic found that the preconditions for significant ozone destruction existed in the Arctic polar vortex. Unfortunately, the

PRECEDING PAGE BLANK NOT FILMED

work was curtailed before the sun rose high enough to affect matters, and whether the vortex broke up before or after the sun rose has not been reported. Improved sounding instruments, such as AIRS, which should be able to give good temperature soundings in that region, should help with defining the extent of the vortex.

E. Lightning strikes used to direct tropospheric sounders – the role of lightning in generating NO and other trace molecular species can be better studied if instruments such as TES (if it is sensitive enough) are directed to, or the data tagged for, regions around lightning.

2. The Decision not to Acquire Data at a Scheduled Time and/or Location

Deciding not to acquire data can increase an instrument's lifetime, especially in the case of lasers that may have a finite number of shots possible before failure, as well as reduce the quantity of the data stream. Examples include:

1. Not firing GLRS if optically dense clouds obscure the ground-based retroreflectors of interest. MISR could give a warning, as could MODIS or instruments on other platforms, such as geosynchronous satellites.
2. Not using HIRIS if the region of interest is sufficiently covered by clouds so that little useful data will result.

3. The Decision to Acquire Additional Data to Improve Data Quality

Here is where a quick-look at the data can indicate weaknesses that can be corrected by acquiring additional data, either with the same or with a different instrument. Examples include:

1. Where low signal-to-noise ratios are found, such as with lidar or active microwave instruments, increase the transmitted power levels, the pulse repetition frequency, or integration time;
2. Where low signal-to-noise ratios are found with passive radiometers and related instruments, increase the aperture or reduce the scan rate; and
3. Where clouds or snow may interfere with the measurement, acquire additional data using other instruments on the extent and nature of the cloud cover.

4. Combining Data from Several Sources to Enhance Data Quality

As mentioned in the Introduction, there are many cases where one instrument cannot measure all of the parameters that are required to adequately analyze the data. If the data sets are not required in near real-time, there is no reason to use ISES for combining the data sets. However, if the data are to be shipped down to a user in near real-time, then it would be important to use ISES. Examples are:

1. When using MODIS data to generate phytoplankton maps, ozone data from TOMS could be used to correct for the attenuation in the 550- to 750-nm spectral region due to absorption by the Chappuis band of ozone.
2. When using MODIS data to generate information on vegetative cover or geological features on land surfaces, water vapor column contents derived from several sources can be used to correct for atmospheric water vapor absorption and improve data quality in the water vapor absorption regions, which is where bound water also absorbs. Water vapor content is difficult to measure well, so it would be advantageous to use a number of sources for the data.
3. As mentioned earlier, information on cloud cover and cloud parameters can be useful for a number of instrumental data sets.
4. When generating data sets that rely on in situ data for calibration, it would be useful to have the in situ data relayed to the platform and included in algorithm. The example that comes to mind is the use of instrumented buoys to give sea surface temperature values for infrared sensing instruments of sea surface temperature. The 10- to 12-micron region traditionally used for sea surface temperature measurements is very sensitive to water vapor and aerosols in the intervening atmosphere (ref. 6). In

order to achieve reasonably high accuracy in this spectral region, in situ data are required to pin down the values at various points.

5. GLRS data on cloud-top heights along the Eos ground track combined with CERES data on cloud-top temperatures can be useful in determining the cloud top height of many clouds outside the Eos ground track, assuming a known vertical temperature profile of the atmosphere. AIRS could also contribute useful data.
6. Accurate determination of snow depth requires both microwave radiometer temperature brightness data as well as thermodynamic temperature data (ITIR) to determine the emissivity of snow.

References

1. P. K. Bhartia, K. F. Klenk, D. Gordon, and J. J. Fleig, "Nimbus-7 Total Ozone Algorithm," Fifth Conference on Atmospheric Radiation, Baltimore, Md., Spons. by Am. Meteorol. Soc. (Oct. 312 to Nov. 4, 1983).
2. C. L. Martin, D. Fitzjarrald, M. Garstang, A. P. Oliveira, S. Greco, and E. Browell, "Structure and Growth of the Mixing Layer Over the Amazonian Rain Forest," JGR 93, 1361 (1988).
3. E. V. Browell, G. L. Gregory, R. C. Harriss, and V. W. J. H. Kirchhoff, "Tropospheric Ozone and Aerosol Distributions Across the Amazon Basin," JGR 93, 1431 (1988).
4. G. L. Gregory, E. V. Browell, and L. S. Warren, "Boundary Layer Ozone: An Airborne Survey Above the Amazon Basin," JGR 93, 1452 (1988).
5. M. Garstang, J. Scala, S. Greco, R. Harriss, S. Beck, E. Browell, G. Sachse, G. Gregory, G. Hill, J. Simpson, W.-K. Tao, and A. Torres, "Trace Gas Exchanges and Convective Transports Over the Amazonian Rain Forest," JGR 93, 1528 (1988).
6. D. E. Hagan, "The Profile of Upwelling 11-Micron Radiance Through the Atmospheric Boundary Layer Overlying the Ocean," JGR 93, 5294 (1988).

Appendix A. Eos Instruments

FACILITY INSTRUMENTS

1. Atmospheric Infrared Sounder (AIRS). Infrared spectral coverage from 3.6 to 16.8 micrometers with 15-km IFOV at nadir. Crosstrack scan of ±48.95°. Will measure atmospheric temperature, moisture, and other properties as a function of height above the ground.

2. Geodynamics Laser Ranging System (GLRS). Will measure crustal movements of the Earth in earthquake-prone regions and across tectonic plate boundaries by precisely determining the locations of special mirrors set up on the ground. Can also measure the surface height profile of glaciers and polar ice sheets. Minimum spot diameter of 80 m (may be selectable to 320 m).

3. High Resolution Imaging Spectrometer (HIRIS). Has 192 channels with average spectral resolution of 9.4 nm from 0.4 to 1 micrometer, and 11.7 nm from 1 to 2.5 micrometers. Swath width is 30 km and IFOV is 30 m. Pointable +60°/ −30° downtrack and +24°/ −24° crosstrack.

4. Laser Atmospheric Wind Sounder (LAWS). Doppler lidar wind sounder with grid spacing order of 100 km and 1 km height intervals, and with an accuracy to the order of 1 ms^{-1}. Has a conical scan angle of 56°.

5. Moderate Resolution Imaging Spectrometer (MODIS). There are two sensors. The nadir-viewing MODIS-N instrument will have 40 channels between 0.4 to 14.2 micrometers, spatial resolutions of 250 m (two channels), 500 m (eight channels), and 1 km (30 channels), and a 1780 km swath width. The tilting MODIS-T instrument will have 64 contiguous bands, 10 nm wide, and between 0.4 to 1.0 micrometers; fore and aft tilt of 50°, and a swath width of 1780 km with 1-km spatial resolution at nadir.

6. Synthetic Aperture Radar (SAR). Multifrequency (L-, C-, and X-band), multipolarization system. Has both east and west viewing at selectable incidence angles from 15° to about 55°. Highest spatial resolution will be approximately 15 m with a swath width of 30 to 120 km in the normal SAR mode. Larger swaths of up to 700 km may be obtained in a SCANSAR mode for the L- and C-band channels.

INSTRUMENT INVESTIGATIONS

1. Clouds and the Earth's Radiant Energy System (CERES). Two broadband scanning radiometers: one crosstrack mode and one rotating plane, similar to ERBE. Each has three channels: total radiance (0.2 to >100 micrometers), shortwave (0.2 to 3.5 micrometers), and longwave (6 to 25 micrometers).

2. Dynamics Limb Sounder (DLS). Fourteen-channel infrared limb-scanning radiometer. Spectral range from 7.04 to 17.06 micrometers with spatial resolution of 200 to 400 km east-west and north-south and 3 km vertical. Will observe global distribution of upper tropospheric, stratospheric, and mesospheric temperature and concentrations of O_3, N_2O, CH_4, CFC11, CFC12, and H_2O.

3. Tropospheric Emission Spectrometer (TES). Downlooking and limb-viewing cryogenic-imaging Fourier transform spectrometer. Will make infrared emission measurements of tropospheric molecules.

4. Lightning Imaging Sensor (LIS). Staring telescope/filter imaging system with 90% detection efficiency under both day and night conditions using background remover and event processor. Has storm-scale (10 km) spatial resolution with 1-ms temporal resolution.

5. Multi-angle Imaging Spectro-Radiometer (MISR). Eight identical CCD-based pushbroom cameras at four viewing angles of 28.5°, 46.5°, 60°, and 72.5°, fore and aft. Continuous simultaneous imaging in

PRECEDING PAGE BLANK NOT FILMED

four narrow spectral bands from 440 nm to 860 nm, with spatial resolutions of 1.73 km and 216 m (local mode).

6. Measurements of Pollution In The Troposphere (MOPITT). Four-channel correlation spectrometer with crosstrack scanning. Measures upwelling radiance in the CO fundamental band around 2,140 cm^{-1}. Uses pressure modulation and length modulation cells to obtain CO concentrations in 3-km layer.

7. Positron Electron Magnet Spectrometer (POEMS). Magnet spectrometer with 6 cm^2 Sr collection power. Measures positrons and electrons in the 5-MeV to 5-GeV range and provides a spectra of protons, helium, and heavier nuclei in the 30-MeV to 10-MeV range.

8. Advanced Scatterometer for Studies in Meteorology and Oceanography (SCANSCAT). Dual-scanning pencil-beam scatterometer at 13.995 GHz. Measures ocean-surface wind speed and direction, with wind speed accuracies of 20% for less than 3 m/s and 10% for 3 to 30 m/s. Directional accuracy 20%, with 25-km spatial resolution and coverage over a 1,100-km swath.

9. High Resolution Research Limb Sounder (HIRRLS). Twelve-channel infrared limb-scanning radiometer with spectral region from 6.08 to 17.99 micrometers and spatial resolution of 5° longitude by 5° latitude by 2.5 km vertical.

10. Ionospheric Plasma and Electrodynamics Instrument (IPEI). Retarding mass analyzer (RPMA) and ion drift meter (IDM). Determines thermal energy distribution and thermal ion arrival angle with respect to spacecraft velocity; also determines relative abundance of ionospheric constituents H$_+$, He$_+$, and O$_+$.

11. Thermal Infrared Ground Emission Spectrometer (TIGER). Thermal infrared imaging spectrometer for surface compositional mapping for geology and volcanology. Provides spectral image measurements of global irradiance in the 3- to 5-micrometer and 8- to 13-micrometer atmospheric windows, with IFOV of 90 m and a swath of 30.2 km.

12. Geomagnetic Observing System (GOS). Boom-mounted vector fluxgate magnetometer; scalar-helium magnetometer, with three star trackers to provide pointing knowledge. Obtains absolute scalar fields at ±1 nanoteslas accuracy; vectors field at ±3 nanoteslas per axis, rss.

13. Energetic Neutral Atom Camera (ENAC). Three sensor heads; charge rejection plates discriminate between ions and energetic neutral atoms (ENA). Obtains spatial images of ENA sources. ENAs sorted as to energy (20 keV to several MeV) and mass species; e.g., H, He, and O.

14. Stratospheric Wind Infrared Limb Sounder (SWIRLS). Gas correlation and filter infrared radiometer. Observes atmospheric infrared emissions in the 7.6- to 17.2-micrometer range. Obtains continuous vertical profiles of horizontal wind vectors (from wind-induced Doppler shifts in the N$_2$O emission spectrum), temperatures and pressures, and mixing ratios of ozone and nitrous oxide. Has a 3-km vertical resolution in a 20- to 60-km altitude range on both the day and night sides of the Earth.

15. Stratospheric Aerosol and Gas Experiment III (SAGE III). Earth-limb scanning grating spectrometer with 1- to 2-km vertical resolution. Obtains global profiles of aerosols, O$_3$, H$_2$, NO$_2$, clouds, and air density in the mesosphere, stratosphere, and troposphere.

16. GPS Geoscience Instrument (GGI). The Global Positioning System (GPS) flight receiver-processor; may include up to 18 dual-frequency satellite channels. Allows real-time platform position and altitude accuracy to 1 m and 20 arc sec, post-processing accuracy to 3 cm and 5 arc sec.

17. X-ray Imaging Experiment (XIE). X-ray pinhole "anger" cameras with NaI(T1) and PM detectors for >20 keV x-rays proportional gas-filled counter for 3–20 keV x-rays. Optional particle package for electrons and protons. FOV + or – 56° (x-rays), + or – 90° (particles).

18. Tropospheric Radiometer for Atmospheric Chemistry and Environmental Research (TRACER). Two-channel gas-filter correlation radiometer with nine separate filters contained in rotating gas-cell chopper. Measures 2.3-micrometer radiance of CO and CH_4, and 4.6 micrometer radiance of CO and N_2O.

19. The Solar Stellar Irradiance Comparison Experiment (SOLSTICE). Four-channel UV spectrometer for daily measurement of full disk solar irradiance, with calibration maintained by comparison to bright, early-type stars (1% accuracy). Has a range of 115 to 440 nm, with three-channel spectral resolution to 0.2 nm and one channel to 0.0015 nm.

20. Spectroscopy of the Atmosphere Using Far-IR Emission (SAFIRE). Seven-channel far-IR Fourier transform spectrometer (0.004 cm^{-1} spectral resolution) and seven-channel mid-IR broadcast LIMS-type radiometer. Covers spectral ranges 80–160, 310–390, and 630–1,560 cm^{-1} with fore and aft viewing. Will make measurements of key gases and dynamical trade gases.

21. High-Resolution Microwave Spectrometer Sounder (HIMSS). High-resolution microwave spectrometer with frequencies between 6.6 and 90 GHz. Resolution varies from 5 km at 90 GHz to 50 km at 6.6 GHz. Will measure precipitation rate, cloud water, water vapor, temperature profiles, sea surface roughness, SST ice, and snow.

22. Earth Observing Scanning Polarimeter (EOSP). Crosstrack scanning polarimeter that simultaneously measures radiances and degree of polarization in 12 spectral channels from 410 to 2,250 nm. Has a 10-km IFOV and will provide cloud properties such as optical thickness and phase, and global aerosol distribution.

23. Microwave Limb Sounder (MLS). Passive microwave limb-sounding radiometer with three spectral bands: 637, 560, and 205 GHz. Obtains vertical profiles of all molecules and radicals believed to be involved in the ozone destruction cycle. Spatial resolution is $100 \times 3 \times 6$ km.

24. Active Cavity Radiometer Irradiance Monitor (ACRIM). Three total irradiance detectors; one sensor monitors solar irradiance fulltime; two sensors calibrate optical degradation of first sensor. SI uncertainty of 0.1%, long-term precision of 5 ppm per year.

National Aeronautics and
Space Administration

Washington, D.C.
20546

RECEIVED

MAR 14, 1989

JOHN WELLMAN

Appendix B. Eos Baseline Planning Scenario

EED

2 March 1989

MEMO TO: NASA Goddard Space Flight Center
Attention: Code 415/Eos Project Manager/Mr. Mackenzie

Jet Populsion Laboratory
Attention: Section 511/Eos Project Manager/Mr. Sander

FROM: EE/Eos Program Manager

SUBJECT: Launch Date Assumptions for Eos Planning

Attached is a revised Eos Baseline Planning Scenario listing instruments and launch dates. These dates should be used in preparation for the NAR and for any other planning activities. The solar instruments identified for a "Flight of Opportunity" should be assumed to be launched on SOHO in March 1995. In addition, you should assume that LAWS will be launched as an attached payload in the third quarter of 1999.

Alexander J. Tuyahov
Alexander Tuyahov

Attachment

cc: EE/Tilford
EE/Huntress
EED/Townsend
EEU/Butler
EEU/Timmons
EEC/Njoku

PRECEDING PAGE BLANK NOT FILMED

Eos Baseline Planning Scenario

Platform	NASA Polar Platform-1	NOAA Free-Flyer	Attached Playloads	NASA Polar Platform-2
Altitude/Equator	NPOP-1			NPOP-2
	705 km	824 km	400 km	705 km
Crossing Time	1:30 pm	1:30 pm	28.5°	1:30 pm
Launch Data	4th quarter 1996	1st quarter 1998	1st quarter 1997	4th quarter 1998
Research Instruments	MODIS-N[a*] MODIS-T[a*] HIRIS[a] ITIR[b] AMSR[b] MIMR[c*]/HIMSS[*] MISR[f] EOSP[f] AIRS[a*] AMSU[a] HIRRLS[f*]/DLS[f*] SAGE III[f] MOPITT[f]/TRACER[f] CERES[f*] ALT-1[a*] NSCAT[f*]/SCANSCAT[f*] GLRS[a] IPEI[f] SEM[a*] GGI[f]		ERBI[f] MODIS-N[a] MODIS-T[a] Rain Radar[f] MIMR[c]/AMSR-2[f] PPS-PODS[f] Scatterometer[f] Ozone Sensor[f] Special Imager[f] Solar Flight of Opportunity 1st quarter 1995 SOLSTICE[f] ACRIM [f]	SAR[a] TES[f] SAFIRE[f] MLS[f] SWIRLS[f] IPEI[f] GOS[f] SEM[a] XIE[f] GGI[f]
Operational Instruments		AMRIR[d] AMSU[d] GOMR[d] SEM[d]		
Other	Communications Package	ARGOS[d] Search & Rescue[d] CCDH[e]		Communications Package

a NASA Research Facility Instrument
b Japanese Research Facility Instrument
c ESA Research Facility Instrument
d Operational Support Instrument
e Operational Support Facility
f Potential PI instrument concept
g Future Japanese instrument concept
* Prototype Operational Instrument

Eos Baseline Planning Scenario (conc.)

Platform	ESA Polar Platform-1	ESA Polar Platform-2	Japanese Polar Platform
Altitude/Equator	EPOP-1/A1	EPOP-2/B1	JPOP
	824 km	705 km	800 km
Crossing Time	10:00-10:30 am	10:00-10:30 am	
Launch Date	1997	2000	4th quarter 1998
Research Instruments	Radiometer[f] Altimeter (incl. precise positioning system)[c] AMI-2[c] MIMR[c]/AMIR[f] or ATLID[c] Chemistry[f] or MERIS[c]	Very High Resolution Stereo Imager[f] SAR-C[c] HRIS[c] ATLID[c] or MIMR[c]/AMIR[f] Chemistry[f]	OCTS[g] AVNIR[g] LAWS[a] AMSR[g] (SAR-L)[g] SAR-X[g]
Operational Instruments	AMSU[d] AMRIR[d] SEM[d]		
Other	ARGOS[d] Search & Rescue[d] Communications[e]		

a	NASA Research Facility Instrument
b	Japanese Research Facility Instrument
c	ESA Research Facility Instrument
d	Operational Support Instrument
e	Operational Support Facility
f	Potential PI instrument concept
g	Future Japanese instrument concept
*	Prototype Operational Instrument

Appendix C. Eos Instrument Acronyms

ACRIM	Active Cavity Radiometer Irradiance Monitor
AIRS	Atmospheric Infrared Sounder
ALT-1	Radar Altimeter
AMI	Active Microwave Instrument
AMIR	Advanced Microwave Imaging Radiometer
AMRIR	Advanced Medium Resolution Infrared Radiometer
AMSR	Advanced Microwave Scanning Radiometer
AMSU	Advanced Microwave Sounding Unit
ARGOS	Advanced Data Collection and Location System
ATLID	Atmospheric Lidar
AVNIR	Advanced Visible & Near Infrared Radiometer
CCDH	Command, Communications, & Data Handling System
CERES	Clouds and the Earth's Radiant Energy System
DLS	Dynamics Limb Scanner
EOSP	Earth Observing Scanning Polarimeter
ERBI	Earth Radiation Budget Instrument
GGI/GPS	Geoscience Instrument/Global Positioning System
GLRS	Geodynamics Laser Ranging System
GOMR	Global Ozone Monitoring Radiometer
GOS	Geomagnetic Observing System
HIMSS	High Resolution Microwave Spectrometer Sounder
HIRIS	High Resolution Imaging Spectrometer
HIRRLS	High Resolution Research Limb Sounder
HRIS	High Resolution Imaging Spectrometer
IPEI	Ionospheric Plasma and Electrodynamics Instrument
ITIR	Intermediate Thermal Infrared Radiometer
LAWS	Laser Atmospheric Wind Sounder
MERIS	Medium Resolution Imaging Spectrometer
MIMR	Multifrequency Imaging Microwave Radiometer
MISR	Multi-Angle Imaging Spectroradiometer
MLS	Microwave Limb Sounder
MODIS-N	Moderate Resolution Imaging Spectrometer - Nadir
MODIS-T	Moderate Resolution Imaging Spectrometer - Tilt
MOPITT	Measurements of Pollution in the Troposphere
NSCAT	Navy Scatterometer
OCTS	Ocean Color & Temperature Sensor
PPS-PODS	Precise Position System - Precise Orbit Determination System
SAFIRE	Spectroscopy of the Atmosphere Using Far-IR Emission
SAGE-III	Stratospheric Aerosol and Gas Experiment III
SAR	Synthetic Aperture Radar
SARSAT	Search and Rescue Instrument
SCANSAT	Scanning Scatterometer
SEM	Space Environment Monitor
SOLSTICE	Solar Stellar Irradiance Comparison Experiment
SWIRLS	Stratospheric Wind Infrared Limb Sounder
TES	Tropospheric Emission Spectrometer

PRECEDING PAGE BLANK NOT FILMED

NASA
National Aeronautics and Space Administration

Report Documentation Page

1. Report No. NASA CP-3072	2. Government Accession No.	3. Recipient's Catalog No.

4. Title and Subtitle Earth Sciences Requirements for the Information Sciences Experiment System	5. Report Date July 1990
	6. Performing Organization Code
7. Author(s) D. E. Bowker, S. J. Katzberg, and R. G. Wilson, Editors	8. Performing Organization Report No. L-16773
9. Performing Organization Name and Address NASA Langley Research Center Hampton, VA 23665-5225	10. Work Unit No. 488-50-01-03
	11. Contract or Grant No.
12. Sponsoring Agency Name and Address National Aeronautics and Space Administration Washington, DC 20546-0001	13. Type of Report and Period Covered Conference Publication
	14. Sponsoring Agency Code

15. Supplementary Notes

16. Abstract

This report contains the papers presented at a workshop sponsored by NASA and held in Williamsburg, Virginia, on May 1–4, 1989. The purpose of the workshop was to further explore and define the Earth sciences requirements for the Information Sciences Experiment System (ISES), a proposed onboard data processor with real-time communications capability intended to support the Earth Observing System (Eos). A review of representative Eos instrument types is given, and a preliminary set of real-time data needs has been established. An executive summary is included.

17. Key Words (Suggested by Authors(s)) Onboard data processing Information extraction Real-time communication	18. Distribution Statement Unclassified—Unlimited Subject Category 43

19. Security Classif. (of this report) Unclassified	20. Security Classif. (of this page) Unclassified	21. No. of Pages 232	22. Price A11

NASA FORM 1626 OCT 86

NASA-Langley, 1990

For sale by the National Technical Information Service, Springfield, Virginia 22161-2171